2018-01-01

Comparative Phylogeography, Taxonomy, And Neuroanatomy Of Montane Chameleons In The Albertine Rift, Central Africa

Daniel Hughes
University of Texas at El Paso, dfh9@humboldt.edu

COMPARATIVE PHYLOGEOGRAPHY, TAXONOMY, AND NEUROANATOMY OF MONTANE CHAMELEONS IN THE ALBERTINE RIFT, CENTRAL AFRICA

DANIEL FREDERICK HUGHES

Doctoral Program in Ecology and Evolutionary Biology

APPROVED:

Eli Greenbaum, Ph.D., Chair

Arshad M. Khan, Ph.D., Co-Chair

Jerry D. Johnson, Ph.D.

Edward Castañeda, Ph.D.

Carl S. Lieb, Ph.D., Advocate

Charles Ambler, Ph.D.
Dean of the Graduate School

COMPARATIVE PHYLOGEOGRAPHY, TAXONOMY, AND NEUROANATOMY OF MONTANE CHAMELEONS IN THE ALBERTINE RIFT, CENTRAL AFRICA

by

DANIEL FREDERICK HUGHES, B.S., M.S.

DISSERTATION

Presented to the Faculty of the Graduate School of

The University of Texas at El Paso

in Partial Fulfillment

of the Requirements

for the Degree of

DOCTOR OF PHILOSOPHY

Department of Biological Sciences

THE UNIVERSITY OF TEXAS AT EL PASO

May 2018

Acknowledgements

"Genius is the summed production of the many with the names of the few attached" – E.O. Wilson

My dissertation captures Wilson's quote because without the help of numerous individuals—both past and present—its completion, and any success I may enjoy from it, would not have been possible. First, I thank my parents Frank and Cheryl for their unconditional support throughout all my endeavors. I thank my best friend Jaclyn for staying with me during it all, especially while I was on several long African trips. I recognize my committee members Drs. Eli Greenbaum, Arshad M. Khan, Jerry D. Johnson, and Edward Castañeda for their constructive contributions to this dissertation. I owe a debt of gratitude to my cohort in the Evolutionary Genetics and Systems Neuroscience labs at UTEP for technical help and excellent companionship.

I would like to give a special thanks to my Ph.D. advisor, Dr. Eli Greenbaum. Eli not only took me in when I had little background in phylogenetics, he also provided me the opportunity to work in Africa, which was a life-changing experience for me. My first African trip was full of biodiversity, hazardous road conditions, and risky encounters with natives—I was hooked. My naiveté showed when I thought the trip went successfully, and Eli later told me it was one of his most difficult and frustrating expeditions yet. Nevertheless, I returned two more times, including a 7-week trip by myself in 2016, and I have plans to return and continue research in 2018. So, in addition to his excellent guidance as a graduate advisor, I thank him for giving me a deep appreciation for African adventures and general wanderlust for unexplored places.

I also owe a distinct debt of gratitude to the co-chair of my Ph.D., Dr. Arshad Khan. Arshad also agreed to work with me when I had limited experience in his discipline, and his genuine

confidence in me was a frequent source of inspiration. I offer my most sincere appreciations to him for always taking the time to not only talk shop with me, but to also give me advice that constantly enriched my view of the scientific process and helped shape my own approach to research. In particular, I internalized a lot from his famed soliloquies, especially when he expounded on ideas parallel to those expressed in Albert Camus's celebrated quote "one must imagine Sisyphus happy", a philosophy that I continue to embrace today.

I thank the graduate school travel grants, graduate scholarship, and the Dodson family for continuously funding my research throughout my tenure at UTEP, without which this project would not have been possible. These finances allowed me to purchase necessary equipment for my research, to travel on three separate occasions to Africa for critical data collection, and to attend several conferences that advanced my professional development.

Abstract

How do traits vary across the tree of life? Our ability to address this question is diminished if: A taxonomic group has a poorly sampled phylogeny, a species goes extinct before their systematic position is resolved, or a trait is inadequately characterized for detailed studies. In the current era of mass extinction, it is imperative to not only accelerate species discovery through traditional studies in taxonomy and expeditionary research, but also to increase rescue efforts for all types of data before poorly understood species and potentially undescribed traits are lost. Here, an integrative taxonomic approach was used and novel methods were developed for preserving neuroanatomy in arboreal lizards (Chamaeleonidae) from the Albertine Rift, a Central African biodiversity hotspot. Species-tree and gene-tree methods were used on DNA data to test several phylogeographic hypotheses regarding the relative influence of geology, climate, and environment on the evolutionary histories of two understudied chameleon species, *Rhampholeon boulengeri* and *Kinyongia adolfifriderici*. Phylogeographic results revealed unanticipated biogeographic scenarios and underestimated species richness in pygmy chameleons (genus *Rhampholeon*). Morphometrics from museum specimens, including type material were compared to results from molecular phylogenies to describe three new forest chameleon species (genus *Kinyongia*). With a greater knowledge of ancestry in these two species groups, a protocol for preserving brains in suboptimal-field conditions was developed. This method was validated to show that samples preserved in the field could be utilized to describe neuroanatomy from gross anatomical down to cellular scales. Significantly, this protocol revealed that the detailed characterization of neuroanatomical traits could be achieved from a novel data source—field-preserved brains. This new methodology represents the beginnings of a comprehensive analysis aimed at studying

vertebrate brain evolution by incorporating greater species diversity. In sum, as we seek to discover Earth's biodiversity during a period when the extinction rate is exceptionally high, we must explore new methods aimed at integrating data across a wide variety of scientific disciplines, while continuing to describe species and traits using traditional approaches in taxonomy and systematics.

Table of Contents

List of Tables

Chapter 2

Chapter 3

Chapter 4

List of Figures

Chapter 2

Chapter 3

Chapter 4

Note to Readers

I have chosen to present my dissertation in five chapters that are broken down as follows: Chapter 1 is a general introduction that provides context to the overall research, Chapters 2–4 represent the body of the dissertation, and Chapter 5 summarizes the main findings and provides avenues for future research. I wrote Chapters 2–4 in the first-person plural because they are a collection of three published research articles that reflect work conducted by myself and collaborators—note that the first-person singular is used in Chapter 1 and Chapter 5 as these were done by me. Importantly, I am the first author on all three of these published papers, and while the final product benefitted from the contributions of co-authors, the lion's share of the writing (including original drafts), editing, analyses, and interpretations were done by me. I have included the first page of each published thesis chapter in the Appendix. Bear in mind that my decision to present the chapters this way inevitably led to overlap in Chapter 1 and to the introduction of all three papers, as well as in Chapter 5, and the discussion of all three papers. Also, in Chapter 3 I have described three new species and I chose to refer to them as *species nova* although the paper has been published. Note that some of the provinces in the Democratic Republic of the Congo were modified in 2015 and I use the names that were in place prior to those changes. Despite the fact that each article has been published in different journals, I compiled all chapters into a consistent format and I congregated all citations into a comprehensive reference list located at the end of this document.

Chapter 1: Introduction

Current rates of species extinction are so high (Alroy, 2015; Ceballos et al., 2015) and the rate of taxonomic discovery so slow (Fontaine et al., 2012; Pante et al., 2014) that numerous species are expected to be lost in the wild before they are even known to science (Costello et al., 2013; Lees and Pimm, 2015). These global problems are exacerbated in Africa's montane forests where high levels of biodiversity are concentrated into very small regions (Plumptre et al., 2007), which are faced with additional threats imposed by an extremely dense human population (Burgess et al., 2007; Carr et al., 2013; Cordeiro et al., 2007). The chameleon fauna of Africa is highly diverse (Tilbury, 2010; Tolley and Herrel, 2013), yet they are also one of the most highly threatened reptile groups—the IUCN Red List of Threatened Species estimates that 36% are currently threatened with extinction compared to 19% of reptiles in general (IUCN, 2018).

Numerous coalescing factors have contributed to African chameleon declines, including habitat loss (Shirk et al., 2014) and overharvesting (Carpenter et al., 2004). A salient—but often overlooked—contributor to chameleon declines is incomplete taxonomy because species that may be threatened but persist as unrecognized cryptic species will not be protected. Further complicating matters is that the taxonomy of chameleons is currently recognized as poorly understood and an underestimation of their true diversity (see Tilbury, 2010; Tolley and Herrel, 2013). This phenomenon manifests itself in several measurable ways. First, priority for protection is given to areas with more species and more endemic species, and as a result, conservation measures cannot be successfully enacted in deserving regions with poorly assessed levels of diversity. Second, chameleons are highly coveted by hobbyists, especially rare species, and incomplete taxonomic knowledge permits loopholes in the trade of live animals to be exploited.

Lastly, inadequate and/or confusing taxonomy obstructs our ability to clearly understand evolutionary processes underlying diversity and this can result in inaccurate findings and inappropriate priorities for conservation.

As one of the largest and arguably most diverse highlands in Africa, the Albertine Rift (AR) likely harbors a significant amount of cryptic chameleon diversity. As currently understood, the region houses more vertebrate and endemic vertebrate species than any other area of similar size on continental Africa (Plumptre et al., 2007), including the highest mammalian tropical forest species richness per unit area on Earth (Demos et al., 2015). The AR was not considered one of the original 25 Biodiversity Hotspots (Myers et al., 2000), yet it was later elevated into the Eastern Afromontane Hotspot (Brooks et al., 2004) and to a Global Biodiversity Hotspot (Küper et al., 2004). Unfortunately, AR biodiversity is currently undervalued because reliable estimates of the level of cryptic diversity are uncommon from the region, which is in part owing to a lack of investigation. The dearth of expeditionary research conducted in the AR stems from an enduring history of civil conflict and political instability from bordering countries (e.g., Butsic et al., 2015; Hanson et al., 2009; Plumptre et al., 2001) that has significantly discouraged exploration (see Greenbaum, 2017; Greenbaum and Kusamba, 2012). Despite such a violent history, the AR still boasts one of the most species-rich chameleon faunas in the world (Spawls et al., 2002; Tilbury, 2010; Tolley and Herrel, 2013), but it is still underestimated.

Understanding chameleon diversity in the AR is particularly pressing because the conservation situation is bleak and has nearly reached its tipping point (Greenbaum, 2017). Of the nine currently recognized endemic chameleon species in the AR, two are listed as Critically Endangered (*Rhampholeon hattinghi* and *Kinyongia mulyai*), two as Near Threatened (*K. carpenteri* and *K. xenorhina*), and one as Data Deficient (*K. gyrolepis*) (IUCN, 2018). In addition

to these endemic species ostensibly facing imminent extinction, several isolated chameleon populations in the AR are anticipated to become extirpated within our lifetime or sooner if swift action is not taken (e.g., Greenbaum et al., 2012; Tilbury and Tolley, 2015). Moreover, several highly vulnerable populations lack genetic data and are known from only a few, often poorly preserved, museum specimens. Therefore, it is not understood whether these populations represent single, widely distributed species of low conservation concern or multiple morphologically similar cryptic species with small ranges of high conservation concern. Because the AR is vastly under-explored and represents one of the most important sites for biodiversity in Africa, it provides an excellent opportunity to advance chameleon conservation by increasing our understanding of the diversity and distribution of a threatened vertebrate group.

The geological history of the AR is highly complex and explains a large part of the species and habitat diversity in the region. The AR represents the western branch of the East African Rift valley system (Chorowicz, 2005), for which the topography began forming from volcanic swells in northeast Africa around the early Oligocene (Paul et al., 2014). The AR was likely initiated approximately 25 million years ago (Mya) (Roberts et al., 2012), with most of its geophysical rifting and volcanic activities occurring from 15–5 Mya (Macgregor, 2015). These lava flows would have altered large woodland areas (Griffiths, 1993; Nonnotte et al., 2008), and thus the age and distribution of AR forests, and the evolution of its forest-dwelling fauna, may be more closely linked to its orogenic history than is currently understood.

Nevertheless, the proposed mechanisms of speciation or environmental processes that have shaped the diversity of the AR are not conclusive. Aridification and refugia formation in response to Pleistocene glaciations have been implicated as drivers of isolation and subsequent lineage formation among some AR montane taxa, including small mammals (Demos et al., 2014, 2015),

land snails (Boxnick et al., 2015), gorillas (Anthony et al., 2007), bats (Hassanin et al., 2015), and birds (Bowie et al., 2006). In contrast, several other African montane taxa, including frogs (Portillo et al., 2015), chameleons (Tolley et al., 2011) and snakes (Menegon et al., 2014; Greenbaum et al., 2015) were suggested to have evolved from pre-Pleistocene events such as the reduction of forests and spread of grasslands across Africa in response to global cooling in the Miocene. Because the AR has a complex orogenic history and is one of the most important sites for biodiversity in Africa (Plumptre et al., 2007), it provides a unique opportunity to test alternative ideas for biotic evolution and understand how historic biogeographic events and concomitant climate change have influenced spatiotemporal aspects of speciation. Using chameleons as a model, I will test various biogeographic hypotheses regarding the evolution of biodiversity in the AR. In particular, I aim to assess whether groups have remained associated with forests over time or adapted to new habitats in open ecosystems. I will determine and compare phylogeographic relationships of two chameleon groups to evaluate whether they follow a refuge-type model with forest-restricted distributions and many diversification events (Measey and Tolley 2011), or far fewer lineages that occupy large distributions (Lorenzen et al., 2012).

Communication can promote speciation by reinforcing reproductive isolation between species, such as observed with the calling frequency and inner-ear anatomy of amphibians (Ryan, 1986). The evolution of species-specific signals depends on the ability of individuals to detect signal variation, which in turn relies on the capability of the brain to process signal information (Boughman, 2002). Chameleons are considered far less agile than other lizards, and thus depend heavily on the accuracy of their visual system and its associated neural circuitry, especially for communication (Tolley and Herrel, 2013). Chameleons communicate through rapid changes in body color that has evolved from selection for social signaling and not for camouflage (Stuart-Fox

and Moussalli, 2008). Chameleons can communicate different information depending on the body region that changes color, color intensity reached, and rate of color change (Ligon and McGraw, 2013). These various factors merge to yield putative species-specific communication, which would reinforce reproductive isolation in areas of sympatry. For example, the information conveyed during social interactions, especially courtship or combat, must be accurately evaluated by recipients or fitness will decline, including unsuccessful reproduction and perhaps physical damage (Ligon, 2014).

Because all Chamaeleonidae possess an ability to change color superior to that of their sister family Agamidae (Teyssier et al., 2015), we can infer that there was likely strong selection in their evolutionary history for individuals to detect subtle variation in signals. The most striking of chameleon color change displays, however, does not seem to be conserved across the family—some species appear better at changing colors than others (e.g., Tilbury, 2010). Chameleon species with highly complex social exchanges may also possess a more sophisticated neuroanatomy to decipher the communication signals compared to species with a narrower repertoire of communication signals. It is reasonable to think that an evolutionary change in the brain that improved the detection of signal variation may have promoted speciation in chameleons, in an analogous manner as that observed in cichlid fish (Maan et al., 2006), electric fish (Carlson et al., 2011), and frogs (Ryan, 1986). Therefore, chameleons provide an excellent opportunity to test the sensory drive hypothesis, which asserts that evolutionary changes in neuroanatomy influenced by signal variation triggered a rapid radiation (e.g., Brauth, 1990). However, a wide sampling of brains across Chamaeleonidae would be necessary to test a hypothesis like this, and procuring the adequate number of high-quality samples for neuroscientific study is greatly hindered by the rules and regulations of live-animal export. For certain countries, exporting live chameleons—all of

which are listed as Appendix II according to the Convention on International Trade in Endangered Species (CITES)—for scientific purposes is discouragingly expensive and complicated, and thus more economical alternatives to acquire well-preserved brain samples are needed.

All of comparative biology depends on knowledge of the evolutionary relationships of organisms. Using an integrative taxonomic approach, I will first test several hypotheses regarding the relative influence of historical forest dynamics and climate change on the evolutionary histories of two understudied chameleon species (*Rhampholeon boulengeri* [Chapter 2] and *Kinyongia adolfifriderici* [Chapter 3]) from the AR and propose phylogeographic hypotheses based on genetic and morphological data. My next goal is to address some of the challenges associated with acquiring chameleon brains by experimentally testing novel approaches to preserve neural tissues in suboptimal conditions (Chapter 4). My overarching objectives will be addressed by integrating molecular and morphological data sets, and investigating methods to overcome issues related to sampling the brains of rare and/or difficult to access species.

1.1 Specific aims

(1) Propose phylogenetic hypotheses and taxonomic solutions for Albertine Rift chameleons

(2) Explore spatiotemporal biogeographical patterns of co-distributed chameleon species

(3) Advance methods to preserve high-quality neuroanatomy in field conditions

Chapter 2: Cryptic diversity in *Rhampholeon boulengeri* (Sauria: Chamaeleonidae), a pygmy chameleon from the Albertine Rift biodiversity hotspot[1]

[1] Published as: **Hughes, D.F.**, K.A. Tolley, W. Lukwago, M. Menegon, J.M. Dehling, J. Stipala, C.R. Tilbury, A.M. Khan, M. Behangana, C. Kusamba, and E. Greenbaum. **2018**. Cryptic diversity in *Rhampholeon boulengeri* (Sauria: Chamaeleonidae), a pygmy chameleon from the Albertine Rift biodiversity hotspot. *Molecular Phylogenetics and Evolution* 122: 125–141. Available online: https://doi.org/10.1016/j.ympev.2017.11.015

2.1 Abstract

Several biogeographic barriers in the Central African highlands have reduced gene flow among populations of many terrestrial species in predictable ways. Yet, a comprehensive understanding of mechanisms underlying species divergence in the Afrotropics can be obscured by unrecognized levels of cryptic diversity, particularly in widespread species. We implemented a multilocus phylogeographic approach to examine diversity within the widely distributed Central African pygmy chameleon, *Rhampholeon boulengeri*. Gene-tree analyses coupled with a comparative coalescent-based species delimitation framework revealed *R. boulengeri* as a complex of at least six genetically distinct species. The spatiotemporal speciation patterns for these cryptic species conform to general biogeographic hypotheses supporting vicariance as the main factor behind patterns of divergence in the Albertine Rift, a biodiversity hotspot in Central Africa. However, we found that parapatric species and sister species inhabited adjacent habitats, but were found in largely non-overlapping elevational ranges in the Albertine Rift, suggesting that differentiation in elevation was also an important mode of divergence. The phylogeographic patterns recovered for the genus-level phylogeny provide additional evidence for speciation by isolation in forest refugia and dating estimates indicated that the Miocene was a significant period for this diversification. Our results highlight the importance of investigating cryptic diversity in widespread species to improve understanding of diversification patterns in environmentally diverse regions such as the montane Afrotropics.

2.2 Introduction

The East African Rift valley system started to form in the early Oligocene from hot mantle plumes causing up-lift of the African plate resulting in rifting, the formation of horst and grabens,

and associated volcanic activity (Chorowicz, 2005; Paul et al., 2014). The Albertine Rift (AR) portion in Central Africa was initiated in the late Oligocene (Roberts et al., 2012) and increased geophysical rifting in the AR occurred during the Miocene (Macgregor, 2015). Rifting oscillations influenced forest environments in the AR, largely through uplift events that altered climate and drainage patterns across the region (Sepulchre et al., 2006). Miocene volcanism has also contributed to the age and distribution of AR forests (Griffiths, 1993). The paleoclimate of the AR was generally stable through the Cretaceous (Maley, 1996), during which tropical Africa was dominated by a nearly continuous rainforest block. African rainforests began to decline in extent throughout the Cenozoic, with a pronounced increase in forest losses after the mid-Miocene (Kissling et al., 2012). Altered precipitation patterns across East Africa, driven by global cooling, contributed to the decline of the African tropical forest ecosystem in the Miocene (Zachos et al., 2001). Decreased Miocene rainfall is linked to the expansion of grass-dominated savannas across East Africa (Jacobs et al., 1999), and as grasslands expanded, forests contracted, and thereby forest connectivity was greatly reduced during this period (Kissling et al., 2012). These ancient geologically and climatically induced forest dynamics during the Miocene have left a profound legacy on the geographic distribution of genetic diversity in forest-distributed fauna in the AR (e.g., Tolley et al., 2011), and may have left a greater genetic imprint than Quaternary ice ages (Hewitt, 2000).

The proposed timing and mechanisms that underlie the remarkably high biodiversity in forests of the AR are not conclusive. One line of evidence supports recent species divergence within Pleistocene (upper limit ca. 1.8 Mya) refugial habitats (i.e., Pleistocene Forest Refuge Hypothesis [Mayr and O'Hara, 1986]), whereas another suggests that divergence occurred before Pleistocene climatic changes and species have been maintained as paleoendemics since the

Miocene (ca. 5–23 Mya) (i.e., Evolutionary Museum Hypothesis, a derivative of the Montane Speciation Hypothesis [Fjeldså and Lovett, 1997]). Both of these hypotheses are based on allopatric models of speciation from isolation in forest refugia, but they differ greatly in their timing of diversification events. Speciation in forest refugia that formed in response to Pleistocene climatic changes have been implicated as biogeographic drivers among small mammals (Demos et al., 2014, 2015), land snails (Boxnick et al., 2015; Wronski and Hausdorf, 2008), and birds (Bowie et al., 2006; Voelker et al., 2013). However, frogs (Larson et al., 2016; Portillo et al., 2015), chameleons (Hughes et al., 2017a; Tolley et al., 2011), and snakes (Greenbaum et al., 2015; Menegon et al., 2014) likely diversified during pre-Pleistocene biogeographic events, such as the reduction of forests in response to global cooling in the Miocene. Afromontane forests have functioned as stable refugia during ancient climate changes and thereby promoted vicariance-driven diversification in some AR taxa (Hughes et al., 2017a); however, this model does not fully account for the lack of genetic structure found in some widespread AR species (e.g., Greenbaum et al., 2013, 2015). Several physical biogeographic barriers have been identified in the AR, including the Virunga volcanoes that have been active from the Plio–Pleistocene to the present (Ebinger and Furman, 2003), and the uplift of the Rwenzori mountains that occurred around the Plio–Pleistocene boundary (ca. 3–2 Mya [Kaufmann et al., 2015]). These physical features have influenced patterns of gene flow for taxa between various highland areas of the AR (e.g., Huhndorf et al., 2007). However, genetic patterns for some AR taxa are not congruent with respect to identified barriers, and thus species-specific responses have been frequently detected. Much of the AR is ancient and several of its prominent geological features emerged before Pleistocene aridification pulses altered African ecosystems (e.g., deMenocal, 1995), and as a result, the AR

represents an ideal region to test several biogeographic hypotheses regarding the timing and environmental mechanisms of biotic evolution.

The pygmy chameleon genus *Rhampholeon* currently contains 19 described taxa that are largely restricted to sub-montane and montane forests distributed across West, Central, and East Africa (Uetz et al., 2017). Many species of *Rhampholeon* are endemic to small forest fragments that face immediate threats of deforestation, and thus nine species are currently considered Endangered or Critically Endangered (IUCN, 2018). The Eastern Arc Mountains and Southern Rift Highlands, stretching from Kenya south to Tanzania, Malawi, and Mozambique, represent the highest regional concentration of species diversity for *Rhampholeon* with 16 species (Tolley and Herrel, 2013). The only pygmy chameleon species in West Africa is *R. spectrum* and its distribution extends from Nigeria and Central African Republic south to Gabon (Tilbury, 2010). *Rhampholeon hattinghi* and *R. boulengeri* occur allopatrically in the AR highlands of Central Africa. The recently described *R. hattinghi* is a Critically Endangered pygmy chameleon endemic to Mount Nzawa, Democratic Republic of the Congo (DRC), a massif in the southern AR (Tolley and Tilbury, 2015a). *Rhampholeon boulengeri* is currently assessed as Least Concern, because it has a relatively large distribution in forest habitats across the AR, west into the Congo Basin (DRC) and east to Kakamega Forest (Kenya), and much of this forest is still relatively intact (Tolley and Plumptre, 2014). In addition to having one of the largest geographic distributions of any *Rhampholeon* species, *R. boulengeri* also occurs in forests across a remarkably wide range of elevations from 500 m to nearly 2300 m (Tilbury, 2010). *Rhampholeon hattinghi* is similar in appearance to *R. boulengeri*, and thus was initially considered to be a disjunct population of the more widespread species (Tilbury, 2010); however, genetic data revealed it as an independently evolving lineage (Tilbury and Tolley, 2015). Steindachner (1911) described *R. boulengeri* from a

series of specimens collected by Rudolf Grauer in 1908. However, the type locality was imprecisely given as "forest beyond the sand hills on the north-western shores of Lake Tanganyika." Tilbury and Tolley (2015) considered the Itombwe Plateau as the type locality because Rudolf Grauer collected specimens in 1908 from forests of the Itombwe Plateau, which is located to the northwest of Lake Tanganyika. However, Grauer did not write books about his travels and the precise localities where he collected on the plateau are unknown (Greenbaum, 2017).

In general, *Rhampholeon* are considered forest specialists with low vagility (Branch et al., 2014), and are thus unlikely to disperse over long distances regardless of suitable habitat corridors (Matthee et al., 2004). As a result, most pygmy chameleon species are endemic to the montane localities from where they were originally described (Uetz et al., 2017). The morphology of *Rhampholeon* is considered highly conservative (Branch et al., 2014), from which a potential for cryptic species results (Bickford et al., 2007), particularly in geographic regions that have received only cursory attention to the biota, such as the AR (Greenbaum, 2017). Moreover, several recent accounts have drawn attention to the likelihood that *R. boulengeri* represents a species complex (Tilbury, 2010; Tilbury and Tolley, 2015; Tolley and Plumptre, 2014). Therefore, *R. boulengeri* is an excellent model for investigating how diverse landscapes with complex histories of geomorphological and climatic changes have influenced the distribution of genetic diversity. In this study, we investigated the evolutionary history of *R. boulengeri* with a statistical framework to test three hypotheses related to cryptic diversity. We use a multilocus gene-tree and a comparative approach with four coalescent-based species-tree estimations to test whether *R. boulengeri* represents a single widespread species in the AR, or a complex of genetically distinct species. We assess phylogeographic patterns and compare species distributions to test whether

allopatric speciation driven by forest fragmentation underlies the diversification in the *R. boulengeri* species complex and for the genus in general. We implement fossil-calibrated Bayesian methods on a large-scale phylogeny to determine whether the timing of diversification in *Rhampholeon* follows a single break-up of African forests followed by isolation, or multiple forest fragmentations and reconnections over time.

2.3 Materials and Methods

2.3.1 Taxon sampling and DNA sequencing

Forty-six samples of *R. boulengeri* were collected during field surveys in various forests across four Central African countries of the AR from 2008–2016, including Burundi, DRC, Rwanda, and Uganda (Table 2.1). Two additional samples were collected from the Yala Nature Reserve, Kakamega Forest, western Kenya. We also included additional sequences in our analyses that were not generated for this study: ND2 fragments and one RAG1 fragment for two individuals from Bwindi Impenetrable National Park, Uganda (CAS 201681–82); a 16S fragment for an individual from Irangi (near Kahuzi-Biega National Park), DRC (ZFMK 47571); and a 16S fragment for an individual from Cyamudongo Forest, Rwanda (ZFMK 55104) (Fisseha et al., 2013). For phylogenetic analyses, we included 18 of the 19 currently recognized *Rhampholeon* species and three species of *Rieppeleon* as outgroups (Branch et al., 2014). We excluded the species *R. beraduccii* from phylogenetic analyses because only a single sequence for the mitochondrial fragment 16S is available on GenBank. *Rhampholeon beraduccii*, from the Mahenge Mountains in southern Tanzania, is a member of the subgenus *Rhinodigitum* with close affinities to *R. acuminatus*; however, this phylogenetic placement was based on analyses of the 16S gene only (Fisseha et al., 2013; Mariaux and Tilbury, 2006).

We harvested tissues from the liver or hind limb muscle of chameleons before formalin fixation and preserved these tissues in 2-ml vials containing 99% ethanol. Genomic DNA was isolated from tissue samples with the Qiagen DNeasy tissue kit (Qiagen Inc., Valencia, CA, USA). PCR amplification and cycle sequencing of two mitochondrial gene fragments were carried out with the following primers for ND2: L4347 (Macey et al., 1997a) and H5934 (Macey et al., 1997b), and 16S: L2510 and H3080 (Palumbi, 1996). A fragment of the nuclear gene RAG1 was sequenced using primers G396 (R13) and G397 (R18) (Groth and Barrowclough, 1999). Although RAG1 is a relatively slowly evolving nuclear gene (Groth and Barrowclough, 1999), it has been demonstrated to be a useful marker for studying deep divergences among vertebrates (San Mauro et al., 2004; Sullivan et al., 2006) and it also has been used extensively in pygmy chameleon systematics (e.g., Tilbury and Tolley, 2015). We used 25 µL PCR reactions with an initial denaturation step of 95 °C for 2 min, followed by denaturation at 95 °C for 35 s, annealing at 50 °C for 35 s, and extension at 72 °C for 95 s, with 4 s added to the extension per cycle for 32 (mitochondrial genes) or 34 (nuclear gene) cycles. Amplification products were visualized on a 1.5% agarose gel stained with Invitrogen SYBR Safe DNA gel stain (Thermo Fisher Scientific, Waltham, MA, USA). Sequencing reactions were purified with Agencourt CleanSEQ magnetic bead solution (Beckman Coulter Inc., Brea, CA, USA) and sequenced with an ABI 3130xl automated sequencer at the University of Texas at El Paso (UTEP) Border Biomedical Research Center (BBRC) Genomic Analysis Core Facility.

Table 2.1 Species identifications, specimen catalog numbers, GenBank accession numbers, and collecting localities for pygmy chameleons (*Rhampholeon*) analyzed in this study. Institutional abbreviations follow Sabaj (2016). See Appendix for abbreviations of field numbers. DRC = Democratic Republic of the Congo; * = data not used due to poor quality; A = allotype; H = holotype; P = paratype; T = topotype.

Species	Catalog or Field No.	16S	ND2	RAG1	Locality
Rhampholeon sp. 1	CAS 201681	*	AY524916	AY524953	Uganda: Kanungu District, Ihihizo River, Bwindi Impenetrable National Park
Rhampholeon sp. 1	CAS 201682	*	AY524915	–	Uganda: Kanungu District, Ihihizo River, Bwindi Impenetrable National Park
Rhampholeon sp. 1	UTEP 21386	MG645819	MG645865	MG645911	Uganda: Kanungu District, Ihihizo River, Bwindi Impenetrable National Park
Rhampholeon sp. 1	UTEP 21685	MG645820	MG645866	MG645912	Uganda: Kanungu District, Ihihizo River, Bwindi Impenetrable National Park
Rhampholeon sp. 1	PEM-R 16517	MG645824	MG645870	–	Uganda: Bushenyi District, Kalinzu Central Forest Reserve
Rhampholeon sp. 1	UTEP 21688	MG645852	MG645898	MG645942	DRC: North Kivu Province, Kaunzo village
Rhampholeon sp. 1	UTEP 21686	MG645853	MG645899	MG645943	DRC: North Kivu Province, Bunyantenge village
Rhampholeon sp. 1	UTEP 21687	MG645854	MG645900	MG645944	DRC: North Kivu Province, Mount Vibende
Rhampholeon sp. 1	JS 41688	MG645855	MG645901	–	Kenya: Kakamega Forest, Yala Nature Reserve
Rhampholeon sp. 1	JS 41690	MG645856	MG645902	–	Kenya: Kakamega Forest, Yala Nature Reserve

Rhampholeon sp. 1	UTEP 21689	MG645848	MG645894	MG645938	DRC: South Kivu Province, Kahuzi-Biega National Park, Luyuyu
Rhampholeon sp. 1	UTEP 21690	MG645849	MG645895	MG645939	DRC: Maniema Province, Kahuzi-Biega National Park, Nkumwa
Rhampholeon sp. 1	MTSN 6898	MG645829	MG645875	MG645919	DRC: South Kivu Province, Kahuzi-Biega National Park, Madiriri
Rhampholeon sp. 1	MTSN 6899	MG645830	MG645876	MG645920	DRC: South Kivu Province, Kahuzi-Biega National Park, Madiriri
Rhampholeon sp. 2	UTEP 21691	MG645845	MG645891	MG645935	DRC: Orientale Province, Bongobongo village
Rhampholeon sp. 2	UTEP 21692	MG645846	MG645892	MG645936	DRC: Orientale Province, Site Lodjo
Rhampholeon sp. 2	UTEP 21693	MG645825	MG645871	MG645915	Uganda: Masindi District, Budongo Central Forest Reserve, Sonso River
Rhampholeon sp. 2	UTEP 21694	MG645826	MG645872	MG645916	Uganda: Masindi District, Budongo Central Forest Reserve, Sonso River
Rhampholeon sp. 2	UTEP 21695	MG645832	MG645878	MG645922	DRC: South Kivu Province, Bizombo village
Rhampholeon sp. 2	UTEP 21696	MG645833	MG645879	MG645923	DRC: South Kivu Province, Bizombo village
Rhampholeon sp. 2	UTEP 21697	MG645834	MG645880	MG645924	DRC: South Kivu Province, Bizombo village
Rhampholeon sp. 2	UTEP 21698	MG645847	MG645893	MG645937	DRC: South Kivu Province, Kahuzi-Biega National Park, Ikundwe

Rhampholeon sp. 2	UTEP 21699	MG645850	MG645896	MG645940	DRC: Maniema Province, Kahuzi-Biega National Park, Kyasa
Rhampholeon sp. 2	ZFMK 47571	AM055647	–	–	DRC: South Kivu Province, Irangi village
Rhampholeon sp. 2	UTEP 21700	MG645859	MG645905	MG645946	Uganda: Kamwenge District, Kibale Forest National Park, Ngogo Research Center
Rhampholeon sp. 3	UTEP 21701	MG645831	MG645877	MG645921	DRC: South Kivu Province, Kalundu village
Rhampholeon sp. 3	UTEP 21702	MG645836	MG645882	MG645926	DRC: South Kivu Province, Kalundu village
Rhampholeon sp. 3	UTEP 21706	MG645837	MG645883	MG645927	DRC: South Kivu Province, Tumungu village
Rhampholeon sp. 3	UTEP 21704	MG645838	MG645884	MG645928	DRC: South Kivu Province, in the vicinity of Irangi village
Rhampholeon sp. 3	UTEP 21705	MG645839	MG645885	MG645929	DRC: South Kivu Province, in the vicinity of Irangi village
Rhampholeon sp. 3	UTEP 21703	MG645844	MG645890	MG645934	DRC: South Kivu Province, Mwana village
Rhampholeon sp. 3	UTEP 21707	MG645851	MG645897	MG645941	DRC: South Kivu Province, Mabwe village
Rhampholeon sp. 3	MTSN 7123	MG645827	MG645873	MG645917	Rwanda: Nyungwe National Park, Cyamudongo Forest
Rhampholeon sp. 3	UTEP 21708	MG645835	MG645881	MG645925	DRC: South Kivu Province, Tshibati village

Rhampholeon sp. 3	JMD 2014-53	MG645857	MG645903	MG645945	Rwanda: Nyungwe National Park, Kamiranzovu Swamp
Rhampholeon sp. 3	JMD 2014-101	MG645858	MG645904	–	Rwanda: Nyungwe National Park, Kamiranzovu Swamp
Rhampholeon sp. 3	ZFMK 55104	AM055645	–	–	Rwanda: Nyungwe National Park, Cyamudongo Forest
Rhampholeon sp. 4	UTEP 21709	MG645818	MG645864	MG645910	Burundi: Bubanza District, Kibira National Park
Rhampholeon sp. 4	MTSN 7213	MG645828	MG645874	MG645918	Rwanda: Nyungwe National Park, Mount Bigugu
Rhampholeon sp. 5	UTEP 21711	MG645814	MG645860	MG645906	Burundi: Bururi District, Bururi Forest Nature Reserve
Rhampholeon sp. 5	UTEP 21710	MG645815	MG645861	MG645907	Burundi: Bururi District, Bururi Forest Nature Reserve
Rhampholeon sp. 5	UTEP 21712	MG645816	MG645862	MG645908	Burundi: Bururi District, Bururi Forest Nature Reserve
Rhampholeon sp. 5	UTEP 21713	MG645817	MG645863	MG645909	Burundi: Bururi District, Bururi Forest Nature Reserve
Rhampholeon sp. 5	UTEP 21714	MG645822	MG645868	MG645914	Uganda: Kasese District, Rwenzori Mountains National Park, near Nyakalengisa entrance
Rhampholeon sp. 5	PEM-R 16518	MG645823	MG645869	–	Uganda: Kasese District, Rwenzori Mountains National Park
Rhampholeon sp. 5	UTEP 21390	MG645821	MG645867	MG645913	Uganda: Kasese District, Rwenzori Mountains National Park, near Nyakalengisa entrance

Rhampholeon sp. Itombwe	UTEP 21715	KM589410	KM589405	KM589416	DRC: South Kivu Province, Bichaka village, Itombwe Plateau
Rhampholeon sp. Itombwe	UTEP 21716	MG645841	MG645887	MG645931	DRC: South Kivu Province, Bichaka village, Itombwe Plateau
Rhampholeon sp. Itombwe	UTEP 21717	MG645842	MG645888	MG645932	DRC: South Kivu Province, Bichaka village, Itombwe Plateau
Rhampholeon sp. Itombwe	UTEP 21718	KM589411	KM589406	KM589417	DRC: South Kivu Province, Bichaka village, Itombwe Plateau
Rhampholeon acuminatus (T)	CT 153	HF570459	–	–	Tanzania: Nguru Mountains
Rhampholeon bruessoworum (T)	PEM-R 20374	HG798975	HG798989	HG798999	Mozambique: Mount Inago
Rhampholeon bruessoworum (T)	PEM-R 20375	HG798976	HG798990	HG799000	Mozambique: Mount Inago
Rhampholeon chapmanorum (T)	PEM-R 16245	AY524881	AY524919	AY524956	Malawi: Malawi Hill
Rhampholeon gorongosae (T)	PEM-R 16252	AY524873	AY524911	AY524949	Mozambique: Mount Gorongosa
Rhampholeon gorongosae (T)	PEM-R 16253	AY524874	AY524912	AY524950	Mozambique: Mount Gorongosa
Rhampholeon hattinghi (P)	PEM-R 19196	KM589414	KM589408	–	DRC: Katanga Province, Mount Nzawa
Rhampholeon hattinghi (P)	PEM-R 19197	KM589415	KM589409	–	DRC: Katanga Province, Mount Nzawa

Rhampholeon maspictus (T)	PEM-R 17911	HG798971	HG798984	HG798997	Mozambique: Mount Mabu
Rhampholeon maspictus (T)	PEM-R 17912	HG798972	HG798985	HG798998	Mozambique: Mount Mabu
Rhampholeon marshalli	PEM-R 16243	AY524870	AY524908	AY524946	Zimbabwe: Vumba Mountains
Rhampholeon marshalli	PEM-R 16244	AY524871	AY524909	AY524947	Zimbabwe: Vumba Mountains
Rhampholeon moyeri (P)	MTSN 001TA	AY524876	AY524914	AY524952	Tanzania: Udzungwa Mountains
Rhampholeon moyeri (P)	MTSN 002TA	–	AY524913	AY524951	Tanzania: Udzungwa Mountains
Rhampholeon nchisiensis (T)	PEM-R 16242	AY524883	AY524921	AY524958	Malawi: Nchisi Mountain
Rhampholeon nchisiensis	PEM-R 16249	AY524886	AY524924	AY524961	Zambia: Nyika Plateau
Rhampholeon nebulauctor (P)	PEM-R 17280	HG798973	HG798987	–	Mozambique: Mount Chiperone
Rhampholeon nebulauctor (A)	PEM-R 17281	HG798974	HG798988	–	Mozambique: Mount Chiperone
Rhampholeon platyceps (T)	PEM-R 16250	AY524880	AY524918	AY524955	Malawi: Mount Mlanje
Rhampholeon platyceps (T)	PEM-R 16251	AY524879	AY524917	AY524954	Malawi: Mount Mlanje

Rhampholeon spectrum	CAS 207682	AY524864	AY524901	AY524939	Equatorial Guinea: Bioko Island
Rhampholeon spectrum	CAS 207683	AY524863	AY524900	AY524938	Equatorial Guinea: Bioko Island
Rhampholeon spinosus	CT 118	HF570460	HF570510	HF570779	Tanzania: West Usambara Mountains
Rhampholeon temporalis (T)	PEM-R 16254	AY524866	AY524904	AY524942	Tanzania: East Usambara Mountains
Rhampholeon temporalis (T)	PEM-R 16255	AY524867	AY524905	AY524943	Tanzania: East Usambara Mountains
Rhampholeon tilburyi (T)	PEM-R 17134	EF114322	EF114330	EF114338	Mozambique: Namuli Massif
Rhampholeon tilburyi (T)	PEM-R 17135	EF114323	EF114331	EF114339	Mozambique: Namuli Massif
Rhampholeon uluguruensis (T)	ZMB 48421	AY524896	AY524934	–	Tanzania: Uluguru Mountains
Rhampholeon uluguruensis (T)	ZMB 48431	AY524897	AY524935	–	Tanzania: Uluguru Mountains
Rhampholeon viridis	CT 204	HF570461	HF570511	HF570780	Tanzania: North Pare Mountains
Rhampholeon viridis (T)	PEM-R 16259	AY524869	AY524907	AY524945	Tanzania: South Pare Mountains
Rhampholeon viridis (T)	PEM-R 16260	AY524868	AY524906	AY524944	Tanzania: South Pare Mountains

Rieppeleon brachyurus	PEM-R 16263	AY524898	AY524936	AY524968	Tanzania: Near Tamota
Rieppeleon brachyurus	PEM-R 16264	AY524899	AY524937	AY524969	Tanzania: Near Tamota
Rieppeleon brevicaudatus (T)	PEM-R 16256	AY524887	AY524925	AY524962	Tanzania: East Usambara Mountains
Rieppeleon brevicaudatus (T)	PEM-R 16257	AY524888	AY524926	AY524963	Tanzania: East Usambara Mountains
Rieppeleon kerstenii	CAS 169939	AY524890	AY524928	AY524965	Kenya: Kilifi
Rieppeleon kerstenii	N/A	AY524892	AY524930	AY524967	N/A

2.3.2 Gene trees and species trees

We interpreted chromatograph data using the program SeqMan Pro (Swindell and Plasterer, 1997) and made alignments for each gene using MUSCLE v. 3.6 (Edgar, 2004) in the program Mesquite v. 3.04 (Maddison and Maddison, 2015). We conservatively trimmed sequences and made other minor manual adjustments in the program MacClade v. 4.08 (Maddison and Maddison, 2005). We used PHASE v. 2.1.1 (Stephens and Donnelly, 2003) in the program DnaSP v. 5.1 (Librado and Rozas, 2009) to phase haplotypes for the nuclear fragment (RAG1). We transformed alignments using SeqPHASE (Flot, 2010) and excluded haplotypes with probabilities lower than 0.7 (Harrigan et al., 2008). In addition, we note that most double peaks in the nuclear marker were remedied in SeqMan Pro because one allele exhibited a much stronger signal than the other did (i.e., unequal heights) (Fontaneto et al., 2015). Phased RAG1 sequences were used for all species-delimitation analyses (see below).

Phylogenetic analyses were initially conducted on mitochondrial and nuclear data sets that revealed similar topologies, and thus we used the concatenated data set for all analyses. Maximum likelihood (ML) analyses were conducted with the GTRGAMMA model in RAxML v. 8.2.2 (Stamatakis, 2006, 2014). All parameters were estimated and a random starting tree was used. Support values for clades inferred by ML analyses were assessed with the rapid bootstrap algorithm with 1,000 replicates (Stamatakis et al., 2008). Bayesian inference (BI) analyses were conducted in MrBayes v. 3.2.2 (Huelsenbeck and Ronquist, 2001; Ronquist and Huelsenbeck, 2003). Our model included seven data partitions, including a single partition for 16S and three independent partitions for each codon position for the protein-coding genes ND2 and RAG1. Concatenated data sets were partitioned identically for ML and BI analyses and were run on the CIPRES Science Gateway v. 3.3 (http://www.phylo.org/). The Akaike Information Criterion

(AIC) and greedy search algorithm in PartitionFinder v. 1.1 (Lanfear et al., 2012) were used to establish the best model of evolution for each marker. The selected models of evolution were used for all BI analyses, but in cases where the model selected in PartitionFinder was not available in MrBayes, we set the number of rate categories and other parameters to match the best model. Bayesian analyses were conducted with random starting trees, run for 20 million generations, and Markov chains were sampled every 1,000 generations. To verify that multiple runs converged, AWTY (Nylander et al., 2008) was used. Burn-in was set at 25%, and thus the initial 5,000 trees were discarded. Phylogenies were visualized using FigTree v. 1.3.1 (Rambaut and Drummond, 2009). Bayesian posterior probabilities ≥ 0.95 (Alfaro et al., 2003; Hillis and Bull, 1993) and bootstrap values $\geq 70\%$ (Felsenstein, 1981, 1985) were considered as strong support. Net sequence divergences (uncorrected *p*-distances) between *Rhampholeon* lineages for each marker were estimated using MEGA v. 7.0 (Kumar et al., 2016).

When inferring species limits from multilocus data, two issues are widely recognized: the underlying species tree can be different from individual gene trees (Maddison, 1997) and that simply increasing the number of loci does not necessarily improve the delimitation of species (Degnan and Rosenberg, 2009). To account for these uncertainties, we implemented a comparative coalescent framework to estimate species trees for the AR *Rhampholeon* clade and we conservatively interpreted species across four separate species-tree approaches. For approach 1, we used the Bayesian *BEAST (Heled and Drummond, 2010) in the program BEAST v. 1.8.4 (Drummond et al., 2012) to estimate a species tree for the focal taxa. *BEAST necessitates the prior assignment of individuals to presumed species, so we based our initial species assignments on reciprocally monophyletic clades recovered in the concatenated gene-tree analyses. As additional evidence for species assignments, we compared uncorrected *p*-distances of the ND2

locus among these clades to described species of *Rhampholeon*. Models of sequence evolution were chosen using the AIC in PartitionFinder. We specified unlinked site, clock, and tree models, and implemented a Yule process tree prior as this analysis investigates interspecific relationships. We estimated species trees with five concurrent runs of 200 million generations that totaled 2 billion generations sampled every 20,000 generations. Each run produced 10,000 trees and all runs were combined using LogCombiner (Drummond et al., 2012) for a total of 50,000 trees. We discarded the initial 10% of trees as burn-in with the program TreeAnnotator (Drummond et al., 2012), and used the program Tracer v. 1.5 (Rambaut and Drummond, 2007) to asses Effective Sample Size (ESS) values, which were > 200 for all parameters. For approach 2, we used the maximum pseudo-likelihood function in the program MP-EST (Liu et al., 2010) on the web-server STRAW (Shaw et al., 2013) to estimate a species tree from our collection of three ML gene trees (16S, ND2, RAG1). Individual gene trees were generated with RAxML under the GTRGAMMA model with 1,000 rapid bootstrap inferences on each genetic data set with three *Rieppeleon* species as the outgroup. The pseudo-likelihood function is derived from coalescent theory, assumes no gene flow, and can be validated with bootstrap support (Liu et al., 2010). For approach 3, we used the Bayesian program bPTP (Zhang et al., 2013) on the web-server (http://species.h-its.org/) to estimate a species tree using our ML tree of the concatenated data. The MCMC analysis was run for 500,000 generations with thinning set to 100 and burn in at 10%. We used a rooted tree and did not exclude the *Rieppeleon* outgroup. Species representation was examined using trace plots to check for convergence of the maximum likelihood's value of each node. For approach 4, we used the coalescent model GMYC (Fujisawa and Barraclough, 2013; Pons et al., 2006) on the web-server (http://species.h-its.org/gmyc/) to estimate a species tree for the focal taxa using both single

and multi-threshold models for the dated phylogeny based on the concatenated data set obtained in BEAST (see below).

2.3.3 Divergence dating

We estimated divergence times for the comprehensive *Rhampholeon* phylogeny using a fossil-calibrated Bayesian approach in the program BEAST v. 1.8.4 (Drummond et al., 2012) run on the CIPRES Science Gateway. We implemented an uncorrelated log-normal relaxed clock model with an estimated clock rate to allow for rate heterogeneity among lineages (Drummond et al., 2006). We estimated tree shape under the Yule prior (pure birth) on our multilocus data set because this prior is best suited for phylogenies describing the relationships between different species and assumes a constant speciation rate. In order to maximize calibration points, and because inadequate outgroup selections can produce misleading dating estimates (Sauquet, 2013), we included at least three species per chameleon genus (when available on GenBank) to provide a robust representation of Chamaeleonidae in these dating analyses. Furthermore, to utilize as many fossil calibrations as possible, we included several major representatives of the superorder Lepidosauria totaling 22 squamate taxa plus *Sphenodon punctatus* (see supplemental information [Table S1] in Hughes et al. [2018a]). In some cases, chimeric sequences were constructed using more than one species from the same genus for these more distantly related groups (Pyron et al., 2013). We enforced monophyly for six chameleon genera based on the relationships recovered in the family level phylogeny of Tolley et al. (2013) (i.e., *Calumma* + *Furcifer*; *Bradypodion* + *Nadzikambia*; *Trioceros* + *Kinyongia*), because initial runs produced topologies inconsistent with interspecific relationships among chameleon genera, most likely due to incomplete taxon sampling at the family level in our phylogeny. Fossil calibrations were placed on nine nodes that correspond

to some of the oldest known fossils of Lepidosauria (Table 2.2). Secondary calibrations were placed on five nodes to achieve temporal congruence with the most comprehensive time-calibrated chameleon phylogeny published to date—dating analyses that were based on 12 genetic markers and included over 90% of all named chameleon species (Tolley et al., 2013). For each calibration, we used a translated log-normal distribution, with an offset equal to the age of the fossil or node split. The treatment of date estimates from independent molecular analyses as point calibrations without consideration of associated error can increase the probability of type I errors (Ho and Phillips, 2009). We attempted to mitigate this potential pitfall by accounting for calibration uncertainty in our use of dates from Tolley et al. (2013) and including multiple primary calibrations rather than relying on a single point calibration (Graur and Martin, 2004). We estimated phylogenetic relationships from five concurrent runs of 100 million generations each and we sampled trees every 5,000 generations. We used the program LogCombiner to combine the trees produced from the five runs, which resulted in 100,000 trees. We discarded 10% of the trees (10,000 trees) as burn-in and summarized parameter values from the posterior probabilities on the maximum clade credibility tree with the program TreeAnnotator. The program Tracer was used to confirm stationarity and adequate ESS of the posterior probabilities (> 200 for each estimated parameter). Bayesian posterior probabilities ≥ 95% were considered as strong support.

Table 2.2 Divergence-date priors for primary (top) and secondary (bottom) calibrations. Node numbers correspond to those indicated in Fig. 2.5. The translated log-normal (TL) zero-offset is presented in millions of years ago (Mya), parameter values (mean and standard deviation) follow in parentheses, and posterior (calculated) ages are presented as median with 95% confidence interval in parentheses.

Primary Calibrations			
Node	TL zero-offset (mean, SD)	Median (95% CI)	Source
1	238 (1.4, 0.7)	242 (239.4–249.6)	Fossil rhynchocephalian from Middle Triassic (Jones et al., 2013)
2	161 (1.8, 1.0)	167 (162.2–192.3)	Stem scincomorph *Balnealacerta* from Middle Jurassic (Evans, 1998)
3	110 (1.8, 1.3)	116 (110.7–161.3)	Stem teiids from Early Cretaceous (Nydam and Cifelli, 2002; Winkler et al., 1990)
4	61 (1.6, 0.8)	66.1 (62.4–80)	Fossil amphisbaenian *Plesiorhineura tsentasi* from Middle Paleocene (Sullivan, 1985)
5	128 (1.0, 0.5)	130.7 (129.2–134.2)	Fossil lizard *Dalinghosaurus longidigitus* from Early Cretaceous (Evans and Wang, 2005)
6	70 (1.8, 1.0)	76.1 (71.2–101.3)	Fossil anguid *Odaxosaurus* from Late Cretaceous (Sullivan and Lucas, 1996)
7	70 (1.8, 1.0)	76.1 (71.2–101.3)	Stem acrodont iguanian clade Priscagaminae from Late Cretaceous (Keqin and Norell, 2000)
8	70 (1.2, 1.9)	73.3 (70.2–145.6)	Fossil pleurodont iguanian *Saichangurvel* from Late Cretaceous (Conrad and Norell, 2007)
9	99 (1.0, 0.5)	101.7 (100.2–105.2)	Stem chameleon from Albian-Cenomanian boundary, Cretaceous (Daza et al., 2016)
Secondary Calibrations			
Node	TL zero-offset (mean, SD)	Median (95% CI)	Source
10	62.8 (1.0, 0.5)	64.8 (63.3–68.3)	Node 1 by codon in Table S4 (Tolley et al., 2013)
11	51.2 (1.0, 0.5)	53.9 (52.4–57.4)	Node 2 by codon in Table S4 (Tolley et al., 2013)

12	47.5 (1.0, 0.5)	50.2 (48.7–53.7)	Node 3 by codon in Table S4 (Tolley et al., 2013)
13	45.6 (1.0, 0.5)	48.3 (46.8–51.8)	Node 4 by codon in Table S4 (Tolley et al., 2013)
14	33.4 (1.0, 0.5)	36.1 (34.6–39.6)	Node 5 by codon in Table S4 (Tolley et al., 2013)

2.4 Results

2.4.1 Sampling, sequencing, and evolutionary models

We generated 138 new sequences of three genetic markers for a multilocus data set consisting of 2045 bp per sample (16S: 450 bp; ND2: 690 bp; RAG1: 905 bp). There were no gaps in the alignments of any of the three loci after we conservatively omitted a hypervariable region consisting of 16 bp from the 16S ribosomal gene. The most appropriate substitution models estimated for each locus were GTR+G for 16S; GTR+G for ND2 1st codon position, HKY+G for ND2 2nd codon position, TrN+G for ND2 3rd codon position; and HKY+G for RAG1 1st and 2nd codon positions, K80 for RAG1 3rd codon position.

2.4.2 Gene trees and genetic distances

Phylogenetic relationships among *Rhampholeon* species, reconstructed from the concatenated data set, were similar and with comparable node support using BI and ML methods (Fig. 2.1). Six distinct clades representing *R. boulengeri* were recovered (Fig. 2.2). The recently described species *R. hattinghi*, endemic to Mount Nzawa in the southern AR, was recovered with strong support as sister to the *R. boulengeri* clade. A population of *R.* cf. *boulengeri*, collected from high-elevation forests of the Itombwe Plateau in eastern DRC (*R.* sp. Itombwe), formed a distinct clade that was weakly supported as sister to *R.* sp. 3. *Rhampholeon* sp. 1 contained samples from populations occupying mid to high-elevation forests in eastern DRC, southwestern Uganda, and the Yala Nature Reserve near Kakamega Forest Reserve in western Kenya. *Rhampholeon* sp. 1 was recovered as sister to *R.* sp. 2 (with strong support in BI analyses), which comprised widely distributed populations from low and mid-elevation forests in eastern DRC and western Uganda (Figs. 2.2–2.4). *Rhampholeon* sp. 3 contained populations from mostly mid-elevation forests of

the Itombwe Plateau and some high-elevation forests around the southern and western sides of Lake Kivu, including Nyungwe National Park in Rwanda and Kahuzi-Biega National Park in DRC (Figs. 2.2–2.4). *Rhampholeon* sp. 4 contained two samples collected from high-elevation forests of the Rugege Highlands, including Mount Bigugu of Nyungwe National Park and Mpishi village near Kibira National Park in Burundi, and was found to be closely related to *R.* sp. 5, which contained populations from high-elevation forests of Bururi Forest Reserve in southern Burundi and Rwenzori Mountains National Park in western Uganda (Figs. 2.2–2.4).

Pairwise sequence divergences (uncorrected p-distances) between the undescribed lineages were generally high and comparable to currently recognized *Rhampholeon* species (see supplemental information [Table S2] in Hughes et al. [2018a]). For the ND2 locus, p-distances ranged from 4.8–6.4% between *R.* sp. 1 and *R.* sp. 2; 6.2–7.3% between *R.* sp. 2 and *R.* sp. 3; 4.1–6.6% between *R.* sp. 3 and *R.* sp. 4; and 5.8–7.4% between *R.* sp. 4 and *R.* sp. 5. Moreover, *p*-distance ranges for this locus between undescribed clades and *R.* sp. Itombwe from the Itombwe Plateau were also relatively high: 4.2–5.9% for *R.* sp. 1; 5.9–6.2% for *R.* sp. 2; 3.2–4.4% for *R.* sp. 3; 5.1–5.2% for *R.* sp. 4; and 5.1–6.4% for *R.* sp. 5 (Fig. 2.2). Lastly, intraspecific *p*-distances among these species were comparatively low.

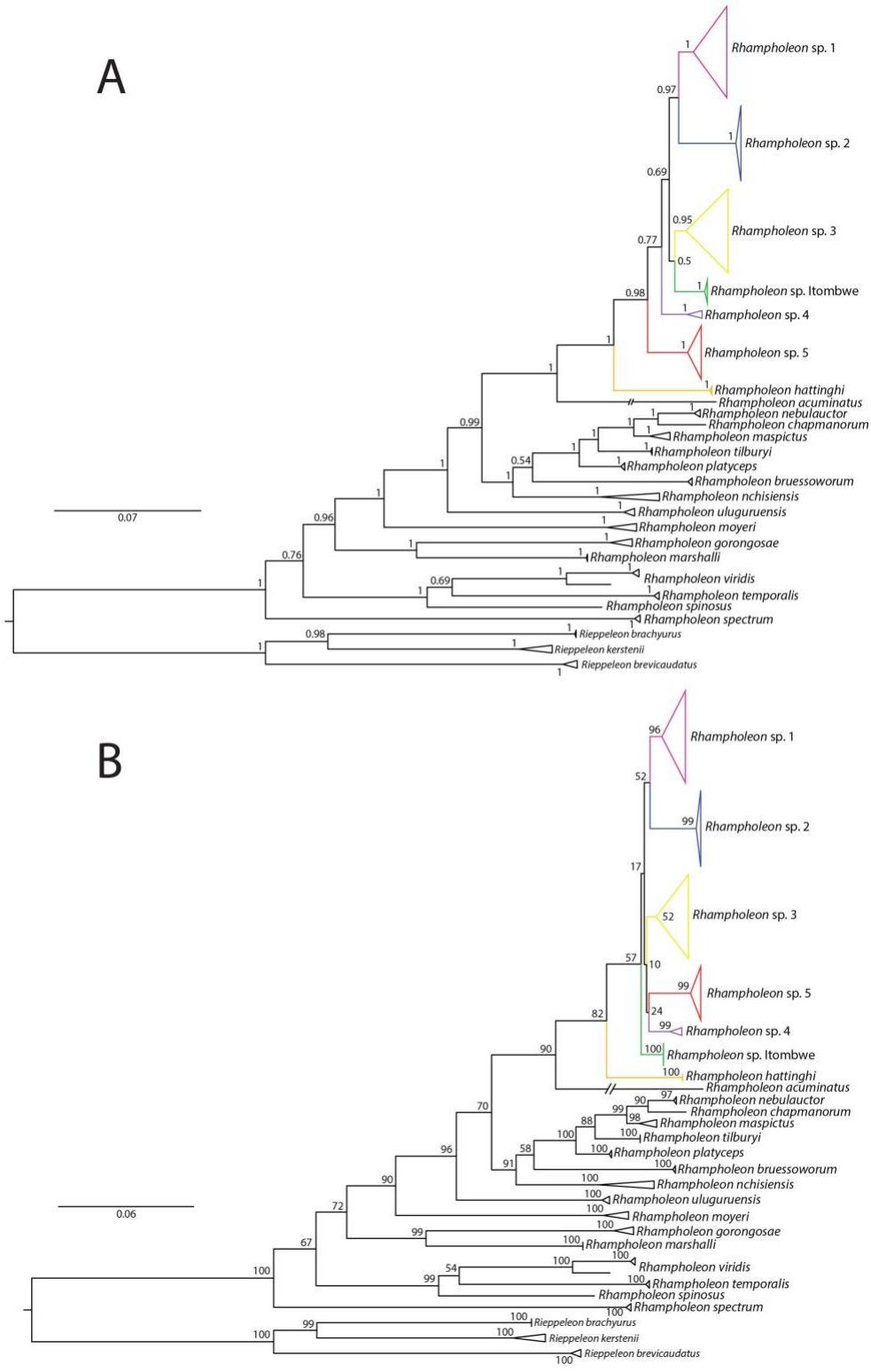

Figure 2.1 Bayesian (A) and maximum likelihood (B) phylogenies of the genus *Rhampholeon* with support values adjacent to nodes.

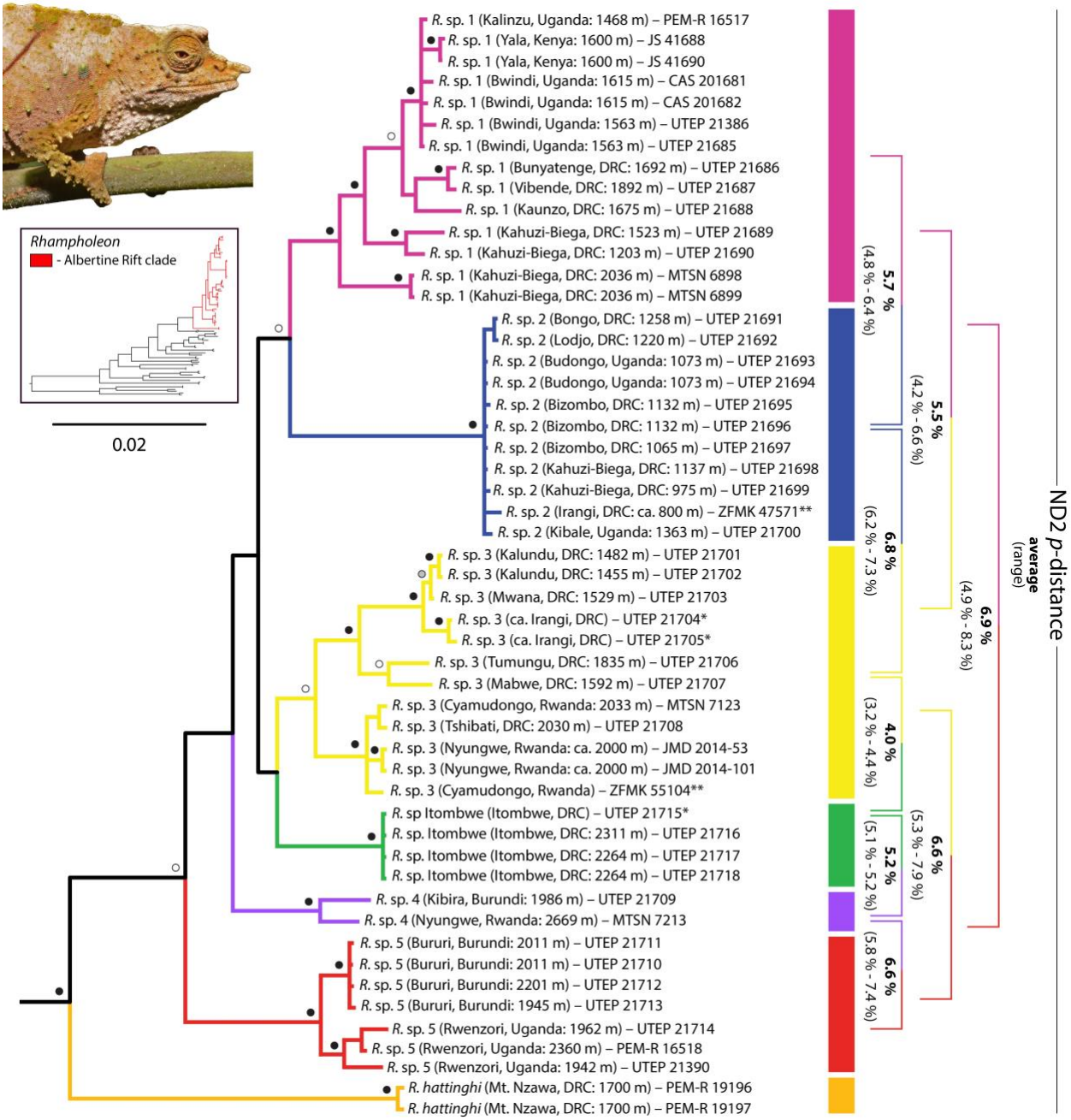

Figure 2.2 Bayesian phylogeny of pygmy chameleon species (genus *Rhampholeon*) from the Albertine Rift, Central Africa, and western Kenya. Color-coded rectangles correspond to the Albertine Rift/western Kenya species as follows (from top of phylogeny down): pink – *R* sp. 1; blue – *R*. sp. 2; yellow – *R*. sp. 3; green – *R. boulengeri*; purple – *R*. sp. 4; red – *R*. sp. 5; orange – *R. hattinghi*. This color scheme is retained throughout all figures. Uncorrected *p*-distances for the ND2 marker are given as a range for selected species on the right. Nodes supported by both ML (≥ 70% bootstrap) and BI (≥ 0.95 posterior probabilities) are denoted with black circles, nodes supported by BI only are denoted with white circles, and nodes supported by ML only are denoted with grey circles. * = specific locality not available. ** = only 16S data were available.

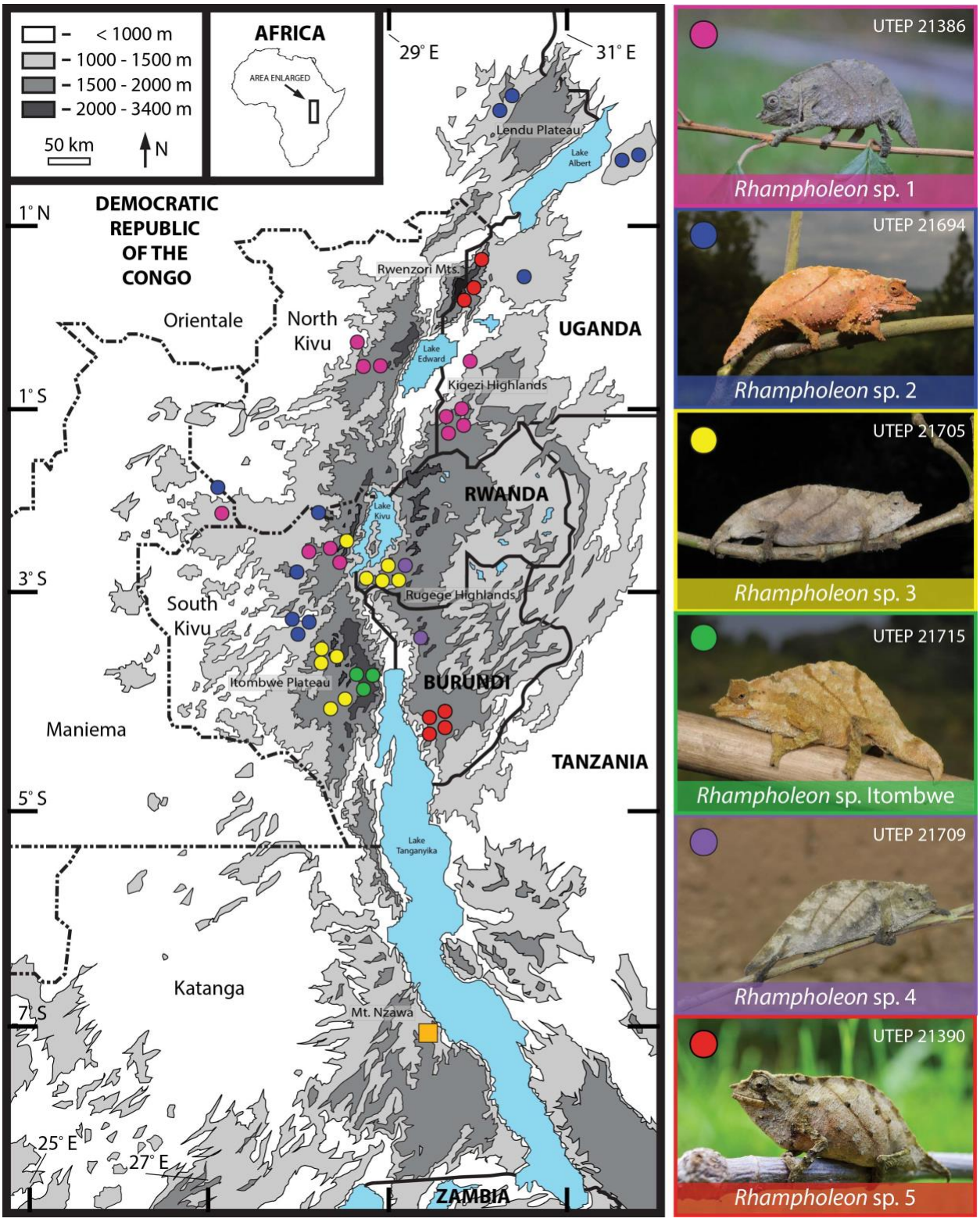

Figure 2.3 Elevation map of the Albertine Rift, Central Africa showing sampling localities of pygmy chameleons (genus *Rhampholeon*) used in this study. Two samples from western Kenya are not shown. Photographs of representative individuals for the new species are displayed on the right. Orange square represents the species *R. hattinghi*.

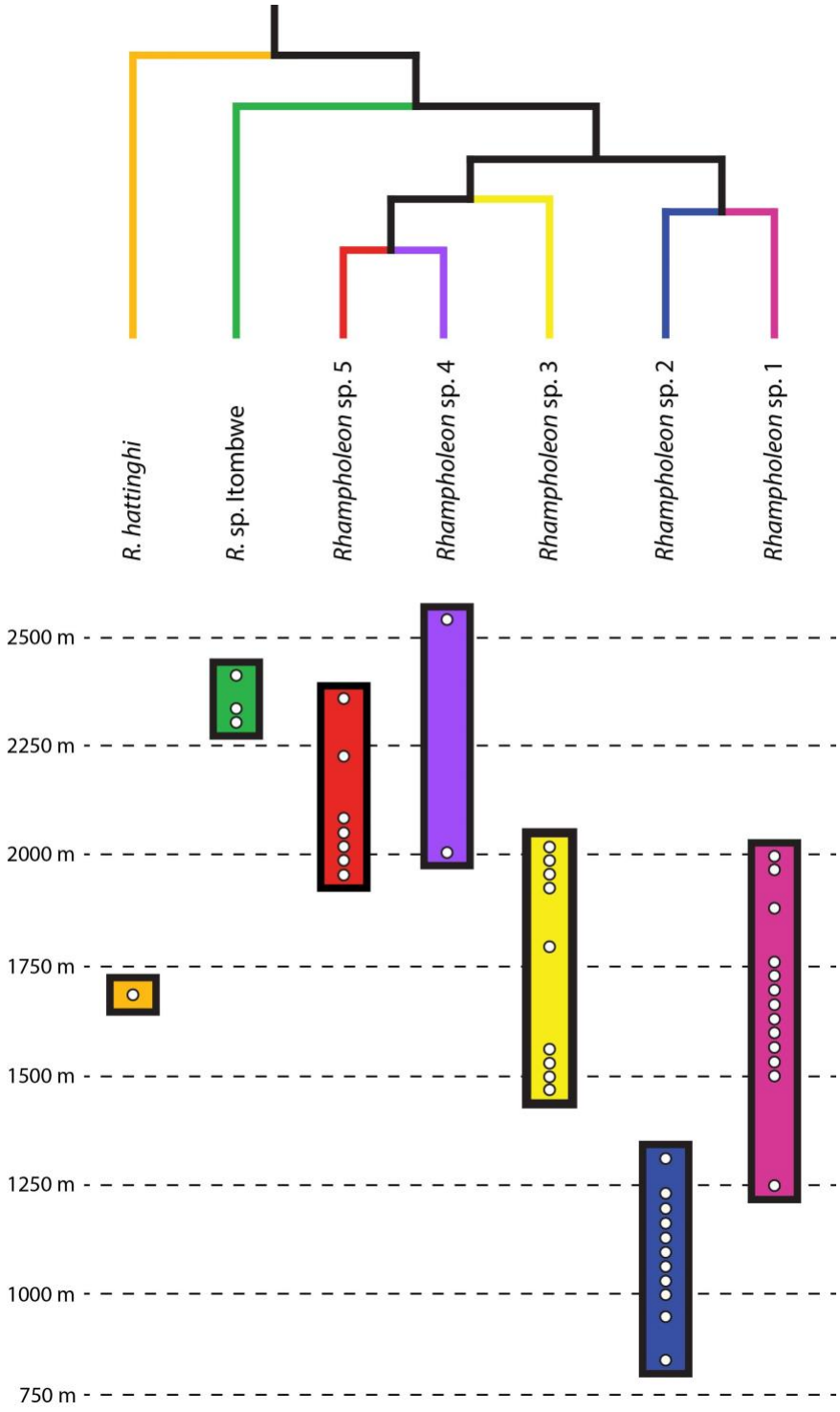

Figure 2.4 Elevational zonation of seven pygmy chameleon species (genus *Rhampholeon*) from the Albertine Rift, Central Africa, and western Kenya. The upper and lower known elevational limits of species distributions are indicated by colored rectangles. White circles within the colored rectangles represent samples used in the phylogenetic analyses. The topology is based on the complete phylogeny in Fig. 2.6.

2.4.3 Divergence dating

Results from the calibrated dating analyses indicate that the genus *Rhampholeon* diverged from other chameleons in the early Eocene at 53.59 Mya (51.92–56.19 Mya, 95% highest posterior densities [HPD]), and initial branching within the genus occurred in the mid-Eocene at 44.99 Mya (39.29–50.44 Mya, HPD) (Fig. 2.5). The majority of species-level diversification occurred in the Miocene, although several lineages arose earlier (Eocene and Oligocene), and a few originated in the Pliocene. The only West African species, *R. spectrum*, diverged in the early Eocene at 41.31 Mya (33.56–47.33 Mya, HPD) from its sister clade, which includes species from the Eastern Arc Mountains of Tanzania. The most southerly species, *R. gorongosae* and *R. marshalli*, also diverged in the Eocene from a sister clade containing primarily East African species. The AR clade diverged in the mid-Miocene at 18.06 Mya (12.59–23.27 Mya, HPD) from its closest relative, *R. acuminatus* from the Nguru Mountains in eastern Tanzania. The earliest divergence of AR *Rhampholeon* (i.e., split between *R. hattinghi* and the *R. boulengeri* clade) occurred in the late Miocene at 11.14 Mya (7.68–14.68 Mya, HPD) (Fig. 2.6). The divergence of *R.* sp. Itombwe from the other five *R.* cf. *boulengeri* species (*R.* sp. 1, *R.* sp. 2, *R.* sp. 3, *R.* sp. 4, and *R.* sp. 5) was dated in the late Miocene around 7.16 Mya (5.34–9.01 Mya, HPD). The initial divergence within the remaining *R. boulengeri* clade was estimated in the late Miocene at 6.25 Mya (4.78–7.72 Mya, HPD), with most of the species-level divergence at the Miocene–Pliocene boundary around 4–5 Mya (Fig. 2.6). For example, estimated splits between *R.* sp. 1 and *R.* sp. 2 occurred at 5.33 Mya (3.84–6.81 Mya, HPD); *R.* sp. 3 was estimated to have diverged from the clade containing *R.* sp. 4 and *R.* sp. 5 at 5.74 Mya (4.27–7.08 Mya, HPD); and the divergence between *R.* sp. 4 and *R.* sp. 5 was estimated to have occurred at 5.54 Mya (3.69–6.61 Mya, HPD).

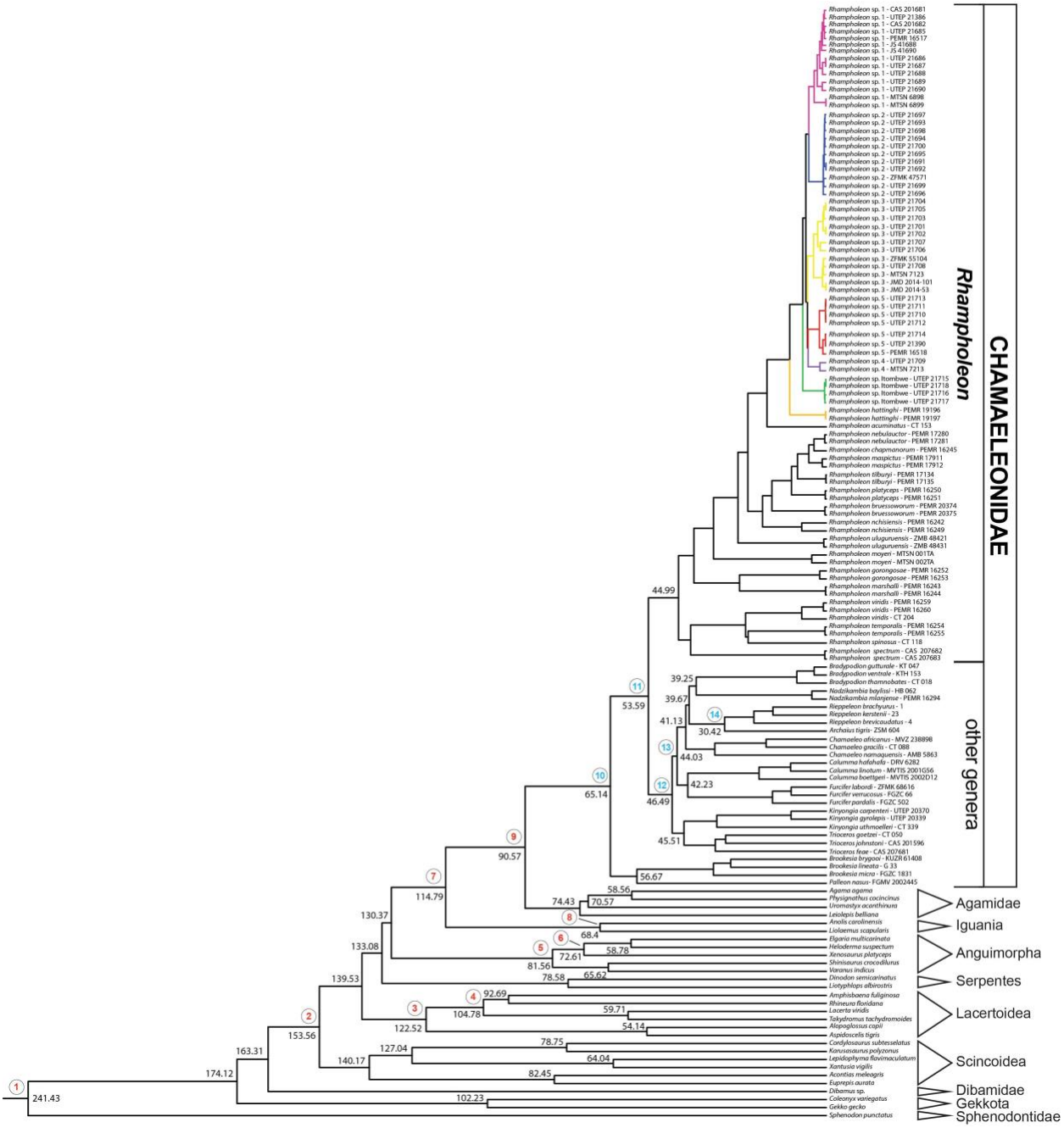

Figure 2.5 Entire Bayesian chronogram of Chamaeleonidae and outgroup. Numbers near nodes denote mean highest posterior densities (HPD). Fossil-calibrated nodes are indicated with encircled red numbers and secondary calibrated nodes with encircled light blue numbers. Diversification dates within the genus *Rhampholeon* are presented in Fig. 2.6.

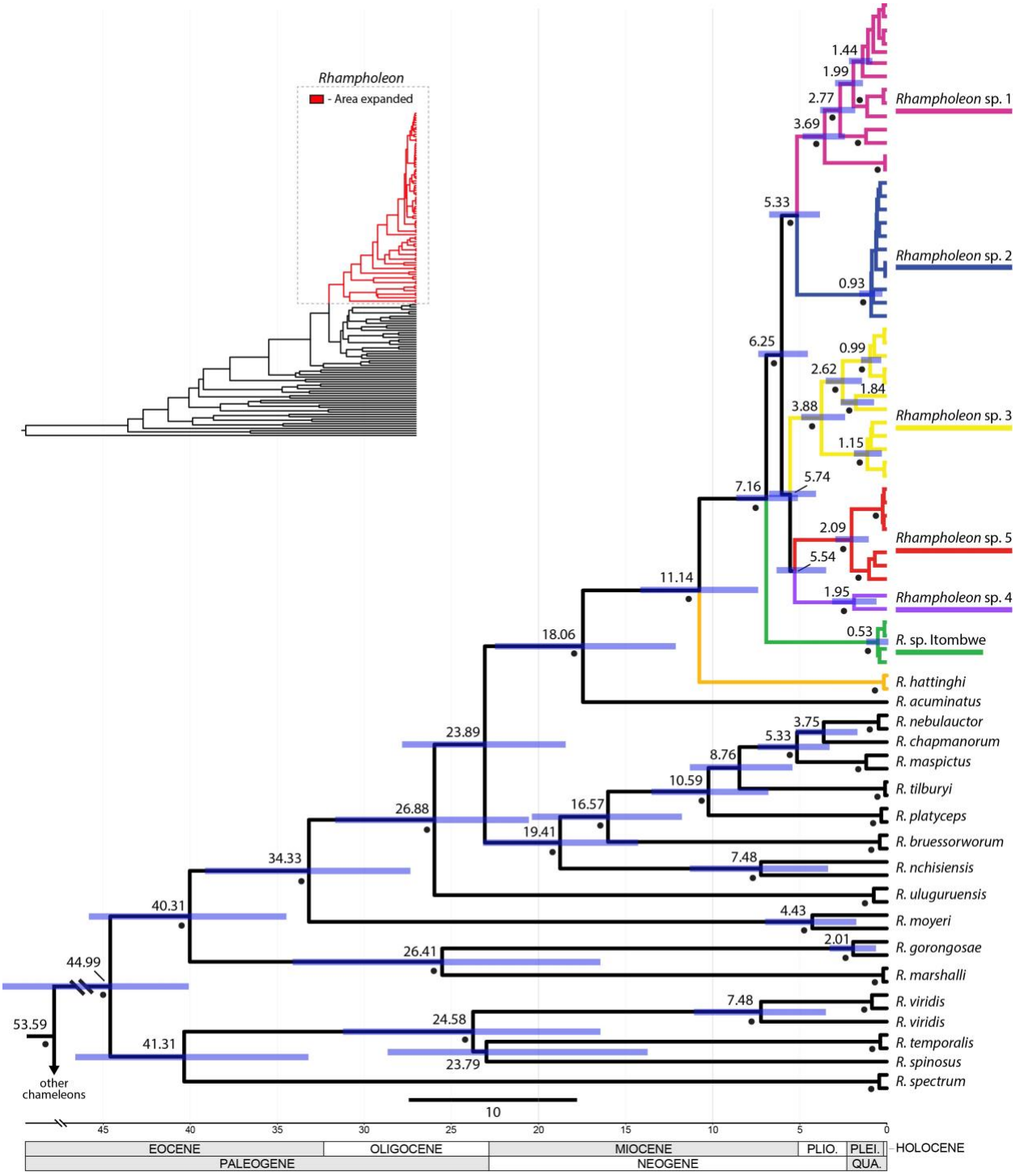

Figure 2.6 Bayesian chronogram of the pygmy chameleon genus *Rhampholeon*. Posterior probabilities ≥ 95% are denoted by filled circles adjacent to nodes. Numbers near nodes denote mean highest posterior densities (HPD) and blue bars at nodes represent 95% HPD.

2.4.4 Species delimitation

The four species-tree analyses recovered similar clade topology and node support values to our concatenated gene-tree analyses. The nodes representing *R. hattinghi* and *R.* sp. Itombwe were generally well-supported across analyses (Fig. 2.7). Similarly, node support values for *R.* sp. 2 were high in the species trees derived from MP-EST and bPTP, yet weaker support for this species was found in the *BEAST species tree. The results from GMYC and bPTP differed from *BEAST and MP-EST in that additional species were delimited beyond the five cryptic species recognized in the gene-tree analyses of the *R. boulengeri* clade. For example, GMYC recovered four additional species and bPTP six additional species, whereas MP-EST and *BEAST both recovered the more conservative estimate of five species (Fig. 2.7). Evaluating the congruent evidence of these four coalescent-based species-tree inferences leads us to recognize five cryptic species within the *R. boulengeri* clade.

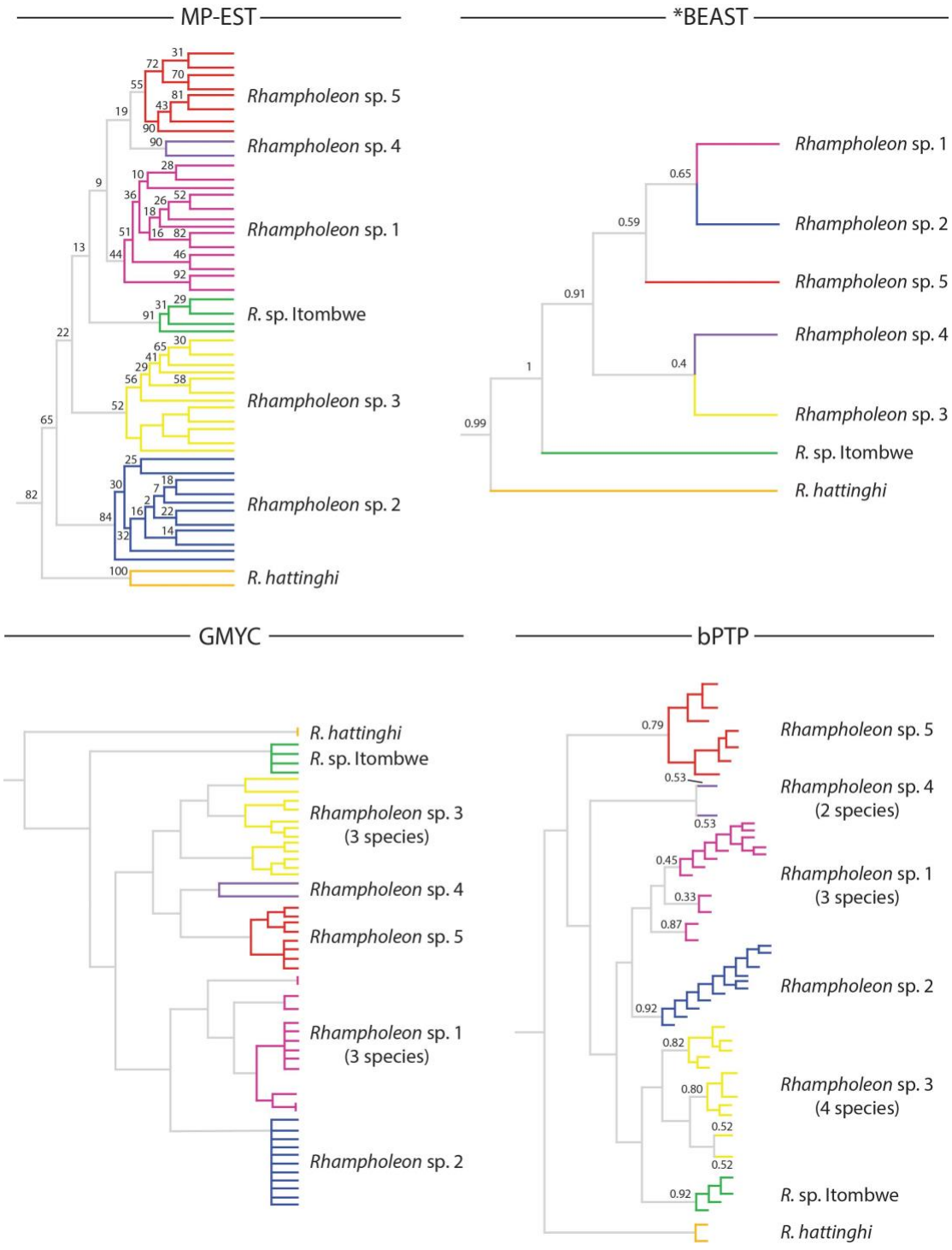

Figure 2.7 Comparative species-tree estimations for seven pygmy chameleon species (genus *Rhampholeon*) from the Albertine Rift, Central Africa, and western Kenya. Numbers above nodes denote posterior probabilities for the Bayesian analyses *BEAST and bPTP, and bootstrap values for MP-EST.

2.5 Discussion

2.5.1 Molecular systematics and species delimitation

While our phylogenetic analyses are consistent with the evolutionary relationships across the genus *Rhampholeon* recovered in previous studies (Branch et al., 2014; Fisseha et al., 2013; Matthee et al., 2004; Mariaux and Tilbury 2006; Tilbury and Tolley, 2015; Tolley et al., 2013), the additional populations sampled from diverse forest environments of the Albertine Rift (AR) represent five previously unrecognized species. All of the AR species were recovered in the same clade, and importantly, none of the new species were conspecific with described *Rhampholeon* from the AR (i.e., *R. hattinghi*). We found three pygmy chameleon species associated with the Itombwe Plateau, which is likely to be the type locality for *R. boulengeri* (see commentary in *Introduction*). Because the type specimens were not consulted, we did not assign the nominal *R. boulengeri* to any of the three lineages with populations from the Itombwe Plateau, South Kivu Province, eastern DRC. Nevertheless, one lineage (*R.* sp. Itombwe) is likely to be the bona fide *R. boulengeri*, because it is currently endemic to the plateau, but an integrative taxonomic assessment is required before names can be appropriately assigned within this clade. The recognition of widespread cryptic diversity in *R. boulengeri* was not entirely unexpected given the extensive range of this species and previous accounts that pointed to the potential for cryptic species. Indeed, a recent phylogeny by Tilbury and Tolley (2015) showed three distinct clades of *R. boulengeri* across three localities in the AR (samples UTEP 21715 (Field no. EBG 1613), UTEP 21718 (Field no. EBG 1702) from the Itombwe Plateau, eastern DRC; two samples CAS 201681–82 from Bwindi Impenetrable National Park, southwestern Uganda; and one sample PEM-R 16518 (Field no. CT 347) from Rwenzori Mountains National Park, western Uganda). The comprehensive sampling in our present study that included those samples and multiple populations across the

range of *R. boulengeri* in the AR and Kenya, allowed for much greater resolution for detecting species, and thus provided a far greater understanding of diversity in *R. boulengeri* across its geographic distribution. In particular, we can confirm the two cryptic species recovered by Tilbury and Tolley (2015) plus the recognition of at least six cryptic species currently recognized under *R. boulengeri*. The species-level phylogeographical patterns we recovered were indicative of diversification in isolation, either due to forest fragmentation (allopatric), or in some cases, elevational zonation (parapatric). Nevertheless, we found that one new species is actually widespread (*R.* sp. 1), extending from eastern DRC to western Kenya, a finding that supports the strong affinities of herpetofauna between these highlands (Bwong et al., 2009; Lötters et al., 2007; Wagner and Böhme 2007; Wagner et al., 2008). Based on our findings, we speculate that observations of *R. boulengeri* from other localities in the AR and western Kenya likely represent one of the new species, or potentially additional novel lineages (e.g., de Witte, 1965; Spawls et al., 2002; Stipala, 2014; Tilbury, 2010).

Across all four approaches to reconstruct species trees, we consistently found support for the recognition of at least six species within *R. boulengeri* sensu lato (including the nominal species). Of the four species-tree reconstruction methods, two directly estimated phylogenies based on the genetic data (*BEAST and MP-EST), and these produced a speciation scenario most similar to the gene-tree analyses. The other two methods (GMYC and bPTP) assessed tree topologies based on the gene trees generated from ML and BI analyses, and these produced inflated speciation scenarios relative to the other approaches. We considered that the additional lineages delimited by GMYC (four) and bPTP (six) to be artifacts of the model and disregarded them as over-split species. The recognition of six species within *R. boulengeri* is based on our conservative interpretation of the results across species-tree and gene-tree estimates, which has improved our

understanding of diversity in this group at a greater resolution than prior studies. These species are morphologically conservative (i.e., cryptic), and thus morphological characters reported in historical accounts on the species (e.g., Schmidt, 1919) are insufficient to delimit species boundaries in this group. The long-standing recognition of *R. boulengeri* as a single species was due to limited sampling across the geographic range of the species, lack of topotypic material in previous molecular studies, and absence of species-tree approaches to delimit species, which have been shown to accurately recover species in empirical tests (e.g., Camargo et al., 2012).

A caveat to the MP-EST results is that the branch lengths in this analysis represent coalescent units and not sequence divergences (Liu et al., 2010). It is likely that incomplete lineage sorting in the deeper branches of the gene tree led to the recovery of low support for some nodes in the species-tree produced by *BEAST (Drummond et al., 2012). Although GMYC has been demonstrated to be a useful tool for species-delimitation (e.g., Talavera et al., 2013), concerns have been raised regarding spatially induced increases in intraspecific genetic variation leading to over-splitting (Bergsten et al., 2012). It has also been demonstrated that GMYC can over-estimate the number of species when compared with other evidence commonly used in taxonomic studies (e.g., morphology) (Miralles and Vences, 2013). Incomplete lineage sorting and loci with different evolutionary rates cannot be ruled out as sources of topological incongruence across species-tree analyses (Sistrom et al., 2014; Xi et al., 2014).

Although our species-tree analyses provide a suitable scenario for speciation among lineages of *R. boulengeri*, multi-species coalescent models can be misleading, recovering high posterior probabilities at the population level rather than the species level (Sukumaran and Knowles, 2017). This can be exacerbated by improper parameter selections (Olave et al., 2014) leading to over-estimation of species delimitation (Carstens et al., 2013; Niemiller et al., 2012).

Regardless, our comparative approach to species-delimitation with a conservative interpretation leads to the same general outcome across the methods, and we are therefore confident in our overall interpretation.

Based on monophyly in phylogenetic analyses and supported by morphological characters (Klaver and Böhme, 1986; Loveridge, 1956; Matthee et al., 2004), *Rhampholeon* are divided into three sub-genera: *Rhampholeon* (*Rhampholeon*) with four species (*spectrum*, *spinosus*, *temporalis*, and *viridis*); *Rhampholeon* (*Rhinodigitum*) with 13 species (*acuminatus*, *beraduccii*, *boulengeri*, *bruessorworum*, *chapmanorum*, *hattinghi*, *maspictus*, *moyeri*, *nchisiensis*, *nebulauctor*, *platyceps*, *tilburyi*, and *uluguruensis*); and *Rhampholeon* (*Bicuspis*) with two species (*gorongosae* and *marshalli*). These sub-generic allocations have been upheld in recent taxonomic investigations of the genus (e.g., Branch et al., 2014). Although our molecular phylogenetic results support the divisions of Matthee et al. (2004), the utility of sub-generic classifications in systematics is equivocal and thus its usage has become generally uncommon in herpetological classifications (e.g., Frost and Hillis, 1990; Frost et al., 2009), with some notable exceptions (e.g., Wallach et al., 2009).

2.5.2 Historical biogeography

The estimated divergence dates we recovered for the genus *Rhampholeon* closely resembled analyses by Townsend et al. (2011) and Tolley et al. (2013), and were roughly similar to those by Matthee et al. (2004). The similarity of our dates to the independent ones of Tolley et al. (2013) was not entirely unexpected given our co-opting of some dates as secondary calibrations. Taxon sampling for *Rhampholeon* varied across these studies: Townsend et al. (2011) included five species; Matthee et al. (2004) included 12; Tolley et al. (2013) included 13; and we included

18. Our dates were also consistent with the estimates provided by Branch et al. (2014) that were derived from a general rate of evolutionary change of the ND2 marker for several Mozambican *Rhampholeon* species. The 95% HPD intervals overlapped across these studies indicating that multiple independent approaches to divergence dating converged on similar estimates for the timing of lineage diversification in *Rhampholeon*.

In contrast to other studies on East African taxa that found genetic legacies left by Quaternary climatic changes (e.g., Cox et al., 2014; Demos et al., 2014; Roy et al., 2014), there was no evidence of Pleistocene radiations in *Rhampholeon* (i.e., no support for the Pleistocene Forest Refuge Hypothesis [Mayr and O'Hara, 1986]). Rather, we found evidence that paleoendemic lineages persisted in montane forest refugia since the Eocene (i.e., support for aspects of the Evolutionary Museum Hypothesis, although in montane regions, whereas the hypothesis originally identified lowlands as refugia [Fjeldså and Lovett, 1997]). These ancient lineages were maintained in small montane forest refugia during the increasingly arid climate of the Pliocene and Pleistocene (e.g., deMenocal, 1995, 2004). Diversification dates for forest-dependent *Rhampholeon* species in our genus-level phylogeny generally overlap with those of Couvreur et al. (2008) for diversification of African tropical rainforests since the Oligocene and follow general patterns of African forest declines during the Miocene presented by Kissling et al. (2012). The high number of ancient species confined to small forest fragments suggests that *Rhampholeon* lineages did not immigrate during the early Pliocene when forest connectivity likely increased across East Africa (e.g., Maley, 1996; Zachos et al., 2001).

The estimated divergence dates recovered within *Rhampholeon* suggest an initial split around 45 Mya (± 10 Mya) (this study; Matthee et al., 2004; Tolley et al., 2013; Townsend et al., 2011). This divergence does not correspond to two spatially disparate clades, but rather, consists

of two deeply divergent clades that are generally sympatric at present. One of the major clades includes the West African *R. spectrum*, which split from an East African group (*R. spinosus*, *R. temporalis*, and *R. viridis*) around 40 Mya (± 10 Mya), generally coincident with the break-up of West/Central and East African forests (Couvreur et al., 2008). The other major *Rhampholeon* clade, which includes all the remaining species in the genus, diverged in the Eocene and has remained on the eastern side of sub-Saharan Africa. The Eastern Arc Mountains and Southern Rift Highlands harbor a particularly species-rich *Rhampholeon* clade, which first diversified in the Eocene and then underwent extensive diversification events during the Miocene, especially in the highlands of Malawi and Mozambique. The Central African clade that is restricted to high-elevation forests of the AR diverged from a common ancestor with the East African *R. acuminatus* in the Miocene around 18 Mya (± 5 Mya) (this study; Matthee et al., 2004; Tolley et al., 2013). This period correlates with some of the initial uplift (Wichura et al., 2010) and subsequent drying of East Africa's climate (Sepulchre et al., 2006), which caused the break-up of forest habitats between Central and East Africa.

We found that the Miocene epoch was an important period for diversification of East African *Rhampholeon* species. In the Miocene, the environment of the AR was experiencing dramatic changes from both climatological and geological factors, which derive from arid conditions induced by a combination of reduced atmospheric CO_2 concentrations globally (Cerling et al., 1997) and tectonic uplifts that altered climatic patterns in East Africa (Sepulchre et al., 2006). Global cooling trends that began after the late Oligocene warming heightened during the Miocene, and these drops in temperature altered precipitation patterns (Jacobs, 2004; Sepulchre et al., 2006), which increased aridity across the African continent (Böhme, 2003; Werdelin and Sanders, 2010; Wichura et al., 2015). A global cooling trend in the Miocene is evident from sedimentation records

(Pickford et al., 1993), and supported by climate-driven faunal turnovers from the fossil record of East Africa (Leakey et al., 1996) and the AR (Senut and Pickford, 1994). Rainfall vicissitudes throughout the Neogene across Central and East Africa (Pickford, 1992; Wynn, 2003) resulted in drastically transformed vegetation patterns (Cerling et al., 1997; Feakins et al., 2005), which manifested in the extensive development of savannas (Cerling, 1992; Jacobs, 2004; Jacobs et al., 1999; Meadows and Linder, 1993) and the interrelated fragmentation of forests (Couvreur et al., 2008; Kissling et al., 2012). Not only was the Miocene climate a significant influence, but tectonic activities were also drivers of major environmental change in the AR. Initial rifting of the AR began around the Oligocene–Miocene boundary (Roberts et al., 2012), and most of the geophysical rifting and volcanism in East Africa occurred during the Miocene (e.g., Wichura et al., 2010), with increased activity from 10–5 Mya around the Miocene–Pliocene boundary (Macgregor, 2015; Paul et al., 2014). These geological changes also shifted climatic patterns towards increased aridity and thus reinforced the global weather trends, which were linked to substantial decreases in the extent of tropical rainforest across sub-Saharan Africa in the Miocene (Kissling et al., 2012). General trends of forest fragmentation during the Miocene likely underlie most of the species-level diversification patterns in *Rhampholeon*, a finding that is similar to East African thicket rats (Bryja et al., 2017) and forest chameleons (Hughes et al., 2017a).

Among the AR *Rhampholeon* species, diversification events since the mid-Miocene were most common, a finding that is similar to several other forest-adapted taxa in the region (e.g., Greenbaum et al., 2015; Hughes et al., 2017a; Larson et al., 2016; Portillo et al., 2015; Tolley et al., 2011). Short internodes and low support among the species in the *R. boulengeri* complex are consistent with a rapid radiation event across the Miocene–Pliocene boundary (ca. 6–4 Mya). Diversification patterns for the entire genus *Rhampholeon* are consistent with vicariance-driven

speciation via forest fragmentation during the Miocene; however, this pattern does not fully explain the diversification within the *R. boulengeri* complex. For example, the distribution of *R.* sp. 5 is extensive yet disjunct, ranging from the Rwenzori Mountains to the highlands of southern Burundi. The geologically young Rwenzori Mountains (Kaufmann et al., 2015) were surrounded by bodies of water since the mid-Pleistocene (Beadle, 1981), which were likely barriers to dispersal. In fact, many vertebrate taxa are endemic to this massif (Butynski and Kalina, 1993), including two forest chameleon species (Tilbury, 2010). However, we found that *R.* sp. 5 was present in high-elevation forests of the Rwenzori Mountains and Bururi Nature Reserve of southern Burundi. These two localities are separated by a great distance (> 450 km), and although samples from these locales formed distinct clades, we detected minimal intraspecific genetic distance between these clades. Furthermore, we estimated that *R.* sp. 5 diverged prior to the uplift of the Rwenzori Mountains (ca. 3–2 Mya), and thus geological uplift alone cannot explain the diversification of this species. It is possible that *R.* sp. 5 occurs at other localities between these sites, but potential populations have yet to be sampled. If the allopatric distribution between populations of *R.* sp. 5 is real, perhaps there were forest connections that are now gone, or fluctuations in the historical water levels of the AR crater lakes (Salzburger et al., 2014) isolated ancestral populations, and subsequent population-level extinctions between these sites produced its present-day distribution. Nevertheless, there are several endemic species that have widespread, yet disjunct distributions in the AR, including one bird (*Bradypterus graueri* [Kahindo et al., 2017]), three tree frogs (*Hyperolius castaneus*, *H. discodactylus*, and *Leptopelis karissimbensis* [Greenbaum et al., 2013; Liedtke et al., 2014; Portillo et al., 2015]), and three small mammals (*Hylomyscus vulcanorum*, *Lophuromys woosnami*, and *Sylvisorex vulcanorum* [Demos et al., 2014, 2015; Huhndorf et al., 2007]).

2.5.3 Elevational zonation and cryptic diversity

A model of allopatric speciation driven by forest fragmentation throughout the Cenozoic has been proposed for forest-dependent chameleons (Branch et al., 2014; Ceccarelli et al., 2014; Matthee et al., 2004; Tolley et al., 2011, 2013; Townsend et al., 2011). This model fits the pattern of cladogenesis for pygmy chameleons from our genus-level phylogeny, but is a poor fit within the *R. boulengeri* complex, because we found evidence that sister species occur in parapatry, yet occupy distinct elevational zones. The complex patterns of cryptic diversity we found in the AR suggest that traditional biogeographic barriers for the region may be inadequate to explain the diversity in *R. boulengeri*, and thus we contend that elevational zonation and parapatric speciation have played more significant roles in generating diversity within this group than previously recognized. Elevational zonation as a mechanism of speciation has been well characterized in the Americas for amphibians and reptiles (e.g., Arteaga et al., 2016; Hutter et al., 2013; Kozak and Wiens, 2010; Wake and Lynch, 1976), yet its role in the divergence of African taxa is not well understood. Fuchs et al. (2011) found species-level genetic differentiation between montane and lowland forms of the bird species *Phyllastrephus debilis* from the Eastern Arc Mountains of Tanzania. However, Cox et al. (2014) found mixed support for an elevational gradient speciation model in their study on the songbird genus *Zosterops* from the Eastern Afromontane highlands of Kenya.

In contrast to the Montane Speciation Hypothesis (Fjeldså and Lovett, 1997) that predicts geographical isolation will result from the inability of species to adapt to new environmental conditions (i.e., allopatric speciation via niche conservatism [Kozak and Wiens, 2010]), we argue that the Gradient Speciation Hypothesis (Moritz et al., 2000) is more appropriate to explain

diversification in the *R. boulengeri* complex. This hypothesis predicts that sister taxa will occupy distinct but adjacent habitats, because new species formation occurred via adaptation to different climatic regimes along an altitudinal gradient (i.e., parapatric speciation via niche differentiation [Moritz et al., 2000]). The six species of the *R. boulengeri* species complex, five of which are endemic to the region, occur along an elevational gradient (800–2,600 m) in the AR and they might be expected to show little genetic differentiation across a relatively small area of continuous habitat, yet they exhibit an extraordinary degree of genetic diversification. This is significant considering that all of the species are members of an ancient clade that diversified in the late Miocene. Furthermore, the elevated levels of genetic variation were not accompanied by pronounced morphological variation, which is likely because the selection pressures exerted upon the phenotype to occupy the leaf-litter ecological niche have been the same across species. Several species in the *R. boulengeri* complex are partly sympatric (e.g., *R.* sp. 1, *R.* sp. 2, *R.* sp. 3, and *R.* sp. Itombwe), but not syntopic, because they occur in largely non-overlapping elevational zones. These patterns of elevational zonation were likely promoted by parapatric speciation, in which adaptation to physical factors such as temperature or differentiation in climatic niches initiated processes that lead to species formation. Specifically, pulses of forest expansion and contraction throughout the Miocene–Pliocene boundary could be invoked to explain a parapatric pattern of high-elevation species (*R.* sp. 1) as sister to a lower-elevation species (*R.* sp. 2). As historical forests migrated up in elevation, ancestral populations may have adapted to novel lower thermal limits and thus physiological thresholds changed. During periods of greater forest connectivity, dispersal to warmer, low-elevation forests may have been hampered. A similar scenario may also explain the divergence of *R.* sp. 3 to the clade containing *R.* sp. 4 and *R.* sp. 5, and perhaps explain the divergence between *R. hattinghi* and *R.* sp. Itombwe.

The highest regional concentration of diversity in the *R. boulengeri* complex (four species) is found in the South Kivu Province of eastern DRC. In Kahuzi-Biega National Park, three species (*R.* sp. 1, *R.* sp. 2, and *R.* sp. 3) occur along an elevational gradient (800–2030 m), and similarly in association with the Itombwe Plateau, three species (*R.* sp. 2, *R.* sp. 3, and *R.* sp. Itombwe) occur along a slightly greater elevational gradient (1060–2311 m). The extensive volcanism and orogeny in this province (e.g., Ebinger and Furman, 2003; Kampunzu et al., 1998; Pasteels et al., 1989), especially during the Miocene, likely contributed to the emergence of new ecological conditions, and thus may account for some of the patterns of increased genetic diversity in pygmy chameleons along elevational gradients in these particular highlands.

2.5.4 Conservation implications

Although pygmy chameleons are considered less threatened by the illegal wildlife trade than by habitat loss, several African countries supply large numbers of chameleon exports to satisfy international demand (Carpenter et al., 2004; Robinson et al., 2015). In an effort to reduce pressure on natural populations for species in the legal trade, all pygmy chameleon species were added to CITES Appendix II in 2016, which represents an important first step towards the sustainable trade in pygmy chameleons. For these reasons and more detailed below, we wish to call attention to several serious threats to the biological integrity of the AR that pose challenges to pygmy chameleon conservation. Although the AR is extremely biologically diverse (see Plumptre et al., 2007), the amount of unrecognized diversity in pygmy chameleons in the AR suggests that the discovery of cryptic taxa in this region is still in its initial stages (see Bickford et al., 2007). Moreover, a recent study demonstrated that Central Africa is one of the three most under-sampled regions on the continent with respect to its herpetofauna (Tolley et al., 2016). The forests that

harbor elevated levels of pygmy chameleon diversity in the AR face severe challenges from an extremely dense human population (Burgess et al., 2007) and international demand for petroleum products (von Einsiedel, 2014). Near ubiquitous occupation of land by humans across the AR has imposed unprecedented pressures upon its natural environments, especially the forest habitats that are being converted to agriculture at an alarming rate (Barnes, 1990; Butsic et al., 2015). Political disputes and armed conflict among the various countries of the AR has also irreparably damaged many of its natural environments (Glew and Hudson, 2007; Hanson et al., 2009; Kanyamibwa, 1998). Adding to these problems is the threat posed by predicted climate change (Carr et al., 2013), and a recent model indicated that by 2070, over 40% of the AR region will be unsuitable for most of its current ecosystems (Ponce-Reyes et al., 2017). Unfortunately, these interwoven threats in the AR (Brooks et al., 2004) are rampant across tropical biodiversity hotspots worldwide (Mittermeier et al., 2011; Myers et al., 2000) and, in part, they underlie the current global extinction crisis (Kolbert, 2014). Exacerbating these issues is the rate of species discovery, which is thought to be so slow (Fontaine et al., 2012) that numerous species will be lost before they are known to science (Costello et al., 2013). Moreover, declines in biodiversity not only affect ecosystem function (see Loreau et al., 2001); they also induce losses to our understanding of character variation via direct losses in data. Our understanding of variation across space and through time is what evolutionary biology and biogeography are founded upon. To that end, no single type of data should be excluded as we endeavor to decipher the history of life on Earth and thus we must increase the rate of rescue for as many types of data as possible (e.g., Hughes et al., 2016). Lastly, we have identified a significant gap between the taxonomy and the diversity of AR pygmy chameleons and because specific names are critical to species conservation, we plan to do a follow-

up study, using an integrative taxonomic approach, to describe these distinct populations as new species.

Chapter 3: Integrative taxonomy of the Central African forest chameleon, *Kinyongia adolfifriderici* (Sauria, Chamaeleonidae), reveals underestimated species diversity in the Albertine Rift[2]

[2] Published as: **Hughes, D.F.**, C. Kusamba, M. Behangana, and E. Greenbaum. **2017**. Integrative taxonomy of the Central African forest chameleon, *Kinyongia adolfifriderici* (Sauria, Chamaeleonidae), reveals underestimated species diversity in the Albertine Rift. *Zoological Journal of the Linnean Society* 181(2): 400–438.
Available online: https://doi.org/10.1093/zoolinnean/zlx005

3.1 Abstract

The Albertine Rift is a center for vertebrate endemism in Central Africa, yet the mechanisms underlying lineage diversification of the region's fauna remain unresolved. We generated a multilocus molecular phylogeny consisting of two mitochondrial (16S and ND2) and one nuclear (RAG1) gene to reconstruct relationships and examine spatiotemporal diversification patterns in the Albertine Rift endemic forest chameleon, *Kinyongia adolfifriderici* (Sternfeld, 1912). This widely distributed species was revealed to be a complex of four genetically distinct and geographically isolated species. Three new species are described based on molecular analyses and morphological examinations. We find that *K. rugegensis* sp. nov. (Rugege Highlands) and *K. tolleyae* sp. nov. (Kigezi Highlands) form a well-supported clade, which is sister to *K. gyrolepis* (Lendu Plateau). *Kinyongia itombwensis* sp. nov. (Itombwe Plateau) was recovered as sister to *K. adolfifriderici* (Ituri rainforest). The phylogeographic patterns we recovered for *Kinyongia* suggest that speciation stemmed from isolation in forest refugia. Our estimated diversification dates in the Miocene indicate that most species of *Kinyongia* diverged prior to the aridification of Africa following climate fluctuations during the Pleistocene. Our results highlight the Albertine Rift as a focal point of diversification for *Kinyongia*, further elevating the global conservation importance of this region.

3.2 Introduction

The Albertine Rift (AR) represents the western branch of the East African Rift valley system (Chorowicz, 2005). The modern topography of the East African Rift started to form ca. 30 million years ago (Mya) from volcanic swells in North and East Africa (Paul et al., 2014). The AR portion of the East African Rift was likely initiated during the Oligocene (ca. 25 Mya) (Roberts et

al., 2012). However, most of the geomorphological changes in the AR took place in the mid- to late Miocene (15–5 Mya) (Macgregor, 2015). Volcanism also principally occurred during the Miocene in the AR (Nonnotte et al., 2008), and extensive lava flows would have contributed to landscape modifications (Griffiths, 1993). The AR is not only geologically unique, it also harbors more endemic vertebrate species than any other area of similar size on continental Africa (Plumptre et al., 2007), including the highest mammalian tropical forest species richness per unit area on Earth (Demos et al., 2015). The AR was not identified by Myers et al. (2000) as one of the original 25 Biodiversity Hotspots. Reassessments with an African emphasis, however, elevated the AR into the Eastern Afromontane Hotspot (Brooks et al., 2004) and to a Global Biodiversity Hotspot (Küper et al., 2004). Nevertheless, the proposed mechanisms of speciation or environmental processes that have sculpted the immense diversity of the region are not conclusive. Aridification and refugia formation in response to Pleistocene glaciations have been implicated as drivers of isolation and subsequent lineage formation among some AR montane taxa, including small mammals (Demos et al., 2014, 2015), land snails (Boxnick et al., 2015; Wronski and Hausdorf, 2008), gorillas (Anthony et al., 2007), and birds (Bowie et al., 2006; Voelker et al., 2010). In contrast, several other AR taxa, including frogs (Larson et al., 2016; Portillo et al., 2015), chameleons (Tolley et al., 2011), and snakes (Greenbaum et al., 2015; Menegon et al., 2014) were suggested to have evolved from pre-Pleistocene events such as the reduction of forests and spread of grasslands across Africa in response to global cooling in the Miocene. Because the AR has a complex orogenic history and is one of the most important sites for biodiversity in Africa (Plumptre et al., 2007), it provides an ideal opportunity to understand the relative influences of historic biogeographic events and climate change on spatiotemporal aspects of speciation.

The forest chameleon genus *Kinyongia* Tilbury, Tolley and Branch, 2006 currently contains 20 described taxa that are distributed in forests across East and Central Africa (Uetz et al., 2017). Monophyly for *Kinyongia* was established using nuclear and mitochondrial markers, but unique morphological synapomorphies have not been identified (Tilbury et al., 2006). Currently recognized *Kinyongia* species were historically classified under the genus *Chamaeleo* Laurenti, 1768 and then reallocated to the South African genus *Bradypodion* Fitzinger, 1843 by Klaver and Böhme (1986). This transfer was not based on similarity, but rather the lack thereof, and the taxonomic rearrangement was not accepted by Branch (1998). Klaver and Böhme (1986) acknowledged the lack of morphological synapomorphies among species in this group (previously referred to as the "*fischeri* complex" [Hillenius, 1959]), and this heterogeneity—among other reasons (see Tolley and Herrel, 2013)—influenced the tangled and controversial taxonomic histories of *Kinyongia* (see Tilbury et al., 2006) and *Bradypodion* (see Tolley et al., 2004). Morphological dissimilarity among *Kinyongia* species is exemplified by differences in cranial ornamentation of this oviparous group, which includes paired rostro-nasal horns (e.g., *K. fischeri* [Reichenow, 1887]), a single blade-like rostral horn (e.g., *K. xenorhina* [Boulenger, 1901]), or no cranial ornamentation (e.g., *K. mulyai* Tilbury and Tolley, 2015). *Kinyongia* was historically thought to be sister to the dwarf chameleons (genus *Bradypodion*) (e.g., Tolley et al., 2011). However, Tolley et al. (2013) found forest chameleons (*Kinyongia*) to be most closely related to horned chameleons (genus *Trioceros* Swainson, 1839) and proposed an ancient split between these sister genera in the mid-Eocene (ca. 45 Mya). *Kinyongia* is composed of mostly ancient lineages originating in the Oligocene and early Miocene (Tolley et al., 2011; Tolley and Herrel, 2013). The speciation patterns in *Kinyongia* recovered by Tolley et al. (2011) did not reflect recent phylogeographic structuring in response to climate changes during the Pleistocene, as recovered

in some African vertebrate taxa (e.g., Arctander et al., 1999). Rather, stronger genetic signatures in *Kinyongia* seemed to stem from the forest dynamics over this time period, including reductions (Plana, 2004) and diversifications (Couvreur et al., 2008). Tolley et al. (2011) proposed an allopatric model of speciation through isolation in forest refugia and supported this model with high genetic divergence between most sister species with a notable absence of sister species occupying the same mountain block. However, a presumed recent divergence of sister species of *Kinyongia* co-occurring on the Rwenzori Mountains (i.e., *K. carpenteri* [Parker, 1929] and *K. xenorhina*) of the AR are in stark contrast to this model, and more investigation is warranted to understand the mechanisms underlying speciation patterns at this geologically young massif (formed ca. 2–3 Mya [Kaufmann et al., 2015]).

In general, all species of *Kinyongia* are restricted to relict montane or sub-montane forest biomes (Tolley and Herrel, 2013) and occupy a relatively high elevation range (1000–3000 m) (Tilbury, 2010). Three genetically divergent and geographically isolated clades have been recognized within *Kinyongia*; one from the AR/Kenya Highlands and two from the Eastern Arc Mountains (EAM) of East Africa (Tolley et al., 2011, 2013). Seven species currently comprise the AR/Kenya Highlands clade, including five from the AR (*K. adolfifriderici* [Sternfeld, 1912], *K. carpenteri*, *K. gyrolepis* Greenbaum et al., 2012a, *K. mulyai*, and *K. xenorhina*) and two from the Kenya Highlands (*K. excubitor* [Barbour, 1911] and *K. asheorum* Nečas et al., 2009). Four of the AR species are endemic to the montane localities of their original descriptions and the fifth species, *K. adolfifriderici*, is currently considered to be widespread throughout the rift (Tilbury, 2010). *Kinyongia adolfifriderici* represents the most westerly species of the genus, extending into the sub-montane forests of eastern Democratic Republic of the Congo (DRC) (Greenbaum et al., 2012a; Tilbury, 2010; Tilbury and Tolley, 2015). The distribution of this species nearly covers the

latitudinal extent of the AR, ranging on either side of the rift from the Itombwe Plateau in eastern DRC and forest remnants in Burundi, to the northeastern extent of the Ituri rainforest in DRC (Tilbury, 2010). As a result of this widespread distribution and overlapping range with some protected areas, the IUCN Red List currently lists this species as Least Concern (Tolley et al., 2014a). *Kinyongia adolfifriderici* was described by Sternfeld (1912) from a single adult female specimen and the type locality was imprecisely given as 'Irumu-Mavambi Urwald [jungle]'. According to Greenbaum et al. (2012a), Irumu and Mavambi (= Mawambi) are villages in the lowland Ituri rainforest of present-day northeastern DRC that were sites visited during the German Central Africa Expedition (1907–1908) led by Adolphus Frederick, Duke of Mecklenburg (Frederick, 1910). Since its original discovery, few specimens of this species have been collected because of its high canopy habits, cryptic coloration, and shy behavior (Tilbury, 2010). Moreover, persistent civil strife within countries of the AR (e.g., van Reybrouck, 2014) has further discouraged biological exploration, and in turn, contributed to the rarity of this species in museum collections and lack of basic biological information (Tilbury, 2010).

At least two studies have proposed that *K. adolfifriderici* represents a complex of species (Greenbaum et al., 2012a; Tilbury and Tolley, 2015). Various searches in isolated forest patches of East and Central Africa have revealed distinct species of *Kinyongia* (e.g., Lutzmann and Nečas, 2002; Menegon et al., 2009, 2015; Nečas, 2009; Nečas et al., 2009), including two new species from the AR (Greenbaum et al., 2012a; Tilbury and Tolley, 2015). Therefore, we anticipate that additional undescribed *Kinyongia* lineages occur in other poorly explored forest fragments of the AR. To that end, we examined spatial and temporal aspects of the phylogenetic relationships among isolated populations of *K. adolfifriderici* across the AR to test three hypotheses. We use multilocus gene-tree and coalescent-based species-tree estimations to determine whether *K.*

adolfifriderici represents a single widespread species in the AR, or is rather a complex of genetically distinct species. We utilize multivariate statistical analyses for morphometric data on over 20 specimens, including the holotype to determine if the lineages recovered from the phylogenetic analyses are supported by morphological differences. We implement Bayesian dating methods to estimate divergence times within *Kinyongia* to determine if climate shifts induced by Pleistocene glaciation have had an impact on the timing of speciation within forest chameleons of the AR. Finally, we describe three new species on the basis of morphological characters, mtDNA pairwise sequence divergences, qualitative observations, and congruence across multiple phylogenetic approaches that support stable hypotheses of independently evolving species.

3.3 Materials and Methods

3.3.1 Taxon sampling

Fourteen samples of *K. adolfifriderici* were collected during field surveys from various forests across the highlands of the AR from 2008–2015. For our morphological examinations, we incorporated an additional eight specimens (*K.* cf. *adolfifriderici*) from various museum collections (see supplemental information [Appendix 1] in Hughes et al. [2017a]). Museum abbreviations follow Sabaj (2016). We also included the holotype of *K. adolfifriderici* (ZMB 22709) in these examinations. For our phylogenetic analyses, we included 19 out of the 20 currently recognized *Kinyongia* species that have published sequences available on GenBank (Table 1). We excluded the species *K. asheorum* from phylogenetic analyses because only a single sequence for the mitochondrial fragment ND2 is currently available on GenBank. *Kinyongia asheorum*, from the Nyiro Range in northern Kenya, is considered to be a member of the

AR/Kenya Highlands clade, however, this phylogenetic placement was based on analyses of the single mtDNA sequence (Nečas et al., 2009; Tolley et al., 2013).

3.3.2 DNA extraction, amplification, and sequencing

Tissues were harvested from the liver or hind limb muscle of chameleons before formalin fixation, and preserved in 2-ml vials containing 100% ethanol. Genomic DNA was isolated from these tissue samples with the Qiagen DNeasy tissue kit (Qiagen Inc., Valencia, CA, USA). PCR amplification and cycle sequencing of two mitochondrial gene fragments were carried out following standard procedures with the following primers for ND2: L4437b (Macey et al., 1997a) and H5934 (Macey et al., 1997b), and 16S: L2510 and H3080 (Palumbi, 1996). A fragment of the nuclear gene RAG1 was sequenced using primers F118 and R1067 (Matthee et al., 2004). We used 25 µL PCR reactions with an initial denaturation step of 95 °C for 2 min, followed by denaturation at 95 °C for 35 s, annealing at 50 °C for 35 s, and extension at 72 °C for 95 s, with 4 s added to the extension per cycle for 32 (mitochondrial genes) or 34 (nuclear gene) cycles. Amplification products were visualized on a 1.5% agarose gel stained with Invitrogen SYBR Safe DNA gel stain (Thermo Fisher Scientific, Waltham, MA, USA). Sequencing reactions were purified with Agencourt CleanSEQ magnetic bead solution (Beckman Coulter Inc., Brea, CA, USA) and sequenced with an ABI 3130xl automated sequencer at the University of Texas at El Paso (UTEP) Border Biomedical Research Center (BBRC) Genomic Analysis Core Facility.

Table 3.1 Species identifications, specimen catalog numbers, GenBank accession numbers, and collecting localities for *Kinyongia* (ingroup) and *Trioceros* (outgroup) samples analyzed in this study. Newly generated sequences are indicated with bold type. Institutional abbreviations follow Sabaj (2016). See Appendix for abbreviations of field numbers. DRC = Democratic Republic of the Congo; T = topotype; H = holotype.

Species	Catalog No.	16S	ND2	RAG1	Locality
Kinyongia rugegensis sp. nov. (T)	UTEP 21481	KY292356	KY292364	KY292372	Burundi: Bubanza Province, Mpishi village, Kibira National Park
Kinyongia rugegensis sp. nov. (H)	UTEP 21485	KY292357	KY292365	KY292373	Burundi: Bubanza Province, Mpishi village, Kibira National Park
Kinyongia rugegensis sp. nov.	UTEP 21484	KY292358	KY292366	KY292374	Burundi: Kayanza Province, Rwegura village, Kibira National Park
Kinyongia tolleyae sp. nov. (T)	UTEP 21486	KY292352	KY292360	KY292368	Uganda: Kabale District, Ruhija village, Bwindi Impenetrable National Park
Kinyongia tolleyae sp. nov. (T)	UTEP 21487	KY292353	KY292361	KY292369	Uganda: Kabale District, Ruhija village, Bwindi Impenetrable National Park
Kinyongia tolleyae sp. nov.	UTEP 21489	KY292354	KY292362	KY292370	Uganda: Kasese District, Ruboni Community Hotel, Rwenzori Mountains National Park
Kinyongia tolleyae sp. nov. (T)	CAS 201593	DQ923820	EF014304	DQ996659	Uganda: Kabale District, Ruhija village, Bwindi Impenetrable National Park
Kinyongia tolleyae sp. nov. (T)	CAS 201594	GQ221944	GQ221965	N/A	Uganda: Kabale District, Ruhija village, Bwindi Impenetrable National Park
Kinyongia itombwensis sp. nov. (H)	UTEP 20371	JN602061	JN602051	JN602056	DRC: South Kivu Province, Bichaka village, Itombwe Plateau
Kinyongia itombwensis sp. nov.	UTEP 21480	KY292351	KY292359	KY292367	DRC: South Kivu Province, Miki village, Itombwe Plateau

Kinyongia adolfifriderici (T)	UTEP 21491	KY292355	KY292363	KY292371	DRC: Orientale Province, Loki village, Ituri rainforest
Kinyongia boehmei (T)	BM 29	GQ221942	GQ221963	GQ221953	Kenya: Taita Hills
Kinyongia boehmei (T)	JM 2946	GQ221948	GQ221969	GQ221958	Kenya: Taita Hills
Kinyongia carpenteri (T)	CT 346	DQ923822	EF014306	FR716622	Uganda: Rwenzori National Park
Kinyongia carpenteri	UTEP 20370	JN602058	JN602048	JN602053	DRC: North Kivu Province, western slope of Ruwenzori Mountains, Mount Teye
Kinyongia excubitor (T)	CT 209	DQ923823	EF014307	DQ996661	Kenya: Mount Kenya
Kinyongia fischeri (T)	CT 334	DQ923829	EF014313	DQ996662	Tanzania: Nguru Mountains
Kinyongia fischeri (T)	MTSN 8490	GQ221951	GQ221971	GQ221960	Tanzania: Nguru Mountains
Kinyongia gyrolepis (T)	UTEP 20339	JN602062	JN602052	JN602057	DRC: Orientale Province, Aboro village, Lendu Plateau
Kinyongia gyrolepis (T)	UTEP 20342	JN602055	JN602050	JN602060	DRC: Orientale Province, Aboro village, Lendu Plateau
Kinyongia magomberae	MTSN 8218	GQ221950	GQ221970	GQ221959	Tanzania: Udzungwa Mountains
Kinyongia magomberae (H)	MTSN 8492	GQ221952	GQ221972	GQ221961	Tanzania: Magombera Forest

Kinyongia matschiei (T)	CAS 168852	FR716605	FR716641	FR716626	Tanzania: East Usambara Mountains
Kinyongia matschiei (T)	CT 105	GQ221946	GQ221967	GQ221956	Tanzania: East Usambara Mountains
Kinyongia multituberculata (T)	CT 111	GQ221947	GQ221968	GQ221957	Tanzania: West Usambara Mountains
Kinyongia mulyai (H)	CT 426	KM589402	KM589404	KM589403	DRC: Katanga Province, Mount Nzawa
Kinyongia msuyae (H)	MTSN9374	LN997635	LN997645	N/A	Tanzania: Livingstone Mountains
Kinyongia msuyae (T)	MTSN9375	LN997636	LN997646	N/A	Tanzania: Livingstone Mountains
Kinyongia oxyrhina (T)	CT 192	DQ923831	EF014315	DQ996669	Tanzania: Uluguru Mountains
Kinyongia oxyrhina (T)	CT 193	DQ923832	EF014316	DQ996670	Tanzania: Uluguru Mountains
Kinyongia tavetana (T)	CT 113	DQ991233	FJ717801	DQ996671	Tanzania: Mount Kilimanjaro
Kinyongia tavetana	CT 207	DQ923833	EF014317	DQ996672	Tanzania: Mount Meru
Kinyongia tenuis (T)	CAS 168917	DQ923834	EF014318	HQ130628	Tanzania: East Usambara Mountains
Kinyongia tenuis (T)	CT 103	DQ923835	EF014319	DQ996673	Tanzania: East Usambara Mountains

Kinyongia uluguruensis (T)	CT 189	DQ923825	EF014309	DQ996667	Tanzania: Uluguru Mountains
Kinyongia uluguruensis (T)	CT 191	DQ923826	EF014310	DQ996666	Tanzania: Uluguru Mountains
Kinyongia uthmoelleri	CT 151	DQ923836	EF014320	DQ996674	Tanzania : South Pare Mountains
Kinyongia uthmoelleri (T)	CT 339	DQ923837	EF014321	DQ996675	Tanzania: Mount Hanang
Kinyongia vanheygeni	SCHP-08-R-50	LN997640	LN997650	N/A	Tanzania: Poroto Mountains
Kinyongia vanheygeni	SCHP-08-R-91	LN997641	LN997651	N/A	Tanzania: Poroto Mountains
Kinyongia vosseleri (T)	CAS 168921	GQ221943	GQ221964	GQ221954	Tanzania: East Usambara Mountains
Kinyongia vosseleri (T)	CT 104	GQ221945	GQ221966	GQ221955	Tanzania: East Usambara Mountains
Kinyongia xenorhina (T)	CT 350	DQ923838	EF014322	DQ996676	Uganda: Rwenzori Mountains National Park
Kinyongia xenorhina (T)	CT 351	DQ923839	EF014323	DQ996677	Uganda: Rwenzori Mountains National Park
Trioceros feae (T)	CAS 207681	FJ717767	AF448749	AF448749	Equatorial Guinea: Bioko Island
Trioceros goetzei	CT 050	FJ717768	FJ717791	FJ746603	Malawi: Nyika Plateau

Trioceros johnstoni	CAS 201596	DQ923812	EF014298	DQ996650	Uganda: Kabale District

3.3.3 Sequence alignment and phylogenetic analyses

Twenty-four new sequences were generated from eight individuals for two mitochondrial markers (16S, ND2) and one nuclear marker (RAG1). Sequences of two individuals from Uganda (CAS 201593–94) and an individual from the Itombwe Plateau (DRC) (UTEP 20371) were published previously (Greenbaum et al., 2012a). New sequences were deposited in GenBank (Table 3.1). Outgroup samples included three species of horned chameleons (*Trioceros*) (Tolley et al., 2013) (Table 3.1). Chromatograph data were interpreted using SEQMAN (Swindell and Plasterer, 1997). Alignments for each gene were generated using MUSCLE 3.6 (Edgar, 2004) in MESQUITE 3.04 (Maddison and Maddison, 2015). Manual adjustments and editing were carried out in MACCLADE 4.08 (Maddison and Maddison, 2005). A hypervariable region in the 16S gene fragment consisting of 44 base pairs was removed prior to phylogenetic analyses because of an ambiguous alignment. Phylogenetic analyses were initially conducted on single-gene data sets. The resulting individual gene-trees revealed nearly identical topologies and thus the following analyses were conducted on the concatenated data set. Maximum likelihood (ML) analyses of concatenated data were conducted with the GTRGAMMA model in RAXML 7.2.6 (Stamatakis, 2006). All parameters were estimated and a random starting tree was used. Support values for clades inferred by ML analyses were assessed with the rapid bootstrap algorithm with 1000 replicates (Stamatakis et al., 2008). Bayesian inference (BI) analyses were conducted in MRBAYES 3.1 (Huelsenbeck and Ronquist, 2001; Ronquist and Huelsenbeck, 2003). Our model included seven data partitions, including a single partition for 16S and three independent partitions for each codon position for the protein-coding genes ND2 and RAG1. Concatenated data sets were partitioned identically for ML and BI analyses. The Akaike Information Criterion (AIC) in PARTITIONFINDER 1.1.0 (Lanfear et al., 2012) was used to establish the best model of evolution

for the nuclear and each of the mitochondrial fragments. The selected models of evolution were used for all BI analyses, but in cases where the model selected in PARTITIONFINDER was not available in MRBAYES, the least restrictive model (GTR) was implemented. Bayesian analyses were conducted with random starting trees, run for 20 million generations, and Markov chains were sampled every 1000 generations. To verify that multiple runs converged, AWTY (Nylander et al., 2008) was used. Burn-in was set at 25%, and thus 5000 of the initial trees were discarded. Phylogenies were visualized using FIGTREE 1.3.1 (Rambaut and Drummond, 2009). Bayesian posterior probabilities ≥ 95% (Alfaro et al., 2003; Hillis and Bull, 1993) and bootstrap values ≥ 70% (Felsenstein, 1981, 1985) were considered as strong support. Net sequence divergences (uncorrected *p*-distances) between *Kinyongia* lineages for each marker were estimated using MEGA 6.0.5 (Tamura et al., 2013).

3.3.4 Species-tree estimation

In accordance with integrative taxonomy, whereby taxonomists should present different lines of evidence to support a stable hypothesis that a population is evolving independently (Padial et al., 2011), and because the underlying species tree can be different than gene trees (Maddison, 1997), we implemented a multi-coalescent model to estimate a species tree for the AR *Kinyongia* clade in *BEAST 1.8 (Drummond et al., 2012). The program assumes lineage sorting is the main source of inconsistency between gene trees and the species tree, it does not require an outgroup (Heled and Drummond, 2010), and it necessitates the prior assignment of individuals to presumed species (Bell et al., 2015). Our species assignments were based on a combination of morphological characters and well-supported, geographically isolated lineages recovered in the concatenated ML and BI gene trees (Figs 3.1–3.2). Double peaks in the nuclear marker (RAG1) were rare and most

were easily remedied at the chromatogram stage in SEQMAN because one allele exhibited a much stronger signal than the other (unequal heights) (Fontaneto et al., 2015). Nevertheless, to account for the possibility of heterozygous individuals in the nuclear data set, haplotypes for RAG1 were phased using PHASE 2.1.1 (Stephens and Donnelly, 2003) in DNASP 5.1 (Librado and Rozas, 2009). Haplotypes with probabilities lower than 0.7 were excluded from the species-delimitation analysis (Harrigan et al., 2008). Phased sequences were used for the subsequent analysis in *BEAST. Models of sequence evolution were chosen using the AIC in PARTITIONFINDER. We only included samples with complete sequence data for all loci. We specified unlinked site, clock, and tree models, and implemented a Yule process tree prior as this analysis largely investigates interspecific relationships. The analysis was run for 50 million generations, sampling every 1000 generations. Multiple independent analyses were run to confirm results produced the same topology. We discarded the initial 25% of trees as burn-in. Convergence was determined from histograms, trace plots, and Effective Sample Size (ESS) values with TRACER 1.5 (Rambaut and Drummond, 2007). Bayesian posterior probabilities ≥ 95% were considered as strong support.

Estimates of species trees can be validated with tree-based coalescent approaches (e.g., Niemiller et al., 2012). By far the most popular of the Bayesian tree-based methods is Bayesian Phylogenetics and Phylogeography (BPP) (Yang and Rannala, 2010). However, BPP requires a fixed, user-specified guide tree, which was recognized by Leaché et al. (2014) as the most obvious pitfall to BPP because inaccuracies in the guide tree can result in artificial increases in genetic divergence between sister lineages, and consequently, over delimitation of species (i.e., false-positives) (Carstens et al., 2013). For example, inappropriate guide trees used by Leaché and Fujita (2010) resulted in biased support for incorrect models, and in turn, inflated taxonomic conclusions (see Bauer et al., 2010). Recently, Olave et al. (2014) identified several significant problems

associated with the sensitivity of tree-based species delimitation analyses to mistakes with upstream analyses (i.e., guide trees for BPP). We align with Carstens et al. (2013) who suggested that results from these analyses should be interpreted with caution and thus we have refrained from implementing a tree-based validation approach until these concerns are fully resolved.

3.3.5 Divergence dating

We used the Bayesian program BEAST 1.8 (Drummond et al., 2012) to estimate divergence dates within *Kinyongia*. We implemented an uncorrelated log-normal relaxed clock model with an estimated clock rate to allow for rate heterogeneity among lineages (Drummond et al., 2006). We used a Yule process tree prior (pure birth) on our multilocus data set because this prior is best suited for phylogenies describing the relationships between different species and assumes a constant speciation rate. Multiple independent analyses were run to confirm results produced the same topology. Analyses were run for 50 million generations, sampling every 1000 generations. TRACER was used to confirm stationarity and adequate ESS of the posterior probabilities (> 200 for each estimated parameter). We discarded the first 25% of trees as burn-in. Parameter values from the posterior probabilities on the maximum clade credibility tree were summarized using the program TREEANNOTATOR 1.7.5 (Drummond et al., 2012). Bayesian posterior probabilities ≥ 95% were considered as strong support.

For the dated tree analysis, we included recent representatives of more distantly related groups as well as representative species from all chameleon genera (at least three species per genus when available) (see supplemental information [Table S1] in Hughes et al. [2017a]). In some instances, hybrid sequences composed of different species from the same genus or a closely related genus (based on Pyron et al., 2013) were used for outgroup samples and these alternate species are

indicated in Table S1 (see supplemental information [Table S1] in Hughes et al. [2017a]). A total of 14 nodes were constrained for divergence dating and most dates for calibration purposes were adopted from Tolley et al. (2013). Primary (fossil) calibrations were placed on a total of nine nodes in the tree corresponding to some of the oldest known fossils of lepidosaurian taxa (Table 2.2). Secondary calibrations were placed on a total of five nodes on the tree to achieve temporal congruence with the most complete time-calibrated chameleon phylogeny published to date—including over 90% of all named species (Tolley et al., 2013) (Table 2.2). For each calibration, we used a translated log-normal distribution, with an offset equal to the age of the fossil or estimated internal node split. The results of an initial dated analysis depicted a tree topology that did not closely reflect the interspecific relationships among chameleon genera recovered by Tolley et al. (2013). Therefore, topological constraints (i.e., enforced monophyly) were imposed on three clades (*Calumma* + *Furcifer*; *Bradypodion* + *Nadzikambia*; *Trioceros* + *Kinyongia*) based on the intergeneric relationships recovered in the family-level phylogeny by Tolley et al. (2013).

3.3.6 Morphological analyses

Specimens examined for this study were preserved in 10% buffered formalin in the field and transferred to 70% ethanol for long-term storage in the UTEP Biodiversity Collections. Other specimens that were examined morphologically are presented in Appendix 1. Morphometric data were recorded from preserved specimens with vernier calipers to the nearest 0.1 mm with the aid of a stereomicroscope. Color descriptions are based on color photographs in life, personal observations, and field notes. Sex was determined by internal examination of gonads, everted hemipenes, or the presence of hemipenal bulges distal to the vent. Drawings of everted hemipenes

were conducted with the aid of an illuminated stereomicroscope. Hemipenal terminology follows Klaver and Böhme (1986).

Measurements (± 0.1 mm) were taken from the right side of the body. Morphometric and meristic data, and their associated abbreviations were modified from Branch and Tolley (2010) and Greenbaum et al. (2012a): snout–vent length (SVL) from tip of snout to anterior edge of vent; tail length (TL) from tip of tail to posterior edge of vent; total length (ToL) from tip of snout to tip of tail; head length (HL) from superior tip of casque to tip of snout; head width (HW) measured at widest point just posterior to eyes; head height (HH) from rictus (i.e., commissure) of jaw to superior tip of casque; mouth length (ML) from tip of rostral to rictus; casque–eye length (CE) measured diagonally from posterior margin of orbit to superior tip of casque; snout length (SL) from tip of snout to anterior margin of orbit; eye diameter (ED) measured horizontally at center of eye; cranial crest gap (CC) measured across the crown between raised supraorbital crests at mid-eye; inter-limb length (IL) from axillary to inguinal attachments of limbs; forelimb length (FLL) from elbow to wrist; hind limb length (HLL) from knee to heel; and three meristic characters, including conical tubercles of dorsal crest (CTD); upper labials (UL) to posterior margin of orbit; lower labials (LL) to posterior margin of orbit. Statistical comparisons of selected measurements and counts were conducted with a two-tailed t-test. To avoid potential problems with the use of ratios in statistics, all measurement data were analyzed in an analysis of covariance (ANCOVA), with body size (SVL) as a covariate (Packard and Boardman, 1999). These analyses were conducted in MINITAB 16 (Minitab Statistical Software, State College, PA, USA).

To examine whether *Kinyongia* from these populations exhibit morphological differences, 10 continuous morphological measurements were used (HL, HW, HH, ML, CE, SL, ED, CC, FLL, and HLL). Two variables (TL and IL) skewed the results of an initial principal components

analysis (PCA) and were thus omitted from the following analyses. These two variables possess potentially meaningful implications regarding differences between sexes for TL (males tend to have longer tails) and gravid females with extended abdomens inflated IL measurements (compared to males of similar SVL). These 10 mensural characters were size corrected using SVL as a covariate and the residuals were included in a PCA. All variables had communalities (> 0.5). A varimax rotation was used, PCs with eigenvalues > 1.0 were extracted, and the resulting PC scores were saved. These PC scores were then used as input variables for a multivariate analysis of variance (MANOVA) with the species as the fixed factor. Posthoc pairwise comparisons were made using Tukey's Honest Significant Difference test and the Bonferroni test. These multivariate analyses were carried out in SPSS 22 (IBM SPSS Statistics for Windows, Armonk, NY, USA).

3.4 Results

3.4.1 Molecular phylogenetics, species-tree inference, and sequence divergence

A total of 2118 bp was obtained from three loci for each of eight individuals of *K.* cf. *adolfifriderici* (16S: 441 bp; ND2: 856 bp; RAG1: 821 bp). There were no gaps in the alignments of any of the three loci after we omitted a hypervariable region consisting of 44 bp from the 16S ribosomal gene. Using AIC in PARTITIONFINDER, we determined that the most appropriate substitution models were, GTR+G for 16S; GTR+I+G for ND2 1st codon position, HKY+G for ND2 2nd codon position, TIM+G for ND2 3rd codon position; HKY+G for RAG1 1st and 2nd codon positions, HKY+I for RAG1 3rd codon position. Relationships among *Kinyongia* species were reconstructed utilizing the concatenated data set and the same topology was recovered using BI and ML methods (Fig. 3.1). The three geographically distinct clades from Tolley et al. (2011) were recovered as monophyletic (i.e., AR/Kenya Highlands, EAM *North*, and EAM *South*) (Fig. 3.1).

The recently described species *K. mulyai* endemic to Mount Nzawa in the southern AR was recovered with strong support as sister to the Rwenzori Massif endemics, *K. xenorhina* and *K. carpenteri* (Fig. 3.1). Four distinct lineages representing geographically isolated populations of *K.* cf. *adolfifriderici* were recovered with strong support (Fig. 3.2). The populations from southwestern Uganda (Rwenzori Mountains + Bwindi Impenetrable National Parks) formed a distinct clade that was most closely related to a clade from northern Burundi (Kibira National Park), whereas a clade from the Itombwe Plateau (eastern DRC) was recovered in a sister relationship with a sample from the Ituri rainforest (northeastern DRC) (Figs 3.1–3.2). The placement of *K. gyrolepis* from the Lendu Plateau in northeastern DRC within the *K. adolfifriderici* clade renders the latter species paraphyletic.

The species-tree analysis recovered identical clade topology to our concatenated gene-tree analyses. The AR *Kinyongia* clade was strongly supported (Fig. 3.3). The *K. adolfifriderici* clade was recovered with strong support and in an identical topology to the gene-tree analyses. *Kinyongia gyrolepis* was nested within the *K. adolfifriderici* clade, supporting the paraphyletic relationship recovered in our multilocus gene tree. The four distinct lineages of *K.* cf. *adolfifriderici* were strongly supported and the sister relationships among them upheld from the gene-tree estimations (Fig. 3.3). Only the placement of *K. mulyai* was equivocal in this analysis (Fig. 3.3). The results of this coalescent-based species-tree inference further supports the recognition of three undescribed, novel lineages of *K.* cf. *adolfifriderici* from the AR.

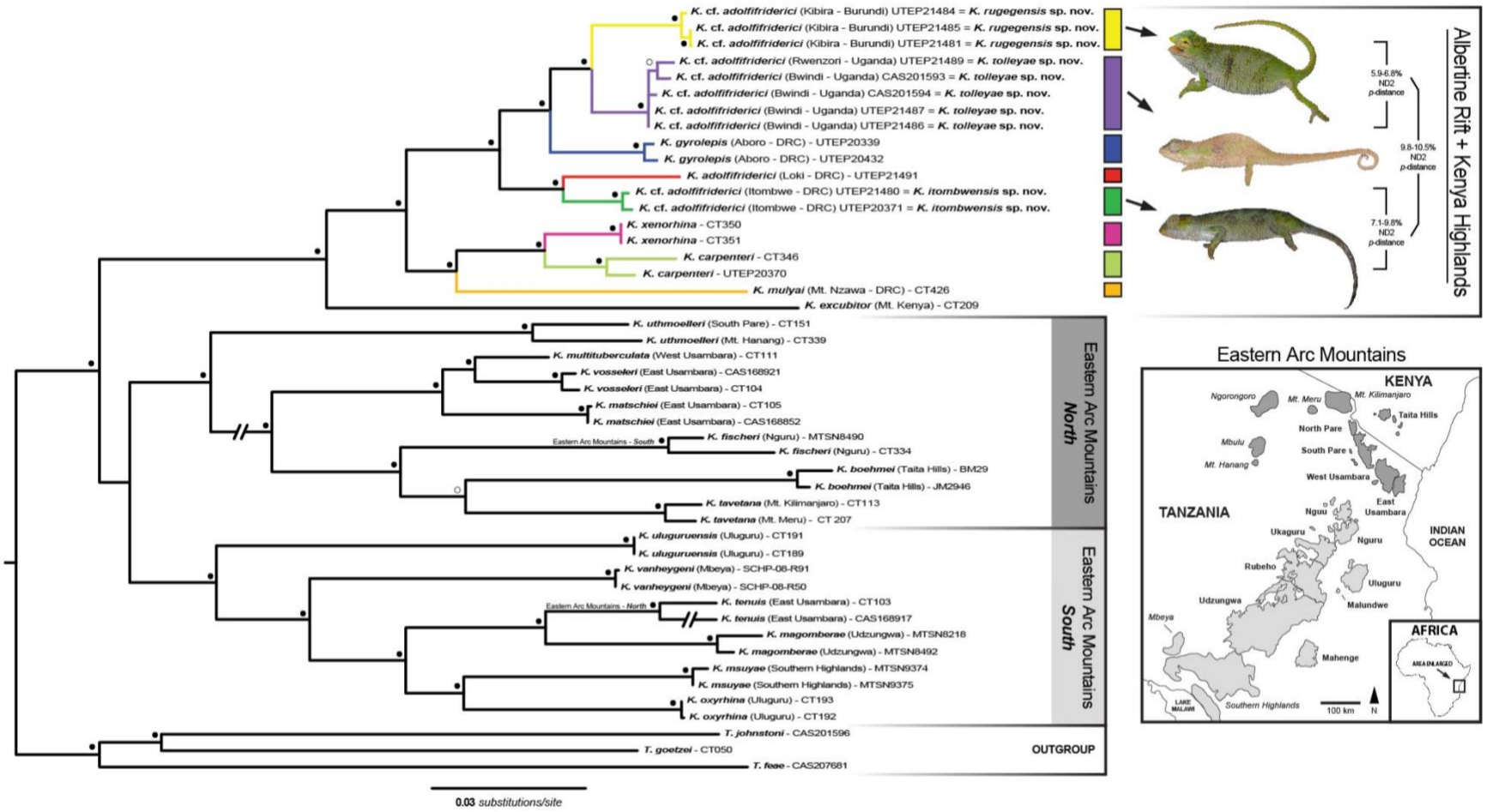

Figure 3.1 Maximum-likelihood phylogeny of the African forest chameleon genus *Kinyongia*. Nodes with strong support from both maximum-likelihood and Bayesian inference analyses are indicated by filled circles (bootstrap ≥ 70% + posterior probability ≥ 0.95), and nodes with support from only maximum-likelihood analyses by open circles. Color-coded rectangles correspond to the Albertine Rift endemic species as follows (in descending order from top of phylogeny): yellow – *K.* cf. *adolfifriderici* (Kibira – Burundi) = *K. rugegensis* sp. nov.; purple – *K.* cf. *adolfifriderici* (Bwindi + Rwenzori – Uganda) = *K. tolleyae* sp. nov.; blue – *K. gyrolepis*; red – *K. adolfifriderici*; dark green – *K.* cf. *adolfifriderici* (Itombwe – DRC) = *K. itombwensis* sp. nov.; pink – *K. xenorhina*; light green – *K. carpenteri*; orange – *K. mulyai*. This color scheme is retained throughout all figures where applicable. Uncorrected *p*-distances for the ND2 marker are given as a range for the three new species (top). The map depicting the northern (dark gray) and southern (light gray) montane regions associated with the Eastern Arc Mountains was modified from Platts et al. (2011).

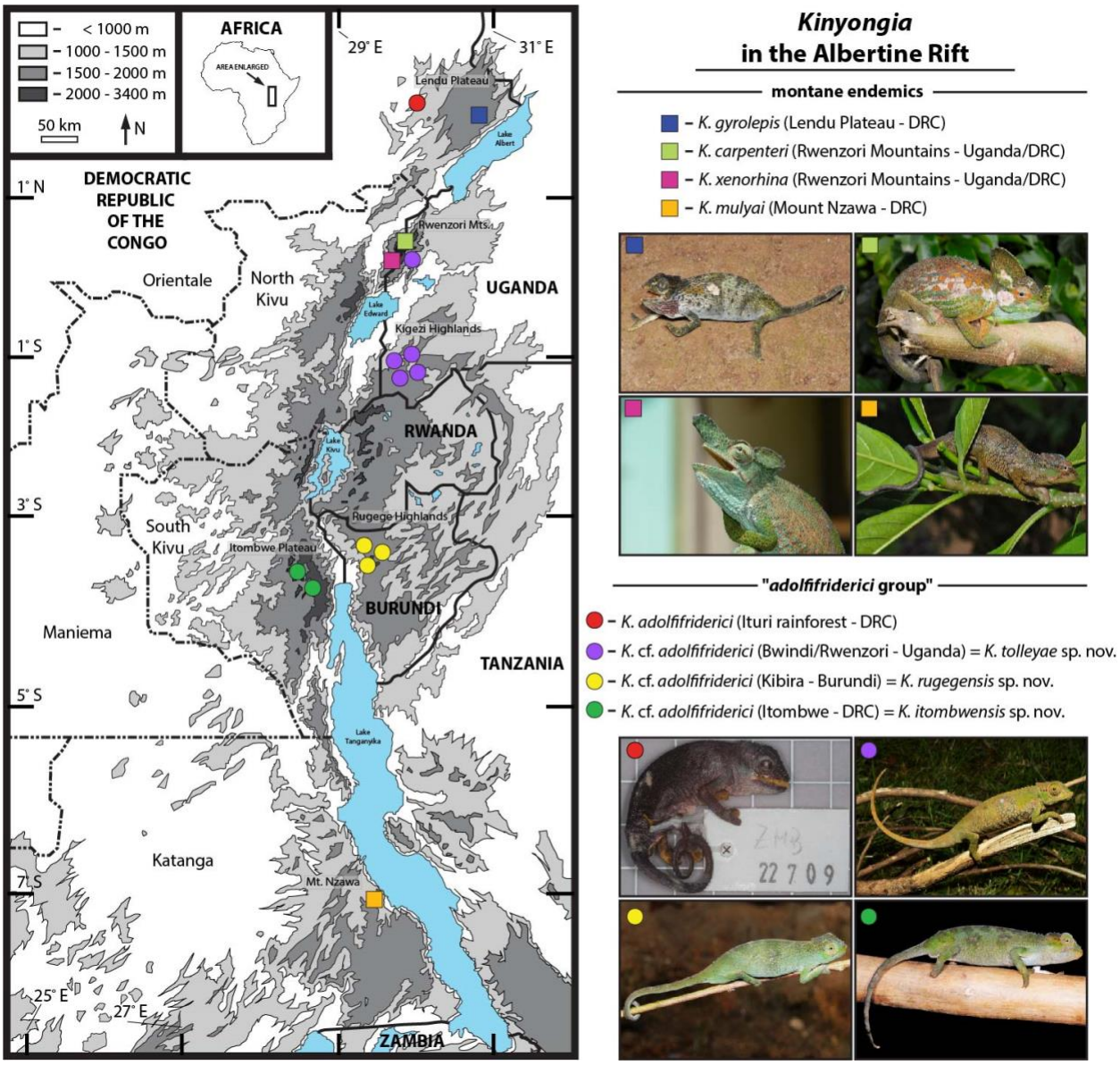

Figure 3.2 Elevation map of the Albertine Rift (Central Africa) showing sampling localities of forest chameleons (*Kinyongia*) used in this study. Photographs of representative individuals for each species are displayed on right; image for *K. mulyai* of the holotype (PEM-R 19199) adapted from Tilbury & Tolley (2015) with permission from Colin R. Tilbury; image for *K. adolfifriderici* is a lateral view of the preserved holotype (ZMB 22709) taken by Frank Tillack; photographs of *K. xenorhina* and *K.* cf. *adolfifriderici* (Bwindi + Rwenzori – Uganda) = *K. tolleyae* sp. nov. were taken by DFH; and photographs of *K. gyrolepis*, *K. carpenteri*, *K.* cf. *adolfifriderici* (Itombwe – DRC) = *K. itombwensis* sp. nov., and *K.* cf. *adolfifriderici* (Kibira – Burundi) = *K. rugegensis* sp. nov. were taken by EG.

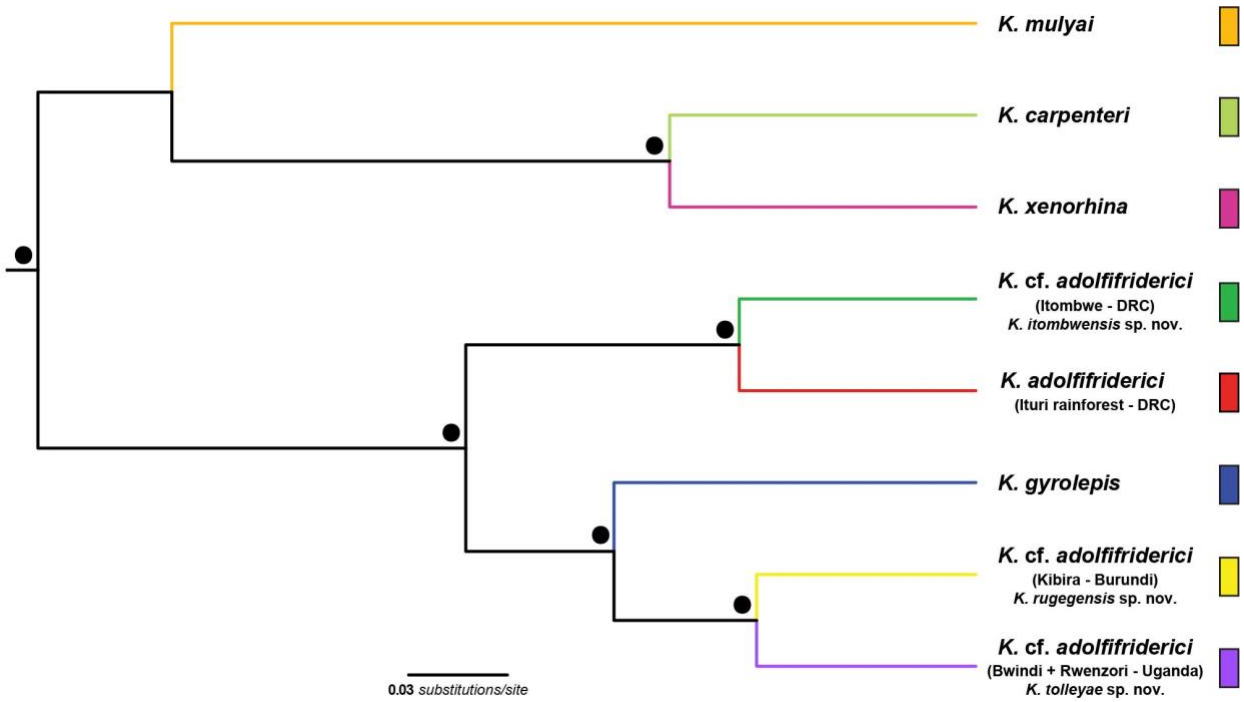

Figure 3.3 *BEAST species-tree inference for combined data set of *Kinyongia* species within the clade endemic to the Albertine Rift (in descending order from top of phylogeny): *K. mulyai* (n = 1), *K. carpenteri* (n = 2), *K. xenorhina* (n = 2), *K.* cf. *adolfifriderici* (Itombwe – DRC) = *K. itombwensis* sp. nov. (n = 2), *K. adolfifriderici* (n = 1), *K. gyrolepis* (n = 2), *K.* cf. *adolfifriderici* (Kibira – Burundi) = *K. rugegensis* sp. nov. (n = 3), and *K.* cf. *adolfifriderici* (Bwindi + Rwenzori – Uganda) = *K. tolleyae* sp. nov. (n = 4). Nodes with Bayesian inference posterior probability values ≥ 95% are denoted by filled circles.

Pairwise sequence divergences (uncorrected *p*-distances) between the undescribed lineages were generally high and comparable to currently recognized *Kinyongia* species endemic to the AR (see supplemental information [Table S2] in Hughes et al. [2017a]). For the ND2 locus, *p*-distances between the western Uganda clade and the Burundi and Itombwe clades ranged from 5.9–6.8% and 7.1–9.8%, respectively (Fig. 3.1). *P*-distances between the Burundi clade and the Itombwe clade for ND2 ranged from 9.8–10.5% (Fig. 3.1). Lastly, *p*-distance ranges for this locus between undescribed clades and the topotypic Ituri lineage were also high: 6.1–6.5% for Itombwe; 8.2–10.6% for Uganda; and 10.3–10.4% for Burundi (see supplemental information [Table S2] in Hughes et al. [2017a]).

3.4.2 Dating estimates

Results from the calibrated dating analysis indicate that *Kinyongia* diverged from *Trioceros* in the Eocene, the three major *Kinyongia* clades emerged around the Eocene-Oligocene boundary, and major lineage diversification within *Kinyongia* took place during the Miocene (Fig. 3.4). Of the 22 distinct *Kinyongia* lineages recovered in this Bayesian analysis, 18 diverged during the Miocene, three diverged during the Oligocene, and one diverged during the Eocene. Most AR *Kinyongia* lineages likely diverged during the Miocene, as evidenced by estimated mean divergence dates within this epoch (Fig. 3.4). An estimated divergence date at the Oligocene-Miocene boundary around 23.39 Mya (17.77–29.6 Mya, 95% highest posterior densities [HPD]) was given for the split between the Kenya Highlands (*K. excubitor*) clade and the AR clade (Fig. 3.4). A basal divergence of AR *Kinyongia* was estimated in the early Miocene at approximately 17.93 Mya (13.58–23.03 Mya, HPD) (Fig. 3.4). The species *K. mulyai* from the southern AR diverged from the Rwenzori Massif endemics (*K. carpenteri* and *K. xenorhina*) around 14.35 Mya (9.63–19.35 Mya, HPD). The two Rwenzori Massif endemic species were estimated to have diverged from each other in the late Miocene around 7.17 Mya (4.1–10.83 Mya, HPD). The root divergence of all lineages in the *K. adolfifriderici* clade was given in the mid-Miocene at 11.45 Mya (8.38–15.3 Mya, HPD). Divergence between *K. gyrolepis* and the Burundi + Uganda clade was dated in the late Miocene around 7.93 Mya (5.28–11.12 Mya, HPD). Topotypic *K. adolfifriderici* diverged from the Itombwe clade also in the late Miocene at 6.37 Mya (3.57–9.78 Mya, HPD). A split between the Burundi and Uganda clades was estimated to occur at the Miocene-Pliocene boundary around 5.05 Mya (2.89–7.63 Mya, HPD).

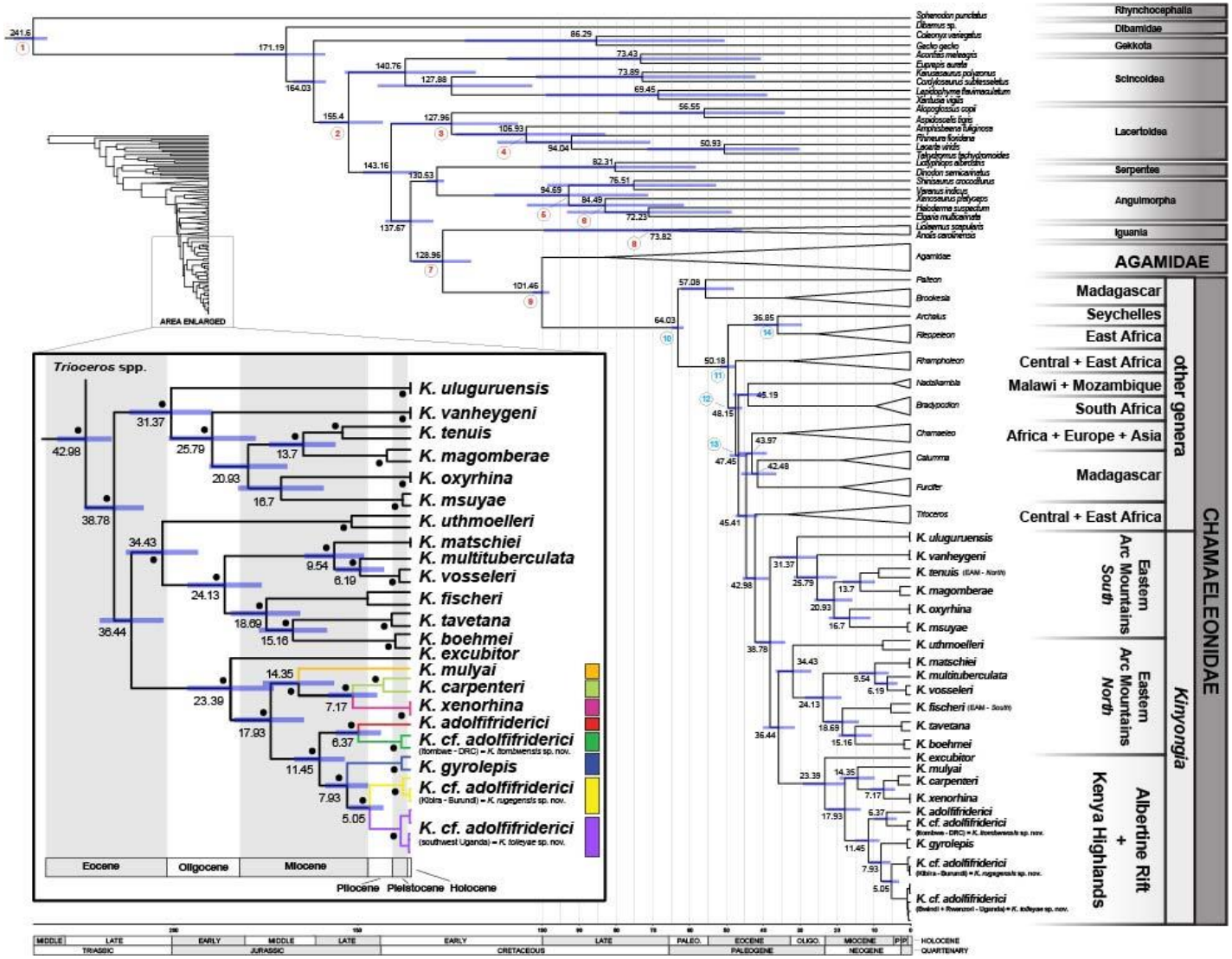

Figure 3.4 Bayesian chronogram of Chamaeleonidae. The genus *Kinyongia* (clade of interest) is expanded for greater detail (left). Posterior probabilities ≥ 95% are denoted by filled circles adjacent to nodes. Numbers above nodes denote mean highest posterior densities (HPD) and blue bars at nodes represent 95% HPD. Fossil-calibrated nodes are indicated with encircled red numbers and secondary calibrated nodes with encircled light blue numbers.

3.4.3 Morphological analyses

Analysis of 10 continuous characters extracted three principal components which accounted for 73.9% of the variation in the data set (see supplemental information [Table S3] in Hughes et al. [2017a]). The first component (PC1) loaded highest for cranial crest gap (CC) and head length (HL), the second (PC2) for snout length (SL) and mouth length (ML), and the third (PC3) for head height (HH) and eye diameter (ED). The MANOVA showed a significant difference between all species for PC1 ($F_{3,18} = 4.07$, $P = 0.023$). Posthoc pairwise comparisons showed differences between topotypic *K. adolfifriderici* and the Burundi specimens for PC1 ($P < 0.05$), and a near significant value between Burundi and Itombwe specimens for PC1 ($P = 0.07$). The scoreplot of the first two PCs regressed against body size (SVL) indicated that there is significant overlap for these continuous measurements, but some population clustering was discernable (i.e., Burundi and Itombwe) (Fig. 3.5). Overall, the morphological characters were conservative across the isolated populations, yet there seem to be some differences between populations in head dimensions and other measurements detailed below.

Burundi samples had a significantly larger average SVL ($t = 2.44$, df = 8, $P = 0.04$), and more upper ($t = 4.48$, df = 8, $P = 0.002$) and lower ($t = 3.11$, df = 8, $P = 0.014$) labial counts than topotypic Ituri samples. Burundi samples had significantly more upper labial counts ($t = 2.6$, df = 12, $P = 0.023$) than Uganda samples. Burundi samples had significantly more conical tubercles on the dorsal crest than Itombwe samples ($t = 4.56$, df = 6, $P = 0.004$). Uganda samples had significantly more upper ($t = 2.56$, df = 12, $P = 0.025$) and lower ($t = 2.59$, df = 12, $P = 0.023$) labial counts than topotypic Ituri samples. Itombwe samples had significantly more lower labial counts than topotypic Ituri samples ($t = 2.86$, df = 6, $P = 0.029$).

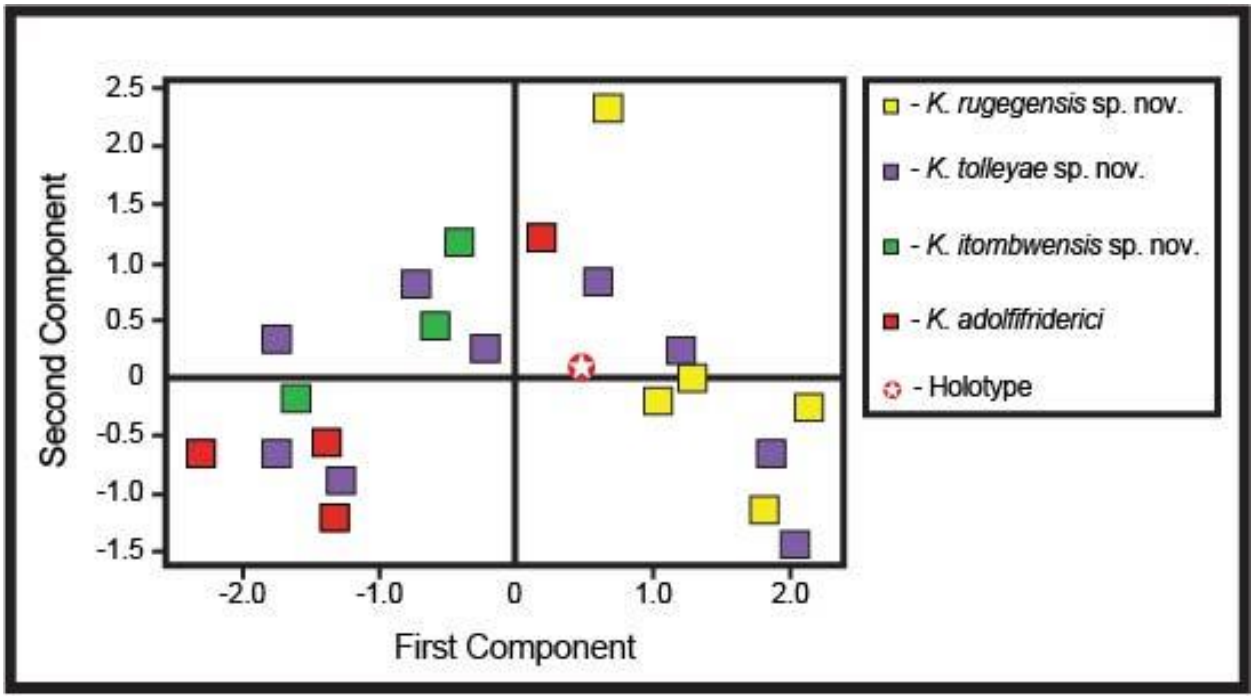

Figure 3.5 Scatterplot of the first two principal components extracted of morphological characters for species from the *Kinyongia adolfifriderici* group. The holotype for *K. adolfifriderici* (ZMB 22709) is indicated with a white star.

Size-corrected ANCOVA analyses detected a significant difference between Uganda and topotypic Ituri populations for snout length (SL), with Uganda samples larger than those from Ituri ($F_{1,13}$ = 14.11, P = 0.003) (Table 3.2). Moreover, a significant difference was found between Uganda and Itombwe samples for SL ($F_{1,11}$ = 6.09, P = 0.036), and values at significance for casque–eye length (CE) ($F_{1,11}$ = 5.08, P = 0.05), FLL ($F_{1,11}$ = 5.05, P = 0.05), and approaching significance for hind limb length (HLL) ($F_{1,11}$ = 4.36, P = 0.06), with Uganda samples having larger mean measurements than Itombwe samples for these four variables (Table 3.2). No size-corrected differences were detected between Burundi samples and topotypic Ituri samples. Size-corrected ANCOVA analyses detected significant differences between Burundi and Itombwe samples for forelimb length (FLL) ($F_{1,7}$ = 55.45, P = 0.001) and hind limb length (HLL) ($F_{1,7}$ = 13.83, P = 0.014), with Burundi samples having larger limbs than Itombwe samples (Table 3). Also, a value at significance between Burundi samples and Uganda samples was found for head

width (HW) ($F_{1,13} = 4.65$, $P = 0.05$), with Burundi samples larger than Uganda ones (Table 3). No size-corrected differences were detected between Itombwe samples and topotypic samples from Ituri. Given the small sample sizes, these results are preliminary and more analyses based on larger samples are warranted to determine if these differences reflect reliable characters. Regardless, these results demonstrate that there are multiple significant morphological differences between the populations.

3.4.4 Taxonomy

The presumably topotypic *K. adolfifriderici* genetic sample from Loki village is located in the Ituri rainforest, Orientale Province, DRC. This site is ca. 75 km (straight line distance) from present-day Irumu village, which is one of the sites provided by Sternfeld (1912) as the type locality for this species (see *Introduction*). Also, the sample was obtained at 1408 m elevation, which is well within the appropriate elevation range for the species (Tilbury, 2010). With putative topotypic genetic material for *K. adolfifriderici*, we are confident that the three geographically separated, genetically divergent lineages in the AR represent new species (Itombwe Plateau in southeastern DRC; Kibira National Park in northern Burundi; Bwindi Impenetrable and Rwenzori Mountains National Parks in western Uganda) (Fig. 3.2). Based on the combined molecular and morphological results presented above, and qualitative differences explained below, we describe three new species that were previously considered to be populations of *K. adolfifriderici*.

Table 3.2 Summary of meristic and mensural characters in adult type specimens of *Kinyongia rugegensis* sp. nov., *K. tolleyae* sp. nov., *K. itombwensis* sp. nov., and examined material of topotypic *K. adolfifriderici* (including the holotype). Linear measurements (in mm) and scale counts are given as mean ± standard deviation, followed by range in parentheses. M = adult male; F = adult female; NP = national park. See text for explanation of character abbreviations.

	Kinyongia rugegensis sp. nov. Kibira Forest NP, Burundi *n = 5* (2M, 3F)	*Kinyongia tolleyae* sp. nov. Bwindi + Rwenzori NPs, Uganda *n = 9* (2M, 7F)	*Kinyongia itombwensis* sp. nov. Itombwe Plateau, DRC *n = 3* (1M, 2F)	*Kinyongia adolfifriderici* Ituri rainforest, DRC *n = 5* (1M, 4F)[1]
SVL	55.9 ± 2.2 (52.8–58.7)	56.6 ± 5.7 (48.5–66.2)	51.1 ± 4.4 (46.1–54.8)	52.1 ± 2.7 (47.9–54.9)
TL	74.1 ± 10.8 (65.6–90.2)	69.4 ± 5.7 (64.0–75.6)	65.4 ± 2.2 (63.8–67.9)	66.4 ± 8.5 (56.4–76.3)
ToL	130.1 ± 12.2 (118.4–148.9)	125.9 ± 9.9 (112.7–141.4)	116.5 ± 5.1 (110.6–120.2)	117.1 ± 11.3 (104.3–131.2)
HL	16.6 ± 1.1 (15.4–18.2)	16.1 ± 0.9 (14.8–17.3)	15.1 ± 0.8 (14.4–15.9)	15.2 ± 0.7 (14.1–15.9)
HW	8.3 ± 0.5 (7.8–8.9)	7.9 ± 0.4 (7.3–8.6)	7.7 ± 0.7 (7.0–8.5)	7.6 ± 0.4 (7.2–8.2)
HH	9.8 ± 0.7 (8.9–10.5)	10.2 ± 0.8 (9.0–11.8)	9.1 ± 0.5 (8.7–9.6)	9.2 ± 0.8 (8.2–10.0)
ML	11.6 ± 1.0 (10.2–12.9)	12.3 ± 1.2 (10.3–13.6)	10.9 ± 1.2 (9.8–12.2)	11.8 ± 1.1 (10.1–13.1)
CE	7.1 ± 0.6 (6.5–7.9)	6.7 ± 0.3 (6.2–7.2)	6.1 ± 0.3 (5.8–6.4)	6.2 ± 0.4 (5.6–6.6)
SL	5.5 ± 0.5 (4.9–6.4)	5.7 ± 0.3 (5.1–6.0)	5.0 ± 0.4 (4.7–5.4)	4.9 ± 0.3 (4.4–5.3)
ED	5.5 ± 0.6 (4.9–6.3)	5.2 ± 0.2 (4.9–5.6)	4.9 ± 0.5 (4.4–5.3)	4.8 ± 0.4 (4.4–5.3)
CC	4.4 ± 0.3 (4.2–4.9)	3.5 ± 0.9 (2.2–4.7)	3.5 ± 0.5 (3.1–4.1)	3.1 ± 1.1 (2.2–4.7)
IL	31.4 ± 2.1 (27.7–32.9)	31.0 ± 3.9 (24.6–37.8)	28.2 ± 1.8 (26.1–29.6)	27.6 ± 2.4 (25.7–31.6)
FLL	11.3 ± 0.3 (10.9–11.6)	10.9 ± 0.9 (9.5–11.9)	9.3 ± 0.1 (9.2–9.4)	10.2 ± 0.8 (9.1–11.1)
HLL	10.4 ± 0.3 (10.1–10.8)	10.0 ± 0.8 (8.36–11.1)	8.6 ± 0.6 (7.9–9.1)	9.0 ± 0.8 (7.8–9.8)
UL	16.4 ± 0.9 (16–18)	14.7 ± 1.3 (13–17)	14.7 ± 1.5 (13–16)	12.6 ± 1.7 (10–14)
LL	15.8 ± 1.1 (14–17)	15 ± 0.9 (14–16)	15.7 ± 0.6 (15–16)	13.6 ± 1.1 (12–15)
TL/SVL	1.3 ± 0.2 (1.2–1.5)	1.2 ± 0.1 (1.1–1.4)	1.3 ± 0.1 (1.2–1.4)	1.3 ± 0.1 (1.1–1.4)

[1]Included in these data are measurements from the holotype (adult female) of *K. adolfifriderici* (ZMB 22709).

3.4.5 Descriptions of three new species

Family Chamaeleonidae *Gray, 1825*

Genus Kinyongia *Tilbury, Tolley and Branch, 2006*

Kinyongia rugegensis Hughes, Kusamba, Behangana and Greenbaum sp. nov.

Figs 3.1, 3.2, 3.3, 3.4, 3.6, 3.7A, 3.10; Tables 3.2, 3.3

Rugege Highlands forest chameleon

Synonymy.

Chamaeleo adolfi-friderici – Fischer and Hinkel, 1992: Figure 110 – Photograph in life and record for Nyungwe forest, Rwanda.

Bradypodion adolfi-friderici – Hinkel, 1993: Record for Cyamudongo forest, Rwanda.

Holotype. UTEP 21485 (field no. ELI 1156), adult female, BURUNDI, Bubanza Province, near Kibira National Park, Mpishi village, 03°4'11.064"S 29°29'4.02"E, 1660 m elevation, 20 December 2011, collected by E. Greenbaum, C. Kusamba, M.M. Aristote, and W.M. Muninga (Fig. 3.6A).

Paratopotypes. Same collection details as holotype, one adult male, UTEP 21481 (field no. ELI 1155) (Fig. 3.6B), and another adult male, UTEP 21482 (field no. ELI 1238), collected on 23 December 2011 (Fig. 3.6C).

Paratypes. One adult female, UTEP 21483 (field no. ELI 1220), BURUNDI, Bubanza Province, Kibira National Park, Mpishi village, 03°3'42.372"S 29°29'36.348"E, 1986 m elevation, 22 December 2011, collected by same collectors of holotype; one adult female, UTEP 21484 (field no. ELI 1256), BURUNDI, Kayanza Province, Kibira National Park, near Rwegura village, 02°56'20.292"S 29°29'54.78"E, 2130 m elevation, 25 December 2011, collected by E. Greenbaum, M.M. Aristote, and W.M. Muninga (Fig. 3.6D).

Diagnosis. Kinyongia rugegensis sp. nov. can be distinguished from all other *Kinyongia* species by the following combination of traits: (1) lack of rostro-nasal ornamentation in both sexes; (2) moderate body size (mean SVL = 55.9 mm); (3) anterior dorsal keel with 8–10 conical tubercles; (4) a slightly elevated casque that tapers posteriorly to a prominent apex; (5) absence of a gular and ventral crest; (6) 16–18 upper and 15–17 lower labials; (7) generally flat shape of the upper casque; (8) tail length longer than SVL in both sexes; (9) indistinct parietal crest with slightly raised tubercles; (10) background body coloration in adult females generally green to yellow-green with darker pigmented regions on the flanks and tail; background body coloration in adult males generally brown with tan and yellow speckling on the flanks; (11) interstitial skin between the tubercles of the body generally black for both sexes; (12) a light brown stripe passes through the middle of the eye and extends from the canthal ridge to the temporal crest; (13) top of the head is typically a darker green/brown color than elsewhere; (14) the gular region is distinctly lighter in color, with a combination of green, white, and tan.

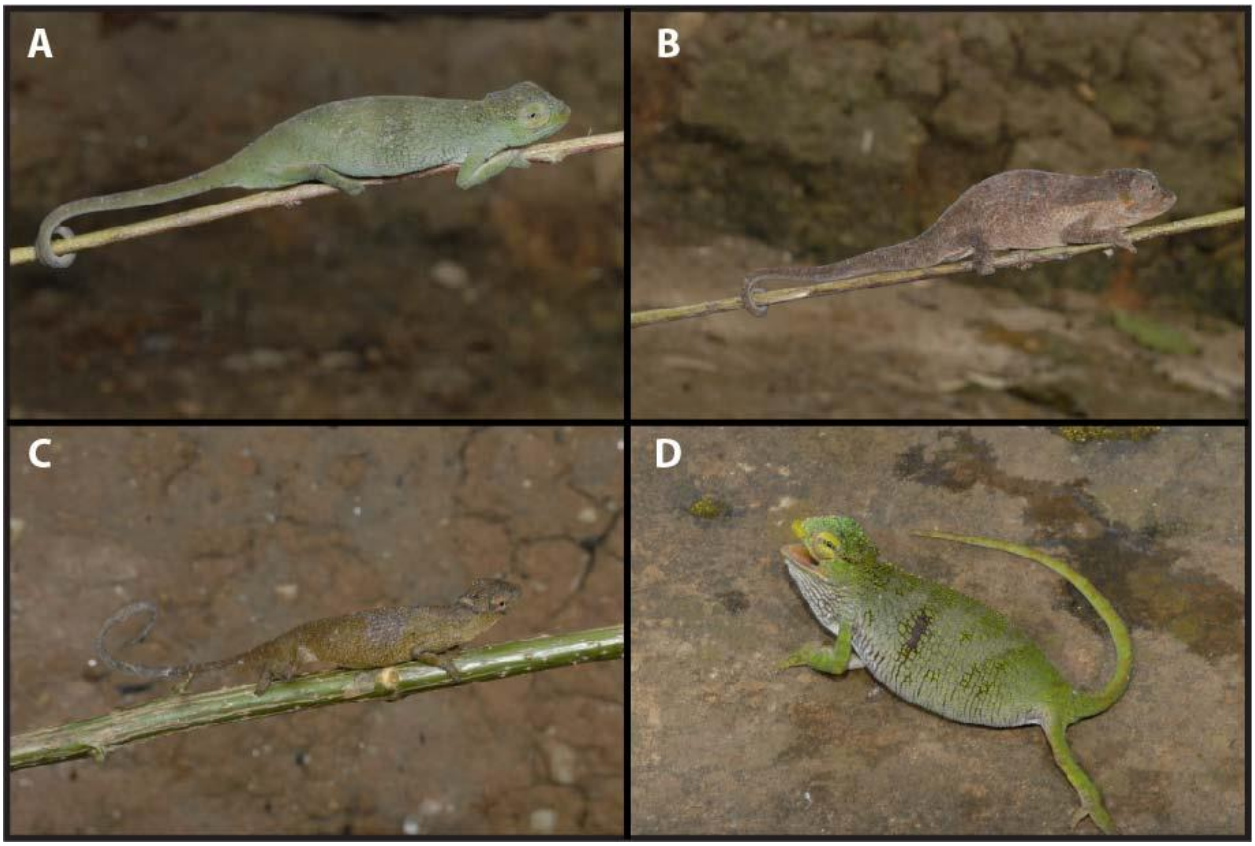

Figure 3.6 Photographs of various individuals of *Kinyongia rugegensis* sp. nov. in life. (A) – Adult female (gravid) lateral view of holotype (UTEP 21485); (B) – Adult male lateral view (UTEP 21481); (C) – Adult male lateral view (UTEP 21482); (D) – Adult female (gravid) in aggressive posture and coloration (UTEP 21484).

Differential diagnosis. A medium-sized forest chameleon that is distinguished from most congeners by the absence of a rostral process in both sexes (*K. asheorum*, *K. boehmei* [Lutzmann and Nečas, 2002], *K. carpenteri*, *K. fischeri*, *K. magomberae* Menegon et al. [2009], *K. matschiei* [Werner, 1895], *K. msuyae* Menegon et al. [2015], *K. multituberculata* [Nieden, 1913], *K. oxyrhina* [Klaver and Böhme, 1988], *K. tavetana* [Steindachner, 1891], *K. tenuis* [Matschie, 1892], *K. uluguruensis* [Loveridge, 1957], *K. uthmoelleri* [Müller, 1938], *K. vanheygeni* Nečas, 2009, *K. vosseleri* [Nieden, 1913], and *K. xenorhina*). The new species can be distinguished from *K. adolfifriderici* by its larger cranial crest gap and head length, larger body size (52.8–58.7 mm versus 47.9–54.9 mm), and more upper (16–18 versus 10–14) and lower labials (14–17 versus 12–

15). The new species can be distinguished from *K. tolleyae* sp. nov. by the lack of two distinctly bulging and rounded portions of the upper casque, slightly larger head width, larger fleshy papillae medial to rotulae on hemipenis, and more upper labials (16–18 versus 13–17). The new species can be distinguished from *K. itombwensis* sp. nov. by its larger fore- and hind limbs, slightly larger cranial crest gap and head length, and more conical tubercles on the dorsal crest (8–10 versus 6–7). The new species can be distinguished from *K. mulyai* and *K. excubitor* by the presence of a dorsal crest with 8–10 conical tubercles and marked mitochondrial sequence divergence. The new species can be distinguished from *K. gyrolepis* by its smaller mean body size (55.9 mm versus 67.3 mm) and current distribution in moist Afromontane rainforest.

Genetic differentiation and variation. A summary of pairwise sequence divergence for each molecular marker (16S, ND2, and RAG1) among individuals of *K. rugegensis* sp. nov. and other species of *Kinyongia* endemic to the AR are presented in Table S2 (see supplemental information [Table S2] in Hughes et al. [2017a]). For the ND2 locus, *p*-distances among *K. rugegensis* sp. nov. samples ranged 0.1–0.7%.

Description of holotype. Adult female, SVL 56.6 mm and TL 67.3 mm. Four oviductal eggs present (see *Reproduction* below). Casque low, slightly raised above nape. Distinct, elevated apex on posterior casque. Neck distinct from head. Parietal crest largely indistinct with few enlarged and flattened tubercles in an inconsistent pattern. Supra-orbital ridges mostly smooth. Temporal crest comprises three enlarged tubercles extending posteriorly from mid-eye and ascending along posterior ridge of casque to its apex. Nares open laterally and in a posterior orientation. Canthal ridge consists of four slightly raised tubercles, one raised higher than others

near snout. Sixteen upper and 14 lower labials are present along tip of snout to posterior margin of orbit. No gular or ventral crests present. Nine small conical tubercles present on anterior portion of dorsal crest, absent near mid-body. Tail and lateral flanks smooth. Body covered in nearly homogenous, flattened tubercles. Some larger polygonal tubercles present on dorsal flanks. Patches of small tubercles in rosette patterns on ventral flanks. Some enlarged flattened tubercles present on outer portions of limbs. Claws typical of *Kinyongia* species.

Coloration of holotype (in ethanol). Photographs of the body and head detail of the holotype (in preservative) are presented in Fig. 3.10. The background coloration is grayish blue with some darker blotches on the flanks and tail. Patches of lighter blues and greens are present near the anterior portions of the body, and the sides of the head and tail. Light yellow (almost white) patches occur near axillary and inguinal regions and a few places on the lateral body flanks. The soles of the feet are yellowish-white.

Coloration of holotype (in life). A photograph of the holotype (in life) is presented in Fig. 3.6A. The top of the head is covered in brown and dark green tubercles with black interstitium. Beginning below the temporal crest, the head is lighter green in color and covered in yellowish-green tubercles with powder-blue interstitium. At mid-eye, there is a dark brown lateral stripe that connects the coloration on the canthal ridge to the temporal crest. Near the tip of the snout is a pronounced yellow coloration that fades posteriorly. The background coloration of the body is yellowish-green with black interstitium. The powder-blue coloration of the head interstitium extends posteriorly on the ventral flanks and gradually changes to black by mid-body, then blue reappears on the posterior third of the body. Tubercles on the venter, near axillary and inguinal

regions, and hidden parts of the limbs, are off-white with flecks of green. The dorsal crest is adorned with darker green tubercles than elsewhere on the body and this coloration extends onto the tail. The posterior third of the tail is darker brown and the greenish coloration of the tail, in general, is less bright compared to the body. Differential distribution of interstitial coloration (light blue or black) on the body forms broad vertical dark brown bands.

Hemipenis. Hemipenal drawings and description are based on specimen UTEP 21481. Line drawings depicting the general hemipenis morphology of *K. rugegensis* sp. nov. are presented in sulcal and lateral views (Fig. 3.7A). Hemipenes are calvate and the pedicel is less than one fifth of the hemipenis length. The truncus is covered with calcyes ranging in size from smaller on the asulcal apex to larger ones near the asulcal pedicel. Distal calcyes are smaller and more hexagonal in shape. The sulcal lips and sulcus spermaticus are smooth and devoid of ornamentation. The flesh on the sulcus is highly envaginated (folded), forming numerous sulcal ridges. Sulcal lips diverge towards the apex and continue as a ridge that encircles the apex. The apex is bilobed and each lobe possesses a large, sharply denticulated rotulae. A sizeable protuberant fleshy papilla is positioned medially from each rotulae.

Table 3.3 Descriptive morphometrics (measurements and meristic counts) for adult type specimens of *Kinyongia rugegensis* sp. nov. See text for explanation of character abbreviations.

	UTEP 21485 Holotype Female[1]	UTEP 21481 Paratopotype Male	UTEP 21482 Paratopotype Male	UTEP 21483 Paratype Female	UTEP 21484 Paratype Female[1]
SVL	56.6	55.0	58.7	56.8	52.8
TL	67.3	80.4	90.2	67.1	65.6
ToL	123.9	135.4	148.9	123.8	118.4
HL	15.4	16.7	18.2	16.6	15.9
HW	7.8	8.3	8.9	8.8	7.9
HH	8.9	10.5	10.3	10.3	9.2
ML	10.2	11.4	13.0	12.0	11.6
CE	6.7	7.9	7.5	7.1	6.5
SL	5.1	5.0	6.4	5.5	5.5
ED	5.0	6.3	6.0	5.3	4.9
CC	4.3	4.2	4.9	4.5	4.4
IL	32.9	31.3	32.8	32.0	27.7
FLL	11.3	11.6	11.4	10.9	11.0
HLL	10.2	10.8	10.2	10.6	10.1
UL	16	16	18	16	16
LL	14	16	16	16	17
CTD	9	9	10	8	10
TL/SVL	1.2	1.5	1.5	1.2	1.2

[1]Enlarged ovarian follicles present in body cavity of specimen.

Variation. Descriptive morphometrics of *K. rugegensis* sp. nov. are presented in Table 3.3, and a summary of mean measurements in Table 3.2. Chameleon photographs displaying color variation in life are presented in Fig. 3.6. Morphological proportions in paratopotypes and paratypes are generally consistent with those in the holotype. Males have longer tails than females (M: 85.3 ± 6.9 [80.4–90.2 mm, $n = 2$]; F: 66.7 ± 0.9 [65.6–67.3 mm, $n = 3$]) ($P < 0.01$), but similar body sizes (M: 56.9 ± 2.6 [55.0–58.7 mm, $n = 2$]; F: 55.4 ± 2.3 [52.8–56.8 mm, $n = 3$]) ($P > 0.05$). Males have an overall yellowish-brown background coloration, in contrast to the lighter green color of females. When agitated, the tip of the snout, eye skin, and various regions on the flanks can be brightly colored with yellow. One female (UTEP 21484) in an aggressive posture and coloration with an open mouth, showed a dark patch laterally at mid-body, white gular and ventral regions, and bright yellow areas on the head (Fig. 3.6D).

Reproduction. The holotype (UTEP 21485) with SVL 56.6 mm and TL 67.3 mm collected on 23 December 2011 was gravid. This individual contained four oviductal (shelled) eggs with mean dimensions (in mm), length 12.75 ± 0.21 (range: 12.49–12.93) and width 6.49 ± 0.25 (range: 6.31–6.84). Exact measurements of eggs were as follows: 12.65 L x 6.84 W; 12.49 L x 6.32 W; 12.91 L x 6.49 W; 12.93 L x 6.31 W. This individual had moderate fat bodies. Another female (UTEP 21484) with SVL 52.8 mm and TL 55.6 mm collected on 25 December 2011 was also gravid. This individual contained four enlarged, yolked ovarian follicles with mean dimensions (in mm), length 7.09 ± 0.19 (range: 6.83–7.25) and width 5.48 ± 0.26 (range: 5.2–5.83). Exact follicular measurements were as follows: 7.25 L x 5.43 W; 7.19 L x 5.2 W; 6.83 L x 5.83 W; 7.09 L x 5.44 W. This individual possessed extensive fat bodies. Conversely, a female (UTEP 21483) with SVL 58.8 mm and TL 67.1 mm collected on 22 December 2011 was not gravid, as

demonstrated by the largest ovarian follicles measuring < 3 mm in diameter and lacking evidence of yolk. This individual had minor fat bodies.

All males had darkly pigmented testes (i.e., black coloration), which is characteristic of all chameleon species examined to date (Tolley and Herrel, 2013). All collected males were sexually mature. One male (UTEP 21481) with SVL 55.0 mm and TL 80.4 mm collected on 20 December 2011 had enlarged testes. The right testis of this individual measured 6.89 mm in length and 5.04 mm in width. Another male (UTEP 21482) with SVL 58.7 mm and TL 90.2 mm collected on 23 December 2011 also had enlarged testes. The right testis of this individual measured 6.45 mm in length and 4.51 mm in width. Fat bodies were minor for both of these individuals.

Diet. All five specimens examined for gut contents had remains of arthropod prey items that could be identified to order. The stomach of one female (UTEP 21484) contained Hemiptera, Lepidoptera, Hymenoptera, and Coleoptera. A second female (UTEP 21485) stomach contained Diptera, Hemiptera, Araneae, and Acari. The stomach of a third female (UTEP 21483) contained Araneae, Orthoptera, and Hemiptera. A male (UTEP 21481) stomach contained Diptera and Hemiptera. Another male (UTEP 21482) stomach contained Diptera, Hemiptera, Araneae, and Psocoptera.

Distribution and natural history. *Kinyongia rugegensis* sp. nov. is found in moist Afrotemperate montane and sub-montane forests at an elevation range from 1660–2130 m. Most specimens were collected from forest edges near and inside Kibira National Park. This montane forest extends from southern Rwanda (Nyungwe Forest National Park) to northern Burundi (Kibira National Park). We speculate that this new species is present throughout the Rugege Highlands in

areas of suitable forest habitat. For example, Hinkel (1993) recorded *Bradypodion adolfi-friderici* (= *Kinyongia adolfifriderici*) from both Nyungwe and Cyamudongo forests (= Nyungwe Forest National Park) in Rwanda, and these records potentially represent this new species. Two specimens (UTEP 21482 and UTEP 21483) were collected inside a banana tree plantation just outside of the national park. One specimen (UTEP 21484) was collected from natural roadside vegetation, and was found ca. 2.5 m above ground in a small tree. Two of the three females were gravid, and both males were sexually mature. No juveniles were detected during the search period (ca. 3.5 weeks). Behavior and activity patterns are essentially unknown, but likely similar to that of *K. adolfifriderici* (Tilbury, 2010). Other lizard species collected near the type locality included typical AR lizard fauna, including *Adolfus africanus*, *Chamaeleo dilepis*, *Congolacerta vauereselli*, *Hemidactylus mabouia*, *Lygodactylus* cf. *gutturalis*, *Rhampholeon boulengeri*, *Trioceros ellioti*, *T. johnstoni*, *Trachylepis striata*, and *T. maculilabris*.

Conservation. Nyungwe Forest National Park is the largest protected area in Rwanda, and Kibira National Park is the largest protected area in Burundi. Together these contiguous parks form one of the largest montane forest blocks in eastern Africa (Barakabuye et al., 2007). However, despite this high level of connectivity, similarity of threats, and biodiversity importance, these forests have been managed in near isolation to the neighboring protected areas (Barakabuye et al., 2007). The highlands of these countries are renowned for their nutrient rich soils. As a result, the regions are burdened with extremely dense human populations that greatly threaten the biological integrity of the remaining forests with severe agricultural pressures. Moreover, a longstanding history of armed conflict in the region has left a legacy of irreparable anthropogenic damage in these fragile ecosystems (Kanyamibwa, 1998).

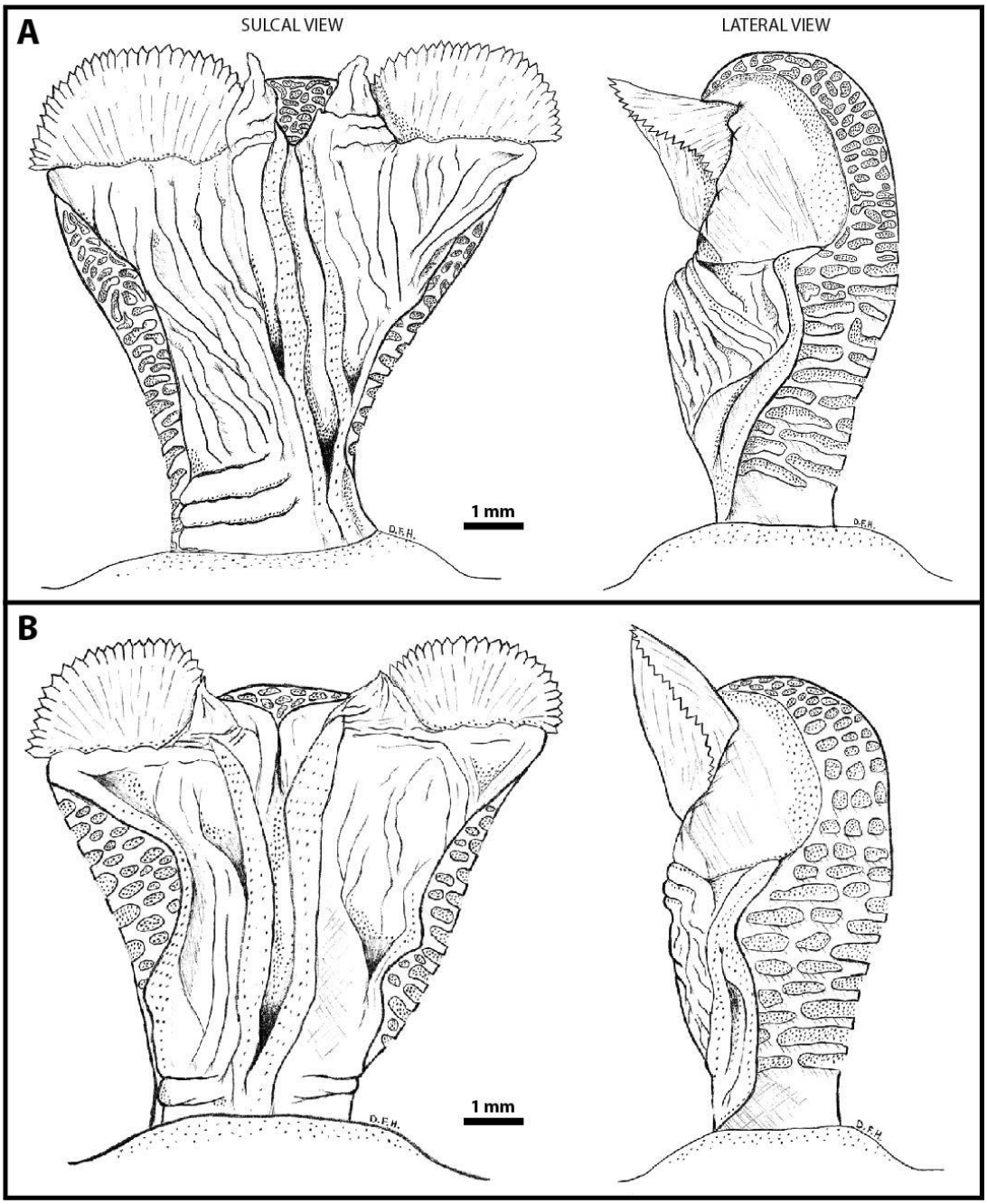

Figure 3.7 Sulcal and lateral views of the male hemipenes. (A) – *Kinyongia rugegensis* sp. nov. (UTEP 21481) demonstrating large fleshy papillae medial to large rotulae; (B) – *Kinyongia tolleyae* sp. nov. (UTEP 21488) illustrating small fleshy papillae medial to large rotulae.

Etymology. The specific epithet is derived from Rugege Highlands, the greater mountainous region where the species was collected, with the Latin suffix *–ensis* denoting a place or locality. Although the holotype was collected from Kibira National Park in northern Burundi,

this Afromontane forest is contiguous with Nyungwe Forest National Park in Rwanda via the Rugege Highlands. This new species likely occurs in suitable forested habitat across this mountain range. The view that these neighboring protected areas are independent is outdated, and unfortunately, park management in bordering countries has sustained this position for some time (Barakabuye et al., 2007). Thus, we felt that the taxonomy should reflect the natural connectivity of the region and chose a broader name accordingly.

Family Chamaeleonidae *Gray, 1825*

Genus Kinyongia *Tilbury, Tolley and Branch, 2006*

Kinyongia tolleyae Hughes, Kusamba, Behangana and Greenbaum sp. nov.

Figs 3.1, 3.2, 3.3, 3.4, 3.7B, 3.8, 3.10; Tables 3.2, 3.4

Tolley's forest chameleon

Synonymy.

Chamaeleo adolfifriderici – Drewes and Vindum, 1998: Table 1, Figure 3 – Photograph in life and basic collection details.

Chamaeleo adolfifriderici – Vonesh, 2001: Table 3 – Record for Kibale National Park.

Kinyongia adolfifriderici – Tilbury et al., 2006: Table 1, Figure 2 – Phylogenetic position.

Kinyongia adolfifriderici – Menegon et al., 2009: Figure 1 – Phylogenetic position.

Kinyongia adolfifriderici – Branch and Tolley, 2010: Figure 4 – Phylogenetic position.

Kinyongia adolfifriderici – Tilbury, 2010: Figure 376 – Photograph in life.

Kinyongia adolfifriderici – Townsend et al., 2011: Figure 1 – Phylogenetic position.

Kinyongia adolfifriderici – Tolley et al., 2011: Figures 2, 3, 4 – Phylogenetic position.

Kinyongia adolfifriderici – Tolley et al., 2013: Figures 1, 2 – Phylogenetic position.

Kinyongia adolfifriderici – Greenbaum et al., 2012a: Figure 2, Appendix II – Phylogenetic position and genetic distances.

Kinyongia adolfifriderici – Tilbury and Tolley, 2015: Figure 4 – Phylogenetic position.

Kinyongia adolfifriderici – Menegon et al., 2015: Figure 3 – Phylogenetic position.

Holotype. UTEP 21490 (field no. ELI 2755), adult female, UGANDA, Western Region, Kigezi sub-region, Kabale District, Bwindi Impenetrable National Park, near Ruhija village, 01°2'54.096"S 29°46'36.624"E, 2284 m elevation, 26 May 2014, collected at night from natural vegetation along a roadside near Institute for Tropical Forest Conservation (ITFC) by C. Kusamba, M.M. Aristote, and W.M. Muninga (Fig. 3.8E).

Paratopotypes. Same collection details as holotype, two adult females, UTEP 21486 (field no. ELI 2754) and UTEP 21487 (field no. ELI 2788 [28 May 2014]), collected at night from forest edges ca. 3 m above ground along a road to ITFC, and one adult male, UTEP 21488 (field no. ELI 2756), collected at night with aid of stick from ca. 5 m above ground in sleeping perch of tree behind ITFC (main office) by D.F. Hughes, K.A. Tolley, S. Davies, and A.A. Turner.

Paratype. One adult male, UTEP 21489 (field no. ELI 2827), UGANDA, Western Region, Rwenzururu sub-region, Kasese District, near Rwenzori Mountains National Park, Ruboni village, 00°20'58.992"N 30°1'47.028"E, 1655 m elevation, 31 May 2014, collected at dusk from ca. 3 m above ground in sleeping perch of vegetation (secondary forest) in front of the Ruboni Community Hotel by D.F. Hughes, E. Greenbaum, and M. Behangana.

Referred specimens. One adult female (CAS 176920 [field no. JVV-1367]), UGANDA, Western Region, Kigezi sub-region, Kabale District, Bwindi Impenetrable National Park, Mubwindi Swamp, ca. 120 m south of swamp, 2133 m elevation, 01º4'12"S 29º45'0"E, 9 December 1990, collected ca. 60 cm above ground on fern by J.P. O'Brien and J.V. Vindum. Three adult females (CAS 201593–95 [field nos. JVV-4058–59, 4577]), UGANDA, Western Region, Kigezi sub-region, Kabale District, Bwindi Impenetrable National Park, ITFC near Ruhija village, 2362 m elevation, 1º2'47.8"S 29º46'28.5"E, 12 September 1996 (CAS 201593–94) and 18 October 1996 (CAS 201595), collected at night ca. 3 m above ground on road-cut vegetation (CAS 201593–94) and ca. 2 m above ground in bush (CAS 201595) by J.V. Vindum (CAS 201593–94), and R.C. Drewes and J.V. Vindum (CAS 201595).

Diagnosis. Kinyongia tolleyae sp. nov. can be distinguished from all other *Kinyongia* species by the following combination of traits: (1) lack of rostro-nasal ornamentation in both sexes; (2) moderate body size (mean SVL = 56.6 mm); (3) anterior dorsal keel with 5–10 conical tubercles; (4) casque slightly elevated above the nape; (5) two smooth, expanded areas present on the casque that appear bilobed when viewed from above; (6) absence of both a gular and ventral crest; (7) 13–17 upper and 14–16 lower labials; (8) tail length longer than SVL in both sexes; (9) parietal crest with several slightly raised tubercles that fork towards the snout; (10) background coloration of the body in adult females is generally light green to yellow-green; background coloration of the body in adult males is generally light brown with anteriorly positioned green patches and peach speckling near the head; (11) large dark brown patches with white centers are present on the lateral flanks of adult females and these lateral patches are typically oriented with a

larger patch positioned anteriorly and sometimes a second smaller patch positioned posteriorly from mid-body; (12) areas of darker brown pigment cover the cloacal region and extend distally onto hidden parts of the hind limbs and tail in adult females; (13) interstitial skin between the tubercles on the body is generally white and sometimes green for both sexes; (14) a brown stripe passes through the middle of the eye and extends from the canthal ridge to the temporal crest, and the eye skin above and below the stripe is powder blue/teal, gradually dissipating dorsally and ventrally; (15) the top of the head is somewhat darker green than elsewhere; (16) gular region and ventral portions of the body are distinctly off-white.

Differential diagnosis. A medium-sized forest chameleon that is distinguished from most other congeners by the absence of a rostral process in both sexes (*K. asheorum*, *K. boehmei*, *K. carpenteri*, *K. fischeri*, *K. magomberae*, *K. matschiei*, *K. msuyae*, *K. multituberculata*, *K. oxyrhina*, *K. tavetana*, *K. tenuis*, *K. uluguruensis*, *K. uthmoelleri*, *K. vanheygeni*, *K. vosseleri*, and *K. xenorhina*). The new species can be distinguished from *K. adolfifriderici* by its larger snout length, and more upper (13–17 versus 10–14) and lower (14–16 versus 12–15) labials. The new species can be distinguished from *K. rugegensis* sp. nov. by the presence of two distinctly expanded and smooth portions of the upper casque (bilobed appearance), slightly smaller head width, fewer upper labials (13–17 versus 16–18), and smaller fleshy papillae medial to rotulae on hemipenis. The new species can be distinguished from *K. itombwensis* sp. nov. by its larger snout length, slightly larger forelimbs and casque–eye distance, and generally more conical tubercles on the dorsal crest (5–10 versus 6–7). The new species can be distinguished from *K. mulyai* and *K. excubitor* by the presence of a dorsal crest with 5–10 conical tubercles and marked mitochondrial

sequence divergence. The new species can be distinguished from *K. gyrolepis* by a smaller mean body size (56.6 mm versus 67.3 mm) and current distribution in moist Afromontane rainforest.

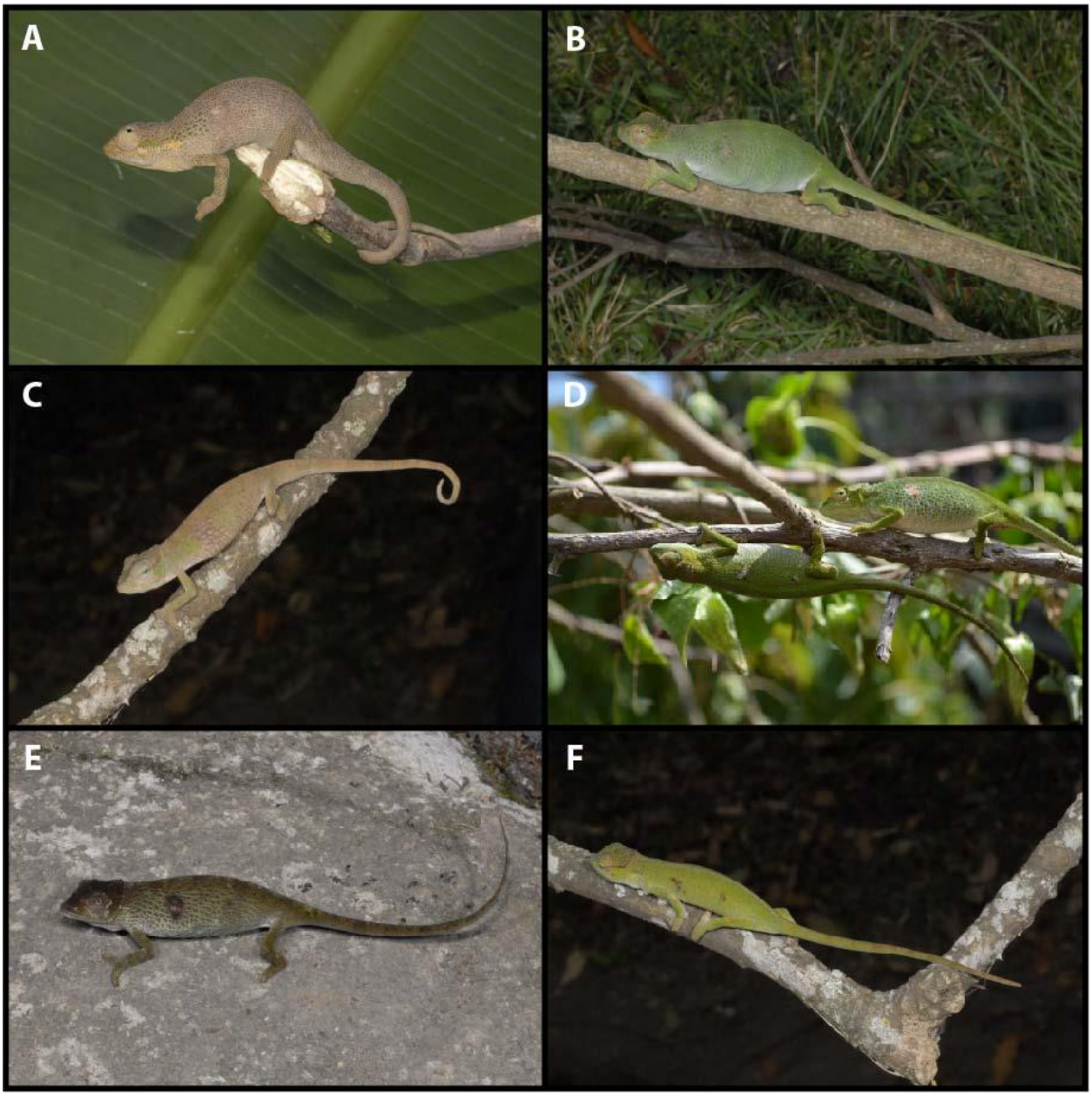

Figure 3.8 Photographs of various individuals of *Kinyongia tolleyae* sp. nov. in life. (A) – Adult male lateral view (UTEP 21489) from Rwenzori Mountains National Park; all others from Bwindi Impenetrable National Park; (B) – Adult female (gravid) lateral view (UTEP 21487); (C) – Adult male lateral view (UTEP 21488); (D) – Two adult females (UTEP 21486, UTEP 21490) in presence of male (not pictured); (E) – Adult female displaying dark coloration (UTEP 21490); (F) – Adult female lateral view (UTEP 21486).

Table 3.4 Descriptive morphometrics (measurements and meristic counts) for adult type specimens of *Kinyongia tolleyae* sp. nov. See text for explanation of character abbreviations.

	UTEP 21490 Holotype Female[1]	UTEP 21486 Paratopotype Female	UTEP 21488 Paratopotype Male	UTEP 21487 Paratopotype Female[1]	UTEP 21489 Paratype Male	CAS 176920 Paratopotype Female	CAS 201593 Paratopotype Female[1]	CAS 201594 Paratopotype Female[1]	CAS 201595 Paratopotype Female
SVL	52.9	51.5	48.5	60.0	51.6	66.2	59.5	59.9	58.9
TL	75.6	64.3	64.2	75.4	65.8	75.2	64.8	75.6	64.0
ToL	128.5	115.8	112.7	135.4	117.3	141.4	124.3	135.5	122.9
HL	16.7	14.8	14.9	16.4	15.8	17.3	16.4	16.9	15.9
HW	8.2	97.7	7.3	8.6	7.7	8.2	7.8	8.1	8.0
HH	10.0	9.0	9.3	10.0	9.5	11.8	10.6	10.6	10.6
ML	12.3	10.6	10.3	12.9	11.5	13.3	13.5	13.6	12.4
CE	7.2	6.7	6.3	6.9	6.7	6.8	6.2	6.7	6.4
SL	6.0	5.1	5.3	5.9	5.7	5.8	5.7	6.0	5.6
ED	5.1	4.9	5.3	5.6	5.3	5.5	5.3	5.0	5.0
CC	4.7	4.1	3.7	4.6	4.3	3.4	2.2	2.5	2.4
IL	28.3	28.3	24.6	32.2	28.7	37.8	32.7	32.8	33.8
FLL	11.8	10.4	9.5	12.0	11.6	11.5	10.2	10.6	10.3
HLL	10.1	9.9	8.4	11.1	10.8	10.6	10.2	9.9	9.4
UL	15	16	17	15	15	13	14	14	13
LL	16	16	16	15	15	15	14	14	14
CTD	9	5	9	5	10	-	-	-	-
TL/SVL	1.4	1.2	1.3	1.3	1.3	1.1	1.1	1.3	1.1

[1]Enlarged ovarian follicles present in body cavity of specimen. Eggs and CTD were not evaluated for CAS specimens.

Genetic differentiation and variation. Summary of pairwise sequence divergence for each molecular marker (16S, ND2, and RAG1) among individuals of *K. tolleyae* sp. nov. and other species of *Kinyongia* endemic to the AR are presented in Table S2 (see supplemental information [Table S2] in Hughes et al. [2017a]). For the ND2 locus, *p*-distances among *K. tolleyae* sp. nov. samples ranged from 0.0–1.4%.

Description of holotype. Adult female, SVL 52.9 mm and TL 75.6 mm. Four rounded ovarian follicles present (see *Reproduction* below). Casque slightly elevated above nape. Posterior apex of casque present, overhanging nape. Two distinct expanded areas of flattened tubercles present on top of casque, bilobed appearance. Neck distinct from head. Parietal crest consists of four discrete, enlarged tubercles extending posteriorly as a ridge to apex of casque. Supra-orbital ridges mostly smooth and one larger conical tubercle near dorsal posterior margin of orbit present. Temporal crest consists of three enlarged tubercles extending posteriorly from mid-eye and ascending posteriorly along ridge of casque to apex. Nares open laterally and posteriorly. Canthal ridge consists of five raised tubercles descending from eye towards snout. Fifteen upper and 16 lower labials present along tip of snout to posterior margin of orbit. No gular or ventral crests present. Nine raised conical tubercles present on anterior portion of dorsal crest, absent near mid-body. Tail and lateral flanks smooth. Body covered in nearly homogenous, flattened tubercles. Some larger polygonal tubercles present dorsally on flanks. Rosette patches of smaller tubercles on ventral portion of body. Mostly enlarged flattened tubercles present on outer portions of limbs. Claws typical of *Kinyongia* species.

Coloration of holotype (in ethanol). Photographs of the body and head detail of the holotype (in preservative) are presented in Fig. 3.10. The background coloration is various shades of blue with darker gray-blue areas covering some dorsal parts of the body and tail. The venter, beginning below nape and extending near the cloacal region, is a pink to off-white coloration. Patches of lighter blues are present behind the eye, near commissure of mouth, side and top of casque, tail, and hind limbs. A large portion, about midway on tail, is off-white. The axillary and inguinal regions are lighter blue-green than elsewhere on body. The soles of the feet are yellowish-white.

Coloration of holotype (in life). A photograph of the holotype (in life) is presented in Fig. 3.8E. The following description is based on color photographs of the holotype, which were taken when the animal was in a slightly defensive display with an overall darker body color (Fig. 3.8E). See *Diagnosis* of *K. tolleyae* sp. nov. for description of more normal coloration, and see photos of other individuals in various physiological states (Fig. 3.8). The top of the head is covered in dark brown tubercles with black interstitium. The head is lighter in color beginning below the temporal crest to canthal ridge, and covered in light brown and yellowish-green tubercles with off-white interstitium. At mid-eye, there is a dark brown lateral stripe that connects the coloration on the canthal ridge to the temporal crest. The eye skin is dark brown and resembles that of the top of head. Labial scales are heterogeneous in color with hues of red. The gular region is off-white, and this coloration extends across the venter and parts of the tail. Areas of darker brown pigment cover the cloacal region, hidden parts of the hind limbs, and part of the tail. Area below jaw on gular is peach color. The background coloration of the body is greenish-brown with off-white to green interstitium. The ventral flanks are adorned with a large dark-brown patch of coloration, positioned

slightly anterior from mid-body. The center of the patch is lighter than the black edges, and almost orange in color. Several faint dark brown vertical bands begin on the dorsal keel and quickly fade ventrally, not to reach mid-body. Smaller body tubercles form rosettes, with light green color filling spaces between tubercles. Tubercles near axillary and inguinal regions, and hidden parts of the limbs, are white with flecks of green. The dorsal crest is ornamented with darker tubercles than elsewhere and this pattern extends onto the tail. The posterior third of the tail is darker green than the rest of the tail, and faint vertical dark brown bands are present, especially towards the distal end of the tail.

Hemipenis. Hemipenal drawings and description are based on specimen UTEP 21488. Line drawings depicting the general hemipenis morphology of *K. tolleyae* sp. nov. are presented in sulcal and lateral views (Fig. 3.7B). The hemipenis of this new species is very similar to that of *K. rugegensis* sp. nov., except that it possesses smaller fleshy papillae medial to each large rotulae. See *Hemipenis* of *K. rugegensis* sp. nov. for description of hemipenis morphology.

Variation. Descriptive morphometrics of *K. tolleyae* sp. nov. are presented in Table 3.4 and a summary of mean measurements in Table 3.2. Chameleon photographs displaying color variation in life are presented in Fig. 3.8. Morphological proportions in paratopotypes and paratypes are generally consistent with those in the holotype. Males and females have similarly sized tails (M: 65.0 ± 1.1 [64.2–65.8 mm, n = 2]; F: 70.7 ± 5.9 [64.0–75.6 mm, n = 7) ($P > 0.05$), but males have smaller body sizes (M: 50.1 ± 2.2 [48.5–51.6 mm, n = 2]; F: 58.4 ± 4.9 [51.5–66.2 mm, n = 7]) ($P = 0.03$). Males have an overall brown background coloration with green pigmented patches anteriorly, in contrast to the light green background coloration of females, which are

largely devoid of brown pigment. Females possess a dark patch (sometimes two) of coloration on the lateral flanks of the body with a lighter center, whereas males do not possess this feature. When agitated, the lateral patches, eye skin, and dorsal region of the head darkened (Fig. 3.8E).

Reproduction. The female holotype (UTEP 21490) with SVL 52.9 mm and TL 75.6 mm collected on 26 May 2014 was in the early stages of folliculogenesis. This individual contained four slightly enlarged ovarian follicles (completely rounded) with mean diameter (in mm) 5.22 ± 0.22 (5.03–5.52). Exact follicular measurements were as follows: 5.25 W; 5.03 W; 5.52 W; 5.09 W. This individual had moderate fat bodies. A female paratopotype (UTEP 21487) with SVL 60.0 mm and TL 75.4 mm collected on 28 May 2014 was gravid. This individual contained five oviductal (shelled) eggs with mean dimensions (in mm), length 14.05 ± 0.33 (range: 13.75–14.44) and width 7.46 ± 0.1 (range: 7.32–7.59). Exact measurements of eggs were as follows: 14.44 L x 7.59 W; 14.38 L x 7.44 W; 13.88 L x 7.32 W; 13.82 L x 7.51 W; 13.75 L x 7.45 W. This individual had minor fat bodies. A paratopotype (UTEP 21486) with a smaller body size (SVL 51.5 mm and TL 64.3 mm) collected on 28 May 2014 was not gravid, as evidenced by the largest ovarian follicles measuring < 2 mm in diameter and lacking yolk. This individual had extensive fat bodies. Two other paratopotype females (CAS 201593 – SVL 59.5 mm and TL 64.8 mm; CAS 201594 – SVL 59.9 mm and TL 75.6 mm) collected on 12 September 1996 were gravid. Clutch characteristics were not measured for these individuals. From a small sample, the temporal incidence of gravidity in females at Bwindi Impenetrable National Park seems to correspond with the two annual peaks in precipitation for this region (i.e., March–May and October–November), which is a common phenomenon among chameleon species (Tilbury, 2010). We speculate that egg production may not occur during only one rainy period per year or females may produce two

clutches per year. More investigation with a larger sample is warranted to determine the seasonal reproductive cycle for females of this new species.

All males had darkly pigmented testes (i.e., black coloration). All collected males were sexually mature. One male paratopotype (UTEP 21488) with SVL 48.5 mm and TL 64.2 mm collected on 26 May 2014 had enlarged testes. The right testis of this individual measured 6.24 mm in length and 4.91 mm in width. This individual had minor fat bodies. A male paratype (UTEP 21489) with SVL 51.6 mm and TL 65.8 mm collected on 31 May 2014 also had enlarged testes. The right testis of this individual measured 6.65 mm in length and 4.93 mm in width. Fat bodies for this individual were moderate.

Diet. Three specimens examined for gut contents had identifiable remains of arthropod prey items, one specimen had an empty stomach (UTEP 21487), and one specimen had only a bolus of unidentifiable remains surrounded by a white mucus membrane (UTEP 21488). The stomach of one female (UTEP 21490) contained Mantodea, Araneae, Hymenoptera, Diptera, Hemiptera, and Coleoptera. A second female (UTEP 21486) stomach contained Araneae and Hymenoptera. A male (UTEP 21489) stomach contained Diptera.

Distribution and natural history. *Kinyongia tolleyae* sp. nov. is found in moist Afrotemperate montane and sub-montane forests at an elevation range from 1655–2362 m. Most specimens were collected from forest edges within Bwindi Impenetrable National Park. Several specimens were found on sleeping perches relatively high in the canopy (ca. 5 m above ground) and some were found lower (ca. 2 m above ground). One specimen (UTEP 21489) was collected from secondary forest on disturbed vegetation (ca. 2.5 m above ground) near the Ruboni

Community Hotel just outside of Rwenzori Mountains National Park. The presence of this species at two disjunct mountain blocks suggests a recent forest connection between these areas and increases the likelihood that this species is more widespread than currently known. For example, Vonesh (2001) recorded *Chamaeleo* (= *Kinyongia*) *adolfifriderici* from Kibale National Park in Uganda, which is less than 50 km from Rwenzori Mountains National Park, and thus the observation was potentially this new species. We speculate that *K. tolleyae* sp. nov. may also occur in other montane protected areas with suitable forest habitat near these two sites (e.g., forest reserves contiguous with Queen Elizabeth National Park and Mgahinga Gorilla National Park). Both collected males seemed sexually mature, and four female specimens were gravid. To the best of our knowledge, no juveniles have been detected to date. Behavior and activity patterns are basically unknown, but likely similar to that of *K. adolfifriderici* (Tilbury, 2010). Intersexual interactions were observed among a few specimens before preservation. When a male was placed in the presence of two females, male body color became milky white, regions on the head greener, powder-blue eye skin became much more striking, and distinct diamond patterns suddenly formed on the tail. Whereas female background color turned a rich green, ventral portions of the body became noticeably whiter, and the lateral body patches became marked with a brown hue at the edges and the center became a purer white (Fig 3.8D). For a detailed list of lizard species present at the type locality see Drewes and Vindum (1998). Other species collected from Rwenzori Mountains National Park comprised typical AR lizard fauna and some endemic species, including *Adolfus jacksoni*, *Kinyongia carpenteri*, *K. xenorhina*, *Leptosiaphos meleagris*, *Rhampholeon boulengeri*, *Trioceros ellioti*, *T. johnstoni*, and *T. rudis*.

Conservation. Bwindi Impenetrable National Park and Rwenzori Mountains National Park are well-established members of the protected area network in the AR. These areas constitute some of the few remaining portions of intact Afromontane forests in the Kigezi Highlands. Nevertheless, these forests face similar anthropogenic threats to other protected areas across the region. The current range of *K. tolleyae* sp. nov. falls within the boundaries of these two protected areas and we suspect it may be present in nearby protected areas with suitable habitat.

Etymology. The specific epithet is named in honor of Krystal A. Tolley for her substantial contributions to chameleon biology, with the Latin suffix *–ae* to denote feminine genitive singular. To date, Krystal has participated in the description of 12 new chameleon species, published copious primary research articles on chameleons covering a remarkable breadth of subjects, and coauthored (or edited) two important books on chameleons (Tolley and Burger, 2007; Tolley and Herrel, 2013).

Family Chamaeleonidae *Gray, 1825*

Genus Kinyongia *Tilbury, Tolley and Branch, 2006*

Kinyongia itombwensis Hughes, Kusamba, Behangana and Greenbaum sp. nov.

Figs 3.1, 3.2, 3.3, 3.4, 3.9, 3.10; Tables 3.2, 3.5

Itombwe forest chameleon

Synonymy.

K. adolfifriderici – Greenbaum et al., 2012a: Figure 2, Appendix II – Phylogenetic placement and genetic distances.

K. adolfifriderici – Tilbury and Tolley, 2015: Figure 4 – Phylogenetic placement.

Holotype. UTEP 20371 (field no. EBG 1605), adult female, DRC, South Kivu Province, Mwenga Territory, Itombwe Plateau, near Bichaka village, 03°20'27.6"S 28°47'40.0"E, 2208 m elevation, 20 June 2008, collected by E. Greenbaum, C. Kusamba, M.M. Aristote, and W.M. Muninga (Fig. 3.9A and D).

Paratypes. One adult female, UTEP 21479 (field no. ELI 3357), DRC, South Kivu Province, Mwenga Territory, Itombwe Plateau, Kilumbi village, 03°25'56.0"S 28°34'34.5"E, 2020 m elevation, 16 June 2015, collected by M.M. Aristote (Fig. 3.9B–C); one adult male, UTEP 21480 (field no. CFS 908), DRC, South Kivu Province, Mwenga Territory, Itombwe Plateau, Miki village, 03°21'24.4"S 28°41'24.4"E, ca. 2200 m elevation, 1 October 2010, collected by M.M. Aristote.

Diagnosis. Kinyongia itombwensis sp. nov. can be distinguished from all other *Kinyongia* species by the following combination of traits: (1) lack of rostro-nasal ornamentation in both sexes; (2) small body size (mean SVL = 51.1 mm); (3) few conical tubercles on dorsal crest (6–7); (4) casque almost indistinct from nape; (5) absence of both a gular and ventral crest; (6) 13–16 upper and 15–16 lower labials; (7) slightly bilobed shape of the upper casque; (8) tail length longer than SVL in both sexes; (9) parietal crest composed of several raised tubercles forming a semi-circle with an extension that connects posteriorly to apex of the casque; (10) background coloration of the body in adult females is generally shades of green and yellow; (11) darker brown pigment covers the cloacal region and extends distally onto hidden parts of the hind limbs and tail in adult

females; (12) interstitial skin between the tubercles on the body is black, which is lighter in color anteriorly and off-white on the nape; (13) a brown stripe passes through the middle of the eye, extending from the canthal ridge to the temporal crest, and the eye skin above and below the stripe is yellowish-green with flecks of blue; (14) the top of the head is darker brown than elsewhere; (15) tubercles on the casque converge to form a weakly raised peak posteriorly; (16) dorsal keel that is darker green-brown than elsewhere, with incomplete vertical black bands.

Differential diagnosis. A small-sized forest chameleon that is distinguished from most other congeners by the absence of a rostral process in both sexes (*K. asheorum*, *K. boehmei*, *K. carpenteri*, *K. fischeri*, *K. magomberae*, *K. matschiei*, *K. msuyae*, *K. multituberculata*, *K. oxyrhina*, *K. tavetana*, *K. tenuis*, *K. uluguruensis*, *K. uthmoelleri*, *K. vanheygeni*, *K. vosseleri*, and *K. xenorhina*). The new species can be distinguished from *K. adolfifriderici* by more lower labials (15–16 versus 12–15). For differences between *K. rugegensis* sp. nov. and *K. tolleyae* sp. nov. to *K. itombwensis* sp. nov., see their respective sections on *Differential diagnosis*. The new species can be distinguished from *K. mulyai* and *K. excubitor* by the presence of a dorsal crest with 6–7 conical tubercles and marked mitochondrial sequence divergence. The new species can be distinguished from *K. gyrolepis* by a smaller mean body size (51.1 mm versus 67.3 mm) and current distribution in moist Afromontane rainforest.

Genetic differentiation and variation. Summary of pairwise sequence divergence for each molecular marker (16S, ND2, and RAG1) among individuals of *K. itombwensis* sp. nov. and other species of *Kinyongia* endemic to the AR are presented in Table S2 (see supplemental information

[Table S2] in Hughes et al. [2017a]). For the ND2 locus, the *p*-distance between two *K. itombwensis* sp. nov. samples was 0.6%.

Description of holotype. Adult female, SVL 54.8 mm and TL 63.8 mm. Casque almost indistinguishably elevated above nape. Short apex on posterior casque. Casque slightly bilobed. Neck indistinct from head. Parietal crest consists of five enlarged tubercles. Parietal crest tubercles in semi-circle pattern at mid-casque and one distinctly larger conical tubercle present on either side. Ridge of parietal tubercles extending to raised apex of casque. Supra-orbital ridges smooth. Temporal crest consists of three enlarged tubercles extending posteriorly from mid-eye and ascending along posterior ridge of casque to apex. Nares open laterally, in posterior orientation. Canthal ridge consists of five raised tubercles descending from eye towards snout and one distinctly larger conical tubercle present anteriorly. Thirteen upper and 15 lower labials present along tip of snout to posterior margin of orbit. No gular or ventral crests present. Six distinctly raised conical tubercles present on anterior portion of dorsal crest, absent far before mid-body. Tail and lateral flanks smooth. Body covered in nearly homogenous, flattened tubercles. Some larger polygonal tubercles present dorsally on flanks. Rosette patches of smaller tubercles present on ventral body. Mostly enlarged flattened tubercles present on outer portions of limbs. Claws typical of *Kinyongia* species.

Table 3.5 Descriptive morphometrics (measurements and meristic counts) for adult type specimens of *Kinyongia itombwensis* sp. nov. See text for explanation of character abbreviations.

	UTEP 20371 Holotype Female	UTEP 21479 Paratype Female	UTEP 21480 Paratype Male
SVL	54.8	46.1	52.2
TL	63.8	64.5	68.0
ToL	118.6	110.6	120.2
HL	15.9	14.4	14.9
HW	8.5	7.0	7.7
HH	9.6	8.9	8.7
ML	12.2	9.8	10.7
CE	5.8	6.2	6.4
SL	5.4	4.7	5.0
ED	5.2	4.4	5.3
CC	3.1	3.4	4.1
IL	29.6	26.1	28.8
FLL	9.2	9.4	9.4
HLL	8.7	7.9	9.1
UL	13	16	15
LL	15	16	16
CTD	6	7	7
TL/SVL	1.4	1.3	1.2

Coloration of holotype (in ethanol). Photographs of the body and head detail of the holotype (in preservative) are presented in Fig. 3.10. The background coloration is various shades of blue and purple with darker gray areas on dorsal parts of the body and tail. The venter, beginning below the nape to the cloacal region, is lighter in color, almost pink to off-white. Patches of lighter purple-blue are present behind the eye, near the commissure of the mouth, and extend onto the gular area. The ventral portions of the tail are off-white. The axillary and inguinal regions are of lighter pigment than elsewhere on the body. The soles of the feet are yellowish-white.

Coloration of holotype (in life). Photographs of the holotype (in life) are presented in Fig. 3.9A and D. The top of the head is covered in dark brown tubercles with black interstitium. Below the temporal crest to the canthal ridge, the head is covered in light brown and yellow tubercles with green interstitium. At mid-eye, there is a dark lateral stripe that connects the brown coloration on the canthal ridge to the temporal crest. The skin above and below the stripe on the eye is yellow-green with minor powder blue speckles. Labial scales are heterogeneous in color with mostly hues of yellow and brown. The gular region just blow the tip of the snout is yellow, which fades to off-white posteriorly until entirely absent at the nape. The ventral regions of the body are light green in color, with shades of white and powder blue. The background coloration of the body is green with yellow-edged tubercles and black interstitium. Two medium-sized gray patches are positioned slightly anteriorly and posteriorly from mid-body on the lateral flanks. These patches are surrounded by slightly darker green tubercles. Several dark vertical bands begin on the dorsal keel and quickly fade ventrally, without reaching to mid-body. Smaller body tubercles form rosettes, with light green color filling spaces between tubercles. Interstitial skin on the venter is lighter than elsewhere. Tubercles near axillary and inguinal regions, and hidden parts of limbs, are

mostly white with flecks of green. The dorsal crest has darker green-brown tubercles than elsewhere and this pattern extends onto the tail. The posterior third of the tail is darker green than other parts of the tail, and in general, coloration of the tail is darker than the body.

Hemipenis. Only a single male specimen was found (UTEP 21480) and the hemipenis was not everted upon collection in the field.

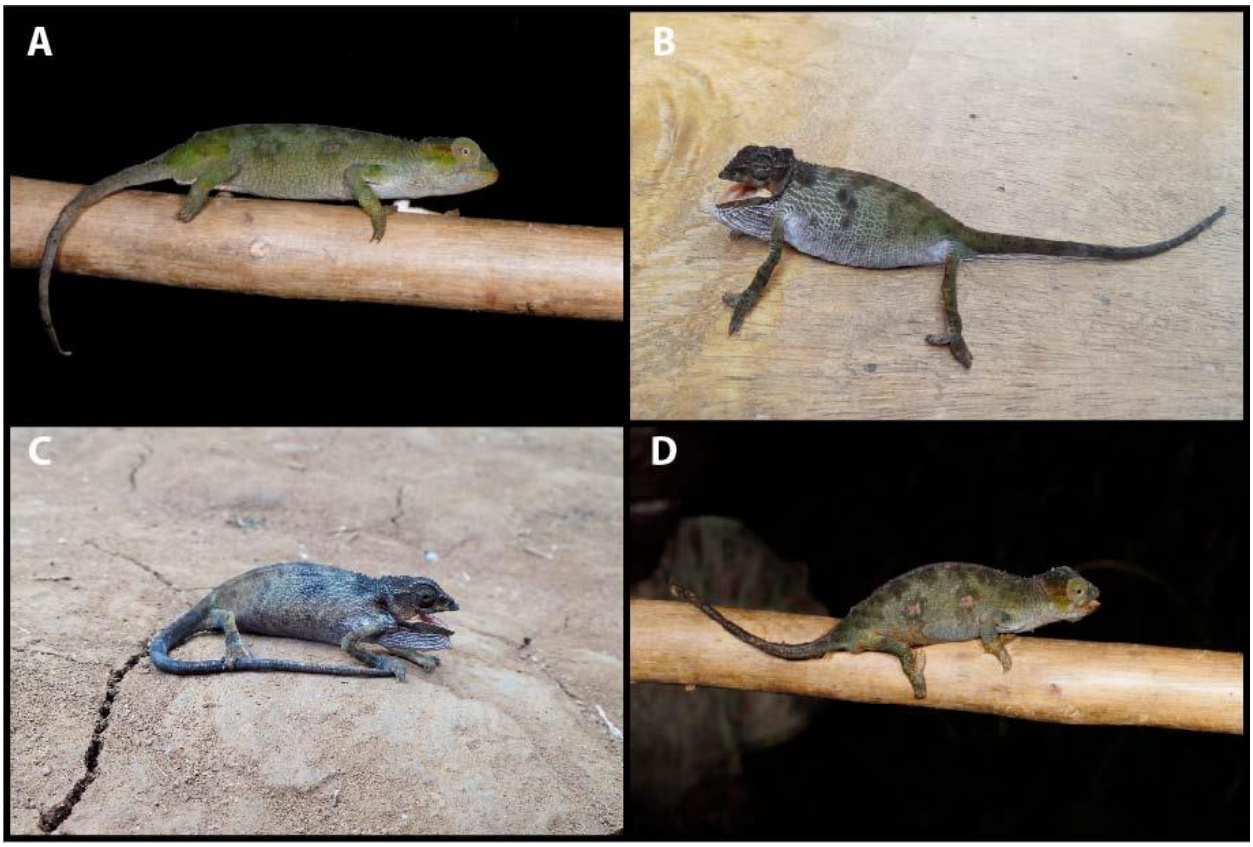

Figure 3.9 Photographs of two individuals of *Kinyongia itombwensis* sp. nov. in life. (A) – Adult female lateral view (UTEP 20371); (B, C) – Adult female displaying aggressive posture and coloration (UTEP 21479); (D) – Adult female slightly posterior lateral view (UTEP 20371).

Variation. Descriptive morphometrics of *K. itombwensis* sp. nov. are presented in Table 3.5 and a summary of mean measurements in Table 3.2. Chameleon photographs for two individuals displaying color variation in life are presented in Fig. 3.9. Morphological proportions

in paratypes are generally consistent with those in the holotype. Too few specimens have been collected to draw reliable inferences regarding intraspecies or intersexual variation. Also, no male photographs were available for comparative descriptions between male and female color patterns in life. The following observations are based on photographs of two female specimens. When agitated, the head was almost entirely black, interstitial skin was lighter and more conspicuous, and large patches on the flanks were dark brown (Fig. 3.9B–C). When the mouth was opened in a defensive posture, the gular region was expanded and displayed an off-white interstitium (Fig. 3.9B–C). Two white patches, one positioned slightly anteriorly and a second slightly posteriorly from mid-body, are present on the lateral flanks of the female holotype, but not present on a female paratype. Photographs of the holotype (Fig. 3.9A and D) likely reflect more normal coloration for the species in life, whereas photographs of a paratype (Fig. 3.9B–C) are of a distressed individual in defensive posture that is displaying aggressive coloration in life.

Reproduction. Two female specimens collected on 16 June 2008 (UTEP 20371) and 20 June 2015 (UTEP 21479) were not gravid. These specimens measured SVL 54.8 mm and 63.8 mm (UTEP 20371), and SVL 52.2 mm and 68.0 mm (UTEP 21479). The largest ovarian follicles for these two individuals measured < 3 mm and the follicles lacked evidence of yolk. Fat bodies were minor for both of these individuals. We speculate that the reproductive status of these females may reflect a period with less rainfall between June–September in the Itombwe Plateau (Jones and Harris, 2008) or that these individuals were not sexually mature despite being of a similar body size to adults of closely related species. More investigation with a larger sample is necessary to determine the reproductive aspects of this new species.

A single adult male (UTEP 21480) had darkly pigmented testes (i.e., black coloration) and was sexually mature. This individual with SVL 52.2 mm and TL 68.0 mm collected on 1 October 2010 had enlarged testes. The right testis of this individual measured 6.16 mm in length and 4.17 mm in width. This individual had minor fat bodies.

Diet. Two female specimens examined for gut contents had empty stomachs (UTEP 20371 and UTEP 21479), and one male specimen (UTEP 21480) had only a few unidentifiable remains of arthropod prey items.

Distribution and natural history. Kinyongia itombwensis sp. nov. is known from only three localities in the montane forest of the Itombwe Plateau at an elevation range from 2020–2208 m. The holotype was found in the vicinity of Bichaka village in a mixed habitat composed of primary forest and agriculture fields. This species seems to be restricted to higher elevation montane rainforest; however, the small number of specimens collected hindered our ability to deduce reliable natural history information. No juveniles were detected during multiple repeated search periods in the plateau and surrounding areas. Behavior and activity patterns are essentially unknown, but likely similar to that of *K. adolfifriderici* (Tilbury, 2010). One male specimen (UTEP 21480) contained a species of parasitic nematode (*Rhabdias* spp.) in its lung (C. Bursey, pers. comm.). Other lizard species collected from Itombwe comprised typical AR lizard fauna and some endemic species, including *Congolacerta vauereselli*, *Holaspis* cf. *guentheri*, *Leptosiaphos blochmanni*, *L. graueri*, *Rhampholeon boulengeri*, *Trachylepis varia*, *Trioceros johnstoni*, and *T. schoutedeni*.

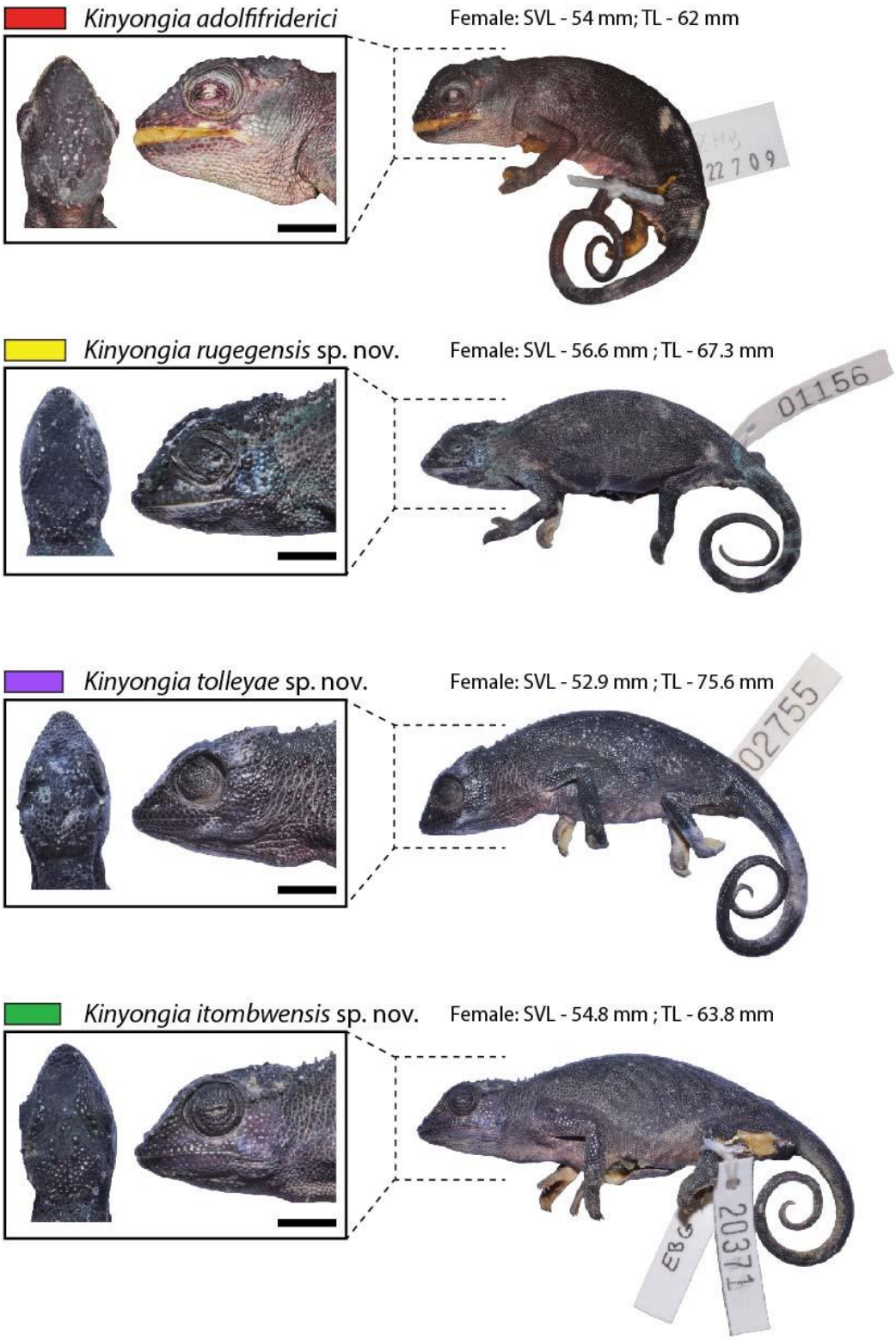

Figure 3.10 Comparison of lateral views and expanded head views of the holotypes (in descending order): *Kinyongia adolfifriderici* ZMB 22709, *K. rugegensis* sp. nov. UTEP 21485, *K. tolleyae* sp. nov. UTEP 21490, and *K. itombwensis* sp. nov. UTEP 20371. Body size as snout–vent length (SVL) and tail-length (TL) are presented above each specimen. Scale bars represent 5 mm.

Conservation. Given the extremely high level of vertebrate endemism harbored in the Itombwe Plateau and the known range of this new species as it currently stands, it is possible that this species is endemic to the Itombwe and Kabobo plateaus. Although gazetted as a reserve in 2006, anthropogenic pressures in this region are substantial and pose serious threats to the biological integrity of Itombwe's forest and its resident fauna (reviewed by Greenbaum and Kusamba, 2012).

Etymology. The specific epithet is derived from the massif, Itombwe, where this species was found, with the Latin suffix *–ensis* donating a place or locality.

3.5 Discussion

3.5.1 Phylogenetic patterns and taxonomic implications

Results presented here are generally consistent with the phylogenetic relationships within *Kinyongia* recovered by Mariaux et al. (2008), Menegon et al. (2009), Tolley et al. (2011), Greenbaum et al. (2012a), Tolley et al. (2013), Menegon et al. (2015), and Tilbury and Tolley (2015). Also, these findings support the phylogenetic positions of *K. msuyae* and *K. mulyai*, two recently described forest chameleon species (Menegon et al., 2015; Tilbury and Tolley, 2015). Furthermore, our phylogenetic results substantiate the molecular relationship of *K. vanheygeni* found by Menegon et al. (2015)—a species for which genetic material was recently made available. A major phylogenetic discrepancy among these studies is the arrangement of species within the Eastern Arc Mountains (EAM) *North* clade. Specifically, the species relationships within the "*fischeri* complex" (*K. boehmei*, *K. tavetana*, and *K. fischeri*) are inconsistent across studies and currently unresolved. A weakly supported sister relationship between *K. fischeri* and *K. boehmei*

was detected by Tolley et al. (2011), Menegon et al. (2015), and Tilbury and Tolley (2015). Menegon et al. (2009), Greenbaum et al. (2012a), Tolley et al. (2013), and this study found a sister relationship between *K. boehmei* and *K. tavetana*, yet this arrangement was poorly supported in these studies. Based solely on mtDNA, Mariaux et al. (2008) found that these three species formed a hard polytomy and thus phylogenetic inferences were rendered ambiguous.

Another notable phylogenetic difference among studies are the unresolved species relationships within the "Usambara clade" (*K. multituberculata*, *K. matschiei*, and *K. vosseleri*). Tolley et al. (2011) and Tilbury and Tolley (2015) both found that this clade formed a well-supported polytomy. Greenbaum et al. (2012a) recovered a poorly supported sister relationship between *K. multituberculata* and *K. matschiei*, with *K. vosseleri* in a sister position to this clade. This study, Mariaux et al. (2008), Menegon et al. (2009), and Menegon et al. (2015) all recovered a sister relationship between *K. multituberculata* and *K. vosseleri*, with *K. matschiei* closely related to this clade. This arrangement was strongly supported in this study, Mariaux et al. (2008), and Menegon et al. (2015), yet weak support for this sister species organization was found by Menegon et al. (2009). Tolley et al. (2013), based on a more comprehensive sampling of individuals and genes, recovered a strongly supported sister relationship between *K. matschiei* and *K. vosseleri*. These relatively minor incongruences in topology and clade support across phylogenetic studies may reflect an underrepresentation of species diversity yet to be discovered in the EAM *North* clade, subtle methodological differences for phylogenetic reconstructions, or accelerated evolutionary rates that influenced long-branch attraction and yielded non-monophyly.

The formal descriptions of these new *Kinyongia* species from the Albertine Rift (AR) clarify previous assertions by Greenbaum et al. (2012a) and Tilbury and Tolley (2015) that the taxonomy of AR forest chameleons did not reflect the true diversity in this region. These two

previous studies—which were focused on AR *Kinyongia*—included genetic data for the newly described *K. tolleyae* sp. nov. (CAS 201593–94) and *K. itombwensis* sp. nov. (UTEP 20371), and both studies recovered two distinct lineages of *K.* cf. *adolfifriderici*. Older studies that predate the availability of genetic material for *K. itombwensis* sp. nov. provided by Greenbaum et al. (2012a) (e.g., Branch and Tolley, 2010; Menegon et al., 2009; Tolley et al., 2011; Townsend et al., 2011), used *K. tolleyae* sp. nov. samples (CAS 201593–94) as representatives of *K. adolfifriderici*. Our study provides the first inclusion of putative topotypic (Ituri rainforest, DRC) material for *K. adolfifriderici*, and because this recently procured population was genetically distinct from all other *K.* cf. *adolfifriderici* samples, we are confident that the three populations we describe represent new species. Furthermore, the phylogeographic patterns we recovered for these cryptic species were indicative of lineage formation in isolation and we speculate that previously published observations of "*K. adolfifriderici*" from remote forest localities in the AR represent either additional undescribed lineages or one of the new species described herein (e.g., Virunga National Park [de Witte, 1941], Kahuzi-Biega National Park [Pupin et al., 2012], and several other AR forest localities [de Witte, 1965; Spawls et al., 2002; Tilbury, 2010]). The recent descriptions of several new cryptic reptile species from the AR Biodiversity Hotspot (e.g., *Congolacerta asukului* Greenbaum et al., 2011; *K. gyrolepis* Greenbaum et al., 2012a; *Cordylus marunguensis* Greenbaum et al., 2012b; *Boaedon radfordi* Greenbaum et al., 2015; *K. mulyai* and *Rhampholeon hattinghi* Tilbury and Tolley, 2015), including these new chameleons, suggests that our understanding of the region's true diversity is far from complete. Moreover, a recent conservation assessment of Africa's reptilian fauna found that Central Africa is one of the three most under-sampled regions on the continent (Tolley et al., 2016). Considering the immense biodiversity already known from the AR (e.g., Plumptre et al., 2007), we believe that the biological discovery

of cryptic taxa in this region is still in its infancy (see Bickford et al., 2007), a situation that is exciting for taxonomists, but problematic for the conservation of Central Africa's herpetofauna (Greenbaum, 2017).

3.5.2 Dating estimates and historical biogeography

The estimated divergence dates we recovered for the genus *Kinyongia* were more ancient than those found by Tolley et al. (2011). Our lineage diversification dates more closely resembled analyses by Townsend et al. (2011) and Tolley et al. (2013). Townsend et al. (2011) included only four species of *Kinyongia*, and in turn, this greatly hampered our ability to draw meaningful comparisons regarding diversification dates for the genus. The younger dates proposed by Tolley et al. (2011) may be a result of methodological differences for calibration priors and outgroup taxa between studies. Tolley et al. (2013), Townsend et al. (2011), and this study all used multiple outgroup taxa, several fossil calibrations outside of Chamaeleonidae, and secondary calibrations within chameleons. In contrast, Tolley et al. (2011) used fossil calibrations within Chamaeleonidae, secondary internal node splits based on molecular dating analyses, and much fewer outgroup taxa. An alternative dating scenario was considered by Tolley et al. (2011) that included more outgroup taxa (sister group Agamidae) and produced much older diversification dates (see Appendix S2 in Tolley et al., 2011). However, the 95% HPD intervals for the latter analysis were suspiciously inflated and thus dating estimates were discredited as artifacts. Given inconsistencies for divergence dating with molecular rates and/or narrow taxonomic scope (Sauquet, 2013), it seems reasonable that studies incorporate sufficient outgroup taxa and calibration priors appropriate for the specific study system.

The divergence dates we recovered for *Kinyongia* were nearly identical to those proposed by Tolley et al. (2013), which included a much more comprehensive sampling of species and genes. For example, Tolley et al. (2013) and this study both found that the initial divergence of the three major clades within the genus occurred in the Eocene, whereas Tolley et al. (2011) found these dates largely occurred in the Oligocene. For *Kinyongia* species endemic to the AR, comparisons to previous studies were rendered more difficult because several new species have been discovered more recently (e.g., Greenbaum et al., 2012; Tilbury and Tolley, 2015). Nevertheless, we found that the sister species *K. xenorhina* and *K. carpenteri*, both endemic to the Rwenzori Mountains, evolved relatively recently with a divergence date in the late Miocene (ca. 7 Mya). Tolley et al. (2011) and Tolley et al. (2013) both found the split between these sister species to have occurred around the same time (ca. 6 Mya). Although our estimated mean divergence dates and those of Tolley et al. (2013) were generally more ancient than dates proposed by Tolley et al. (2011), there was a great deal of overlap for the 95% HPD of divergences. As a result, we are confident that our dates are representative of the broad biogeographic history of this group. For example, we found a split between the AR and Kenya Highlands species *K. excubitor* dated in the late Oligocene (ca. 23 Mya), as did Tolley et al. (2013) (ca. 22 Mya). However, Tolley et al. (2011) found this split to have occurred much earlier, in the mid-Miocene (ca. 17 Mya). The 95% HPD for this divergence recovered by Tolley et al. (2011) ranged from ca. 6–28 Mya, and this large interval overlapped with our findings (ca. 17–29 Mya) and Tolley et al. (2013) (ca. 16–29 Mya). Although these dates are somewhat contrasting, the phylogenetic patterns are much the same. An ancient split between the AR and Kenya Highlands supports the older forested connection proposed by Fjeldså and Lovett (1997). However, genetic signatures left from more recent forested connections between these areas have been detected in other East African taxa (e.g.,

birds [Bowie et al., 2005] and small mammals [Demos et al., 2014]). These conflicting biogeographic patterns suggest that historical geo-climatic changes have had different influences on the genetic patterns for various co-distributed African taxa (i.e., taxon-specific patterns). For example, the formation of the East African Rift affected paleo-drainage patterns that in turn influenced the biogeographic affinities for some of Africa's aquatic fauna (e.g., Daniels et al., 2015; Schultheiß et al., 2014), a biogeographic scenario that differs from the patterns recovered for some of Africa's terrestrial fauna (this study and citations herein).

Our dated-phylogenetic results further support the Miocene epoch as an important period for diversification and endemism of vertebrate taxa in the AR, a finding that is consistent with *Amietia* river frogs (Larson et al., 2016), *Leptopelis* tree frogs (Portillo et al., 2015), *Boaedon* house snakes (Greenbaum et al., 2015), *Atheris* tree vipers (Menegon et al., 2014), and *Kinyongia* forest chameleons (Tolley et al., 2011). Global cooling trends began after the late Oligocene warming and heightened during the Miocene, and these drops in temperature altered precipitation patterns across East Africa (Jacobs, 2004; Sepulchre et al., 2006). A global cooling trend in the Miocene is documented from sedimentation records (Pickford et al., 1993), and supported by climate-driven faunal turnovers recorded in the fossil record of East Africa (Leakey et al., 1996) and the AR (Senut and Pickford, 1994). Mammalian fossil and palaeosol-carbonate records also show evidence of a long-term decrease in precipitation throughout the Neogene in East Africa (Pickford, 1992; Wynn, 2003). Rainfall vicissitudes over time resulted in drastically transformed African vegetation (Cerling et al., 1997; Feakins et al., 2005) and this aridification influenced the expansion of grass-dominated savannas across Central and East Africa in the mid-Miocene (Cerling, 1992; Meadows and Linder, 1993). Pollen and carbon isotope records indicate that this biome became widespread across East Africa in the late Miocene (ca. 8 Mya) (Jacobs et al., 1999;

Jacobs, 2004). Afromontane forests have been implicated as stable refugia for species during ancient aridification pulses (e.g., Loader et al., 2014). However, dispersal into novel habitats following the Miocene climatic optimum has been linked to a recent, adaptive radiation in the South African chameleon genus *Bradypodion* (Tolley et al., 2004, 2006, 2008). A recent radiation out of forests was not discernable from our phylogeny, but rather, stasis in putative forest refugia and allopatric speciation seemed more likely based on the patterns of cladogenesis we recovered. We speculate that potentially poor dispersal and limited immigration by *Kinyongia* species during more recent moist periods with higher forest connectivity (e.g., Zachos et al., 2001) underlies the abundance of paleoendemic lineages and lack of contemporary radiations found in the phylogenies of our study, Tolley et al. (2011), and Tolley et al. (2013). Moreover, the genetic legacy left by Quaternary ice ages—characteristic of numerous biota globally (e.g., Araújo et al., 2008; Davis and Shaw, 2001; Hewitt, 2000), including some East Africa taxa (e.g., Roy, 1997)—was not detectable in *Kinyongia* (Tolley et al., 2011, 2013). The paleoclimate during the Pliocene–Pleistocene fluctuated widely (deMenocal, 1995, 2004), yet AR *Kinyongia* lineages that formed during the Miocene do not seem to have dispersed between forest refugia during recent, climatically stable periods (Maley, 1996). We found evidence that AR *Kinyongia* lineages diversified from persistence in montane forests as allopatric populations, a result that reinforces the speciation by isolation model proposed by Tolley et al. (2011) for forest-dwelling chameleons. Initiation of the AR in the late Oligocene (Roberts et al., 2012), geophysical rifting in the Miocene (Macgregor, 2015), and global cooling after the climatic optimum in the mid-Miocene (Böhme, 2003; Werdelin and Sanders, 2010; Wichura et al., 2015) are all likely linked to the diversification of AR *Kinyongia* species.

A number of potential biogeographic barriers have been suggested or identified in the AR. Volcanic areas, specifically the Virunga volcanic province (Ebinger and Furman, 2003) and South-Kivu volcanic province (Pasteels et al., 1989), could have hampered dispersal of terrestrial fauna between suitable forested areas. Initial volcanism commenced in these two active provinces no later than 10 Mya (Ebinger and Furman, 2003), and extensive volcanic activity occurred in the late Miocene, approximately 5–7 Mya (Pasteels et al., 1989). We found evidence that a significant geographical barrier to gene flow existed between forests of the Kigezi Highlands (Uganda) and those of the Rugege Highlands (Rwanda/Burundi). Sister species from these forests (*K. tolleyae* sp. nov. [Kigezi Highlands] and *K. rugegensis* sp. nov. [Rugege Highlands]) diverged between 3 and 7 Mya, around the late Miocene-Pliocene boundary, suggesting that volcanic activity in the Virunga volcanic province (Kampunzu et al., 1998) may have destroyed suitable dispersal corridors between these highlands, and thereby isolated ancestral populations. An identical genetic split was recovered between populations of an arboreal mammal, the moon-striped mouse (*Hybomys lunaris*), by Huhndorf et al. (2007). Furthermore, Bryja et al. (2017) found that the forest thicket rat (*Grammomys dryas*), an AR endemic mammal species, harbors a genetically distinct clade that is restricted to the Rugege Highlands. Nevertheless, diversification dates among clades of *H. denniae* and *G. dryas* from these highlands were estimated in the mid-Pleistocene and thus much earlier than our date. It is possible that volcanic pulses occurred periodically over a large time scale and differentially affected dispersal routes for various taxa (i.e., taxon-specific patterns). This biogeographic scenario needs to be investigated further with more comprehensive sampling from additional localities across the region, especially Virunga and Kahuzi-Biega National Parks. The Rwenzori Mountains are geologically young (ca. 2–3 Mya; Kaufmann et al., 2015), yet they have been surrounded by bodies of water since the mid-Pleistocene (Beadle, 1981), which were

likely significant barriers to dispersal. In fact, many vertebrate taxa are endemic to this massif (Butynski and Kalina, 1993), including the two forest chameleon species *K. carpenteri* and *K. xenorhina*. We found that these sympatric sister species diverged 4–10 Mya, long before the estimated emergence of the Rwenzori Mountains, suggesting that geological uplift alone does not explain their diversification. For one of the new species (*K. tolleyae* sp. nov.), we found genetic evidence of a recent forested connection between Bwindi Impenetrable and Rwenzori Mountains National Parks. A similar lack of phylogeographic structure for other AR taxa has also been found between disjunct populations occupying these two forested regions (e.g., *H. lunaris* sensu stricto [Huhndorf et al., 2007]; *G. dryas* sensu stricto [Bryja et al., 2017]; and the river frog *Amietia lubrica* [Larson et al., 2016]).

3.5.3 Conservation implications

Current rates of species extinction are so high (Dirzo et al., 2014) and the rate of taxonomic discovery so slow (Fontaine et al., 2012; Pante et al., 2014) that numerous species are expected to be lost in the wild before they are known to science (Costello et al., 2013; Lees and Pimm, 2015). Moreover, our understanding of trait variation is further reduced as species are lost, and as a result, we must make every effort to offset data losses with higher rates of data rescue (e.g., Hughes et al., 2016). These global problems are exacerbated in Central Africa's montane forests where high levels of biodiversity are concentrated into very small regions (Plumptre et al., 2007) that are faced with added pressures from an extremely dense human population (Burgess et al., 2007; Carr et al., 2013). A longstanding history of civil conflict and political instability (Butsic et al., 2015) has considerably discouraged expeditionary research in the region (Greenbaum, 2017; Greenbaum and Kusamba, 2012). Currently, two of the newly described species benefit from distributions that

overlap with three national parks (i.e., Bwindi Impenetrable, Rwenzori Mountains, and Kibira). However, these new chameleon species seem to have small geographical ranges and might be rare within those ranges, as evidenced by the small number of collected specimens. Moreover, the species are likely restricted to montane forests and are probably sensitive to habitat transformations—a common phenomenon among most *Kinyongia* species (Tilbury, 2010). The genus overall is one of the most threatened groups of chameleons on continental Africa. Of the 19 *Kinyongia* species assessed by the IUCN, seven are threatened with extinction (i.e., Critically Endangered, Endangered, or Vulnerable), and an additional seven are considered Near Threatened—three of which are experiencing decreasing population trends (IUCN, 2018). The AR endemic *K. mulyai* was recently evaluated as Critically Endangered, the only *Kinyongia* species currently classified under this category (Tolley and Tilbury, 2015b). This species was described from a single male specimen (Tilbury and Tolley, 2015), yet the assessment was appropriately influenced by an urgency for conservation, because the species occurs in an extremely small geographic area devoid of any formal protected status (Mount Nzawa in southeastern DRC). The species *K. gyrolepis* (currently listed as Data Deficient [Tolley et al., 2014b]) might be assessed similarly to *K. mulyai*, because the species is known only from the Lendu Plateau in northeastern DRC, which also lacks protected status.

Montane forests of the AR are continually threatened from illegal mining, logging, and poaching that date back to the 19th century (Barnes, 1990; Hanson et al., 2009), and severe pressures from an increasingly dense human population that is converting forests to agriculture at an astounding rate (Burgess et al., 2007; Plumptre et al., 2003). Persistent armed conflict has led to rebel groups occupying protected areas, and in turn, devastating local communities, poaching rare animals, and damaging the much-needed infrastructure required to mitigate illegal activities

(Glew and Hudson, 2007; Plumptre et al., 2001). These interwoven threats are escalating, and are arguably the greatest risk to the biological integrity of the AR. For these new chameleon species, the most immediate and daunting challenges will categorically face *K. itombwensis* sp. nov. from the Itombwe Plateau in eastern DRC, which was initially gazetted in 2006 as Reserve Naturelle d'Itombwe (Itombwe Natural Reserve) and only established official boundaries in 2016 (Greenbaum, 2017). This reserve is an important conservation area because it harbors numerous endemic taxa, including plants (Doumenge, 1998), butterflies (Carcasson, 1964), birds (Prigogine, 1977), reptiles (Greenbaum et al., 2011), amphibians (Evans et al., 2008; Portillo and Greenbaum, 2014a, 2014b), and mammals (Omari et al., 1999), and its biodiversity significance will certainly increase if expeditionary research continues. The imminent threats facing the Itombwe Plateau are formidable (reviewed by Greenbaum and Kusamba, 2012) and biodiversity concerns across DRC are pervasive (reviewed by Inogwabini, 2014). If conservation efforts in this country cannot rapidly improve, many rare and potentially new species will be lost. We are hopeful that the formal descriptions of these three endemic chameleon species will be used to increase conservation awareness and galvanize transboundary protection efforts across these irreplaceable regions.

Chapter 4: Rescuing perishable neuroanatomical information from a threatened biodiversity hotspot: Remote field methods for brain tissue preservation validated by cytoarchitectonic analysis, immunohistochemistry, and x-ray microcomputed tomography[3]

[3] Published as: **Hughes, D.F.**, E.M. Walker, P.M. Gignac, A. Martinez, K. Negishi, C.S. Lieb, E. Greenbaum, and A.M. Khan. **2016**. Rescuing perishable neuroanatomical information from a threatened Biodiversity Hotspot: Remote field methods for brain tissue preservation validated by cytoarchitectonic analysis, immunohistochemistry, and x-ray microcomputed tomography. *PLoS ONE* 11(5): e0155824.
Available online: https://doi.org/10.1371/journal.pone.0155824

4.1 Abstract

Biodiversity hotspots, which harbor more endemic species than elsewhere on Earth, are increasingly threatened. There is a need to accelerate collection efforts in these regions before threatened or endangered species become extinct. The diverse geographical, ecological, genetic, morphological, and behavioral data generated from the on-site collection of an individual specimen are useful for many scientific purposes. However, traditional methods for specimen preparation in the field do not permit researchers to retrieve neuroanatomical data, disregarding potentially useful data for increasing our understanding of brain diversity. These data have helped clarify brain evolution, deciphered relationships between structure and function, and revealed constraints and selective pressures that provide context about the evolution of complex behavior. Here, we report our field-testing of two commonly used laboratory-based techniques for brain preservation while on a collecting expedition in the Congo Basin and Albertine Rift, two poorly known regions associated with the Eastern Afromontane biodiversity hotspot. First, we found that transcardial perfusion-fixation and long-term brain storage, conducted in remote field conditions with no access to cold storage laboratory equipment, had no observable impact on cytoarchitectural features of lizard-brain tissue when compared to tissue sets processed under laboratory conditions. Second, field-perfused brain tissue subjected to prolonged post-fixation remained readily compatible with subsequent immunohistochemical detection of neural antigens, with immunostaining that was comparable to that of laboratory-perfused brain tissue. Third, immersion-fixation of lizard brains, prepared under identical environmental conditions, was readily compatible with subsequent iodine-enhanced X-ray microcomputed tomography, which facilitated the non-destructive imaging of the intact brain within its skull. In summary, we have validated multiple approaches to preparing intact lizard brains under entirely remote field conditions with

limited access to supplies and a high degree of environmental exposure. This protocol should serve as a malleable framework intended for future researchers attempting to rescue perishable and irreplaceable morphological and molecular data from regions of disappearing biodiversity. Our approach can be harnessed to extend the numbers of species being actively studied by the neuroscience community, by reducing some of the difficulty associated with acquiring brains of animal species that are not readily available in captivity.

4.2 Introduction

By one estimate (Mora et al., 2011), 86% of the world's extant eukaryotic species still await identification and description. It is believed that our current classification and taxonomic efforts are too slow to overcome biodiversity loss (Mora et al., 2011). As a result, a multitude of species may go extinct before their existence is even known to us. Terrestrial biodiversity is concentrated in at least 35 biodiversity hotspots. Although they account for only 2.3% of the Earth's land surface, these areas harbor over 50% of the world's endemic plant species and an estimated 43% of endemic terrestrial vertebrate species (Mittermeier et al., 2011). Intensive efforts are now underway to fully characterize and document the biota within these hotspots, which are anticipated to yield the highest amount of data in the shortest amount of time (Myers, 2003). Thus, even if rapid global biodiversity loss cannot be fully prevented, efforts can be made at these hotspots to mitigate data losses with targeted efforts at data rescue. Such efforts can slow the rate of global biodiversity decline (Hoffman et al., 2010) and help increase our understanding of how traits vary across species.

An important part of such data rescue involves documenting biodiversity through the careful and responsible on-site collection of individual members of poorly known species

(Iwaniuk, 2011; Rocha et al., 2014). On-site collection allows for a variety of information to be gathered for such species, including geographical, ecological, genetic, biochemical, morphological, and behavioral datasets (e.g., Kamath et al., 2013; Kamath and Stuart, 2015; Kolbe et al., 2004; Lieb et al., 1983; Stuart et al., 2014). Having diverse datasets for a species, in turn, affords investigators flexibility in how the data can later be used for a host of analytical approaches across molecular to macro-evolutionary scales (Albert et al., 2012; Balanoff et al., 2013; Carlson et al., 2011; Charvet et al., 2010; Gonzalez-Voyer et al., 2009; Huelsenbeck et al., 1996; Levasseur and Lapointe, 2001; Sylvester et al., 2010), even if current paradigms of analysis favor some datasets over others.

A potentially useful—but often overlooked—source of variation is the brain. Mapping of neuroanatomical characters onto molecular-based phylogenies has revealed new information about differences in brain region size and encephalization among species (Charvet et al., 2010; Gonzalez-Voyer et al., 2009; Sylvester et al., 2010), the evolution of species-specific communication (Carlson et al., 2011), and the evolutionary origins of the neurological configuration of the brain for certain taxa (Balanoff et al., 2013). Moreover, comparing neuroanatomical characters in wild-caught animals with those in their domesticated counterparts has provided insights about the genetic routes through which domestication becomes manifest in different species (Albert et al., 2012). Unfortunately, field methods used to preserve collected specimens traditionally have been incompatible with the preservation of neuroanatomy for several reasons. First, biodiversity hotspots are often located in remote regions of developing countries where infrastructure is inadequate to support laboratory-based neuroanatomical and neuromolecular research (Editorial, 2003; Yusuf et al., 2014). Second, in remote field locations there is limited access to resources that ensure optimal preservation of brain tissue, such as appropriate fixatives or stable cold storage

conditions free from environmental exposure. Finally, local regulations often prohibit the export of live animals to outside countries where adequate laboratory-based infrastructure may exist, further discouraging researchers without access to regional laboratories from preserving brain tissues optimally.

In addition to these challenges, the collection of rare and previously undocumented species affords additional considerations related to brain tissue processing. In particular, dissecting and sectioning preserved brains destroys important gross anatomical information that is potentially useful for advancing knowledge of the brains of newly discovered or previously undocumented species. Such information includes craniometric relationships between the skull and underlying brain tissue structures that could potentially inform future stereotaxic procedures, as well as three-dimensional relationships within the brain and between cranially derived sensory and motor organs and the neural networks to which they are connected. This information in turn can help enable classification of cell types, neural configurations, and structure-function relationships for specific brain circuits across a far wider diversity of vertebrate taxa than is currently understood.

In this study, we have developed a validated field protocol for brain tissue preservation that overcomes these challenges. Specifically, we undertook a 58-day collecting expedition to the Congo Basin and Albertine Rift of Central Africa, both poorly known regions that form portions of the Eastern Afromontane biodiversity hotspot (Mittermeier et al., 2004; Plumptre et al., 2007), and performed on-site euthanasia of lizards and fixation of their intact brains under entirely remote conditions, with limited access to supplies, and during a high degree of environmental exposure. We field-tested two tissue fixation methods commonly used in the laboratory: immersion and transcardial perfusion with buffered formalin. We evaluated the efficacy of these methods in the laboratory by examining the field-fixed samples collected in Central Africa at the

cytoarchitectural, chemoarchitectural, and gross-neuroanatomical levels by using semi-quantitative Nissl-based structural analysis, immunohistochemistry, and diffusible iodine-based contrast-enhanced computed tomography (diceCT) (Gignac and Kley, 2014; Gignac et al., 2016), respectively. Our field protocols not only generated high-quality tissue preservation at the cellular and regional tissue levels, but they are also compatible with non-destructive imaging, at the gross neuroanatomical level, of the intact skull and underlying soft brain tissue. These fixation methods are simple to implement in the field, require few resources that would otherwise be difficult to obtain in remote locations, and are extensible to collection efforts for a variety of poorly known or undiscovered vertebrates found in the world's most fragile ecosystems.

4.3 Materials and Methods

4.3.1 Approvals and permissions

Permission to collect lizards in Uganda was obtained from the Uganda Wildlife Authority (UWA), the National Biodiversity Data Bank at Makerere University, Institut Superieur d'Ecologie pour la Conservation de la Nature (ISEC), and Uganda's CITES License (2888). Permission to collect in Democratic Republic of Congo (DRC) was granted by the Centre de Recherche en Sciences Naturelles (CRSN – LW1/27/BB/KB/BBY/60/2014) and the Institut Congolais pour la Conservation de la Nature (ICCN – 1007/ICCN/DG/ADG/DT/04). The University of Texas at El Paso's (UTEP) Institutional Animal Care and Use Committee (IACUC – A-200902-1) approved field and laboratory methods.

Table 4.1 Details regarding the animals that underwent euthanasia and fixation under field conditions for this study. Abbreviations used: BW, body weight (g); F, female; I, immersion fixation; ID, identification number (UTEP Biodiversity Collections); Jv, juvenile; M, male; NA, not applicable (these specimens did not go to cold storage); P, perfusion fixation; SVL, snout–vent length (mm); TL, tail length (mm). Note that coordinates are expressed in decimal degrees. Specimens indicated by underlining are those for which tissue photographs have been furnished in this study (brackets note the specific figures). * The interval between sedation of the subject to storage of the fixed brain.

Species	ID	SVL	TL	BW	Sex	Coordinates	Elevation	Fixation Type, Time*	Duration w/o Cold Storage
Location 1: Uganda: Western Region, Kabale-Kanungu Districts, Bwindi Impenetrable National Park									
Trioceros johnstoni [see Figs. 4.2 & 4.6A]	UTEP 21385	109	121	31.9	M	S01.04836, E29.77684	2284 m	P, 58 min	54 d
Rhampholeon boulengeri	UTEP 21386	48	13	2.5	Jv, M	S00.97828, E29.69354	1563 m	P, 42 min	54 d
Location 2: Uganda: Western Region, Kasese District, Rwenzori Mountains National Park									
Trioceros ellioti	UTEP 21387	59	53	3.9	M	N00.34972, E30.02973	1655 m	P, 51 min	51 d
Trioceros johnstoni [see Fig. 4.7B,C]	UTEP 21388	100	107	31.2	F	N00.36033, E30.00975	1909 m	I, 18 min	NA
Rhampholeon boulengeri [see Fig. 4.7A]	UTEP 21389	47	12	3.6	F	N00.36029, E30.00922	1942 m	I, 25 min	NA
Rhampholeon boulengeri [see Fig. 4.6C]	UTEP 21390	46	14	3.1	M	N00.36029, E30.00922	1942 m	P, 33 min	51 d
Location 3: DR Congo: Orientale Province, Bas-Uele District, Boda village									
Agama cf. *finchi* [see Fig. 4.4]	UTEP 21391	108	171	40.9	M	N03.52319, E26.39019	653 m	P, 46 min	21 d

4.3.2 Expedition details and experimental subjects collected for this study

The expedition took place May–July 2014. Table 4.1 lists the animals collected for this study, including the locations where they were collected. Location 1 is in Bwindi Impenetrable National Park, Uganda; Location 2 is in Rwenzori Mountains National Park, Uganda; and Location 3 is in the small village of Boda in northeastern DRC. These collection sites are located in the Albertine Rift (Locations 1, 2) and Congo Basin (Location 3), two regions that form portions of the Eastern Afromontane biodiversity hotspot (Mittermeier et al., 2004; Plumptre et al., 2007).

In addition to animals collected in the field, control animals listed in Table 4.2 and processed at UTEP under laboratory conditions were purchased from Underground Reptiles (Deerfield Beach, FL).

Table 4.2 Details regarding the animals that underwent euthanasia and fixation under lab conditions for this study. See Table 4.1 for abbreviations used. Specimens indicated by underlining are those for which tissue photographs have been furnished in this study (brackets note the specific figures). *The interval between sedation of the subject to storage of the fixed brain on ice.

Species	ID	SVL	TL	BW	Sex	Fixation Type	Time*	Duration w/o Cold Storage
Trioceros jacksonii [see Fig. 4.3]	UTEP 21382	111	92	40.9	F	P	34 min	0 d
Trioceros jacksonii	UTEP 21383	119	114	43.5	M	P	50 min	0 d
Rieppeleon kerstenii [see Fig. 4.6B,D]	UTEP 21384	49	10	3.2	F	P	29 min	0 d

4.3.3 Formaldehyde sources

The buffered formalin solution used in this study was derived from either of two sources: (1) stock formalin sold commercially in bottled liquid form in Kampala, Uganda; and (2) paraformaldehyde powder obtained from the University of Kisangani, DRC. These sources of formaldehyde were used to freshly prepare 1 L batches of 4% and 10% buffered formalin (100 ml

v/v of source (1) or 100 g w/v of source (2) added to 900 ml of water) in the field using 4 g of sodium phosphate monohydrate ($NaH_2PO_4H_2O$) and 6.5 g of dibasic sodium phosphate anhydrate (Na_2HPO_4) per liter of formalin. Notably, the powdered formaldehyde differed from the liquid commercial-grade formalin in that it was not filtered after being prepared as a solution, contained a concentration of 10% formaldehyde, and also lacked methanol, a common stabilizer that can affect certain immunological reactions. Field-prepared formalin was mixed without heat-mediated depolymerization, due to a lack of electricity and laboratory facilities. The chameleons listed in Table 4.1 (*Locations 1 and 2*) were all fixed using liquid stock solution (4% formaldehyde), whereas the agamid (*Location 3*) was perfused using solution prepared from powdered fixative (10% formaldehyde). Although the pH values for these solutions were not measured in the field, they were likely near neutral pH, based on the buffering ranges of the salts we used.

The fixative used was prepared from freshly depolymerized and cleared granular *p*-formaldehyde (Electron Microscopy Sciences Inc.; Hatfield, PA; Catalog #19210) as a 4% w/v solution in sodium borate buffer (pH 9.5 at 4°C). First validated by Berod and colleagues (1981), this high pH solution is used routinely in our laboratory for locating neural antigens with immunohistochemistry (Khan and Watts, 2004; Khan et al., 2007, 2011, 2014).

4.3.4 Transcardial perfusions under field conditions

Figure 4.1 shows details of our field procedures, and Table 4.3 lists the supplies used to perform them. Lizards were deeply sedated by placing them in closed plastic containers containing two cotton balls saturated with liquid isoflurane. When the animals were sedated enough to remain immobile, they were briefly removed from the container to record body weight and snout–vent length before being returned to the container to complete the sedation. Other more detailed

morphometric measurements necessary for biodiversity studies, especially of the head, were also recorded at this time (e.g., head length and width, snout length, etc.). Once fully anesthetized (i.e., no Labyrinthine righting reflex), animals were affixed to a silicone mat by a single pin pierced through each appendage (Fig. 4.1B).

Table 4.3 List of materials used for the field perfusion procedures.

Item	Quantity	Supplier	Catalog #
1. Containers			
Falcon™ conical centrifuge tube (polypropylene, 50 ml)	5	Fisher	352070
field box with handle (11.6" x 5.1" x 7.1")	1	Plano Molding	131200
Fisherbrand™ bottle (polyethylene, 125 ml)	10	Fisher	02911952
2. Reagents and solutions			
4% and 10% formalin, sodium phosphate buffered	varied	*See Methods*	NA
Isosol™ (isoflurane, USP) (250 ml)	2	Vedco	NDC 50989-150-15
normal saline solution, sterile (250 ml)	2	Vedco	NDC 50989-641-15
sucrose (5 kg)	30 x 3 g	Sigma-Aldrich	S8501
3. Perfusion and dissecting instruments			
hypodermic needle (18 ga)	10	Nipro	AH+1825
syringe (3 cc)	3	Nipro	JD+03L
Dumont #5SF forceps (inox steel, super fine, straight tip)	1	Fine Science Tools	11252-00
Friedman-Pearson rongeurs (1 mm cup size, straight tip)	1	Fine Science Tools	16020-14
interchangeable blades (angled, 10 mm cutting edge)	10	Fine Science Tools	10035-15
Moria fine scissors (inox steel, extra sharp, straight tip)	1	Fine Science Tools	14370-22
insect pin (size 3, 0.5 mm diameter, 4 cm length)	10	Fine Science Tools	26001-50
scalpel handle #3 (stainless steel, 12 cm length)	1	Fine Science Tools	10003-12
spatula & probe (stainless steel, 14 cm length)	1	Fine Science Tools	10090-13
student surgical scissors (stainless steel, 14.5 cm length)	1	Fine Science Tools	91402-14
Vannas spring scissors (straight tip, 2 mm cutting edge)	1	Fine Science Tools	15000-03
4. Miscellaneous supplies			
cotton ball (500/pack)	1	U.S. Cotton	
digital balance, battery-operated	1	Ohaus	
Parafilm "M" (2" x 250')	10 (strips)	Bemis	PM992
silicone mat	2	OXO	372100V2
plastic ruler	1		

For perfusion, the lizard's snout was placed inside a 50-ml conical tube that contained an isoflurane-soaked cotton ball at its base. To open the mediastinum (thoracic cavity), scissors, aided with finer incisions from a scalpel, were used to cut anterior–posterior from mid-neck to lower-abdomen. The thoracic cavity was opened without collapsing the pectoral girdle on the brachiocephalic trunks and carotid arteries. The thoracic wall was removed—the sternum was cut free from the ribs, connective tissue was excised, and portions of the ribs and lungs were removed to further expose the heart, right atrium, and carotid arteries (Fig. 4.1 C and D). The common carotid artery was gently seized with forceps to elevate the heart from the pericardial cavity and better observe the flow of injected solutions toward the head (Fig. 4.1 C and D). Lizards were exsanguinated from an incision to the right atrium with fine scissors. Two 3-ml syringes, equipped with 18-gauge needles, were used for successive injections into the apex of the heart (Fig. 4.1C and D). The needle tip was inserted carefully into the apex and extended through the ventricle to settle visibly just beyond the base of the common carotid. Saline was injected first, followed by buffered formalin solution. In both cases, due to lack of ice or cold storage, the solutions injected were not cold. The small amount of liquid formalin waste (ca. 2 ml) collected after perfusion was diluted with water to a nonhazardous concentration of < 0.1% and disposed of down a drain.

4.3.5 Transcardial perfusions under laboratory conditions

Control animals (Table 4.2) perfused transcardially under laboratory conditions at UTEP underwent identical procedures to those described above for field perfusions with a few notable differences. First, the formulation and source of formaldehyde used were different than the sources used in the field. Second, when saline and fixative were successively injected into the animal, both solutions were ice cold. Finally, perfusions were performed in a chemical fume hood.

Figure 4.1 Images of field-based perfusion technique. The field laboratory setup (A); pinned lizard on silicone mat prior to opening of the thoracic cavity (B); injections of solution through opening in apex of heart (C, D); partially dissected and exposed formaldehyde-fixed brains (E, F, G).

4.3.6 Brain dissections in the field

The head of the euthanized and perfused animal was removed above the shoulders with large surgical scissors. If still attached, cervical vertebrae were removed with rongeurs. To uncover

the occipital and parietal skull bones, the postcranial musculature and surrounding connective tissue were gently removed with fine scissors or scraped away by scalpel. To facilitate manipulation of the cranium, the lower mandible was separated from the head with rongeurs. Dorsal portions of the parietal and temporal skull bones were removed, and the entire occipital skull bone was excised. Saline irrigation helped to maintain moisture levels in the brain tissue once it was exposed to the environment. All connective tissues between the skull and brain (i.e., meninges) were gently teased apart, and the roots of the cranial nerves severed, thereby releasing the brain from its remaining attachments to the skull. The unattached brain was removed from the cranial cavity and placed immediately into storage solution.

4.3.7 Brain dissections in the laboratory

One major difference between field-based dissections and those performed in the laboratory involved temperature control. Specifically, following transcardial perfusions in the laboratory, the heads were removed and placed immediately on ice. Fixed and chilled brains were excised a few hours later as described previously.

4.3.8 Brain storage conditions in the field

Following dissection, brains were stored in individually labeled 100 ml plastic vials filled with a buffered formalin solution containing 12% w/v sucrose ("storage solution") (Khan and Watts, 2004; Khan et al., 2007, 2011, 2014). The solution was topped off to minimize evaporative loss and to ensure that the brain would be wholly submerged. Infiltration of sucrose was confirmed when each brain lost buoyancy and sank to the bottom of the vial. Liquid levels in the vials were checked daily and replenished if low. Care was taken to avoid exposing the vials to excessive heat.

4.3.9 Brain storage conditions in the laboratory

Each brain remained in storage solution (the same fixative solution noted in *Section 2.3b*, but with 12% w/v sucrose; [Khan and Watts, 2004; Khan et al., 2007, 2011, 2014]) at 4°C, until sinking to the bottom of its vial.

4.3.10 Freezing of brains and histology

The following procedures were conducted at the UTEP Systems Neuroscience Laboratory. Brains collected in the field or in the laboratory were removed from their respective storage solutions, blotted dry, and then flash frozen in a plastic container filled with hexane supercooled over a bed of powdered dry ice. The frozen brains were then stored at –80°C until further processing. To prepare them for sectioning, all brain samples were placed into small plastic molds, embedded in Tissue-Tek OCT embedding medium (10.24% polyvinyl alcohol, 4.26% polyethylene glycol, and 85.5% non-reactive ingredients; Sakura Finetek USA, Inc., Torrance, CA), and returned to the –80°C storage until the embedding medium hardened. The OCT medium helped to maintain tissue stability, especially for the smallest lizard brain samples, throughout the sectioning process. Each OCT-embedded brain block was cut into 20–30 µm-thick sections on the freezing stage of a Reichert-Jung OmE sliding microtome. Four serial series of brain sections were collected in 24-well plates filled with anti-freeze cryoprotectant solution (50% 0.1 M sodium phosphate buffer, 30% ethylene glycol, and 20% glycerol; [Watson et al., 1986]). Sections were maintained in cryoprotectant at –20°C until further processing.

4.3.11 Nissl staining

Freely floating sections were rinsed twice in an isotonic Tris-buffered saline solution (pH 7.6) to wash out cryoprotectant. Sections were mounted on gelatin-coated slides using a fine-tipped paintbrush. Mounted sections were dried overnight (24 h) at room temperature (ca. 20°C) in a vacuum chamber. They were then dehydrated in ascending ethanol concentrations (50–100%; 3 min each), defatted in xylene, stained in 0.5% w/v thionine solution (thionin acetate, Catalog #T7029; Sigma-Aldrich Corporation, St. Louis, MO [Lenhossék, 1895; Kiernan, 2001]), and differentiated in 0.4% anhydrous glacial acetic acid. Slides were coverslipped with DPX mounting medium (Catalog # 06522; Sigma-Aldrich) and stored flat within covered slide trays.

4.3.12 Photomicrography and post-acquisition image processing

Stained tissues were examined under bright field illumination using a Zeiss M2 AxioImager microscope equipped with an X-Y-Z motorized stage (Carl Zeiss Corporation, Thornwood, NY). Wide field mosaic images of stained histological sections were obtained using a cooled EXi Blue camera (QImaging, Inc., Surrey, British Columbia, Canada) driven by Volocity Software (Version 6.1.1; Perkin-Elmer, Inc., Waltham, MA) installed on the Apple Mac Pro computer driving the Zeiss microscope. Images were exported from Volocity as lossless TIFF formatted files and imported into Adobe Photoshop (Version CS6; Adobe Systems, Inc., San Jose, CA). In Photoshop, images were cropped via the lasso tool, converted and resampled to 300 dpi gray scale, and brightness- and contrast-adjusted via the curves tool. For hollow spaces within the tissue (e.g., third ventricle), any background illumination of the slide remaining after white balancing was not cropped. Care was taken to make all adjustments judiciously across

photomicrographs of field- and lab-processed tissue sections and also to track changes in scale during any size conversion.

4.3.13 Semi-quantitative histological evaluation

To evaluate the relative efficacies of the lab- and field-based perfusion methods, the condition of the sections obtained using each procedure was evaluated using a semi-quantitative approach. Three members of the UTEP Systems Neuroscience Laboratory, who were blind to the treatment conditions of the tissue, independently rated tissue sections from both treatments using a three-point quality scale: poor (1), good (2), and excellent (3). This rating was performed by viewing the tissue sections under bright field illumination. To understand the effect of perfusion treatment (laboratory vs. field) on various aspects of both tissue and stain quality, independent raters were instructed to apply this scale across six criteria: (A) presence of blood in the tissue; (B) evenness of stain; (C) integrity of tissue at the center of the section; (D) integrity of tissue at the edges of the section; (E) clarity of lamination patterns; and (F) visibility and clarity of nuclei and cell clusters. A total of 204 stained tissue sections were evaluated, representing 166 sections prepared under laboratory conditions and 38 sections prepared under field conditions. The sample size discrepancy between treatments was not believed to influence the overall results because the model-based statistical approach we used (see below) is a function of the size of the largest cluster rather than of the number of clusters (i.e., population-averaged estimates).

4.3.14 Statistical analyses

A heat map of the scores generated by our independent observers was first generated using R function heat map (R Core Team, 2015). Because criteria C–F are not independent from criteria

A and B (i.e., the criteria are interdependent) and because both fixed effects (field vs. lab conditions) and random effects (order of tissue sampling onto slides, variable sample thickness, and subject selected for perfusion fixation) were present, we employed a variation of a general linear mixed model to analyze the results. Specifically, to best compare the scores between the two fixation methods, a generalized-estimating equations (GEE) approach (Heagerty and Zeger, 1996) was used to account for the dependence structure among clustered ordinal scores, as implemented in *geepack* package (Halekoh et al., 2006) in R. We tested each variable separately. The analyses were conducted based on the raw data and a reduced dataset using the mode score for each slide from each observer. This data reduction did not influence the results.

4.3.15 Immunohistochemistry

To evaluate the effect of the perfusion method on the immunoreactivity of neural antigens in the tissue samples, we performed a series of indirect immunohistochemistry experiments using distinct primary antibodies (Table 4.4) across both field- and laboratory-perfused tissue samples. In the first set of experiments, we incubated tissue sections from field- (*Trioceros johnstoni*) and laboratory-perfused (*Rieppeleon kerstenii*) chameleons with a rabbit polyclonal antibody targeting the catecholamine-synthesizing enzyme tyrosine hydroxylase (TH). Importantly, the specificity of this TH antibody has been validated in Western blots as recognizing a single, 62 kDa protein band from both amphibian and reptile brain homogenates and shown to be immunogenically identical to that of mammalian TH (Morona and González, 2008; Moreno et al., 2012). In some initial experiments, we also co-incubated the TH antibody with an antibody targeting dopamine beta-hydroxylase (DβH) (Table 4.4). However, since this antibody did not reveal any staining, it was not used in subsequent immunohistochemical runs. In a second set of experiments, field-

(*Rhampholeon boulengeri*) and laboratory-perfused (*Rieppeleon kerstenii*) chameleon tissue sections were co-incubated with antibodies targeting neuropeptide Y (NPY) and the calcium-binding protein, calbindin (Calb). Tissues were processed for immunohistochemistry as described previously (Khan and Watts, 2004; Khan et al., 2007, 2011, 2014). Briefly, all primary and secondary antibodies were prepared in blocking solution, which consisted of normal donkey serum (2%; EMD Millipore; Catalog #S30-100ML, Lot #2510142), Triton X-100 (0.1%; Sigma-Aldrich; Catalog #T8532-500ML, Lot #MKBH4307V) and Tris-buffered saline (TBS; pH 7.4 at room temperature). After five washes in TBS, each for five min (5 × 5), sections were incubated in a cocktail of secondary antibodies (Table 4.4) prepared in blocking solution. Sections were washed again (5 × 5) in TBS, reacted with fluorophore conjugates also prepared in blocking solution, and counterstained (Table 4.4). Following another 5 × 5 rinse in TBS, sections were mounted onto Superfrost slides and coverslipped with sodium bicarbonate buffered glycerol (pH 8.6 at room temperature) and sealed with clear nail polish. Sections were visualized under the appropriate filters using a Zeiss M2 AxioImager epifluorescence microscope driven by Volocity software.

Table 4.4 Summary of antibody combinations used for immunohistochemistry across distinct reaction sets. [1] Reagents used in a common reaction set are grouped by reaction number in the left column. Each number represents a common set of reagents applied to one series of tissue sections. [2] Superscript letters next to each catalog number refer to the following lot numbers for the batches of reagent used: *a*, 2219225; *b*, 120991; *c*, 2029625; *d*, 107814; *e*, 1037281; *f*, 1159932; *g*, 1112001; *h*, 116529; *i*, GR61453-4; *j*, 118982. [3] The dilutions listed are calculated from suppliers' stock. All secondary antibody and conjugate stocks from suppliers were diluted 1:2 in glycerol (i.e., 50% glycerol, 50% buffer), and the dilution listed (e.g., 1:500) is the final dilution. Thus, we calculated a 1:250 dilution of the 1:2 working stock to obtain the final 1:500 dilution. [4] The total duration of incubation (in hours) is expressed as a range based on the parameters of reactions run on separate occasions, followed by the temperature at which the incubations proceeded. See abbreviations in Appendix.

Reagent[1]	Antibody, Conjugate, or Counterstain	Host	Type	Source	Catalog # [2]	Titer[3]	Incubation (h,ºC)[4]
1:Primary	anti-TH	Rb	poly IgG	E	AB152[a]	1:5,000	17, 4
1:Secondary	anti-rabbit Cy3	Dk	IgG	J	711-165-152[b]	1:500	5, RT
1:Primary	anti-DBH	Ms	mono IgG	E	MAB308[c]	1:10,000	17, 4
1:Secondary	anti-mouse IgG	Dk	biotinylated	J	715-065-150[d]	1:500	5, RT
1:Fluorophore	streptavidin	-	Alexa 488	L	S11223[e]	1:2,000	1, RT
1:Counterstain	DAPI	-	UV label	T	D1306[f]	1:4,000	1, RT
2:Primary	anti-NPY	Rb	mono IgG	I	22940[g]	1:1,000	17, 4
2:Secondary	anti-rabbit IgG	Dk	biotinylated	J	711-065-152[h]	1:500	5, RT
2:Fluorophore	streptavidin	-	Alexa 488	L	S11223[e]	1:2,000	1, RT
2:Primary	anti-calbindin	Ms	mono IgG	A	AB66185[i]	1:1,000	17, 4
2:Secondary	anti-mouse Cy3	Dk	IgG	J	715-165-150[j]	1:500	5, RT
2:Counterstain	DAPI	-	UV label	T	D1306[f]	1:4,000	1, RT

4.4 Results

4.4.1 Fixation and storage

Five lizards were perfused under similar conditions in the field (Table 4.1) and three lizards were perfused in the laboratory (Table 4.2). For the five wild-caught lizards, the field-perfusion process, from initial sedative exposure to storage, averaged 47.8 min (range 33–58 min), comprising 32 min (range 21–39 min) from exsanguination to brain storage. For the two lizards whose brains were immersion-fixed in the field, the process averaged 21.5 min (range 18–25 min), which included time for full sedation and for morphometric measurements. Field-perfused brains remained in storage solution and unfrozen for an average of 46.2 days (range 21–54 days) (Table

4.1). Upon arrival at the UTEP Systems Neuroscience Laboratory, field-fixed brains were initially placed in a cold room (4°C). After a brief period (ca. 48 hours), the perfusion-fixed brains were frozen in hexane supercooled over a bed of powdered dry ice and placed in long-term storage (–80°C). The three lizard brains perfusion-fixed in the laboratory were immediately—after dissection—stored at 4°C until sucrose saturation (24–36 hours). Once saturation was evident, these brains were also frozen in supercooled hexane and placed in long-term storage (–80°C).

4.4.2 Qualitative evaluation of tissue integrity and cytoarchitecture of perfusion-fixed tissues

With the unaided eye surface vessels and sinuses free of blood, in addition to a uniformly pale, opaque color (Figs. 4.1E–G), indicated successful formaldehyde infusion and fixation of the brain under field conditions. Qualitatively, the light microscope revealed that the Nissl staining for the field-perfused animals was robust (Fig. 4.2) and appeared comparable, in terms of color richness and stain evenness, to stained sections obtained from brains perfused under our standard laboratory protocol (Fig. 4.3; see Khan and Watts [2004]). Specific brain regions and landmarks were delimited easily in the stained sections under both field and lab perfusion fixation conditions (Figs. 4.2–4.4). Figure 4.4 shows how a field-perfused agamid, the only specimen perfused with the fixative containing a concentration of 10% formaldehyde, displayed clearly defined cytoarchitectural features, including discernible laminated structures (e.g., cortex medialis, C *m*, Fig. 4.4A) and white matter tracts (e.g., optic tract, Op tr, Fig. 4.4B). Both largely acellular (Fig. 4.4D, *Layer 2*) and cell-dense layers (Fig. 4.4D, *Layers 3/4*), with observable Nissl substance in neuronal perikarya, were visible, lending further support to successful tissue fixation and high staining intensity.

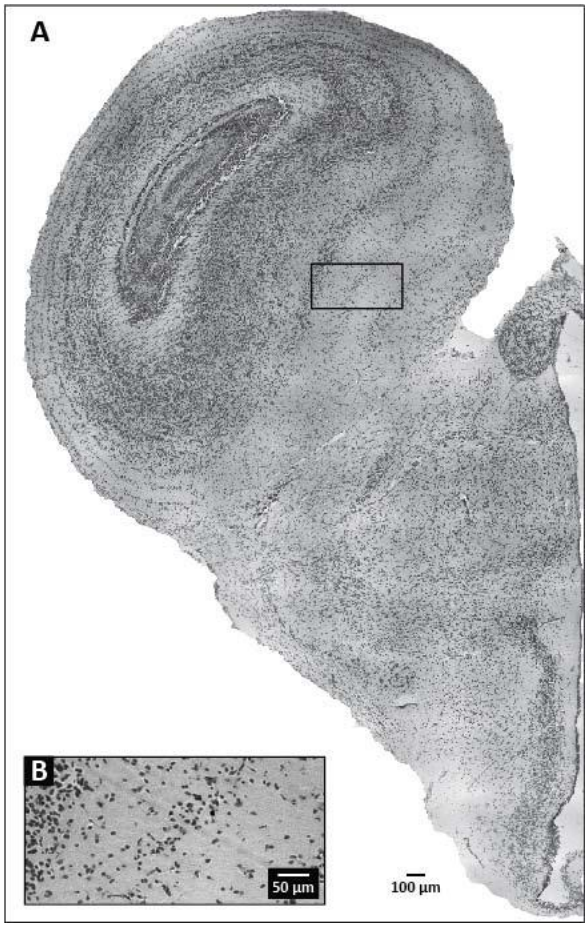

Figure 4.2 Representative tissue section at the level of the optic tectum, obtained from a field-perfused specimen of *Trioceros johnstoni*. (A) Wide field image of a hemisphere from a section of the specimen. The black box outlines the area enlarged in (B), which provides details regarding the level of background staining and cellular labeling demonstrable by our Nissl-based staining procedure.

4.4.3 Semi-quantitative evaluation of tissue integrity and cytoarchitecture of perfusion-fixed tissues

The raw scored data obtained from the tissue evaluations of three independent raters are represented as a heat map in Figure 4.5. The map clearly shows distinct patterns between the two perfusion methods. For example, inter-observer variability was high, but intra-observer variability across criteria was generally not. In some cases, all observers agreed well on the conditions of the tissue (Fig. 4.5, *see black box outlines*). Table 4.5 shows the GEE analysis results for the correlated ordinal response based on the reduced mode scores. The analyses based on the raw data yielded

similar conclusions (data not shown). Specifically, no significant difference was found between perfusion methods for criteria A and B (i.e., degree of blood in brain [$P = 0.59$] and evenness of stain [$P = 0.63$]). We did detect significant differences between perfusion methods for the remaining four criteria (C–F), with p-values varying from 0.0386 to < 0.0001. More specifically, tissue sections obtained from field perfusions received generally higher scores for these criteria, as suggested by the positive signs of the beta estimates and patterns readily deducible in the heat map (Fig. 4.5).

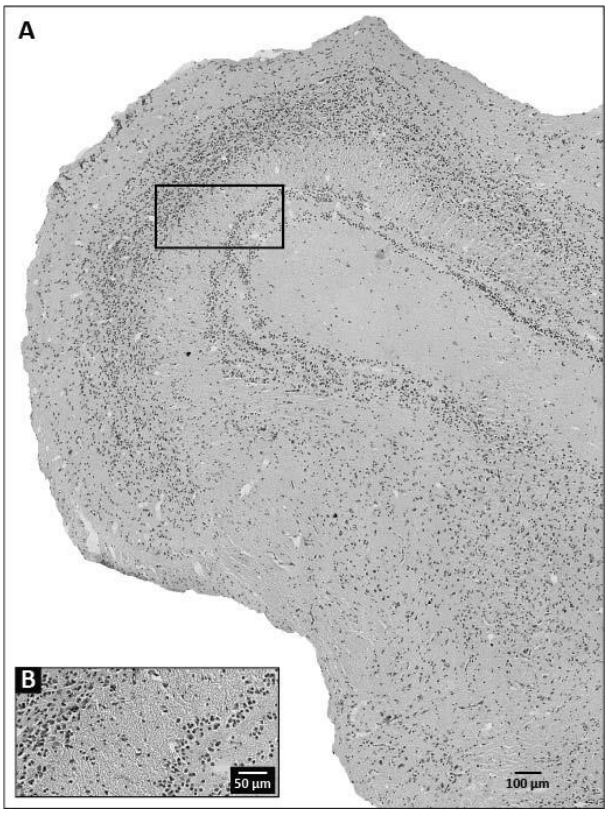

Figure 4.3 Representative tissue section at the level of the optic tectum, obtained from a laboratory-perfused specimen of *Trioceros jacksonii*. (A) Wide field image of a hemisphere from a section of the specimen. The black box outlines the area enlarged in (B), which provides details regarding the level of background staining and cellular labeling demonstrable by our Nissl-based staining procedure.

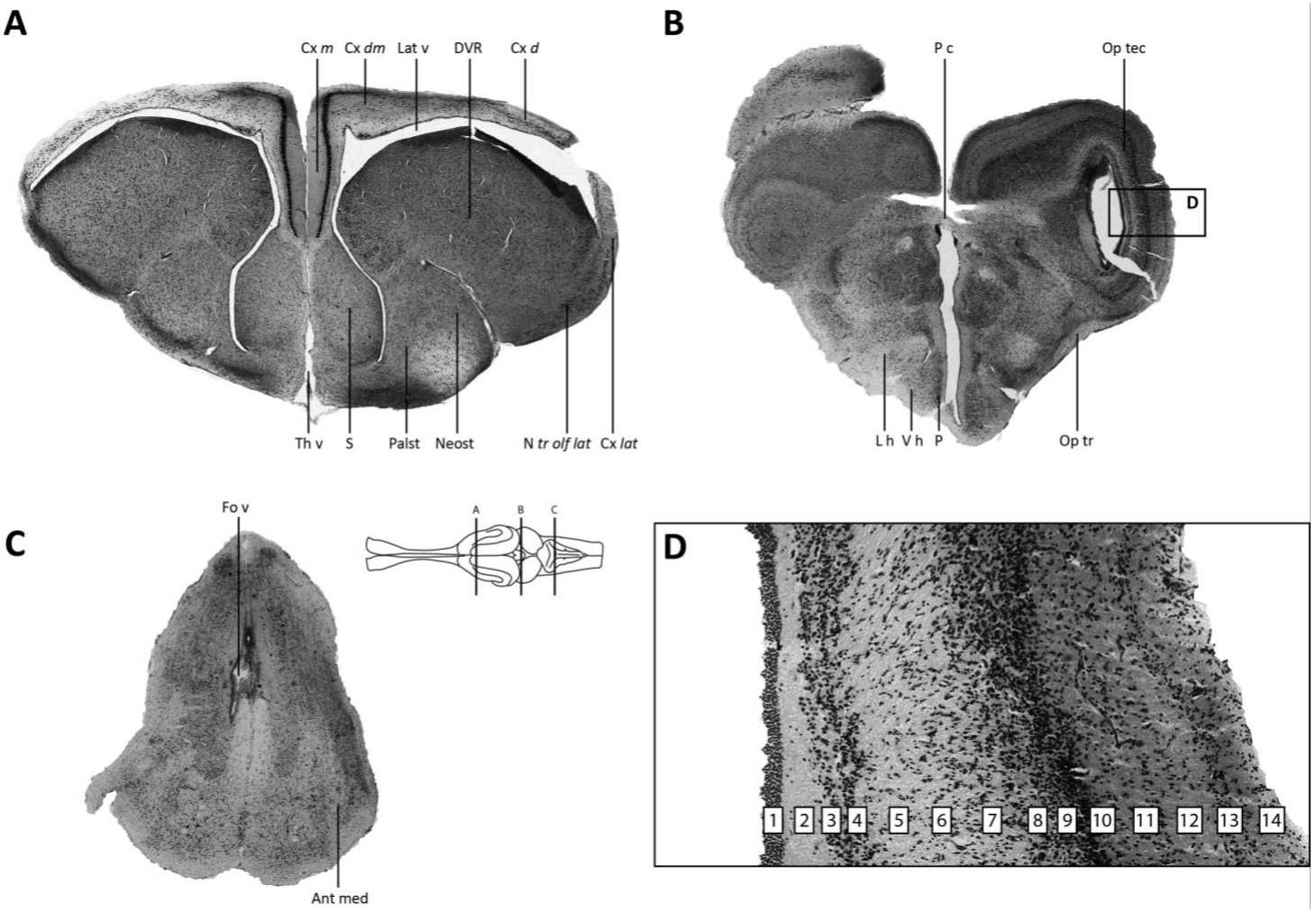

Figure 4.4 Photomicrographs of Nissl-stained brain sections from an agamid. (A–C) Major brain regions are represented (A – forebrain; B – midbrain; C – hindbrain). (D) Detailed image of the optic tectum. The brain schematic was modified from a drawing of a lizard rendered by artist Christiaan van Huijzen for Poster 2 of the poster book accompanying (Nieuwenhuys et al., 1998). Delineation of major brain regions (A–C), with only cosmetic changes made to the abbreviation style, generally follows: Butler and Northcutt, 1971, 1973; Foster and Hall, 1975; Greenberg, 1982; Northcutt, 1967, 1978; Senn and Northcutt, 1973; Shanklin, 1930; and Smeets et al., 1986. The laminar organization of the optic tectum (D) follows Ramón (1986). See Appendix for abbreviations.

4.4.4 Immunohistochemical staining of perfusion-fixed tissue

The results of our immunohistochemical staining are presented in Figure 4.6A–D. Robust TH-immunoreactive (-ir) neurons were observed in the periventricular hypothalamus of tissues fixed under field conditions for *Trioceros johnstoni* (Fig. 4.6A, *white arrows*). Fine TH-ir neurites (many of them likely axonal) were also observed within this region (Fig. 4.6A, *solid yellow horizontal lines*). Fluorescent counterstaining additionally revealed that delicate structures, such as the ependymal layer lining the third ventricle, were largely intact under field fixation conditions (Fig. 4.6A, *large arrowheads*). Similarly, laboratory-fixed tissues revealed robust TH-ir neurons in the periventricular hypothalamus of *Rieppeleon kerstenii* (Fig. 4.6B), yet the ependymal layer lining the third ventricle did not remain entirely intact and fine TH-ir neurites were less prominently visible. Additionally, NPY-labeled neurons were prominently localized in the field-fixed tissues of *Rhampholeon boulengeri* (Fig. 4.6C), and the laboratory-fixed tissues of *Rieppeleon kerstenii* (Fig. 4.6D). In contrast, Calb staining was poor in both tissue sets (Fig. 4.6C–D).

4.4.5 Immersion-fixed samples scanned using diffusible iodine-based contrast-enhanced computed tomography (diceCT)

Two lizards (*Rhampholeon boulengeri* and *Trioceros johnstoni*) were prepared for diceCT scanning under the field conditions described in *Section 4.3*. In addition to bony tissues that are typically captured with X-ray imaging techniques, our contrast-enhanced specimens revealed, in great detail, differentiation between muscular, epithelial, glandular, and neurological tissues (Fig. 4.7). This was equally true for superficial structures (e.g., hyobranchial muscles, distal branches of peripheral nerves) as it was for tissues located more deeply within the head, such as the brain.

Indeed, even the internal anatomy of the brain was visualized clearly owing to the ability for Lugol's iodine to differentiate between myelinated and non-myelinated components of the central (and peripheral) nervous system (compare, for example, optic tectum [Op tec] and the optic tract [Op tr] in Fig. 4.7C). The high levels of contrast for these scans make them amenable to successful 3-D reconstruction of the soft anatomy (e.g., the brain and its peripheral cranial nerves), registration with the surrounding skull, and finer, Nissl-based imaging techniques.

Table 4.5 Results of GEE analyses of clustered ordinal scores for scored data from stained tissue sections comparing field and lab fixation treatments using solutions containing 4% formaldehyde.

Variable	Description	beta Estimate	Robust SE	Z	P-Value
A	presence of blood	0.376	0.702	0.536	0.5922
B	evenness of stain	–0.375	0.771	–0.487	0.6261
C	tissue integrity at center	1.579	0.763	2.068	0.0384
D	tissue integrity at edge	7.091	0.631	11.231	0.0000
E	lamination patterns visible	26.920	0.492	54.726	0.0000
F	cell clusters and nuclei visible	23.577	6.194	3.806	0.0001

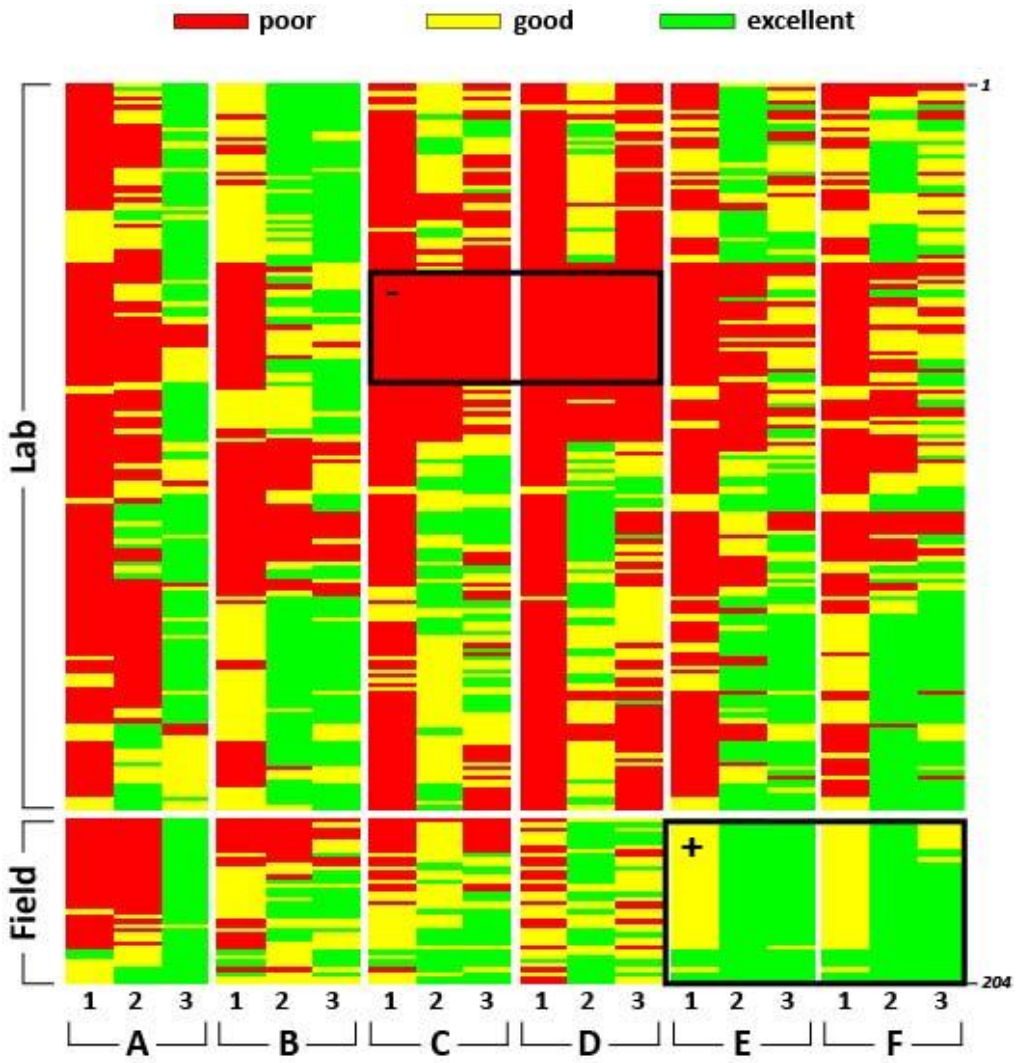

Figure 4.5 Heat map of scored semi-quantitative data for six qualitative variables from three independent observers. Observers evaluated Nissl-stained tissue sections (n = 204) from laboratory and field treatments using solutions containing 4% formaldehyde. Each column indicated with a small number (1, 2, or 3) represents an observer. Columns are grouped according to the qualitative variable being rated: presence of blood in tissue (A); evenness of stain (B); integrity of tissue at center of section (C); integrity of tissue at edges of section (D); clarity of lamination patterns (E); visibility of cell areas and nuclei (F). Tissue sections prepared under laboratory conditions are positioned on top (n = 166) and those prepared under field conditions on bottom (n = 38). The color code for the scored data is shown above the heat map. The black box outlines denoted with a '-' or a '+' indicate selected regions of tissue ratings (negative or positive, respectively) that were largely uniform across observers.

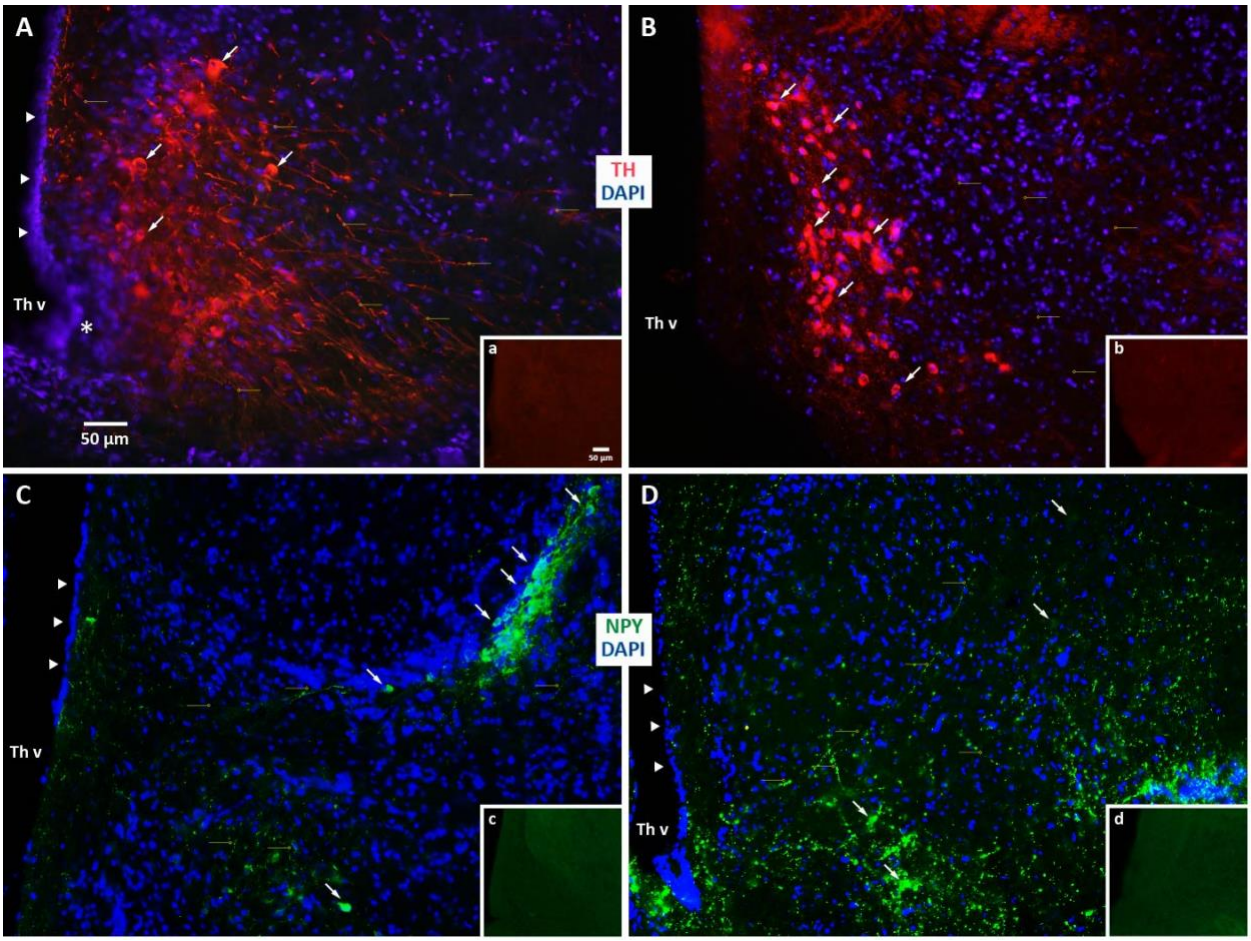

Figure 4.6 Comparison of immunohistochemical staining of brain tissue fixed under field and laboratory conditions. (A, B). The images show tyrosine hydroxylase immunoreactivity (-ir) (TH; *red*) with DAPI fluorescent counterstain (*blue*) for (A) *Trioceros johnstoni* fixed under field conditions, and (B) *Rieppeleon kerstenii* fixed under laboratory conditions. (C, D). The images show neuropeptide Y-ir (NPY; *green*), again with DAPI (*blue*) for (C) *Rhampholeon boulengeri* fixed under field conditions and (D) *Rieppeleon kerstenii* fixed under laboratory conditions (note that tissues in B and D are from the same animal). Both immunoreactive neurons (*arrows*) and neuronal extensions (*small solid horizontal lines ending in hollow circles*) are clearly visible, many of the latter being identifiable axons with varicosities. The ependymal cell layers lining the third ventricle (Th v) in A, C and D are indicated by arrowheads. The single-plane image in A rendered a portion of the image slightly out of focus (*asterisk*). Insets (a–d) show views of sections processed in the absence of the primary antibody. For inset b, the image has been brightened linearly so that the tissue section can be clearly seen in the photo. Scale bars (panel A, inset a) apply to all remaining panels and insets, respectively.

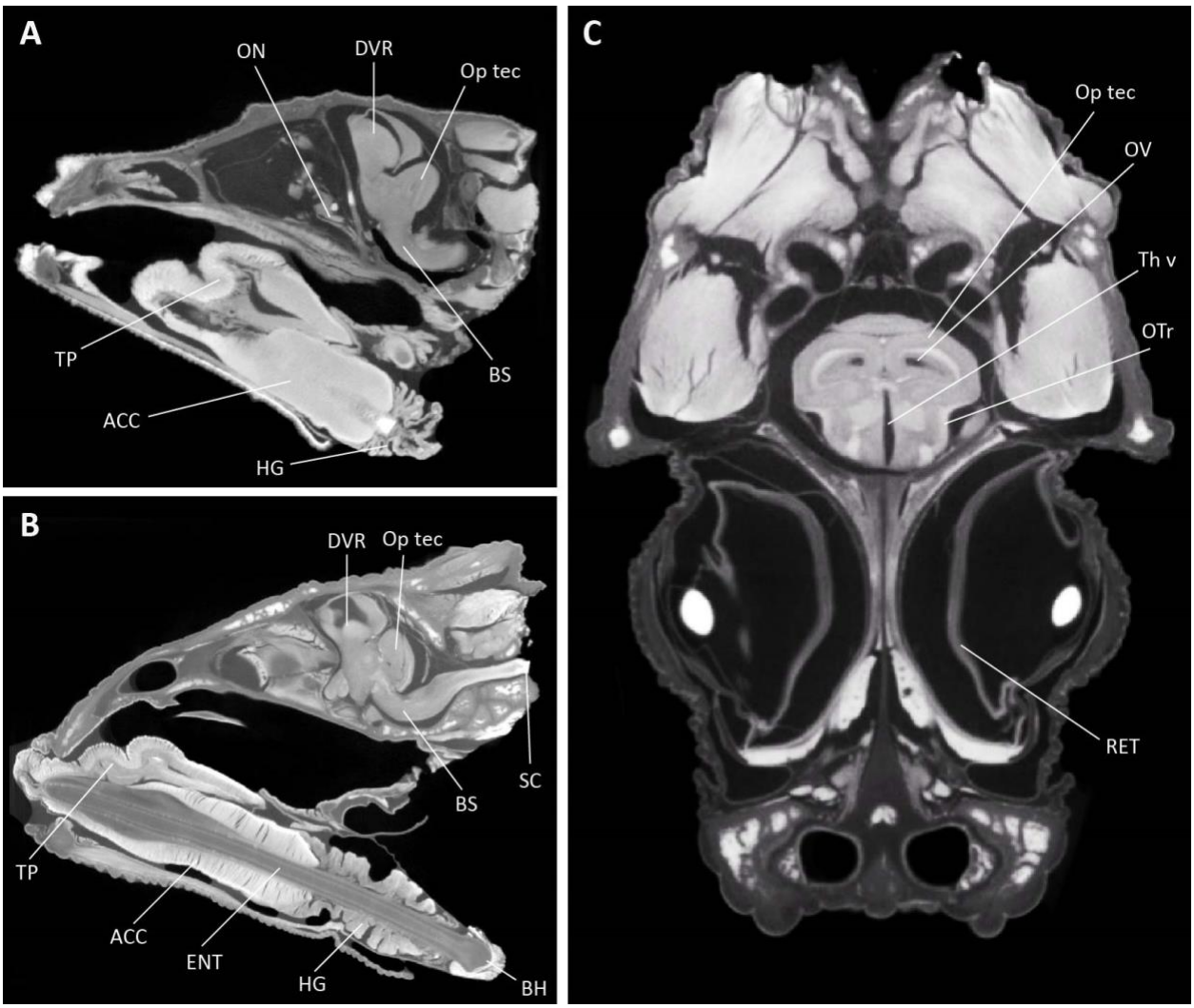

Figure 4.7 Diffusible iodine-based contrast-enhanced computed tomography (DiceCT) through the heads of two chameleon species. (A) Parasagittal view of an adult male representative of *Rhampholeon boulengeri*; (B) parasagittal and (C) frontal views of an adult female representative of *Trioceros johnstoni*. These images illustrate the extraordinary diversity of soft anatomical structures that can be clearly visualized with our approach, including myelinated and unmyelinated components of the brain. Abbreviations for selected structures: ACC – M. accelerator linguae; BH – basihyoid; BS – brain stem; DVR – dorsal ventricular ridge; ENT – entoglossal process; HG – M. hyoglossus; ON – optic nerve; Op tec – Optic tectum; OTr – olfactory tract; OV – optic ventricle; RET – retina; SC – spinal cord; Th v – third ventricle; TP – tongue pad.

4.5 Discussion

In this study, we have evaluated two standard laboratory brain fixation methods for use in remote field locations where resources are limited and environmental conditions for tissue preservation are suboptimal. First, we found that transcardial perfusion-based methods to preserve lizard brain tissue, performed in parts of a remote biodiversity hotspot, are comparable to laboratory-based use of these methods in maintaining tissue quality at the cellular level. This conclusion is based on careful validation of the field fixation methods against laboratory methods by semi-quantitative cytoarchitectonic analysis of the processed brain tissue and by indirect immunohistofluorescence cytochemistry. Second, we found that immersion fixation in the field preserves gross neuroanatomical features of the brain very well, as evaluated using diceCT imaging. Moreover, the visualization of myelinated and unmyelinated components of the brain using diceCT imaging supports the efficacy of our field immersion fixation approach. To our knowledge, this paper is the first published account of a successful attempt to perform and rigorously validate protocols for transcardial perfusion and immersion fixation of brain tissue in a completely mobile field setting.

4.5.1 Methodological considerations

We found that field-perfused lizard brains are similar to lizard brains perfused under standard laboratory conditions. In particular, cytoarchitectural features normally found in Nissl-stained brain sections were evident within the field specimens we processed, including discrete nuclear boundaries and structurally intact patterns of lamination. Moreover, the general appearance of the tissue, cleared completely of any blood, indicated complete perfusion. Although attempts were made to avoid extreme environmental exposure, our field-collected samples were subjected

to high ambient temperatures (33–37°C) and a wide range of climates during their shipment from Central Africa to the southwestern United States. Moreover, traditional methods to preserve brain tissue involve perfusing animals with ice-cold 4% paraformaldehyde (Aitken et al., 1995; Lipton et al., 1995), but our collected animals were perfused with 10% buffered formalin during the rainy season of a humid tropical climate, with no access to ice or cold storage. Considering the potential damage to delicate brain tissues from exposure to environmental variables, warm solutions, and buffered formalin with a relatively high concentration of formaldehyde, our observations of no demonstrable differences between field- and lab-processed tissues for the first two criteria we evaluated (presence of blood and evenness of staining) is somewhat surprising. However, it has been shown that varying formaldehyde concentration within fixative solutions has little effect on the size of nuclei over a 10-fold range (1–20%), and extreme changes have only been observed in tissues fixed in at least 40% formaldehyde (Fox et al., 1985). Furthermore, tissue shrinkage was not evident with the naked eye, which is known to occur in tissues incompletely fixed in formaldehyde or those subjected to varying temperatures (Fox et al., 1985).

The greatest negative effect on tissue quality for Nissl staining is arguably the interval between the time *post mortem* and the time of fixation (Scudamore et al., 2011). It has been observed that fixation within 10 h *post mortem* has no effect on the intensity of stains, yet the ability for the tissue to be stained gradually deteriorates as the time interval increases, until staining capacity is entirely lost if fixation occurs 60–72 h *post mortem* (Gu et al., 1985). On average, our field-collected animals were fixed in under an hour. Therefore, the mean duration between the time *post mortem* and the time of fixation for our field procedure does not compromise tissue quality. However, to minimize operational time, adequate training and multiple practice runs in a controlled environment are warranted before trying this procedure in the field.

4.5.2 Cytoarchitectonics

We used a semi-quantitative approach to evaluate the cytoarchitecture of the tissue sets processed under laboratory and field conditions of perfusion fixation. A recent survey of semi-quantitative methods used to evaluate histology has found that there is no accepted standard for the types of criteria used for such evaluations (Klopfleisch, 2013). Given the many diverse approaches used to rate the quality of brain tissue, it was recommended that at the very least, investigators should provide a rationale for the specific criteria they use (Klopfleisch, 2013). In line with this recommendation, we note here that the criteria we used were selected on the basis of the goals of our larger experimental research program involving these species, which are to examine the gross neuroanatomical relationships among their gray and white matter structures and the general cytoarchitectonic features of their brain tissue such as aggregations of neurons forming nuclei and laminae. These scales of comparative analysis are informed, in part, by seminal comparative neuroanatomical studies published at the turn of the twentieth century by Ramón (1896), Edinger (1899), and Brodmann (1909). Our approach necessarily constrains the criteria we use to those listed in *Section 2.10*, guided as we are by a rationale of general histological evaluation at the tissue level rather than its examination at the single-cell or subcellular levels. If the focus were on more fine-grained studies of the morphology of the cells (e.g., the appearance of neurites, the condition of the organelles within the stained cells), then the criteria chosen using Nissl-based methods would likely be different (e.g., see Chapters X–XIV of Barker [1899]), and alternatives to the Nissl method would also have been considered (e.g., see Chapter II in Vol. I of Cajal [1909]).

Our statistical analyses show that, on the basis of the two major criteria we used to evaluate fixation efficacy (presence of blood and evenness of stain), no differences in tissue quality were observed between field- and laboratory-perfused specimens. This result supports our qualitative observations of the tissue samples. Further, on the basis of the remaining four criteria (integrity of tissue in center, integrity of tissue at edges, visualization of lamination patterns, visualization of cell clustering and nuclei), the field-perfused tissue actually displayed significantly better tissue quality than lab-perfused tissue. While these results may be somewhat surprising given the more controllable fixation conditions generally available in a laboratory setting, we must interpret these findings with caution for a few reasons. First, from a qualitative standpoint, it is difficult to separate these four criteria from underlying effects that could be due to other factors, such as tissue damage that was incurred during the mounting of the tissue sections onto glass slides, tissue adherence to the slides during their mechanical transfer through separate reagent reservoirs during the Nissl staining procedure, and any differences in tissue stability resulting from variations in section thickness. Second, our analysis is limited by the variability we observed among the three independent raters, despite the fact that the mixed model we used to analyze our results mitigates this issue to some extent. Third, the dissimilarity in buffers used to prepare the laboratory and field fixative solutions presents a confounding variable to comparisons between respective tissue sets. Nevertheless, we do not feel that this buffer difference contributed significantly to the statistical (or qualitative patterns) deduced from the comparative analyses because the use of borate and sodium phosphate buffers for fixative solutions is common and both have been validated in cytoarchitectonic and chemoarchitectonic studies of the brain [27-30, 43, 63, 65, this study]. Finally, these latter four criteria are interdependent to a large degree on the first two criteria; this interdependence of predictors makes it possible that the statistically significant effects we obtained

may be more apparent than real, given that the first two major criteria (which are not dependent, or as dependent, on issues such as mounting and mechanical transfer) show no differences between the two groups.

4.5.3 Immunohistochemistry

In addition to providing validation of our fixation procedures in the field by evaluating cytoarchitectonic criteria within Nissl-stained tissue sections, we sought indications that our fixation was compatible with standard chemoarchitectural localization methods. In particular, given that the field conditions required prolonged post-fixation in formalin-sucrose, we were concerned about the possibilities of over-fixing the tissue. The duration of formaldehyde fixation may lead to absent or weak binding for some epitopes, preventing effective chemoarchitectural studies with immunohistochemistry (Srinivasan et al., 2002). At times, poor penetration of the fixative can occur with too short of an exposure time and excessive cross-linkage can occur from prolonged exposure (Werner et al., 2000). In addition, the effects of prolonged formalin fixation can cause irreversible damage to some epitopes, but this is largely dependent on the antibody used (Wasielewski et al., 1994).

For our immunohistochemical procedures, we aimed to identify dopamine-containing neurons in the periventricular hypothalamus, a well-studied neuronal subpopulation that has been documented previously to be present within the lizard brain (Bennis et al., 1991; González and Smeets, 1994; Smeets, 1994). Our results demonstrating robust TH-immunoreactivity (-ir) in neurons of field-fixed tissues that is comparable to that observed in laboratory-fixed tissues, confirms the findings of others (Bennis et al., 1991; González and Smeets, 1994; Smeets, 1994) that characterize this cell population as dopaminergic and extends them by demonstrating that the

field conditions of prolonged post-fixation did not prevent chemical identification of these neurons. Relative to the field-fixed sample, the lab-fixed sample displayed apparently elevated levels of TH expression in cell bodies and low levels in fibers. Whether this staining difference indicates a difference in fixation efficacy or that of peptide transport from the cell bodies to distal neurites between animals, is unclear. We also found comparable labeling of NPY-ir, reported to be present in chameleon brain (Bennis et al., 2001), in cell bodies and/or axonal fibers within field- and lab-fixed tissues. These findings demonstrate the extensibility of our field-based methods to antigens of different types (i.e., those that mark the presence of small neurotransmitters or those that mark neuropeptides). Although immunohistochemical labeling and visualization was feasible using our approach, further research is required to understand the degree of immunohistochemical reactivity across a broader range of antigens within field-perfused brains under our protocol conditions.

4.5.4 DiceCT imaging

In addition to cytoarchitectonic and immunohistochemical validation of our procedures in the field, diceCT scans from immersion-fixed field-collected samples show that our field protocol is compatible with the non-destructive visualization of gross neuroanatomical features in relation to other soft-tissue structures of the head as well as the skull. Our approach to prepare specimens for diceCT scans, immersion fixation and prolonged storage in fixative followed by iodine-enhancement, was demonstrated to have no negative effects on the contrast and visual quality of the scans. Gray and white matter regions were clearly distinguishable in the soft tissue, further demonstrating that our specimen preparation was successful. Importantly, diceCT can be achieved without encephalectomy, allowing for the interrelationships between central and peripheral

components of the nervous system to be preserved. Another advantage of diceCT is that 3-D rendering software can be used to rapidly visualize the high-resolution scans as complex, 3-D soft-tissue anatomy (Gignac and Kley, 2014; Gignac et al., 2016). In turn, these datasets can be analyzed to quantify and compare neuroanatomical structures among different body regions and species (Gold et al., 2016). Indeed, the possibility with field-fixed samples to visualize neural circuitry from the cellular level to that of entire brain regions sets up the potential for a comprehensive mapping of brain interconnectedness in three dimensions across multiple scales.

In sum, the robust staining and tissue integrity of our field-perfused brains demonstrates that neither the concentration of formalin used nor the degree of exposure to environmental variables was sufficient to inflict any serious negative effects on the tissue quality or any superficial diminishing effects of the tissues' ability to be stained (or, with immersion-fixed samples, visualized) under the techniques described here.

4.5.5 Considerations in the field

Access and/or availability of supplies are the major limiting factors for field research, especially for long-term expeditions in remote locations with poor infrastructure. Biodiversity hotspots (Mittermeier et al., 2011) are distributed disproportionally in tropical countries, which have generally high levels of poverty (Sachs et al., 2001). Most of the equipment and supplies detailed herein should be procured before travel, as they may not be available in certain countries, especially underdeveloped ones. Our expedition was no different from other carefully planned herpetological collecting expeditions in which it was realized in retrospect that certain supplies should have been brought to the field (Jackson, 2008; James, 2008). For example, including pH test strips (pH paper) or a battery-powered pH meter in our field kit would have allowed for us to

make accurate pH measures of our fixatives, and we recommend researchers to include this item before embarking on their own collecting trips. Indeed, our list of supplies was far from complete, and can also be modified to facilitate more specialized perfusion approaches intending to address specific research questions. With respect to essential supplies, particular attention should be paid to formaldehyde, a hazardous material that is not permitted on commercial airlines. Researchers attempting this procedure in underdeveloped countries or countries without reliable access to formaldehyde (at a range of concentrations) must ensure that this material can be acquired upon their arrival as it will be a major limiting factor. Typical sources of formaldehyde include universities, morgues, or laboratory supply companies. Researchers should also bear in mind the disposal of chemical waste generated from this procedure, which takes the form of a very small amount of waste formalin (~2 ml/perfusion). We recommend researchers attempting this procedure to store any amount of hazardous waste in a labeled container and dispose of this waste at a proper facility when one is made available.

To accomplish this procedure under completely mobile conditions in the field over a relatively long period of time without access to a laboratory, both a substantial amount of fluids and replacements of most supplies are required. Ideally, a researcher would have access to some sort of basecamp with basic shelter from the elements, where most of the supplies can be stored. In this case, animals can be captured and transported to basecamp for the fixation procedure, which will likely cut down on waste, sample exposure to environmental conditions, and potential equipment loss.

Perfusion fixation of brain tissue has been performed in various forms for at least the better part of a century (e.g., Carmichael, 1929; Koenig et al., 1945). Clearly, our methodology is only one approach to conduct perfusion fixation of brain tissue. Pump-assisted perfusions, for example,

can also be used. Electric pumps are optimal because both the hydrostatic pressure and flow rate of the fixative solutions are controllable (Eichhammer et al., 1987; Hoops, 2015). However, pumps require a reliable source of electricity, which is often not available in the field. Gravity assisted approaches are also a viable alternative to transcardial perfusions (Rieke et al., 1981) and are arguably superior to syringes for controlling the pressure of injected solutions. However, it can be challenging to bring an entire gravity-fed perfusion system (e.g., containers, fluid lines) when working in very remote locations; yet, a resourceful scientist can utilize a variety of common items to replace containers, such as water bottles. Nevertheless, if the containers are too small, it can be difficult to properly regulate the flow rate of solutions in the fluid lines as they are drained from their elevated positions (E. D. Roth, personal communication). Immersion fixation is arguably the easiest fixation method to achieve in the field. This approach can help avoid inflicting physical damage to the brain tissue during dissection. However, it is widely recognized that transcardial perfusion fixation produces superior results to immersion fixation with respect to staining efficacy and visible immunoreactivity (Beach et al., 1987; Bondonna et al., 1977; Gertz et al., 1975; Tago et al., 1986). Finally, our procedure works well for small lizards; however, larger animals require greater amounts of fixative to penetrate deep brain tissues and a small syringe will likely not suffice. This problem should be recognized before an expedition is undertaken and can be easily resolved with the use of a larger syringe or gravity-assisted perfusion set-up with a sizable elevated container. For very large animals where such a set-up is not feasible, some unique brain fixation methods in the field have been described (Knudsen et al., 2002; Manger et al., 2009).

4.5.6 Concluding remarks

We have shown that field-based brain fixation methods can preserve effectively the cytoarchitecture, chemoarchitecture, and gross neuroanatomy of the brains of wild-caught herpetofauna. Specifically, performing transcardial perfusion fixation in a mobile field setting is an advantageous alternative to laboratory-based perfusion. The tissue integrity and stain intensity obtained in this study indicate, qualitatively and semi-quantitatively, that the degree of environmental exposure and amount of formaldehyde concentration did not negatively impact our visualization of neural substrates within the tissues. Also, we found that immersion fixation of the intact brain and skull is highly feasible for preserving gross anatomy and for preparing specimens for diceCT imaging. Collectively, these protocols should serve as a flexible framework for researchers attempting field-based fixation of brain tissue. Our approach also has the potential to liberate researchers from laboratory limitations imposed by traditional methods and can be harnessed to explore species diversity that is critically needed for neuroscientific and gross anatomical research.

Accelerated declines in global biodiversity are associated inescapably with losses in unknown amounts of trait variation. We must endeavor to mitigate these losses with higher rates of rescue for as many types of data as possible. Our understanding of the anatomical diversity of the vertebrate brain is rudimentary; for this reason, there recently have been efforts to increase the level of species diversity in neuroscientific research (Striedter et al., 2014). Although novel ways to salvage existing brain specimens will undoubtedly help in this effort (Iwaniuk, 2011), this goal will best be accomplished by the continued active collection of brain specimens from wild animals in the field.

Chapter 5: Conclusion

5.1 Comparative biogeography of Albertine Rift chameleons

The Albertine Rift (AR) is the most diverse highland region in continental Africa, and thus an ideal region to test hypotheses of squamate evolution. Nevertheless, it is not well known whether sympatric taxa share diversification patterns in relation to the historical biogeographic events of this region. I investigated the relative roles of environmental and taxon-specific factors in influencing spatiotemporal patterns of genetic diversity in two sympatric chameleon species. The Ituri Forest Chameleon (*Kinyongia adolfifriderici*) and Boulenger's Pygmy Chameleon (*Rhampholeon boulengeri*) share distributions and habitats in the AR, yet differ in microhabitat use and foraging behavior. *Rhampholeon boulengeri* is considered terrestrial and forages on the forest floor, whereas *K. adolfifriderici* is considered arboreal and forages high in the forest canopy. Considering their prominent ecomorphological differences, it is reasonable to think that ancestral populations of these two species would have experienced slightly diverse selective conditions and thereby responded differently to the same change in the environment.

Results from gene-tree and species-tree reconstructions indicated that these two species were not widespread in the rift, but rather each is composed of several genetically distinct, cryptic species. Phylogeographic patterns demonstrated that similar geographic areas for both species harbored distinct clades with restricted distributions, yet idiosyncratic distribution patterns were detected for several of these lineages. In particular, I detected a high level of undescribed species diversity in the genus *Rhampholeon* from the AR. The five new pygmy chameleon lineages presented an alternative to the allopatric speciation via forest retraction biogeographic scenario, which is the most commonly cited mode of vertebrate evolution in the region. Rather, pygmy

chameleon diversification patterns were better explained by parapatric speciation via niche differentiation across an elevational gradient. In contrast, patterns of diversification for the forest chameleon genus *Kinyongia* were more closely aligned with the isolation in forest refugia model.

Diversification dates identified the Miocene as the most important time for lineage formation in both species groups, yet *Kinyongia* species were generally more ancient than *Rhampholeon* species. Dates for lineage formation in *Rhampholeon* indicated that the group in the AR exhibited a pulse of speciation at the Miocene-Pliocene boundary. The divergence dates for clades of both species suggest that historical biogeographic events affected speciation dynamically, such that congruent and taxon-specific patterns emerged. The distribution of genetic diversity I found supported several putative biogeographic barriers in the region that were identified in previous studies, yet an unfrequently cited mechanism was revealed to be a driver of pygmy chameleon diversity in the region, and it may be more widespread than currently thought.

5.2 Applications of field-preserved brains in comparative neuroanatomy

It is self-evident that we need to accelerate collection efforts in biodiversity hotspots before poorly understood and/or undocumented species become extinct. Further, the lack of species diversity in comparative studies of neuroanatomy has led to a rudimentary understanding of vertebrate brain evolution. A rational solution to these problems is to sample more species for neuroanatomy, especially species for which nothing is known. However, traditional specimen preparations do not permit researchers to retrieve neuroanatomical data at a high resolution. For this reason, I field-tested two traditional laboratory-based techniques for brain preservation (transcardial perfusion and immersion fixation) while collecting specimens of Agamidae and Chamaeleonidae in a Central African biodiversity hotspot.

Field- and laboratory-perfused brain samples were compared for tissue cytoarchitecture and chemoarchitecture using Nissl-based staining and fluorescence immunocytochemistry, respectively. I found that transcardial perfusion fixation and long-term storage, conducted under remote field conditions without access to cold storage, had no observable impact on cytoarchitectural integrity or stain evenness. Further, immunostaining for small neurotransmitter and neuropeptide biomarkers was similar between our comparisons. With respect to immersion-fixation methods, field-preserved chameleon brains were readily compatible with subsequent diffusible iodine-based contrast-enhanced computed tomography (diceCT) imaging, which facilitated the non-destructive imaging of the intact brain within the skull. In particular, diceCT images revealed excellent contrast of brain tissue structures, including myelinated and unmyelinated portions of the brain. Pairing diceCT with cytoarchitectural and immunocytochemical techniques allows for the study of brains across multiple scales of analysis.

Armed with this novel, malleable framework for preserving neural tissue, researchers can now set their sights on capturing the species diversity needed to optimally explore vertebrate brain evolution. The fields of study that most commonly utilize museum specimens to address questions in taxonomy, systematics, and evolution have largely ignored the brain as a source of data. Just as taking tissues from wild animals for DNA sequencing and phylogenetic analyses became standard for all expeditionary biologists in the 21st century—including those that knew nothing of genetics—I am hopeful that this brain-preservation protocol can become part of the specimen collector's tool kit. My optimism is heightened for researchers from countries that are poised logistically to sample the brains of rare and poorly known species, even for those researchers that lack training in neuroscience.

5.3 Future directions

While this study achieved measureable goals, it also laid bare several unanticipated gaps in knowledge and thus multiple avenues for further research. With that in mind, I intend to build upon, significantly extend, and carefully follow through with these endeavors. As a first step towards this goal, I will use this section to outline future projects, describe their current status, and highlight some preliminary findings.

Based on phylogenetic analyses of DNA data, I identified five new pygmy chameleon lineages that were previously recognized under the name *Rhampholeon boulengeri*. From preliminary analyses on the morphology of museum specimens from various *R. boulengeri* populations, I also identified size-corrected differences among some of the putative species identified with genetic analyses (e.g., Hughes and Greenbaum, 2014). I intend to incorporate linear measurements from additional populations and, importantly, from the type specimens for *R. boulengeri* into novel statistical analyses aimed at reconciling morphology with the genetic lineages. Rudolf Grauer collected three specimens that are currently registered as syntypes in the Naturhistoriches Museum Wien (NMW 16000: 1–3) in Vienna, Austria. In the absence of examining these three specimens, we chose not to undertake any nomenclatural acts and we have not identified the "real" *R. boulengeri*. As a priority future direction, I will assign the bona fide *R. boulengeri* and describe various lineages as new taxa based on a morphological comparisons to the original type series and newly collected voucher specimens.

The biogeography of montane chameleons in the AR is far from resolved. I found evidence for two separate modes of speciation, including allopatry and parapatry, with each mode better suited to explain species-level divergence events in either *Kinyongia* or *Rhampholeon*, respectively (e.g., Hughes et al., 2017b). Nevertheless, the species in those two genera are not the only

chameleons in the region. The horned chameleons of the genus *Trioceros* are represented by several species in the area, including three widespread, montane species: *T. johnstoni*, *T. ellioti*, and *T. rudis*. Preliminary phylogenetic results (data not shown) from several populations representing these three species corroborate both idiosyncratic and expected responses to the biogeographic barriers that were identified for *Kinyongia* and *Rhampholeon*. I intend to generate a comprehensive analysis that incorporates montane species from all three genera and this study aims to provide a large-scale, multispecies perspective on chameleon evolution and biogeography in the Central African highlands.

Species extinctions beget losses to our understanding of trait variation, so sampling such rare taxa demands extraordinary care in accelerating data-rescue efforts before poorly understood species are lost. I experimentally validated a protocol using novel field-based procedures for brain preservation while collecting chameleons in Africa. I found that brain tissues preserved under remote field conditions were comparable to laboratory prepared tissues and tractable with diffusible iodine-based contrast-enhanced computed tomography (diceCT), allowing for the documentation of soft-tissue structures. As a future direction, I will integrate the field-based protocol into a pipeline that aims to examine the cranial diversity of rare species (e.g., Hughes et al., 2018b). This pipeline involves CT-scanning field-collected specimens to reconstruct high-density tissues (bone). The same specimens are next stained with Lugol's iodine (I_2KI) and re-scanned to visualize soft-tissue structures, including the brain. Finally, samples are then de-stained, brains dissected from the skull, and used for histological preparations to examine cyto- and chemoarchitectural features. A pipeline for reciprocal illumination of field-fixed brains from the gross anatomical to the cellular levels sets up the potential for a comprehensive mapping of brain interconnectedness across spatial scales for rare species that lack neuroanatomical information.

References

Aitken PG, Breese GR, Dudek FF, Edwards F, Espanol MT, Larkman PM, Lipton P, Newman GC, Nowak Jr TS, Panizzon KL, Raley-Susman KM. 1995. Preparative methods for brain slices: A discussion. *Journal of Neuroscience Methods* 59: 139–49.

Albert FW, Somel M, Carneiro M, Aximu-Petri A, Halbwax M, Thalmann O, Blanco-Aguiar JA, Plyusnina IZ, Trut L, Villafuerte R, Ferrand N. 2012. A comparison of brain gene expression levels in domesticated and wild animals. *PLoS Genetics* 8: e1002962.

Alfaro ME, Zoller S, Lutzoni F. 2003. Bayes or bootstrap? A simulation study comparing the performance of Bayesian Markov chain Monte Carlo sampling and bootstrapping in assessing phylogenetic confidence. *Molecular Biology and Evolution* 20: 255–266.

Alroy J. 2015. Current extinction rates of reptiles and amphibians. *Proceedings of the National Academy of Sciences, USA* 112: 13003–13008.

Anthony NM, Johnson-Bawe M, Jeffery K, Clifford SL, Abernethy KA, Tutin CE, Lahm SA, White LJT, Utley JF, Wickings EJ, Bruford MW. 2007. The role of Pleistocene refugia and rivers in shaping gorilla genetic diversity in central Africa. *Proceedings of the National Academy of Sciences, USA* 104: 20432–20436.

Araújo MB, Nogués-Bravo D, Diniz-Filho JAF, Haywood AM, Valdes PJ, Rahbek C. 2008. Quaternary climate changes explain diversity among reptiles and amphibians. *Ecography* 31: 8–15.

Arctander P, Johansen C, Coutellec-Vreto MA. 1999. Phylogeography of three closely related African bovids (tribe Alcelaphini). *Molecular Biology and Evolution* 16: 1724–1739.

Arteaga A, Pyron RA, Peñafiel N, Romero-Barreto P, Culebras J, Bustamante L, Yánez-Muñoz MH, Guayasamin JM. 2016. Comparative phylogeography reveals cryptic diversity and repeated patterns of cladogenesis for amphibians and reptiles in northwestern Ecuador. *PLoS ONE* 11: e0151746.

Balanoff AM, Bever GS, Rowe TB, Norell MA. 2013. Evolutionary origins of the avian brain. *Nature (London)* 501: 93–96.

Barakabuye N, Mulindahabi F, Plumptre AJ, Kaplin K, Munanura I, Ndagijimana D, Ndayiziga O. 2007. Conservation of chimpanzees in the Congo-Nile Divide forests of Rwanda and Burundi. Unpublished report No. 98210-G-GO95/GA 0282. Arlington, VA: United States Fish and Wildlife Service (USFWS).

Barbour T. 1911. A new race of chameleon from British East Africa. *Proceedings of the Biological Society of Washington* 24: 219–220.

Barker LF. 1899. *The Nervous System and its Constituent Neurones*. New York: D. Appleton and Co.

Barnes RFW. 1990. Deforestation trends in tropical Africa. *African Journal of Ecology* 28: 161–173.

Bauer AM, Parham JF, Brown RM, Stuart BL, Grismer L, Papenfuss TJ, Böhme W, Savage JM, Carranza S, Grismer JL, Wagner P, Schmitz A, Ananjeva NB, Inger RF. 2010. Availability of new Bayesian-delimited gecko names and the importance of character-based species descriptions. *Proceedings of the Royal Society of London B: Biological Sciences* 278: 490–492.

Beach TG, Tago H, Nagai T, Kimura H, McGeer PL, McGeer EG. 1987. Perfusion-fixation of the human brain for immunohistochemistry: Comparison with immersion-fixation. *Journal of*

Neuroscience Methods 19: 83–192.

Beadle LC. 1981. *The Inland Waters of Tropical Africa: An Introduction to Tropical Limnology*, 2nd edition. London, UK: Longman Group, Ltd.

Bell RC, Drewes RC, Channing A, Gvoždík V, Kielgast J, Lötters S, Stuart BL, Zamudio KR. 2015. Overseas dispersal of *Hyperolius* reed frogs from Central Africa to the oceanic islands of São Tomé and Príncipe. *Journal of Biogeography* 42: 65–75.

Bennis M, Calas A, Geffard M, Gamrani H. 1990. Distribution of dopamine immunoreactive systems in brain stem and spinal cord of the chameleon. *Biological Structures and Morphogenesis* 3: 13–19.

Bennis M, Bam'hamed S, Rio JP, Le Cren D, Repérant J, Ward R. 2001. The distribution of NPY-like immunoreactivity in the chameleon brain. *Anatomy and Embryology* 203: 121–128.

Bergsten J, Bilton DT, Fujisawa T, Elliott M, Monaghan MT, Balke M, Hendrich L, Geijer J, Herrmann J, Foster GN, Ribera I. 2012. The effect of geographical scale of sampling on DNA barcoding. *Systematic Biology* 61: 851–869.

Berod A, Hartman BK, Pujol JF. 1981. Importance of fixation in immunohistochemistry: Use of formaldehyde solutions at variable pH for the localization of tyrosine hydroxylase. *Journal of Histochemistry and Cytochemistry* 29: 844–850.

Bickford D, Lohman DJ, Sodhi NS, Ng PKL, Meier R, Winker K, Ingram KK, Das I. 2007. Cryptic species as a window on diversity and conservation. *Trends in Ecology and Evolution* 22: 148–155.

Böhme M. 2003. The Miocene climatic optimum: Evidence from ectothermic vertebrates of Central Europe. *Palaeogeography, Palaeoclimatology, Palaeoecology* 195: 389–401.

Bondonna TJ, Jacquet Y, Wolf G. 1977. Perfusion-fixation procedure for immediate histologic

processing of brain tissue. *Physiology and Behavior* 19: 345–347.

Boughman JW. 2002. How sensory drive can promote speciation. *Trends in Ecology and Evolution* 17: 571–577.

Boulenger GA. 1901. Description of two new *Chamaeleon* from Mount Ruwenzori, British East Africa. *Proceedings of the Zoological Society of London* 71: 135–136.

Bowie RCK, Voelker G, Fjeldså J, Lens L, Hackett SJ, Crowe TM. 2005. Systematics of the olive thrush *Turdus olivaceus* species complex with reference to the taxonomic status of the endangered Taita thrush *T. helleri*. *Journal of Avian Biology* 36: 391–404.

Bowie RCK, Fjeldså J, Hackett SJ, Bates JM, Crowe TM. 2006. Coalescent models reveal the relative roles of ancestral polymorphism, vicariance, and dispersal in shaping phylogeographical structure of an African montane forest robin. *Molecular Phylogenetics and Evolution* 38: 171–188.

Boxnick A, Apio A, Wronski T, Hausdorf B. 2015. Diversity patterns of the terrestrial snail fauna of Nyungwe Forest National Park (Rwanda), a Pleistocene refugium in the heart of Africa. *Biological Journal of the Linnean Society* 114: 363–375.

Branch, WR. 1998. *Field Guide to Snakes and Other Reptiles of Southern Africa*, revised edition. Cape Town, South Africa: Struik Publishers, Ltd.

Branch WR, Tolley KA. 2010. A new species of chameleon (Sauria: Chamaeleonidae: *Nadzikambia*) from Mount Mabu, central Mozambique. *African Journal of Herpetology* 59: 157–172.

Branch WR, Bayliss J, Tolley KA. 2014. Pygmy chameleons of the *Rhampholeon platyceps* complex (Squamata: Chamaeleonidae): Description of four new species from isolated ‘sky islands’ of northern Mozambique. *Zootaxa* 3814: 1–36.

Brauth SE. 1990. Histochemical strategies in the study of neural evolution. *Brain, Behavior and Evolution* 36: 100–115.

Brodmann K. 1909. *Vergleichende Lokalisationslehre der Großhirnrinde in ihren Prinzipien dargestellt auf Grund des Zellenbaues*. Leipzig, Germany: Johann Ambrosius Barth. German. Translated by Laurence J. Garey. 2006. *Brodmann's Localisation in the Cerebral Cortex: The Principles of Comparative Localisation in the Cerebral Cortex Based on Cytoarchitectonics*, 3rd edition. New York: Springer Science + Business Media.

Brooks T, Hoffmann M, Burgess N, Plumptre AJ, Williams S, Gereau RE, Mittermeier RA, Stuart S. 2004. Eastern afromontane. Pp. 241–242. In: Mittermeier RA, Robles-Gil P, Hoffmann M, Pilgrim JD, Brooks TM, Mittermeier CG, Lamoreux JL, Fonseca G, eds. *Hotspots Revisited: Earth's Biologically Richest and Most Endangered Ecoregions*, 2nd edition. Mexico: CEMEX.

Bryja J, Šumbera R, Peterhans JCK, Aghová T, Bryjová A, Mikula O, Nicolas V, Denys C, Verheyen E. 2017. Evolutionary history of the thicket rats (genus *Grammomys*) mirrors the evolution of African forests since late Miocene. *Journal of Biogeography* 44: 182–194.

Burgess ND, Balmford A, Cordeiro NJ, Fjeldså J, Kuper W, Rahbek C, Sanderson EW, Scharlemann JPW, Sommer JH, Williams PH. 2007. Correlations among species distributions, human density and human infrastructure across the high biodiversity tropical mountains of Africa. *Biological Conservation* 134: 164–177.

Butler AB, Northcutt RG. 1971. Retinal projections in *Iguana* and *Anolis carolinensis*. *Brain Research* 26: 1–13.

Butler AB, Northcutt RG. 1973. Architectonic studies of the diencephalon of *Iguana iguana* (Linnaeus). *Journal of Comparative Neurology* 149: 439–461.

Butsic V, Baumann M, Shortland A, Walker S, Kuemmerle T. 2015. Conservation and conflict in the Democratic Republic of Congo: The impacts of warfare, mining, and protected areas on deforestation. *Biological Conservation* 191: 266–273.

Butynski TM, Kalina J. 1993. Three new mountain national parks for Uganda. *Oryx* 27: 214–224.

Bwong BA, Chira R, Schick S, Veith M, Lötters S. 2009. Diversity of ridged frogs (Ptychadenidae: *Ptychadena*) in the easternmost remnant of the Guineo-Congolian rain forest: An analysis using morphology, bioacoustics and molecular genetics. *Salamandra* 45: 129–146.

Cajal SR y. 1909. *Histologie du Système Nerveux de L'homme et des Vertébrés* (2 vols.). French. Translated by Neely Swanson and Larry W. Swanson. 1995. *Histology of the Nervous System of Man and Vertebrates*. New York, NY: Oxford University Press.

Camargo A, Morando M, Avila LJ, Sites JW, 2012. Species delimitation with abc and other coalescent-based methods: A test of accuracy with simulations and an empirical example with lizards of the *Liolaemus darwinii* complex (Squamata: Liolaemidae). *Evolution* 66: 2834–2849.

Carcasson RH. 1964. A preliminary survey of the zoogeography of African butterflies. *East African Wildlife Journal* 2: 122–157.

Carlson BA, Hasan SM, Hollmann M, Miller DB, Harmon LJ, Arnegard ME. 2011. Brain evolution triggers increased diversification of electric fishes. *Science (Washington)* 332: 583–586.

Carmichael EA. 1929. Microglia: An experimental study in rabbits after intracerebral injection of blood. *Journal of Neurology and Psychopathology* 9: 209–216.

Carpenter AI, Rowcliffe JM, Watkinson AR. 2004. The dynamics of the global trade in chameleons. *Biological Conservation* 120: 291–301.

Carr JA, Outhwaite WE, Goodman GL, Oldfield TEE, Foden WB. 2013. Vital but vulnerable: Climate change vulnerability and human use of wildlife in Africa's Albertine Rift. *Occasional Paper of the International Union for Conservation of Nature (IUCN) Species Survival Commission No. 48*. Gland, Switzerland; and Cambridge, UK: IUCN.

Carstens BC, Pelletier TA, Reid NM, Satler JD. 2013. How to fail at species delimitation. *Molecular Ecology* 22: 4369–4383.

Ceballos G, Ehrlich PR, Barnosky AD, García A, Pringle RM, Palmer TM. 2015. Accelerated modern human–induced species losses: Entering the sixth mass extinction. *Science Advances* 1: e1400253.

Ceccarelli FS, Menegon M, Tolley KA, Tilbury CR, Gower DJ, Laserna MH, Kasahun R, Rodriguez-Prieto A, Hagmann R, Loader SP. 2014. Evolutionary relationships, species delimitation and biogeography of Eastern Afromontane horned chameleons (Chamaeleonidae: *Trioceros*). *Molecular Phylogenetics and Evolution* 80: 125–36.

Cerling TE. 1992. Development of grasslands and savannas in East Africa during the Neogene. *Paleogeography, Paleoclimatology, Paleoecology* 97: 241–247.

Cerling TE, Harris JM, MacFadden BJ, Leakey MG, Quade J, Eisenmann V, Ehleringer JR. 1997. Global vegetation change through the Miocene/Pliocene boundary. *Nature (London)* 389: 153–158.

Charvet CJ, Sandoval AL, Striedter GF. 2010. Phylogenetic origins of early alterations in brain region proportions. *Brain, Behavior and Evolution* 75: 104–110.

Chorowicz J. 2005. The East African Rift system. *Journal of African Earth Sciences* 43: 379–410.

Conrad JL, Norell MA. 2007. A complete Late Cretaceous iguanian (Squamata, Reptilia) from the Gobi and identification of a new iguanian clade. *American Museum Novitates* 3584: 1–47.

Cordeiro NJ, Burgess ND, Dovie DB, Kaplin BA, Plumptre AJ, Marrs R. 2007. Conservation in areas of high population density in sub-Saharan Africa. *Biological Conservation* 134: 155–163.

Costello MJ, May RM, Stork NE. 2013. Can we name Earth's species before they go extinct? *Science (Washington)* 339: 413–416.

Couvreur TLP, Chatrou LW, Sosef MSM, Richardson JE. 2008. Molecular phylogenetics reveal multiple tertiary vicariance origins of the African rain forest trees. *BMC Biology* 6: 54.

Cox SC, Prys-Jones RP, Habel JC, Amakobe BA, Day JJ. 2014. Niche divergence promotes rapid diversification of East African sky island white-eyes (Aves: Zosteropidae). *Molecular Ecology* 23: 4103–4118.

Daniels SR, Phiri EE, Klaus S, Albrecht C, Cumberlidge N. 2015. Multilocus phylogeny of the Afrotropical freshwater crab fauna reveals historical drainage connectivity and transoceanic dispersal since the Eocene. *Systematic Biology* 64: 549–567.

Davis MB, Shaw RG. 2001. Range shifts and adaptive responses to Quaternary climate change. *Science (Washington)* 292: 673–679.

Daza JD, Stanley EL, Wagner P, Bauer AM, Grimaldi DA. 2016. Mid-Cretaceous amber fossils illuminate the past diversity of tropical lizards. *Science Advances* 2: e1501080.

de Witte G-F. 1941. Batraciens et reptiles. Exploration du Parc National Albert, Mission GF de Witte 1933–1935. *Institut des Parcs Nationaux du Congo Belge, Bruxelles* 33: i–xvii, 1–261 + pl. I–LXXVI + map.

de Witte G-F. 1965. Les caméléons de l'Afrique Centrale (République Démocratique du Congo, République du Rwanda et Royaume du Burundi). *Annales Musée Royal de l'Afrique Centrale, Sciences Zoologiques* 142: 1–215 + pl. I–XII.

Degnan JH, Rosenberg NA. 2009. Gene tree discordance, phylogenetic inference and the multispecies coalescent. *Trends in Ecology and Evolution* 24: 332–340.

Dirzo R, Young HS, Galetti M, Ceballos G, Isaac NJB, Collen B. 2014. Defaunation in the Anthropocene. *Science (Washington)* 345: 401–406.

deMenocal PB. 1995. Plio-Pleistocene African climate. *Science (Washington)* 270: 53–59.

deMenocal PB. 2004. African climate change and faunal evolution during the Pliocene–Pleistocene. *Earth and Planetary Science Letters* 220: 3–24.

Demos TC, Peterhans JCK, Agwanda B, Hickerson MJ. 2014. Uncovering cryptic diversity and refugial persistence among small mammal lineages across the Eastern Afromontane biodiversity hotspot. *Molecular Phylogenetics and Evolution* 71: 41–54.

Demos TC, Peterhans JCK, Joseph TA, Robinson JD, Agwanda B, Hickerson MJ. 2015. Comparative population genomics of African montane forest mammals support population persistence across a climatic gradient and quaternary climatic cycles. *PLoS ONE* 10: e0131800.

Doumenge C. 1998. Forest diversity, distribution, and dynamique in the Itombwe Mountains, South-Kivu, Congo Democratic Republic. *Mountain Research and Development* 18: 249–264.

Drewes RC, Vindum JV. 1998. Reptiles of the impenetrable forest including an addendum and corrigenda to the amphibian fauna. Unpublished report. San Francisco, CA: California Academy of Sciences.

Drummond AJ, Ho SYW, Phillips MJ, Rambaut A. 2006. Relaxed phylogenetics and dating with confidence. *PLoS Biology* 4: e88.

Drummond AJ, Suchard MA, Xie D, Rambaut A. 2012. Bayesian phylogenetics with BEAUti and

the BEAST 1.7. *Molecular Biology and Evolution* 29: 1969–1973.

Ebinger C, Furman T. 2003. Geodynamical setting of the Virunga volcanic province, East Africa. *Acta Vulcanologica* 14: 1–8.

Edgar RC. 2004. MUSCLE: Multiple sequence alignment with high accuracy and high throughput. *Nucleic Acids Research* 32: 1792–1797.

Edinger L. 1899. Untersuchungen über die vergleichende Anatomie des Gehirnes. 4. Studien über das Zwischenhirn der Reptilien. *Treatises of the Senckenberg Nature Research Society* 20: 21–197.

Editorial. 2003. Worldwide neuroscience. *Nature Neuroscience* 6: 901.

Eichhammer P, Zeller R, Rohkamm R. 1987. Fixation of neural tissue for electron microscopy with an electronically controlled perfusion pump. *Tissue and Cell* 19: 153–157.

Evans SE. 1998. Crown-group lizards from the Middle Jurassic of Britain. *Palaeontographica A* 250: 1–32.

Evans SE, Wang Y. 2005. The Early Cretaceous lizard *Dalinghosaurus* from China. *Acta Palaeontologica Polonica* 50: 725–742.

Evans BJ, Carter TF, Tobias ML, Kelley DB, Hanner R, Tinsley RC. 2008. A new species of clawed frog (genus *Xenopus*) from the Itombwe Massif, Democratic Republic of the Congo: Implications for DNA barcodes and biodiversity conservation. *Zootaxa* 1780: 55–68.

Feakins SJ, deMenocal PB, Eglinton TI. 2005. Biomarker records of late Neogene changes in northeast African vegetation. *Geology* 33: 977–980.

Felsenstein J. 1981. Evolutionary trees from DNA sequences: A maximum likelihood approach. *Journal of Molecular Evolution* 17: 368–376.

Felsenstein J. 1985. Confidence limits on phylogenies: An approach using the bootstrap. *Evolution* 39: 783–791.

Fischer E, Hinkel H. 1992. *Natur Ruandas: Einführung in die Flora und Fauna Ruandas*. Germany: Ministerium des Innern und für Sport.

Fisseha M, Mariaux J, Menegon M. 2013. The "*Rhampholeon uluguruensis* complex" (Squamata: Chamaeleonidae) and the taxonomic status of the pygmy chameleons in Tanzania. *Zootaxa* 3746: 439–453.

Fitzinger LJFJ. 1843. *Systema Reptilium, Fasciculus Primus, Amblyglossae*. Vienna, Austria: Braumüller et Seidel.

Fjeldså J, Lovett JC. 1997. Geographical patterns of old and young species in African forest biota: The significance of specific montane areas as evolutionary centres. *Biodiversity Conservation* 6: 325–346.

Flot JF. 2010. SeqPHASE: A web tool for interconverting PHASE input/output files and FASTA sequence alignments. *Molecular Ecology Resources* 10: 162–166.

Fontaine B, Perrard A, Bouchet P. 2012. 21 years of shelf life between discovery and description of new species. *Current Biology* 22: R943–R944.

Fontaneto D, Flot JF, Tang CQ. 2015. Guidelines for DNA taxonomy, with a focus on the meiofauna. *Marine Biodiversity* 45: 433–451.

Foster RE, Hall WC. 1975. The connections and laminar organization of the optic tectum in a reptile (*Iguana iguana*). *Journal of Comparative Neurology* 163: 397–425.

Fox CH, Johnson FB, Whiting J, Roller PP. 1985. Formaldehyde fixation. *Journal of Histochemistry and Cytochemistry* 33: 845–853.

Frederick A. 1910. *In the Heart of Africa*. London, UK; Toronto, Canada; and Melbourne,

Australia: Cassell and Company, Ltd.

Frost DR, Hillis DM. 1990. Species in concept and practice: Herpetological applications. *Herpetologica* 46: 86–104.

Frost DR, McDiarmid RW, Mendelson III JR. 2009. Response to the Point of View of Gregory B. Pauly, David M. Hillis, and David C. Cannatella, by the anuran subcommittee of the SSAR/HL/ASIH scientific and standard English names list. *Herpetologica* 65: 136–153.

Fuchs J, Fjeldså J, Bowie RCK. 2011. Diversification across an altitudinal gradient in the Tiny Greenbul (*Phyllastrephus debilis*) from the Eastern Arc Mountains of Africa. *BMC Evolutionary Biology* 11: 117.

Fujisawa T, Barraclough TG. 2013. Delimiting species using single-locus data and the Generalized Mixed Yule Coalescent approach: A revised method and evaluation on simulated data sets. *Systematic Biology* 62: 707–724.

Gertz SD, Rennels ML, Forbes MS, Nelson E. 1975. Preparation of vascular endothelium for scanning electron microscopy: A comparison of the effects of perfusion and immersion fixation. *Journal of Microscopy* 105: 309–313.

Gignac PM, Kley NJ. 2014. Iodine-enhanced micro-CT imaging: Methodological refinements for the study of the soft-tissue anatomy of post-embryonic vertebrates. *Journal of Experimental Zoology Part B: Molecular and Developmental Evolution* 322: 166–176.

Gignac PM, Kley NJ, Clarke JA, Colbert MW, Morhardt AC, Cerio D, Cost IN, Cox PG, Daza JD, Early CM, Echols MS. 2016. Diffusible iodine-based contrast-enhanced computed tomography (diceCT): An emerging tool for rapid, high-resolution, 3-D imaging of metazoan soft tissues. *Journal of Anatomy* 228: 889–909.

Glew L, Hudson MD. 2007. Gorillas in the midst: The impact of armed conflict on the conservation

of protected areas in sub-Saharan Africa. *Oryx* 41: 140–150.

Gold MEL, Schulz D, Budassi M, Gignac PM, Vaska P, Norell MA. 2016. Flying starlings, PET and the evolution of volant dinosaurs. *Current Biology* 26: R265–R267.

González A, Smeets WJAJ. 1994. Catecholamine systems in the CNS of amphibians. Pp. 77–102. In: Smeets WJAJ, Reiner A, eds. *Phylogeny and Development of Catecholamine Systems in the CNS of Vertebrates*. Cambridge, MA: Cambridge University Press.

Gonzalez-Voyer A, Winberg S, Kolm N. 2009. Brain structure evolution in a basal vertebrate clade: Evidence from phylogenetic comparative analysis of cichlid fishes. *BMC Evolutionary Biology* 9: 238.

Graur D, Martin W. 2004. Reading the entrails of chickens: Molecular timescales of evolution and the illusion of precision. *Trends in Genetics* 20: 80–86.

Gray JE. 1825. A synopsis of the genera of reptiles and Amphibia, with a description of some new species. *Annals of Philosophy* 2: 193–217.

Greenbaum E, Villanueva CO, Kusamba C, Aristote MM, Branch WR. 2011. A molecular phylogeny of equatorial African Lacertidae, with the description of a new genus and species from eastern Democratic Republic of the Congo. *Zoological Journal of the Linnean Society* 163: 913–942.

Greenbaum E, Kusamba C. 2012. Conservation implications following the rediscovery of four frog species from the Itombwe Natural Reserve, eastern Democratic Republic of the Congo. *Herpetological Review* 43: 253–259.

Greenbaum E, Tolley KA, Joma A, Kusamba C. 2012a. A new species of chameleon (Sauria: Chamaeleonidae: *Kinyongia*) from the northern Albertine Rift, Central Africa. *Herpetologica* 68: 60–75.

Greenbaum E, Stanley EL, Kusamba C, Moninga WM, Goldberg SR, Bursey CR. 2012b. A new species of *Cordylus* (Squamata: Cordylidae) from the Marungu Plateau of south-eastern Democratic Republic of the Congo. *African Journal of Herpetology* 61: 14–39.

Greenbaum E, Sinsch U, Lehr E, Valdez F, Kusamba C. 2013. Phylogeography of the tree frog *Hyperolius castaneus* (Anura: Hyperoliidae) from the Albertine Rift of Central Africa: Implications for taxonomy, biogeography and conservation. *Zootaxa* 3731: 473–494.

Greenbaum E, Portillo F, Jackson K, Kusamba C. 2015. A phylogeny of Central African *Boaedon* (Serpentes: Lamprophiidae), with the description of a new species from the Albertine Rift. *African Journal of Herpetology* 64: 18–38.

Greenbaum E. 2017. *Emerald Labyrinth: A Scientist's Adventures in the Jungles of the Congo*. Lebanon, NH: University Press of New England.

Greenberg N. 1982. A forebrain atlas and stereotaxic technique for the lizard, *Anolis carolinensis*. *Journal of Morphology* 174: 217–236

Griffiths CJ. 1993. The geological evolution of East Africa. Pp. 9–21. In: Lovett JC, Wasser SK, eds. *Biogeography and Ecology of the Rain Forests of Eastern Africa*. Cambridge, UK: Cambridge University Press.

Groth JG, Barrowclough GF. 1999. Basal divergences in birds and the phylogenetic utility of the nuclear RAG-1 gene. *Molecular Phylogenetics and Evolution* 12: 115–123.

Gu J, Huang WM, Polak JM. 1985. Stability of immunocytochemical reactivity of neuronal substances following delayed fixation. *Journal of Neuroscience Methods* 12: 297–302.

Halekoh U, Højsgaard S, Yan J. 2006. The R Package *geepack* for generalized estimating equations. *Journal of Statistical Software* 15: 1–11.

Hanson T, Brooks TM, Da Fonseca GAB, Hoffmann M, Lamoreux JF, Machlis G, Mittermeier

CG, Mittermeier RA, Pilgrim JD. 2009. Warfare in biodiversity hotspots. *Conservation Biology* 23: 578–587.

Harrigan RJ, Mazza ME, Sorenson MD. 2008. Computation vs. cloning: Evaluation of two methods for haplotype determination. *Molecular Ecology Resources* 8: 1239–1248.

Hassanin A, Khouider S, Gembu GC, Goodman SM, Kadjo B, Nesi N, Pourrut X, Nakoune E, Bonillo C. 2015. The comparative phylogeography of fruit bats of the tribe Scotonycterini (Chiroptera, Pteropodidae) reveals cryptic species diversity related to African Pleistocene forest refugia. *Comptes Rendus Biologies* 338: 197–211.

Heagerty PJ, Zeger SL. 1996. Marginal regression models for clustered ordinal measurements. *Journal of the American Statistical Association* 91: 1024–1036.

Heled J, Drummond AJ. 2010. Bayesian inference of species trees from multilocus data. *Molecular Biology and Evolution* 27: 570–580.

Hewitt G. 2000. The genetic legacy of the Quaternary ice ages. *Nature (London)* 405: 907–913.

Hillenius D. 1959. The differentiation within the genus *Chamaeleo* Laurenti, 1768. *Beaufortia* 8: 1–92.

Hillis DM, Bull JJ. 1993. An empirical test of bootstrapping as a method for assessing confidence in phylogenetic analysis. *Systematic Biology* 42: 182–192.

Hinkel H. 1993. Zur Biogeographie und Ökoethologie der Reptilienfauna von montanen Feuchtwäldern in Ruanda und Ost-Zaïre unter Berücksichtigung der Amphibien. Unpublished D. Phil. Thesis, Johannes Gutenberg-Universität.

Ho SY, Phillips MJ. 2009. Accounting for calibration uncertainty in phylogenetic estimation of evolutionary divergence times. *Systematic Biology* 58: 367–380.

Hoffmann M, Hilton-Taylor C, Angulo A, Böhm M, Brooks TM, Butchart SH, Carpenter KE,

Chanson J, Collen B, Cox NA, Darwall WR, et al. 2010. The impact of conservation on the status of the world's vertebrates. *Science (Washington)* 330: 1503–1509.

Hoops D. 2015. A perfusion protocol for lizards, including a method for brain removal. *MethodsX* 2: 165–173.

Huelsenbeck JP, Bull JJ, Cunningham CW. 1996. Combining data in phylogenetic analysis. *Trends in Ecology and Evolution* 11: 152–158.

Huelsenbeck JP, Ronquist F. 2001. MrBayes: Bayesian inference of phylogeny. *Bioinformatics* 17: 754–755.

Hughes DF, Greenbaum, E. 2014. Molecular phylogenetics of the pygmy chameleon *Rhampholeon boulengeri* from Africa's Albertine Rift. Oral Presentation (Abstract #90): 8 June 2014. Kisagani, Democratic Republic of the Congo: 1st International Conference on the Biodiversity of the Congo Basin.

Hughes DF, Walker EM, Gignac PM, Martinez A, Negishi K, Lieb CS, Greenbaum E, Khan AM. 2016. Rescuing perishable neuroanatomical information from a threatened biodiversity hotspot: Remote field methods for brain tissue preservation validated by cytoarchitectonic analysis, immunohistochemistry, and x-ray microcomputed tomography. *PLoS ONE* 11: e0155824.

Hughes DF, Kusamba C, Behangana M, Greenbaum E. 2017a. Integrative taxonomy of the Central African forest chameleon, *Kinyongia adolfifriderici* (Sauria: Chamaeleonidae), reveals underestimated species diversity in the Albertine Rift. *Zoological Journal of the Linnean Society* 181: 400–38.

Hughes DF, Lukwago W, Behangana M, Menegon M, Dehling JM, Stipala J, Tilbury CR, Tolley KA, Khan AM, Kusamba C, Greenbaum E. 2017b. From the floor, to the canopy:

Comparative phylogeography of two sympatric chameleon species in Central Africa's Albertine Rift. Poster Presentation (Abstract #0229): 14 July 2017. Austin, TX: Joint Meetings of Ichthyologists and Herpetologists.

Hughes DF, Tolley KA, Behangana M, Lukwago W, Menegon M, Dehling JM, Stipala J, Tilbury CR, Khan AM, Kusamba C, Greenbaum E. 2018a. Cryptic diversity in *Rhampholeon boulengeri* (Sauria: Chamaeleonidae), a pygmy chameleon from the Albertine Rift biodiversity hotspot. *Molecular Phylogenetics and Evolution* 122: 125–141.

Hughes DF, Gignac PM, Greenbaum E, Khan AM. 2018b. Field-Based brain tissue preservation methods and comparative multi-scale structural analyses reveal the cranial diversity of chameleons. Oral Presentation (Session 96-7): 6 January 2018. San Francisco, CA: Society for Integrative and Comparative Biology.

Huhndorf MH, Peterhans JCK, Loew SS. 2007. Comparative phylogeography of three endemic rodents from the Albertine Rift, east central Africa. *Molecular Ecology* 16: 663–674.

Hutter CR, Guayasamin JM, Wiens JJ. 2013. Explaining Andean megadiversity: The evolutionary and ecological causes of glassfrog elevational richness patterns. *Ecology Letters* 16: 1135–1144.

Inogwabini B-I. 2014. Conserving biodiversity in the Democratic Republic of Congo: A brief history, current trends and insights for the future. *PARKS* 20: 101–110.

IUCN 2018. The IUCN Red List of Threatened Species. Version 2017-3. Accessed on 27 January 2018. Available at: www.iucnredlist.org

Iwaniuk AN. 2011. The importance of scientific collecting and natural history museums for comparative neuroanatomy. *Annals of the New York Academy of Sciences* 1225: E1–E19.

Jackson K. 2008. *Mean and Lowly Things: Snakes, Science, and Survival in the Congo*.

Cambridge, MA: Harvard University Press.

Jacobs BF, Kingston JD, Jacobs LL. 1999. The origin of grass-dominated ecosystems. *Annals of the Missouri Botanical Garden* 86: 590–643.

Jacobs BF. 2004. Palaeobotanical studies from tropical Africa: Relevance to the evolution of forest, woodland and savannah biomes. *Philosophical Transactions of the Royal Society B: Biological Sciences* 359: 1573–1583.

James J. 2008. *The Snake Charmer: A Life and Death in Pursuit of Knowledge*. New York: Hyperion.

Jones PD, Harris I. 2008. Climatic Research Unit (CRU): Time-series datasets of variations in climate with variations in other phenomena. *NCAS British Atmospheric Data Centre.* Available at: http://catalogue.ceda.ac.uk/uuid/3f8944800cc48e1cbc29a5ee12d8542d

Jones MEH, Anderson CL, Hipsley CA, Müller J, Evans SE, Schoch RR. 2013. Integration of molecules and new fossils supports a Triassic origin for Lepidosauria (lizards, snakes, and tuatara). *BMC Evolutionary Biology* 13: 208.

Kahindo CM, Bates JM, Bowie RCK. 2017. Population genetic structure of Grauer's Swamp Warbler *Bradypterus graueri*, an Albertine Rift endemic. *Ibis* 159: 415–429.

Kamath A, Stuart YE, Campbell TS. 2013. Behavioral partitioning by the native lizard *Anolis carolinensis* in the presence and absence of the invasive *Anolis sagrei* in Florida. *Breviora* 535: 1–10.

Kamath A, Stuart YE. 2015. Movement rates of the lizard *Anolis carolinensis* (Squamata: Dactyloidae) in the presence and absence of *Anolis sagrei* (Squamata: Dactyloidae). *Breviora* 546: 1–7.

Kampunzu AB, Bonhomme MG, Kanika M. 1998. Geochronology of volcanic rocks and evolution of the Cenozoic Western Branch of the East African Rift System. *Journal of African Earth Sciences* 26: 441–461.

Kanyamibwa S. 1998. Impact of war on conservation: Rwandan environment and wildlife in agony. *Biodiversity and Conservation* 7: 1399–1406.

Kaufmann G, Hinderer M, Romanov D. 2015. Shaping the Rwenzoris: Balancing uplift, erosion, and glaciation. *International Journal of Earth Sciences* 104: 1–18.

Keqin G, Norell MA. 2000. Taxonomic composition and systematics of Late Cretaceous lizard assemblages from Ukhaa Tolgod and adjacent localities, Mongolian Gobi Desert. *Bulletin of the American Museum of Natural History* 249: 1–118.

Khan AM, Watts AG. 2004. Intravenous 2-deoxy-D-glucose injection rapidly elevates levels of the phosphorylated forms of p44/42 mitogen-activated protein kinases (extracellularly regulated kinases 1/2) in rat hypothalamic parvicellular paraventricular neurons. *Endocrinology* 145: 351–359.

Khan AM, Ponzio TA, Sanchez-Watts G, Stanley BG, Hatton GI, Watts AG. 2007. Catecholaminergic control of mitogen-activated protein kinase signaling in paraventricular neuroendocrine neurons *in vivo* and *in vitro*: A proposed role during glycemic challenges. *Journal of Neuroscience* 27: 7344–7360.

Khan AM, Kaminski KL, Sanchez-Watts G, Ponzio TA, Kuzmiski JB, Bains JS, Watts AG. 2011. MAP kinases couple hindbrain-derived catecholamine signals to hypothalamic adrenocortical control mechanisms during glycemia-related challenges. *Journal of Neuroscience* 31: 18479–18491.

Khan AM, Walker EM, Dominguez N, Watts AG. 2014. Neural input is critical for arcuate

hypothalamic neurons to mount intracellular signaling responses to systemic insulin and deoxyglucose challenges in male rats: Implications for communication within feeding and metabolic control networks. *Endocrinology* 155: 405–416.

Kiernan JA. 2001. Classification and naming of dyes, stains and fluorochromes. *Biotechnic and Histochemistry* 76: 261–278.

Kissling WD, Eiserhardt WL, Baker WJ, Borchsenius F, Couvreur TL, Balslev H, Svenning JC. 2012. Cenozoic imprints on the phylogenetic structure of palm species assemblages worldwide. *Proceedings of the National Academy of Sciences, USA* 109: 7379–7384.

Klaver CJJ, Böhme W. 1986. Phylogeny and classification of the Chamaeleonidae (Sauria) with special reference to hemipenis morphology. *Bonner zoologische Monographien* 22: 1–64.

Klaver CJJ, Böhme W. 1988. Systematics of *Bradypodion tenue* (Matschie, 1892) (Sauria: Chamaeleonidae) with a description of a new species from the Uluguru and Uzungwe Mountains, Tanzania. *Bonner zoologische Beiträge* 39: 381–393.

Klopfleisch R. 2013. Multiparametric and semiquantitative scoring systems for the evaluation of mouse model histopathology—a systematic review. *BMC Veterinary Research* 9: 123.

Knudsen SK, Mørk S, Øen EO. 2002. A novel method for in situ fixation of whale brains. *Journal of Neuroscience Methods* 120: 35–44.

Koenig H, Groat RA, Windle WF. 1945. A physiological approach to perfusion-fixation of tissues with formalin. *Biotechnic and Histochemistry* 20: 13–22.

Kolbe JJ, Glor RE, Schettino LR, Lara AC, Larson A, Losos JB. 2004. Genetic variation increases during biological invasion by a Cuban lizard. *Nature (London)* 431: 177–181.

Kolbert E. 2014. *The Sixth Extinction: An Unnatural History*. London, UK: Bloomsbury Publishing.

Kozak KH, Wiens JJ. 2010. Niche conservatism drives elevational diversity patterns in Appalachian salamanders. *The American Naturalist* 176: 40–54.

Kumar S, Stecher G, Tamura K. 2016. MEGA7: Molecular Evolutionary Genetics Analysis version 7.0 for bigger datasets. *Molecular Biology and Evolution* 33: 1870–1874.

Küper W, Sommer JH, Lovett JC, Mutke J, Linder HP, Beentje HJ, Van Rompaey RSAR, Chatelain C, Sosef M, Barthlott W. 2004. Africa's hotspots of biodiversity redefined. *Annals of the Missouri Botanical Garden* 91: 525–535.

Lanfear R, Calcott B, Ho SY, Guindon S. 2012. PartitionFinder: Combined selection of partitioning schemes and substitution models for phylogenetic analyses. *Molecular Biology and Evolution* 29: 1695–1701.

Larson TR, Castro D, Behangana M, Greenbaum E. 2016. Evolutionary history of the river frog genus *Amietia* (Anura: Pyxicephalidae) reveals extensive diversification in Central African highlands. *Molecular Phylogenetics and Evolution* 99: 168–181.

Laurenti JN. 1768. *Specimen Medicum, Exhibens Synopsis Reptilium Emendatam cum Experimentis circa Venena et Antidota Reptilium Austriacorum*. Vienna, Austria: Johann Thomas Edlen von Trattnern.

Leaché AD, Fujita MK. 2010. Bayesian species delimitation in West African forest geckos (*Hemidactylus fasciatus*). *Proceedings of the Royal Society B: Biological Sciences* 277: 3071–3077.

Leaché AD, Fujita MK, Minin VN, Bouckaert RR. 2014. Species delimitation using genome-wide SNP data. *Systematic Biology* 63: 534–542.

Leakey MG, Feibel CS, Bernor RL, Harris JM, Cerling TE, Stewart KM, Storrs GW, Walker A, Werdelin L, Winkler AJ. 1996. Lothagam: A record of faunal change in the Late Miocene

of East Africa. *Journal of Vertebrate Paleontology* 16: 556–570.

Lees AC, Pimm SL. 2015. Species, extinct before we know them? *Current Biology* 25: R177–R180.

Lenhossék M. 1895. *Der Feinere Bau Des Nervensystems im Lichte Neuester Forsuchungen*, 2nd editon. German. Berlin, Germany: H. Kornfeld.

Levasseur C, Lapointe F-J. 2001. War and peace in phylogenetics: A rejoinder on total evidence and consensus. *Systematic Biology* 50: 881–891.

Librado P, Rozas J. 2009. DnaSP v5: A software for comprehensive analysis of DNA polymorphism data. *Bioinformatics* 25: 1451–1452.

Lieb CS, Buth DG, Gorman GC. 1983. Genetic differentiation in *Anolis sagrai*: A comparison of Cuban and introduced Florida populations. *Journal of Herpetology* 17: 90–94.

Liedtke HC, Huegli D, Dehling JM, Pupin F, Menegon M, Plumptre AJ, Kujirakwinja D, Loader SP. 2014. One or two species? On the case of *Hyperolius discodactylus* Ahl, 1931 and *H. alticola* Ahl, 1931 (Anura: Hyperoliidae). *Zootaxa* 3768: 253–290.

Ligon RA, McGraw KJ. 2013. Chameleons communicate with complex colour changes during contests: Different body regions convey different information. *Biology Letters* 9: 20130892.

Ligon RA. 2014. Defeated chameleons darken dynamically during dyadic disputes to decrease danger from dominants. *Behavior Ecology and Sociobiology* 68: 1007–1017.

Lipton P, Aitken PG, Dudek FE, Eskessen K, Espanol MT, Ferchmin PA, Kelly JB, Kreisman NR, Landfield PW, Larkman PM, Leybaert L. 1995. Making the best of brain slices: Comparing preparative methods. *Journal of Neuroscience Methods* 59: 151–156.

Liu L, Yu L, Edwards SV. 2010. A maximum pseudo-likelihood approach for estimating species

trees under the coalescent model. *BMC Evolutionary Biology* 10: 302.

Loader SP, Ceccarelli FS, Menegon M, Howell KM, Kassahun R, Mengistu AA, Saber SA, Gebresenbet F, de Sá R, Davenport TR, Larson JG, Müller H, Wilkinson M, Gower DJ. 2014. Persistence and stability of Eastern Afromontane forests: Evidence from brevicipitid frogs. *Journal of Biogeography* 41: 1781–1792.

Loreau M, Naeem S, Inchausti P, Bengtsson J, Grime JP, Hector A, Hooper DU, Huston MA, Raffaelli D, Schmid B, Tilman D. 2001. Biodiversity and ecosystem functioning: Current knowledge and future challenges. *Science (Washington)* 294: 804–808.

Lorenzen ED, Heller R, Siegismund HR. 2012. Comparative phylogeography of African savannah ungulates. *Molecular Ecology* 21: 3656–3670.

Lötters S, Wagner P, Bwong BA, Schick S, Malonza PK, Muchai V, Wasonga DV, Veith M. 2007. *A Fieldguide to the Amphibians and Reptiles of the Kakamega Forest*. Frankfurt am Main, Germany: National Museum of Kenya and University of Mainz.

Loveridge A. 1956. A new subgenus of *Chamaeleo* from Rhodesia and a new race of *Mabuya* from Kenya Colony. *Breviora* 59: 1–4.

Loveridge A. 1957. On a third collection of reptiles taken in Tanganyika by C. J. P. Ionides, Esq. *Tanganyika Notes and Records* 43: 1–19.

Lutzmann N, Nečas P. 2002. Zum Status von *Bradypodion tavetanum* (Steindachner, 1891) aus den Taita Hills, Kenia, mit Beschreibung einer neuen Unterart (Reptilia: Sauria: Chamaeleonidae). *Salamandra* 38: 5–14.

Maan ME, Hofker KD, van Alphen JJ, Seehausen O. 2006. Sensory drive in cichlid speciation. *The American Naturalist* 167: 947–954.

Macey JR, Larson A, Ananjeva NB, Papenfuss TJ. 1997a. Evolutionary shifts in three major

structural features of the mitochondrial genome among iguanian lizards. *Journal of Molecular Evolution* 44: 660–674.

Macey JR, Larson A, Ananjeva NB, Fang ZL, Papenfuss TJ. 1997b. Two novel gene orders and the role of light-strand replication in rearrangement of the vertebrate mitochondrial genome. *Molecular Biology and Evolution* 14: 91–104.

Macgregor D. 2015. History of the development of the East African Rift System: A series of interpreted maps through time. *Journal of African Earth Sciences* 101: 232–252.

Maddison DR, Maddison WP. 2005. MacClade: Analysis of phylogeny and character evolution. Version 4.08. Available at: http://macclade.org/index.html

Maddison WP. 1997. Gene trees in species trees. *Systematic Biology* 46: 523–536.

Maddison WP, Maddison DR. 2015. Mesquite: A modular system for evolutionary analysis. Version 3.04. Available at: http://mesquiteproject.org

Maley J. 1996. The African forest – main characteristics of changes in vegetation and climate from Upper Cretaceous to the Quaternary. *Proceedings of the Royal Society of Edinburg* 104: 31–73.

Manger PR, Pillay P, Maseko BC, Bhagwandin A, Gravett N, Moon DJ, Jillani N, Hemingway J. 2009. Acquisition of brains from the African elephant (*Loxodonta africana*): Perfusion-fixation and dissection. *Journal of Neuroscience Methods* 179: 16–21.

Mariaux J, Tilbury CR. 2006. The pygmy chameleons of the Eastern Arc Range (Tanzania): Evolutionary relationships and the description of three new species of *Rhampholeon* (Sauria: Chamaeleonidae). *The Herpetological Journal* 16: 315–331.

Mariaux J, Lutzmann N, Stipala J. 2008. The two-horned chamaeleons of East Africa. *Zoological Journal of the Linnean Society* 152: 367–391.

Matschie P. 1892. Über eine kleine Sammlung von Säugethieren und Reptilien, welche Herr L. Conradt aus Usambara (Deutsch Ostafrika) heimgebracht hat. *Sitzungsberichte der Gesellschaft naturforschender Freunde zu Berlin* 1892: 101–110.

Matthee CA, Tilbury CR, Townsend T. 2004. A phylogenetic review of the African leaf chameleons: Genus *Rhampholeon* (Chamaeleonidae): The role of vicariance and climate change in speciation. *Proceedings of the Royal Society of London Series B: Biological Sciences* 271: 1967–1975.

Mayr E, O'Hara RJ. 1986. The biogeographic evidence supporting the Pleistocene forest refuge hypothesis. *Evolution* 40: 55–67.

Meadows ME, Linder HP. 1993. A palaeoecological perspective on the origin of Afromontane grasslands. *Journal of Biogeography* 20: 345–355.

Measey GJ, Tolley KA. 2011. Sequential fragmentation of Pleistocene forests in an East Africa biodiversity hotspot: Chameleons as a model to track forest history. *PLoS ONE* 6: e26606.

Menegon M, Tolley KA, Jones T, Rovero F, Marshall AR, Tilbury CR. 2009. A new species of chameleon (Sauria: Chamaeleonidae: *Kinyongia*) from the Magombera Forest and the Udzungwa Mountains National Park, Tanzania. *African Journal of Herpetology* 58: 59–70.

Menegon M, Loader SP, Marsden SJ, Branch WR, Davenport TRB, Ursenbacher S. 2014. The genus *Atheris* (Serpentes: Viperidae) in East Africa: Phylogeny and the role of rifting and climate in shaping the current pattern of species diversity. *Molecular Phylogenetics and Evolution* 79: 12–22.

Menegon M, Loader SP, Davenport TR, Howell KM, Tilbury CR, Machaga S, Tolley KA. 2015. A new species of chameleon (Sauria: Chamaeleonidae: *Kinyongia*) highlights the

biological affinities between the Southern Highlands and Eastern Arc Mountains of Tanzania. *Acta Herpetologica* 10: 111–120.

Mittermeier RA, Turner WA, Larsen FW, Brooks TM, Gascon C. 2011. Global biodiversity conservation: The critical role of hotspots. Pp. 3–22. In: Zachos FE, Habel JC, eds. *Biodiversity Hotspots: Distribution and Protection of Conservation Priority Areas*. Berlin, Germany: Springer-Verlag.

Miralles A, Vences M. 2013. New metrics for comparison of taxonomies reveal striking discrepancies among species delimitation methods in *Madascincus* lizards. *PLoS ONE* 8: e68242.

Mora C, Tittensor DP, Adl S, Simpson AGB, Worm B. 2011. How many species are there on Earth and in the ocean? *PLoS Biology* 9: e1001127.

Moritz C, Patton JL, Schneider CJ, Smith TB. 2000. Diversification of rainforest faunas: An integrated molecular approach. *Annual Review of Ecology and Systematics* 31: 533–563.

Moreno N, Domínguez L, Morona R, González A. 2012. Subdivisions of the turtle *Pseudemys scripta* hypothalamus based on the expression of regulatory genes and neuronal markers. *Journal of Comparative Neurology* 520: 453–478.

Morona R, González A. 2008. Calbindin-D28k and calretinin expression in the forebrain of anuran and urodele amphibians: Further support for newly identified subdivisions. *Journal of Comparative Neurology* 511: 187–220.

Müller L. 1938. Über die von Herren W. Uthmöller und L. Bohmann im britischen Madatsgebiet "Tanganyika Territory" gesammelten Chamäleons. *Zoologischer Anzeiger* 122: 20–23.

Myers N, Mittermeier RA, Mittermeier CG, Da Fonseca GAB, Kent J. 2000. Biodiversity hotspots for conservation priorities. *Nature (London)* 403: 853–858.

Myers N. 2003. Biodiversity hotspots revisited. *BioScience* 53: 916–917.

Nečas P. 2009. Ein neues Chamäleon der Gattung *Kinyongia* Tilbury, Tolley and Branch, 2006 aus den Poroto-Bergen, Süd-Tansania (Reptilia: Sauria: Chamaeleonidae). *Sauria* 31: 41–48.

Nečas P, Sindaco R, Koreny J, Malonza PK, Modry D. 2009. *Kinyongia asheorum* sp. nov., a new montane chameleon from the Nyiro Range, northern Kenya (Squamata: Chamaeleonidae). *Zootaxa* 2028: 41–50.

Nieden F. 1913. *Chamaeleon fischeri* Rchw. und seine Unterarten. *Sitzungsberichte der Gesellschaft naturforschender Freunde zu Berlin* 1913: 231–249.

Niemiller ML, Near TJ, Fitzpatrick BM. 2012. Delimiting species using multilocus data: Diagnosing cryptic diversity in the southern cavefish, *Typhlichthys subterraneus* (Teleostei: Amblyopsidae). *Evolution* 66: 846–866.

Nieuwenhuys R, Ten Donkelaar HJ, Nicholson C. 1998. *The Central Nervous System of Vertebrates*. Berlin, Germany: Springer.

Nonnotte P, Guillou H, Gall BL, Benoit M, Cotton J, Scaillet S. 2008. New K–Ar age determinations of Kilimanjaro volcano in the North Tanzanian diverging rift, East Africa. *Journal of Volcanology and Geothermal Research* 173: 99–112.

Northcutt RG. 1967. Architectonic studies of the telencephalon of *Iguana iguana*. *Journal of Comparative Neurology* 130: 109–147.

Northcutt RG, Butler AB. 1974. Evolution of reptilian visual systems: Retinal projections in a nocturnal lizard, *Gecko gecko* (Linnaeus). *Journal of Comparative Neurology* 157: 453–466.

Northcutt RG. 1978. Forebrain and midbrain organization in lizards and its phylogenetic significance. Pp. 11–64. In: Greenberg N, MacLean PD, eds. *Behavior and Neurology of Lizards*. Rockville, MD: National Institute of Mental Health.

Nydam RL, Cifelli RL. 2002. Lizards from the Lower Cretaceous (Aptian–Albian) Antlers and Cloverly Formations. *Journal of Vertebrate Paleontology* 22: 286–298.

Nylander JA, Wilgenbusch JC, Warren DL, Swofford DL. 2008. AWTY are we there yet? A system for graphical exploration of MCMC convergence in Bayesian phylogenetics. *Bioinformatics* 24: 581–583.

Olave M, Solà E, Knowles LL. 2014. Upstream analyses create problems with DNA-based species delimitation. *Systematic Biology* 63: 263–271.

Omari I, Hart JA, Butynski TM, Birhashirwa NR, Upoki A, M'Keyo Y, Bengana F, Bashonga M, Bagurubumwe N. 1999. The Itombwe Massif, Democratic Republic of Congo: Biological surveys and conservation with an emphasis on Grauer's gorilla and birds endemic to the Albertine Rift. *Oryx* 33: 301–322.

Packard GC, Boardman TJ. 1999. The use of percentages and size-specific indices to normalize physiological data for variation in body size: Wasted time, wasted effort? *Comparative Biochemistry and Physiology Part A: Molecular Integrative Physiology* 122: 37–44.

Padial JM, Miralles A, la Riva ID, Vences M. 2010. The integrative future of taxonomy. *Frontiers in Zoology* 7: 1–14.

Palumbi S. 1996. Nucleic acids II: The polymerase chain reaction. Pp. 205–247. In: Hillis DM, Moritz C, Mable BK, eds. *Molecular Systematics*, 2nd edition. Sunderland, MA: Sinauer Associates.

Pante E, Schoelinck C, Puillandre N. 2014. From integrative taxonomy to species description: One step beyond. *Systematic Biology* 64: 152–160.

Parker HW. 1929. A new *Chamaeleon* from Mt. Ruwenzori. *Annals and Magazine of Natural History* 3: 280–281.

Pasteels P, Villeneuve M, De Paepe P, Klerkx J. 1989. Timing of the volcanism of the southern Kivu province: Implications for the evolution of the western branch of the East African Rift system. *Earth and Planetary Science Letters* 94: 353–363.

Paul JD, Roberts GG, White N. 2014. The African landscape through space and time. *Tectonics* 33: 898–935.

Pickford M. 1992. Evidence for an arid climate in western Uganda during the Middle Miocene. *Comptes Rendus de l'Académie des Sciences*. *Série 2, Mécanique, Physique, Chimie, Sciences de l'univers, Sciences de la Terre* 315: 1419–1424.

Pickford M, Senut B, Hadoto DPM. 1993. Geology and palaeobiology of the Albertine Rift valley, Uganda-Zaire: Geology, Vol. I. Publication Occasionnelle. Orléans, France: Centre International pour la Formation et les Echanges Geologiques.

Plana V. 2004. Mechanisms and tempo of evolution in the African Guineo-Congolian rainforest. *Philosophical Transactions of the Royal Society B: Biological Sciences* 359: 1585–1594.

Platts PJ, Burgess ND, Gereau RE, Lovett JC, Marshall AR, McClean CJ, Pellikka PKE, Swetnam RD, Marchant R. 2011. Delimiting tropical mountain ecoregions for conservation. *Environmental Conservation* 38: 312–324.

Plumptre AJ, Masozera M, Vedder A. 2001. Effect of civil war on the conservation of protected areas in Rwanda. Washington, DC: Biodiversity Support Program.

Plumptre AJ, Behangana M, Davenport TRB, Kahindo C, Kityo R, Ndomba E, Nkuutu D, Owiunji I, Ssegawa P, Eilu G. 2003. The biodiversity of the Albertine Rift. *Albertine Rift Technical Reports No. 3*. Available at: https://albertinerift.wcs.org/

Plumptre AJ, Davenport TRB, Behangana M, Kityo R, Eilu G, Ssegawa P, Ewango C, Meirte D, Kahindo C, Herremans M, Peterhans JCK, Pilgrim JD, Wilson M, Languy M, Moyer D. 2007. The biodiversity of the Albertine Rift. *Biological Conservation* 134: 178–194.

Ponce-Reyes R, Plumptre AJ, Segan D, Ayebare S, Fuller RA, Possingham HP, Watson JEM. 2017. Forecasting ecosystem responses to climate change across Africa's Albertine Rift. *Biological Conservation* 209: 464–472.

Pons J, Barraclough TG, Gomez-Zurita J, Cardoso A, Duran DP, Hazell S, Kamoun S, Sumlin WD, Vogler AP. 2006. Sequence-based species delimitation for the DNA taxonomy of undescribed insects. *Systematic Biology* 55: 595–609.

Portillo F, Greenbaum E. 2014a. At the edge of a species boundary: A new and relatively young species of *Leptopelis* (Anura: Arthroleptidae) from the Itombwe Plateau, Democratic Republic of the Congo. *Herpetologica* 70: 100–119.

Portillo F, Greenbaum E. 2014b. A new species of the *Leptopelis modestus* complex (Anura: Arthroleptidae) from the Albertine Rift of Central Africa. *Journal of Herpetology* 48: 394–406.

Portillo F, Greenbaum E, Menegon M, Kusamba C, Dehling JM. 2015. Phylogeography and species boundaries of *Leptopelis* (Anura: Arthroleptidae) from the Albertine Rift. *Molecular Phylogenetics and Evolution* 82: 75–86.

Prigogine A. 1977. The composition of Itombwe forest's avifauna. *Bonner zoologische Beiträge* 28: 369–383.

Pupin F, Hügli D, Loader SP, Sekisambu R, Menegon M. 2012. Baseline for herpetological monitoring in the Albertine Rift montane forests. Unpublished report. New York, NY: Wildlife Conservation Society. Available at: https://albertinerift.wcs.org/

Pyron RA, Burbrink FT, Wiens JJ. 2013. A phylogeny and revised classification of Squamata, including 4161 species of lizards and snakes. *BMC Evolutionary Biology* 13: 93.

R Core Team. 2015. R: A language and environment for statistical computing. Vienna, Austria: R Foundation for Statistical Computing. Available at: https://www.R-project.org/

Rambaut A, Drummond AJ. 2007. Tracer v1.5. Available at: http://tree.bio.ed.ac.uk/software/tracer/

Rambaut A, Drummond AJ. 2009. FigTree v1.3.1. Available at: http://tree.bio.ed.ac.uk/software/figtree/

Ramón P. 1896. El structura de encéfalo del cameléon. *Revista Trimestral Micrográfica* 1: 146–182.

Reichenow A. 1887. Neue Wirbelthiere des Zoologischen Museums in Berlin. *Zoologischer Anzeiger* 10: 369–372.

Rieke GK, Bowers DE, Silvy NJ. 1981. A technique for improved fixation of the pigeon central nervous system for electron microscopy. *The Anatomical Record* 200: 121–125.

Roberts EM, Stevens NJ, O'Connor PM, Dirks PHGM, Gottfried MD, Clyde WC, Armstrong RA, Kemp AIS, Hemming S. 2012. Initiation of the western branch of the East African Rift coeval with the eastern branch. *Nature Geoscience* 5: 289–294.

Robinson JE, Griffiths RA, John FAS, Roberts DL. 2015. Dynamics of the global trade in live reptiles: Shifting trends in production and consequences for sustainability. *Biological Conservation* 184: 42–50.

Rocha LA, Aleixo A, Allen G, Almeda F, Baldwin CC, Barclay MV, Bates JM, Bauer AM, Benzoni F, Berns CM, Berumen ML, et al. 2014. Specimen collection: An essential tool. *Science (Washington)* 344: 814–815.

Ronquist F, Huelsenbeck JP. 2003. MrBayes 3: Bayesian phylogenetic inference under mixed models. *Bioinformatics* 19: 1572–1574.

Roy J, Arandjelovic M, Bradley BJ, Guschanski K, Stephens CR, Bucknell D, Cirhuza H, Kusamba C, Kyungu JC, Smith V, Robbins MM. 2014. Recent divergences and size decreases of eastern gorilla populations. *Biology Letters* 10: 20140811.

Ryan MJ. 1986. Neuroanatomy influences speciation rates among anurans. *Proceedings of the National Academy of Sciences, USA* 83: 1379–1382.

Sabaj MH. 2016. Standard symbolic codes for institutional resource collections in herpetology and ichthyology: An online reference. Version 6.5 (16 August 2016). Washington, DC: American Society of Ichthyologists and Herpetologists. Available at: http://www.asih.org/

Sachs JD, Mellinger AD, Gallup JL. 2001. The geography of poverty and wealth. *Scientific American* 284: 70–75.

Salzburger W, Van Bocxlaer B, Cohen AS. 2014. Ecology and evolution of the African Great Lakes and their faunas. *Annual Review of Ecology, Evolution, and Systematics* 45: 519–545.

San Mauro D, Gower DJ, Oommen OV, Wilkinson M, Zardoya R. 2004. Phylogeny of caecilian amphibians (Gymnophiona) based on complete mitochondrial genomes and nuclear RAG1. *Molecular Phylogenetics and Evolution* 33: 413–427.

Sauquet H. 2013. A practical guide to molecular dating. *Comptes Rendus Palevol* 12: 355–367.

Schmidt KP. 1919. Contributions to the herpetology of the Belgian Congo based on the collection of the American Museum Congo Expedition, 1909–1915. Part I: Turtles, crocodiles, lizards, and chamaeleons. *Bulletin of the American Museum of Natural History* 39: 385–624.

Schultheiß R, Van Bocxlaer B, Riedel F, von Rintelen T, Albrecht C. 2014. Disjunct distributions of freshwater snails testify to a central role of the Congo system in shaping biogeographical patterns in Africa. *BMC Evolutionary Biology* 14: 42.

Scudamore CL, Hodgson HK, Patterson L, Macdonald A, Brown F, Smith KC. 2011. The effect of post-mortem delay on immunohistochemical labelling—a short review. *Comparative Clinical Pathology* 20: 95–101.

Senn DG, Northcutt RG. 1973. The forebrain and midbrain of some squamates and their bearing on the origin of snakes. *Journal of Morphology* 140: 135–152.

Senut B, Pickford M. 1994. Geology and palaeobiology of the Albertine Rift valley, Uganda-Zaire: Palaeobiology, Vol. II. Publication Occasionnelle. Orléans, France: Centre International pour la Formation et les Echanges Geologiques.

Sepulchre P, Ramstein G, Fluteau F, Schuster M, Tiercelin JJ, Brunet M. 2006. Tectonic uplift and Eastern Africa aridification. *Science (Washington)* 313: 1419–1423.

Shanklin WM. 1930. The central nervous system of *Chameleon vulgaris*. *Acta Zoologica* 11: 425–490.

Shaw TI, Ruan Z, Glenn TC, Liu L. 2013. STRAW: Species TRee Analysis Web server. *Nucleic Acids Research* 41: W238–W241.

Shirk PL, Linden DW, Patrick DA, Howell KM, Harper EB, Vonesh JR. 2014. Impact of habitat alteration on endemic Afromontane chameleons: Evidence for historical population declines using hierarchical spatial modelling. *Diversity and Distributions* 20: 1186–1199.

Sistrom M, Hutchinson M, Bertozzi T, Donnellan S. 2014. Evaluating evolutionary history in the face of high gene tree discordance in Australian *Gehyra* (Reptilia: Gekkonidae). *Heredity* 113: 52–63.

Smeets WJAJ, Hoogland PV, Lohman AHM. 1986. A forebrain atlas of the lizard *Gekko gecko*. *Journal of Comparative Neurology* 254: 1–19.

Smeets WJAJ. 1994. Catecholamine systems in the CNS of reptiles: Structure and functional correlations. Pp. 103–134. In: Smeets WJAJ, Reiner A, eds. *Phylogeny and Development of Catecholamine Systems in the CNS of Vertebrates*. Cambridge, MA: Cambridge University Press.

Spawls S, Howell K, Drewes RC, Ashe J. 2002. *A Field Guide to the Reptiles of East Africa: Kenya, Tanzania, Rwanda and Burundi*. London, UK: Academic Press.

Srinivasan M, Sedmak D, Jewell S. 2002. Effect of fixatives and tissue processing on the content and integrity of nucleic acids. *The American Journal of Pathology* 161: 1961–1971.

Stamatakis A. 2006. RAxML-VI-HPC: Maximum likelihood-based phylogenetic analyses with thousands of taxa and mixed models. *Bioinformatics* 22: 2688–2690.

Stamatakis A, Hoover P, Rougemont J. 2008. A rapid bootstrap algorithm for the RAxML web servers. *Systematic Biology* 57: 758–771.

Stamatakis A. 2014. RAxML version 8: A tool for phylogenetic analysis and post-analysis of large phylogenies. *Bioinformatics* 30: 1312–1313.

Steindachner F. 1891. Bericht über die von Herrn Linienschiffsleutenant Ritter von Höhnel während der Graf Samuel Telekis ostafrikanischer Expedition gesammelten Reptilien. *Sitzungsberichte der Akademie der Wissenschaften in Wien, Mathematisch-naturwissenschaftliche Klasse, Abteilung I* 100: 307–313.

Steindachner F. 1911. Vorläufiger Bericht über drei neue Arten aus der Familie Chamaeleontidae. *Wien Anzeiger der Akademie der Wissenschaften* 10: 177–179.

Stephens M, Donnelly P. 2003. A comparison of Bayesian methods for haplotype reconstruction from population genotype data. *The American Journal of Human Genetics* 73: 1162–1169.

Sternfeld R. 1912. ‘‘1913’’ Reptilia. Pp. 197–279 + figs. 1–4 + pl. VI–IX. In: Schubotz H, ed. *Wissenschaftliche Ergebnisse der Deutschen Zentral-Afrika-Expedition 1907–1908 Unter Führung Adolf Friedrichs, Herzogs zu Mecklenberg. Band IV, Zoologie II*. Leipzig, Germany: Klinkhardt Biermann.

Stipala J. 2014. *Mountain Dragons: In Search of Chameleons in the Highlands of Kenya*. Singapore: Tien Wah Press.

Striedter GF, Belgard TG, Chen CC, Davis FP, Finlay BL, Güntürkün O, Hale ME, Harris JA, Hecht EE, Hof PR, Hofmann HA, et al. 2014. NSF workshop report: Discovering general principles of nervous system organization by comparing brain maps across species. *Brain, Behavior and Evolution* 83: 1–8.

Stuart YE, Campbell TS, Hohenlohe PA, Reynolds RG, Revell LJ, Losos JB. 2014. Rapid evolution of a native species following invasion by a congener. *Science (Washington)* 346: 463–466.

Stuart-Fox D, Moussalli A. 2008. Selection for social signalling drives the evolution of chameleon colour change. *PLoS Biology* 6: e25.

Sukumaran, J., Knowles, L.L., 2017. Multispecies coalescent delimits structure, not species. *Proceedings of the National Academy of Sciences, USA* 114: 1607–1612.

Sullivan JP, Lundberg JG, Hardman M. 2006. A phylogenetic analysis of the major groups of catfishes (Teleostei: Siluriformes) using *rag1* and *rag2* nuclear gene sequences. *Molecular Phylogenetics and Evolution* 41: 636–662.

Sullivan RM. 1985. A new Middle Paleocene (Torrejonian) rhineurid amphisbaenian, *Plesiorhineura tsentasi* new genus, new species, from the San Juan Basin, New Mexico. *Journal of Paleontology* 59: 1481–1485.

Sullivan RM, Lucas SG. 1996. *Palaeoscincosaurus middletoni*, new genus and species (Squamata: Scincidae) from the Early Paleocene (Puercan) Denver Formation, Colorado. *Journal of Vertebrate Paleontology* 16: 666–672.

Swainson W. 1839. On the natural history and classification of fishes, amphibians, and reptiles, or monocardian animals. Pp. 1–452. In: Lardner D, ed. *The Cabinet Cyclopaedia, Vol. II*. London, UK: Longman, Orme, Brown, Green, Longmans, and Taylor.

Swindell SR, Plasterer TN. 1997. SEQMAN. Pp. 75–89. In: Swindell SR, ed. *Sequence Data Analysis Guidebook. Methods in Molecular Medicine* v. 70. Totowa, NJ: Humana Press.

Sylvester JB, Rich CA, Loh YE, van Staaden MJ, Fraser GJ, Streelman JT. 2010. Brain diversity evolves via differences in patterning. *Proceedings of the National Academy of Sciences, USA* 107: 9718–9723.

Tago H, Kimura HI, Maeda TO. 1986. Visualization of detailed acetylcholinesterase fiber and neuron staining in rat brain by a sensitive histochemical procedure. *Journal of Histochemistry and Cytochemistry* 34: 1431–1438.

Talavera G, Dincă V, Vila R. 2013. Factors affecting species delimitations with the GMYC model: Insights from a butterfly survey. *Methods in Ecology and Evolution* 4: 1101–1110.

Tamura K, Stecher G, Peterson D, Filipski A, Kumar S. 2013. MEGA6: Molecular evolutionary genetics analysis version 6.0. *Molecular Biology and Evolution* 30: 2725–2729.

Teyssier J, Saenko SV, Van Der Marel D, Milinkovitch MC. 2015. Photonic crystals cause active colour change in chameleons. *Nature Communications* 6: 6368.

Tilbury CR, Tolley KA, Branch WR. 2006. A review of the systematics of the genus *Bradypodion* (Sauria: Chamaeleonidae), with the description of two new genera. *Zootaxa* 1363: 23–38.

Tilbury CR. 2010. *Chameleons of Africa: An Atlas Including the Chameleons of Europe, the Middle East and Asia*. Frankfurt am Main, Germany: Edition Chimaira.

Tilbury CR, Tolley KA. 2015. Contributions to the herpetofauna of the Albertine Rift: Two new species of chameleon (Sauria: Chamaeleonidae) from an isolated montane forest, south eastern Democratic Republic of Congo. *Zootaxa* 3905: 345–364.

Tolley KA, Tilbury CR, Branch WR, Matthee CA. 2004. Phylogenetics of the southern African dwarf chameleons, *Bradypodion* (Squamata: Chamaeleonidae). *Molecular Phylogenetics and Evolution* 30: 354–365.

Tolley KA, Burger M, Turner AA, Matthee CA. 2006. Biogeographic patterns and phylogeography of dwarf chameleons (*Bradypodion*) in an African biodiversity hotspot. *Molecular Ecology* 15: 781–793.

Tolley KA, Burger M. 2007. *Chameleons of Southern Africa*. Cape Town, South Africa: Struik Publishers.

Tolley KA, Chase BM, Forest F. 2008. Speciation and radiations track climate transitions since the Miocene climatic optimum: A case study of southern African chameleons. *Journal of Biogeography* 35: 1402–1414.

Tolley KA, Tilbury CR, Measey GJ, Menegon M, Branch WR, Matthee CA. 2011. Ancient forest fragmentation or recent radiation? Testing refugial speciation models in chameleons within an African biodiversity hotspot. *Journal of Biogeography* 38: 1748–1760.

Tolley KA, Herrel A, eds. 2013. *The Biology of Chameleons*. Berkeley, CA: University of California Press.

Tolley KA, Townsend TM, Vences M. 2013. Large-scale phylogeny of chameleons suggests African origins and Eocene diversification. *Proceedings of the Royal Society B: Biological Sciences* 280: 20130184.

Tolley KA, Plumptre AJ, Behangana M, Greenbaum E, Menegon M. 2014a. *Kinyongia adolfifriderici*. The IUCN Red List of Threatened Species 2014: e.T172578A1346125. Accessed on 3 December 2016. Available at: http://www.iucnredlist.org/details/172578/0

Tolley KA, Plumptre AJ, Menegon M. 2014b. *Kinyongia gyrolepis*. The IUCN Red List of Threatened Species 2014: e.T42760124A42760127. Accessed on 3 December 2016. Available at: http://www.iucnredlist.org/details/42760124/0

Tolley KA, Plumptre AJ. 2014. *Rhampholeon boulengeri*. The IUCN Red List of Threatened Species 2014: e.T172523A1344185. Accessed on 26 March 2017. Available at: http://www.iucnredlist.org/details/172523/0

Tolley KA, Tilbury CR. 2015a. *Rhampholeon hattinghi*. The IUCN Red List of Threatened Species 2015: e.T75976755A75976771. Accessed on 26 March 2017. Available at: http://www.iucnredlist.org/details/75976755/0

Tolley KA, Tilbury CR. 2015b. *Kinyongia mulyai*. The IUCN Red List of Threatened Species 2015: e.T75976903A75976914. Accessed on 3 December 2016. Available at: http://www.iucnredlist.org/details/75976903/0

Tolley KA, Alexander GJ, Branch WR, Bowles P, Maritz B. 2016. Conservation status and threats for African reptiles. *Biological Conservation* 204: 63–71.

Townsend TM, Tolley KA, Glaw F, Böhme W, Vences M. 2011. Eastward from Africa: Palaeocurrent-mediated chameleon dispersal to the Seychelles islands. *Biology Letters* 7: 225–228.

Uetz P, Freed P, Hošek J, eds. 2017. The Reptile Database. Accessed on 17 March 2017. Available at: http://www.reptile-database.org

van Reybrouck D. 2014. *Congo: The Epic History of a People*. Translated by S. Garrett. London, UK: HarperCollins.

Voelker G, Outlaw RK, Bowie RCK. 2010. Pliocene forest dynamics as a primary driver of African bird speciation. *Global Ecology and Biogeography* 19: 111–121.

Voelker G, Marks BD, Kahindo C, A'genonga U, Bapeamoni F, Duffie LE, Huntley JW, Mulotwa E, Rosenbaum SA, Light JE. 2013. River barriers and cryptic biodiversity in an evolutionary museum. *Ecology and Evolution* 3: 536–545.

Vonesh JR. 2001. Natural history and biogeography of the amphibians and reptiles of Kibale National Park, Uganda. *Contemporary Herpetology* 4: 1–14.

von Einsiedel O, dir. 2014. *Virunga* [movie]. London, UK: Grain Media, Ltd.

Wagner P, Böhme W. 2007. Herpetofauna Kakamegensis–the amphibians and reptiles of Kakamega Forest, western Kenya. *Bonner zoologische Beiträge* 55: 123–150.

Wagner P, Köhler J, Schmitz A, Böhme W. 2008. The biogeographical assignment of a west Kenyan rain forest remnant: Further evidence from analysis of its reptile fauna. *Journal of Biogeography* 35: 1349–1361.

Wake DB, Lynch JF. 1976. The distribution, ecology, and evolutionary history of plethodontid salamanders in tropical America. *Natural History Museum of Los Angeles County, Science Bulletin* 25: 1–65.

Wallach V, Wüster W, Broadley DG. 2009. In praise of subgenera: Taxonomic status of cobras of the genus *Naja* Laurenti (Serpentes: Elapidae). *Zootaxa* 2236: 26–36.

Wasielewski RV, Werner M, Nolte M, Wilkens L, Georgii A. 1994. Effects of antigen retrieval by microwave heating in formalin-fixed tissue sections on a broad panel of antibodies. *Histochemistry* 102: 165–172.

Watson RE, Wiegand SJ, Clough RW, Hoffman GE. 1986. Use of cryoprotectant to maintain long-term peptide immunoreactivity and tissue morphology. *Peptides* 7: 155–159.

Werdelin L, Sanders WJ, eds. 2010. *Cenozoic Mammals of Africa*. Berkeley, CA: University of California Press.

Werner F. 1895. Über einige Reptilien aus Usambara (Deutsch-Ostafrika). *Verhandlungen der zoologisch-botanischen Gesellschaft in Wien* 45: 190–194.

Werner M, Chott A, Fabiano A, Battifora H. 2000. Effect of formalin tissue fixation and processing on immunohistochemistry. *The American Journal of Surgical Pathology* 24: 1016–1019.

Wichura H, Bousquet R, Oberhänsli R, Strecker MR, Trauth MH. 2010. Evidence for middle Miocene uplift of the East African Plateau. *Geology* 38: 543–546.

Wichura H, Jacobs LL, Lin A, Polcyn MJ, Manthi FK, Winkler DA, Strecker MR, Clemens M. 2015. A 17-My-old whale constrains onset of uplift and climate change in East Africa. *Proceedings of the National Academy of Sciences, USA* 112: 3910–3915.

Winkler DA, Murry PA, Jacobs LL. 1990. Early Cretaceous (Comanchean) vertebrates of central Texas. *Journal of Vertebrate Paleontology* 10: 95–116.

Wronski T, Hausdorf B. 2008. Distribution patterns of landsnails in Ugandan rain forests support the existence of Pleistocene forest refugia. *Journal of Biogeography* 35: 1759–1768.

Wynn J. 2003. Miocene and Pliocene paleosols of Lothagam. Pp. 31–38. In: Leakey MG, Harris J, eds. *Lothagam: The Dawn of Humanity in Eastern Africa*. New York, NY: Columbia University Press.

Xi Z, Liu L, Rest JS, Davis CC. 2014. Coalescent versus concatenation methods and the placement of *Amborella* as sister to water lilies. *Systematic Biology* 63: 919–932.

Yang Z, Rannala B. 2010. Bayesian species delimitation using multilocus sequence data. *Proceedings of the National Academy of Sciences, USA* 107: 9264–9269.

Yusuf S, Baden T, Prieto-Godino LL. 2014. Bridging the gap: Establishing the necessary infrastructure and knowledge for teaching and research in neuroscience in Africa. *Metabolic Brain Disease* 29: 217–220.

Zachos JC, Pagani M, Sloan L, Thomas E, Billups K. 2001. Trends, rhythms, and aberrations in global climate 65 Ma to present. *Science (Washington)* 292: 686–693.

Zhang J, Kapli P, Pavlidis P, Stamatakis A. 2013. A general species delimitation method with applications to phylogenetic placements. *Bioinformatics* 29: 2869–2876.

Appendix

Abbreviations for known field numbers in Table 2.1 and Table 3.1: JS – Jan Stipala; JMD – J. Maximilian Dehling; CT – Colin Tilbury.

Abbreviations for Table 4.4: A – Abcam, Cambridge, MA; DAPI – 4',6-diamidino-2-phenylindole dihydrochloride; DBH – dopamine β-hydroxylase; Dk – donkey; E – EMD-Millipore, Billerica, MA; I – ImmunoStar, Hudson, WI; IgG – immunoglobulin G; J – Jackson ImmunoResearch Labs, West Grove, PA; L – Life Technologies, Carlsbad, CA; mono – monoclonal; Ms – mouse; NPY – neuropeptide Y; poly – polyclonal; Rb – rabbit; RT – room temperature; T – ThermoFisher Scientific, Waltham, MA; TH – tyrosine hydroxylase; UV – ultraviolet.

Abbreviations for Figure 4.4: Ant med – Anterior medulla; Cx *d* – Cortex dorsalis (dorsal cortex); Cx *dm* – Cortex dorsomedialis (dorsomedial cortex); Cx *lat* – Cortex lateralis (lateral cortex); Cx *m* – Cortex medialis (medial cortex); DVR – Dorsal Ventricular Ridge; Fo v – Fourth ventricle; L h – Lateral hypothalamus; Lat v – Lateral ventricle; Neost – Neostriatum; N *tr olf lat* – Nucleus tractus olfactori lateralis (nucleus of the lateral olfactory tract); Op tr – Optic tract; Op tec – Optic tectum; Palst – Paleostriatum; P – Periventricular hypothalamus; P c – Posterior commissure; S – septal nuclei; Th v – Third ventricle; V h – Ventral hypothalamus.

The first page of each published chapter:

Molecular Phylogenetics and Evolution 122 (2018) 125–141

Contents lists available at ScienceDirect

Molecular Phylogenetics and Evolution

journal homepage: www.elsevier.com/locate/ympev

Cryptic diversity in *Rhampholeon boulengeri* (Sauria: Chamaeleonidae), a pygmy chameleon from the Albertine Rift biodiversity hotspot

Daniel F. Hughes[a,*], Krystal A. Tolley[b,c], Mathias Behangana[d], Wilber Lukwago[d], Michele Menegon[e], J. Maximilian Dehling[f], Jan Stipala[g], Colin R. Tilbury[h], Arshad M. Khan[a], Chifundera Kusamba[i], Eli Greenbaum[a]

[a] Department of Biological Sciences, University of Texas at El Paso, El Paso, TX 79968, USA
[b] South African National Biodiversity Institute, Private Bag X7, Claremont, Cape Town, South Africa
[c] Centre for Ecological Genomics and Wildlife Conservation, Department of Zoology, University of Johannesburg, Auckland Park 2000, Johannesburg, South Africa
[d] Department of Environmental Sciences, Makerere University, P.O. Box 7062, Kampala, Uganda
[e] Tropical Biodiversity Section, MUSE – The Science Museum of Trento, Corso del Lavoro e della Scienza 3, Trento 38123, Italy
[f] Institut für Integrierte Naturwissenschaften, Abteilung Biologie, AG Zoologie, Universität Koblenz-Landau, Universitätsstraße 1, 56070 Koblenz, Germany
[g] School of Biosciences, University of Exeter, Tremough Campus, Penryn, Cornwall TR10 9EZ, United Kingdom
[h] Department of Botany & Zoology, University of Stellenbosch, Private Bag X1, Matieland, 7602 Stellenbosch, South Africa
[i] Laboratoire d'Herpétologie, Département de Biologie, Centre de Recherche en Sciences Naturelles, Lwiro, Democratic Republic of the Congo

ARTICLE INFO

Keywords:
Biodiversity
Biogeography
Burundi
Diversification
Democratic Republic of the Congo
Kenya
Molecular systematics
Phylogeography
Rwanda
Uganda

ABSTRACT

Several biogeographic barriers in the Central African highlands have reduced gene flow among populations of many terrestrial species in predictable ways. Yet, a comprehensive understanding of mechanisms underlying species divergence in the Afrotropics can be obscured by unrecognized levels of cryptic diversity, particularly in widespread species. We implemented a multilocus phylogeographic approach to examine diversity within the widely distributed Central African pygmy chameleon, *Rhampholeon boulengeri*. Gene-tree analyses coupled with a comparative coalescent-based species delimitation framework revealed *R. boulengeri* as a complex of at least six genetically distinct species. The spatiotemporal speciation patterns for these cryptic species conform to general biogeographic hypotheses supporting vicariance as the main factor behind patterns of divergence in the Albertine Rift, a biodiversity hotspot in Central Africa. However, we found that parapatric species and sister species inhabited adjacent habitats, but were found in largely non-overlapping elevational ranges in the Albertine Rift, suggesting that differentiation in elevation was also an important mode of divergence. The phylogeographic patterns recovered for the genus-level phylogeny provide additional evidence for speciation by isolation in forest refugia, and dating estimates indicated that the Miocene was a significant period for this diversification. Our results highlight the importance of investigating cryptic diversity in widespread species to improve understanding of diversification patterns in environmentally diverse regions such as the montane Afrotropics.

1. Introduction

The East African Rift valley system started to form in the early Oligocene from hot mantle plumes causing up-lift of the African plate resulting in rifting, the formation of horst and grabens, and associated volcanic activity (Chorowicz, 2005; Paul et al., 2014). The Albertine Rift (AR) portion in Central Africa was initiated in the late Oligocene (Roberts et al., 2012) and increased geophysical rifting in the AR occurred during the Miocene (Macgregor, 2015). Rifting oscillations influenced forest environments in the AR, largely through uplift events that altered climate and drainage patterns across the region (Sepulchre et al., 2006). Miocene volcanism has also contributed to the age and distribution of AR forests (Griffiths, 1993). The paleoclimate of the AR was generally stable through the Cretaceous (Maley, 1996), during which tropical Africa was dominated by a nearly continuous rainforest block. African rainforests began to decline in extent throughout the Cenozoic, with a pronounced increase in forest losses after the mid-Miocene (Kissling et al., 2012). Altered precipitation patterns across East Africa, driven by global cooling, contributed to the decline of the African tropical forest ecosystem in the Miocene (Zachos et al., 2001).

* Corresponding author.
E-mail address: dfhughes@miners.utep.edu (D.F. Hughes).

https://doi.org/10.1016/j.ympev.2017.11.015
Received 3 June 2017; Received in revised form 3 October 2017; Accepted 27 November 2017
Available online 02 December 2017

Zoological Journal of the Linnean Society, 2017, **181**, 400–438. With 10 figures.

Integrative taxonomy of the Central African forest chameleon, *Kinyongia adolfifriderici* (Sauria: Chamaeleonidae), reveals underestimated species diversity in the Albertine Rift

DANIEL F. HUGHES[1]*, CHIFUNDERA KUSAMBA[2], MATHIAS BEHANGANA[3] and ELI GREENBAUM[1]

[1]*Department of Biological Sciences, University of Texas at El Paso, El Paso, TX 79968, USA*
[2]*Laboratoire d'Herpétologie, Département de Biologie, Centre de Recherche en Sciences Naturelles, Lwiro, République Démocratique du Congo*
[3]*Department of Environmental Sciences, Makerere University, P.O. Box 7298, Kampala, Uganda*

Received 4 December 2015; revised 8 December 2016; accepted for publication 15 January 2017

The Albertine Rift (AR) is a centre for vertebrate endemism in Central Africa, yet the mechanisms underlying lineage diversification of the region's fauna remain unresolved. We generated a multilocus molecular phylogeny consisting of two mitochondrial (*16S* and *ND2*) and one nuclear (*RAG1*) gene to reconstruct relationships and examine spatiotemporal diversification patterns in the AR endemic forest chameleon, *Kinyongia adolfifriderici* (Sternfeld, 1912). This widely distributed species was revealed to be a complex of four genetically distinct and geographically isolated species. Three new species are described based on molecular analyses and morphological examinations. We find that ***K. rugegensis* sp. nov.** (Rugege Highlands) and ***K. tolleyae* sp. nov.** (Kigezi Highlands) form a well-supported clade, which is sister to *K. gyrolepis* (Lendu Plateau). ***Kinyongia itombwensis* sp. nov.** (Itombwe Plateau) was recovered as sister to *K. adolfifriderici* (Ituri Rainforest). The phylogeographic patterns we recovered for *Kinyongia* suggest that speciation stemmed from isolation in forest refugia. Our estimated diversification dates in the Miocene indicate that most species of *Kinyongia* diverged prior to the aridification of Africa following climate fluctuations during the Pleistocene. Our results highlight the AR as a focal point of diversification for *Kinyongia*, further elevating the global conservation importance of this region.

ADDITIONAL KEYWORDS: biodiversity – biogeography – Burundi – conservation – Democratic Republic of the Congo – diversification – molecular systematics – new species – phylogeography – Uganda.

INTRODUCTION

The Albertine Rift (AR) represents the western branch of the East African Rift valley system (Chorowicz, 2005). The modern topography of the East African Rift started to form *c.* 30 Mya from volcanic swells in North and East Africa (Paul, Roberts &White, 2014). The AR portion of the East African Rift was likely initiated during the Oligocene (*c.* 25 Mya) (Roberts *et al.*, 2012). However, most of the geomorphological changes in the AR took place in the mid- to late Miocene (15–5 Mya) (Macgregor, 2015). Volcanism also principally occurred during the Miocene in the AR (Nonnotte *et al.*, 2008), and extensive lava flows would have contributed to landscape modifications (Griffiths, 1993). The AR is not only geologically unique, it also harbours more endemic vertebrate species than any other area of similar size on continental Africa (Plumptre *et al.*, 2007), including the highest mammalian tropical forest species richness per unit area on Earth (Demos *et al.*, 2015). The AR was not identified by Myers *et al.* (2000) as one of the original 25 Biodiversity Hotspots. Reassessments with an African emphasis, however, elevated the AR into the Eastern Afromontane Hotspot (Brooks *et al.*,

*Corresponding author. E-mail: dfhughes@miners.utep.edu [Version of Record, published online 20 May 2017; http://zoobank.org/ urn:lsid:zoobank.org:pub:FAAE0F53-0BED-4D04-BB71-15A392FC9195]

PLOS | ONE

RESEARCH ARTICLE

Rescuing Perishable Neuroanatomical Information from a Threatened Biodiversity Hotspot: Remote Field Methods for Brain Tissue Preservation Validated by Cytoarchitectonic Analysis, Immunohistochemistry, and X-Ray Microcomputed Tomography

Daniel F. Hughes[1,2,3,4]*, Ellen M. Walker[1,2,5], Paul M. Gignac[6], Anais Martinez[1,2,5], Kenichiro Negishi[1,2,6], Carl S. Lieb[1,3], Eli Greenbaum[1,3,7], Arshad M. Khan[1,2,7]*

1 Department of Biological Sciences, University of Texas at El Paso, El Paso, Texas, United States of America, **2** UTEP Systems Neuroscience Laboratory, University of Texas at El Paso, El Paso, Texas, United States of America, **3** UTEP Biodiversity Collections, University of Texas at El Paso, El Paso, Texas, United States of America, **4** Doctoral Program in Ecology & Evolutionary Biology, University of Texas at El Paso, El Paso, Texas, United States of America, **5** Doctoral Program in Environmental Pathobiology, University of Texas at El Paso, El Paso, Texas, United States of America, **6** Masters Program in Biology, University of Texas at El Paso, El Paso, Texas, United States of America, **7** Border Biomedical Research Center, University of Texas at El Paso, El Paso, Texas, United States of America, **8** Department of Anatomy and Cell Biology, Oklahoma State University Center for Health Sciences, Tulsa, Oklahoma, United States of America

* amkhan2@utep.edu (AMK); dfhughes@miners.utep.edu (DFH)

Citation: Hughes DF, Walker EM, Gignac PM, Martinez A, Negishi K, Lieb CS, et al. (2016) Rescuing Perishable Neuroanatomical Information from a Threatened Biodiversity Hotspot: Remote Field Methods for Brain Tissue Preservation Validated by Cytoarchitectonic Analysis, Immunohistochemistry, and X-Ray Microcomputed Tomography. PLoS ONE 11(5): e0155824. doi:10.1371/journal.pone.0155824

Editor: Antal Nógrádi, University of Szeged, HUNGARY

Received: November 19, 2015

Accepted: May 4, 2016

Published: May 19, 2016

Data Availability Statement: All relevant data are within the paper and its Supporting Information files.

Funding: This work was supported by National Science Foundation grant DEB-1145459 (to EG and DFH), National Institutes of Health grant GM109817 (to AMK), UTEP Office of Research and Sponsored Projects Grand Challenges Grant (to AMK), a Howard Hughes Medical Institute STEM Education Grant (to AMK and EG), Keelung Hong Graduate

Abstract

Biodiversity hotspots, which harbor more endemic species than elsewhere on Earth, are increasingly threatened. There is a need to accelerate collection efforts in these regions before threatened or endangered species become extinct. The diverse geographical, ecological, genetic, morphological, and behavioral data generated from the on-site collection of an individual specimen are useful for many scientific purposes. However, traditional methods for specimen preparation in the field do not permit researchers to retrieve neuroanatomical data, disregarding potentially useful data for increasing our understanding of brain diversity. These data have helped clarify brain evolution, deciphered relationships between structure and function, and revealed constraints and selective pressures that provide context about the evolution of complex behavior. Here, we report our field-testing of two commonly used laboratory-based techniques for brain preservation while on a collecting expedition in the Congo Basin and Albertine Rift, two poorly known regions associated with the Eastern Afromontane biodiversity hotspot. First, we found that transcardial perfusion fixation and long-term brain storage, conducted in remote field conditions with no access to cold storage laboratory equipment, had no observable impact on cytoarchitectural features of lizard brain tissue when compared to lizard brain tissue processed under laboratory

Vita

Daniel Hughes was awarded his B.Sc. in Zoology from Humboldt State University (Arcata, CA) in 2011 and his M.Sc. in Biology from Shippensburg University (Shippensburg, PA) in 2013. While a student at UTEP, Daniel held several positions that overlapped: Research Associate in the UTEP Biodiversity Collections from 2013–2015; Dr. Keelung Hong Graduate Fellow from 2015–2017; Teaching Assistant for Molecular Systematics course during Spring 2016; and Adjunct Faculty with Excelsior College's Department of Natural Sciences at the US Army Sergeants Major Academy from 2016–2018. Daniel will start a post-doctoral research position at the University of Illinois Urbana-Champaign in 2018 to work on applied aspects of amphibian conservation.

Daniel has presented his research at many scientific conferences, including the Society for Neuroscience (SfN), Society for Integrative and Comparative Biology (SICB), and Joint Meeting of Ichthyologists and Herpetologists (JMIH). At JMIH in 2017, he won the Society for the Study of Amphibians and Reptile's best student poster award. While at UTEP, Daniel was awarded the Frank B. Cotton Estate Fund Scholarship (2015), George Krutilek Memorial Graduate Fellowship (2015), Outstanding Doctoral Student award (2016), Dodson research grant (2014, 2015, 2016, 2017), and Student Travel grant (2014, 2015, and 2016). To date, Daniel has authored or co-authored 14 major scientific publications on reptiles and amphibians and he has also published 12 natural history notes on various herpetofaunal observations.

Daniel enjoys all aspects science, especially exploration in Africa where he has spent over six-months across three expeditions looking for new species. Outside of academia, he enjoys books and movies, and happily squanders many days searching the countryside for creepy-crawlies.

This dissertation was typed by Daniel Frederick Hughes.